Mars Express

MARS EXPRESS ORBITER RADIO SCIENCE
MaRS

FLIGHT OPERATIONS MANUAL
EXPERIMENT USER MANUAL

Reference: **MEX-MRS-IGM-MA-3008**
Issue: **2**
Revision: **2**

Rheinisches Institut für Umweltforschung
An der Universität zu Köln
Aachenerstr. 201 - 209
50931 Cologne
Germany

Prepared by:

_____
Axel Hagermann, RSI Experiment Manager

Approved by:

_____
Martin Pätzold, Principal Investigator

PAGE LEFT FREE

Contents

List of figures

List of tables

Document Change Record

Issue	Rev.	Section	Date	Changes
Draft	0	All	08.05.2000	All pages
Draft	1	All	01.10.2000	All sections after EFDR
Draft	2	All	05.06.2001	all sections
Draft	3	4.5	10.10.2001	section 4.5 added
		5	10.10.2001	section 5 added
		4	10.10.2001	section 4 updated
		3.3.3	10.10.2001	section updated
		3.3.4	10.10.2001	section updated
		2	10.10.2001	section edited
		7.1	10.10.2001	section added
		4.1-4.4	10.10.2001	sections updated with regard to DSN involvement
Draft	4	3.1.1.1	24.01.2002	science objective added
		3.1.1.4		section added (Phobos)
		3.1.1.6		Fig 3.1.1-7 updated
				Table 3.4-6 updated
		3.4.2.3		auxiliary data updated
		3.4.2		section 3.4.2.1.1 updated
		3.5		Table 3.5.1-2 updated
		3.5.2		section Phobos added
				Table 3.5.2-1 updated
		4.1.2		Table 4.1.2-1 updated
				Table 4.1.2-2 updated
		4.1.3		Table 4.1.3-1 updated
		4.1.4		Table 4.1.4-1 updated
		4.1.5		Table 4.1.5-1 updated
				section Phobos added
				Figure 4.1.5-5 added
				Figure 4.1.5-4 added
		4.4		section 4.4.4 added
				Tables 4.4.1 – 4.4.6 updated
				Table 4.4.5-2 updated
				Figure 4.4.2-1 deleted
				Figure 4.4.5-1 updated
		5		all timelines updated
		8		section 8 fully updated
Draft	5	all	24-May-02	Document restructured, Interface info added
1	0	3.4.3	11.11.02	IFMS openloop data volume
1	1	7	03.03.2003	Section 7 revised and updated New section 7.1 OCC request list introduced in section 7.2 GRA target list introduced in section 7.3 BSR target list introduced in section 7.4 PHO flyby list introduced in section 7.5 SCO request list introduced in section 7.6
1	2	all	10.03.03	Editing
1	3	6.1	31.03.03	EPS syntax section included
2	0	all	18.5.03	Editing Include new section 1.3: Contact Persons of MaRS Move section 4.3 to section 7.1 Updating of DSN data files from ATDF to TRK-2-34
2	1	6	21.05.03	“Handling of configuration data” included
2	2	6	21.05.03	Adress “Institut für Geophysik und Meteorologie”

				changed in “Rheinisches Institut für Umweltforschung“.

Distribution List

Recipient	Institution	No. of copies
	ESTEC	5
	ESOC	2
	MMS	5
	B. Häusler	2
	M. Pätzold	2
	MaRS Team	10

PAGE LEFT FREE

1 Introduction

1.1 Purpose

This document presents the Experiment User Manual and Flight Operations Manual for the RSI experiment. It is intended as a reference for the implementation of MaRS science operations during the Mars Express mission.

1.2 Scope

The document defines the science objectives, describes the observational methods, and the configuration and operational modes of the MaRS experiment, with regard to the space and ground station segments.
Section 2 describes the science objectives, the experiment operations and pointing requirements. Section 3 covers characteristics of the experiment, section4 covers operations. In section 5 Functions are explained. An interface definition is given in section 6, in section 7 a detailed description of functional procedures and an estimate of the total data volume is given. In section 8 a timeline including operation procedure tables for the individual procedures is given. References are listed in section 9.

1.3 Contact Persons of MaRS

Function	Name	Adress	E-mail	Telephone/ Fax
Principal Investigator	Martin Pätzold	Institut für Geophysik und Meteorologie, Universität zu Köln, Albertus-Magnus-Platz, D-50923 Köln, Germany	paetzold@geo.uni-koeln.de	phone: (49)-221-470-3385 Fax: (49)-221-470-5198
Experiment Manager	Bernd Häusler	Institut für Raumfahrt-technik, Universität der Bundeswehr, München, D-85577 Neubiberg, Germany	bernd.haeusler@unibw-muenchen.de	phone: (49)-89-6004-2138 Fax: (49)-89-6004-2138
Data Manager	Richard A. Simpson	Dept. of Electrical Engineering, Stanford University, Packard Building 350, Serra Mall, Stanford, CA 94305-9515, USA	rsimpson@magellan.stanford.edu	phone: (1)-650-723-3525 Fax: (1)-650-723-9251
Operations Manager	Joerg Selle	Institut für Raumfahrt-technik, Universität der Bundeswehr, München, D-85577 Neubiberg, Germany	joerg.selle@unibw-muenchen.de	phone : (49)-89-6004-3598 Fax: (49)-89-6004-2138
JPL	Sami W. Asmar	Jet propulsion Laboratory, California Institute of Technology, 4800 Oak Grove Drive, Pasadena CA 91009, USA	sami.w.asmar@jpl.nasa.gov	phone: (1)-818-354-6288 Fax: (1)-818-393-9282
Stanford University	G. Leonard Tyler	Dept. of Electrical Engineering, Stanford University, Packard Building 350, Serra Mall, Stanford, CA 94305-9515, USA	: tyler@ee.stanford.edu	phone: (1)-650-723-3535 Fax: (1)-650-723-9251

1.4 Applicable Documents

Reference Number	Title	Issue	Date
GRST-TTC-GS-ICD-0518-TOSG	IFMS-to-OCC Interface Control Document	1.0	14-Mar-2000
TRK-2-34	DSMS Tracking System Data Archival Data	B	30.4.200
JPL D-16765 (159-SCIENCE)	Radio Science Receiver RSR	Draft	5.2.2001
RSC 11-13	Original Data Record ODR		
TRK 2-25	Archival Tracking Data File ATDF		
MEX-MRS-IGM-RS-3014	IFMS User Requirement Document		
MEX-MRS-IGM-RS-3007	MaRS EID-B	1	02.11.1999
RO-RSI-IGM-TN-3057			
GRST-TTC-GS-ICD-0518-TOSG	IFMS-to-OCC Interface Control Document	1.0	14.07.2000
MEX-RAL-TN-0026	Handling of MaRS configuration data	0.1	04.05.2003
SOP-SSD-RG-001	Experiment Planning System Reference Guide	?	?

1.5 Referenced Documents

Reference Number	Title	Issue	Date
RO-EST-TN-3053	Rosetta Mission Scenarios: Pointing	Draft d	11-Mar-2002
SOP-RSSD-SO-002	Science Operations for Planetary Missions EPS PTR SSD	1.2	26-Apr-2002
DSN810-5	Deep Space Network / Flight Project Interface Design Book, Document 810-5, JPL, Pasadena, CA.	**?**	**?**

1.6 Abbreviations

ADC Analog Digital Converter
ADEV Allan Deviation
AGC Automatic Gain Controll
AOCS Attitude and Orbit Control Subsystem
AOU Astronomical Institute, Uppsala University
ATDF Archival Tracking Data File
AVAR Allan Variance
BSR Bistatic Radar Procedure
BVA High performance, low phase noise type of quartz oscillator
BWG Beam Wave Guide
CAN Canberra
CFE Common Front End
CPU Central Processor Unit
CNES Centre National d'Etude Spatiale
DC Direct Current
DSN Deep Space Network
DSP Digital Signal Processor
DSS Deep Space Network Station
DTM Digital Topographic Model
DUT Device under test
EM Engineering Model
EPS Experiment Planning System
EQM Electrical Qualification Model
ERT Earth (pointing)

ESA	European Space Agency
ESO	European Southern Observatory
ESOC	European Space Operations Centre
FFT	Fast Fourier Transformation
FM	Flight Model
FOM	Flight Operations Manual
FS	Flight Spare
FTP	File Transfer Protocoll
GDSP	Generic Digital Signal Processing
GRA	Gravity Mapping of Anomalies
GSFC	Ground Communications Facility
GST	Goldstone
G/S	Ground Station
HDEV	Hadamard Deviation
HEF	High Efficiency
HGA	High Gain Antenna
HRSC	High Resolution Stereo Camera
HS	High Speed
HSB	High- Speed BWG
HVAR	Hadamard Variance
IFMS	Intermediate Frequency Modulation System
IGM	Institut für Geophysik und Meteorologie, Universität zu Köln
IPP	Inter-Process Protocoll
IRIG	Interrange Instrumentation Group
IF	Intermediate Frequency
ITA	Institute of Theoretical Astrophysics, Oslo University
JPL	Jet Propulsion Laboratory
LCP	Left Circular Polarization
LGA	Low Gain Antenna
LHC	Left Handed Circulated Polarization
LO	Local Oscillator
LOS	Line-of-Sight
MAD	Madrid
MaRS	Mars Express orbiter Radio Science Experiment
MB/s	Mega Byte per second
Mb/s	Mega Bit per second
MKP	Max-Planck-Intitut für Kernphysik
MPAe	Max-Planck Institut für Aeronomie
MPTS	Multi-Protocoll Transport Service
NASA	National Aeronautics and Space Administration
NNO	New Norcia
NOCC	Network Operations and Control System
OCC	Occultation Procedures
OL	Open-loop
ONES	One-way single-frequency mode
ODR	Original Data Record
PA	Power Amplifier
PC	Personal Computer
PFM	Proto Flight Model
PHO	Phobos encounter procedure
PLL	Phase-lock loop
PSD	Power Spectral Density
RAIUB	Radioastronomisches Institut der Universität Bonn
RFDU	Radio Frequency Distribution Unit
RCP	Right Circular Polarization
RF	Radio Frequency
RHC	Right Handed Circulated Polarization
R_S	Sun Radius
RSI	Radio Science Investigation

RSR	Radio- Science Receiver
S-RX	S-band Receiver
SA	Solar Arrays
S/C	Spacecraft
SCP	Solar Conjunction Procedures
SFDU	Standard Formatted Data Unit
SGICD	Surface Ground Interface Control Document
SJSU	San Jose State University
SNR	Signal-Noise-Ratio
SOHO	Solar and Heliospheric Observatory
SoM	School of Mathematics, University of Wales
SPC	Signal Processing Center
STAT	Science Time Analysis Tool
STC	Station Computer
S-TX	S-Band Transmitter
TCXO	Temperature controlled crystal oscillator
TEC	Total Electron Content
TBC	To be confirmed
TBD	To be determined
TC	Telecommanding
TM	Telemetry
T_{sys}	System Temperature
TT&C	Telemetry Tracking & Comanding
TVT	Tracking Verification Test
TWOD	Two-way dual-frequency mode
TWOS	Two-way single-frequency mode
TWTA	Travelling wave tube amplifier
U-CPU	Unix CPU
UniBW	Universität der Bundeswehr
USM	Universitätssternwarte München
USO	Ultra Stable Oscillator
VCXO	Voltage controlled crystal oscillator
VME	Versa Module Eurocard (standard bus)
X-TX	X-band Transmitter

2 An Introduction to Radio Science

2.1 Introduction

Although initially conceived as an exploratory tool, radio science techniques have provided considerable detail—originally unanticipated—regarding the atmospheres and gravity of the planets. Previous experiments at Mars have demonstrated accuracies in measurements of Martian atmospheric surface pressure and temperature that rival or surpass those of in situ measurements made with the Viking Landers. This performance can be duplicated or bettered for occultation immersion measurements with Mars Express.

2.2 Background

Radio Science is the general study of phenomena affecting the propagation, scattering, and reception of electromagnetic transmissions in the wavelength regime longward of roughly 0.1 millimeters. A broad array of phenomena and the techniques used in studying them fall in this category, including much of electromagnetism in the natural world. The distinction between 'radio science' and 'electromagnetics,' as used especially in an engineering sense, is the emphasis in the former on study of phenomena observed in nature. In the context of planetary study and exploration, however, the term radio science has come generally to indicate a focus on the use of radio signals traveling between spacecraft and an Earth terminal for scientific investigation of planets and their environs. This specialized usage arises from the historical development of space applications. Thus, for example, topside sounding and passive reception of natural emissions properly would be `radio science' in a terrestrial context, but these topics likely would be identified in terms of the specific techniques when applied in space. In the context of planetary studies the term radio science also includes the scientific application of radio tracking data in the precise determination of a spacecraft's orbit and scientific information that can be derived from such information. Radio signals provide an extremely precise measurement of the radio path between the ground station and the spacecraft, and such measurements in turn are employed to infer important characteristics of planetary systems.

Radio Science techniques are applied to the study of planetary atmospheres (including the ionosphere), cometary atmospheres, the solar corona, rings, surfaces, and gravity. Much of our modern fundamental knowledge of these subjects has been derived from radio science observations. Early flight missions incorporating radio science investigations include the Mariners, Pioneers, and Viking, as well as Soviet projects. Examples of recent and current radio science investigations include those conducted with Voyager (Eshleman et al. 1977; Tyler 1987), Ulysses (Bird et al., 1994; Pätzold et al., 1995), Giotto (Pätzold et al., 1991a; 1991b; 1993), Galileo (Howard et al. 1992), Mars Observer (Tyler et al. 1992), and Mars Global Surveyor (Tyler et al. 2000). Missions carrying radio science investigations currently en route or planned include Cassini (Bird et al., 1995), Rosetta (Pätzold et al., 2000a), and Mars Express (Pätzold et al., 2000b).

Radio science investigations fall into three broad categories of experimentation and observation. First, for the study of planetary environments, the orbit or trajectory of the spacecraft is arranged so that the spacecraft passes behind the planetary body as seen from the tracking station on the Earth. In this instance the spacecraft is said to be 'occulted' by the planet during those intervals when the atmosphere or body of the planet lies between the radio source and receiver. In a typical occultation experiment conducted with an orbiter, the spacecraft sequentially passes behind the ionosphere, the neutral atmosphere, and body of the planet as seen from the tracking station, and then reemerges in the reverse sequence. During an occultation event one 'senses' the media of interest—atmosphere and ionosphere—by the effect of the gas on the radio signal. The method can be extended to any one of several separable 'atmospheres' including the planetary rings and magnetospheres, as well as the relativistic gravitational effects of stars (Eshleman 1973). In conducting such observations the geometry and other experimental conditions must be controlled so that the only significant unknown factors are the properties of the medium along the radio path.

The modern value for the surface pressure of Mars was first determined in 1965 by use of the radio occultation method with Mariner 4 providing the signal source (Kliore et al. 1965). Prior to the Mariner 4 experiment, the scientific and popular literature indicated a consensus that the surface pressure was in the range of 100 mb, or about 10 percent of that of Earth, based on difficult spectroscopic observations from the ground. Further, many believed that oxygen was a major atmospheric constituent. In a time when Mt. Everest had been conquered many believed that it would be possible to live on Mars without mechanical aids after a period of adjustment! The science fiction stories of Edgar Rice Burroughs reflect this earlier view.

At the beginning of the space age, however, a precise value became important in the context of designs for entry craft and landers destined for the surface of Mars then under study by teams led by Werner von Braun. At the time of the Mariner 4 launch and cruise new ground based observations of the atmosphere had begun to cast doubt on the 100 mb value, suggesting that the true value could be substantially lower. As a result of this situation an accurate determination became critical in an engineering sense. After considerable debate in which one side declared that the loss of data during an occultation event could lead to a spacecraft catastrophe, mission managers at NASA elected to direct Mariner 4 to fly behind the body of Mars for the purpose of performing radio occultation measurements. Although the early analysis methods were primitive compared with current techniques, it was immediately clear that atmospheric pressure at the occultation point was approximately 4 mb, a factor of 20 less than the consensus value; dramatically and very significantly less that many expected! Further, since spectrographic studies indicated that the partial pressure of CO2 on Mars was in this range, the atmosphere was almost entirely carbon dioxide with little if any oxygen. Radio occultation measurements have been included on all planetary mission flown since that time. Similarly, a radio occultation experiment conducted with Voyager 2 was able to determine for the first time that the surface pressure of Neptune's satellite Triton is 14 microbars (Tyler et al. 1989; Gurolla 1995).

Second, oblique incidence scattering investigations using carom paths between spacecraft, a planetary or satellite surface, and an Earth station can be used to explore the surface properties through study of the microwave scattering

function. Such investigations are referred to a 'bistatic radar' after the military nomenclature for radar systems in which the transmitter and receiver are separated by significant angular distances or ranges. In this instance the first experiment in space was conducted on the moon. The oblique scattering geometry afforded by the Luna II, Luna III and Lunar Orbiter spacecrafts, provided the signal source. Recording of signals transmitted to Earth by that satellite also contained echos of the transmissions from the lunar surface. As it happened, the plane of the spacecraft spin axis and the antenna polarization made it possible to measure the Brewster angle of the lunar crust, leading to an unambiguous value for the relative dielectric constant of lunar soil between 2.9 and 3.1, and thereby confirming that a future landing spaceship would be on firm (lunar) ground.

Third, when the radio path is well-clear of occulting material, the spacecraft can be treated as a classical 'test particle' falling in the gravity field of the planetary system with the component of its velocity along the line-of-sight to the tracking station measured by the Doppler effect. In contrast to occultation experiments, which sense the effect of the medium along a path between two known points, gravity experiments are based on determining the motion of the spacecraft in response to the variations in mass distribution within a planet or its satellites. This is a classical physics laboratory experiment carried out on planetary scales. Our global knowledge of Earth's gravity comes from such studies. In space, our only knowledge of the gravity field of Mercury is from the three flybys of Mariner 10 (Howard et al., 1974). Similarly, recent inferences as to the internal structures of the Galilean satellites, for example that there is an ocean on Europa, are based on the behavior of the trajectory of Galileo spacecraft during close flybys. A precise determination of the total mass of Uranus and Neptune has led to the conclusion that there is no need for a 'Planet X' to explain the orbits of these bodies (Standish, 1993), although some important mysteries in the motions of the out planets and very remote spacecraft remain. The method has been extended to small bodies as well, for example in the mass determination of asteroid Mathilde (Yeomans et al., 1997) and gravity field of asteroid Eros (Yeomans et al., 2000). At Mars, techniques similar to those used for asteroids can be applied to a precise determination of the masses of Phobos and Diemos.

These three techniques—radio occultation, bistatic radar, and determinations of gravity from radio tracking—have roots and counterparts in classical astronomy: (I) Classical stellar occultation observations make use of the chance passage of a planet between Earth and a star. Such an occurrence permits determination of the existence or absence of an atmosphere by observing the extinction of starlight as the planet obscures the star (*v., e.g.,* Elliot et al. 1989). When an atmosphere is present some of its properties can be determined. Stellar occultation has been extended to the study of planetary rings by observing the degree extinction as a function of radius (*v., e.g.,* Elliot and Nicholson 1984). Sometimes the unexpected occurs; the rings of Uranus were discovered by this technique by investigators attempting to understand the planet's upper atmosphere. (ii) Measurements of the classical scattering phase function, *i.e.*, the angular distribution of scattered energy flow, are the optical predecessor of bistatic radar, in which the source typically is the sun and observations are made with terrestrial telescopes. (iii) Early determinations of the small-scale properties of the lunar surface, for example, were carried out in this manner. Classical Earth-based measurements of the motions of natural satellites are used to determine the low-order gravity fields of planets. When available, radio

science methods provide much greater accuracy and dynamic range than these classical approaches. The power of radio science methods as compared with the classical techniques arises from the use of coherent radio signals that permit the measurement of radio frequency phase and deterministic polarization as precise tools for probing planetary environments. An additional, fundamental distinction between the classical approaches and those of radio science is the ability of the investigation geometry to be controlled through manipulation of the spacecraft relative to the Earth, thereby considerable flexibility in the selection of the geometric experimental parameters. Future missions in which such experiments are organized utilizing transmission between or among multiple satellites in orbit about the same planet would permit complete control of experimental conditions. An early such occultation experiment, GPS/MET, has been conducted in Earth orbit using the GPS constellation of satellites as signal sources with reception on a low-Earth orbiter (Kursinski et al. 1996; Ware et al. 1996).

Short of in situ measurements by entry probes, radio occultation studies of atmospheres provide the most detailed information available on the vertical structure of the neutral atmosphere, the ionosphere, and atmospheric waves. In principle, vertical structure as fine as a few meters can be discerned, and a resolution as fine as 100 m has been demonstrated for Mars. Recent analyses of MGS radio occultations at Mars have shown that a sequence of radio occultation measurements can provide adequate sampling and accuracy to provide a useful determination of atmospheric fields; wind velocity, temperature, and pressure can all be determined as a function of altitude. An unusual aspect of this is the use of the occultation determination of the atmospheric parameters in terms of the absolute radius, thereby enabling the use of new techniques to address problems in atmospheric dynamics. For example, the gradient wind equation can be used to determine absolute winds vs. altitude across a path connecting two nearby occultation points (Hinson 1999). Radio occultation measurements strongly complement and extend other spacecraft and Earth-based remote sensing techniques, such as infrared spectroscopy, which provide detailed information on atmospheric constituents and low vertical resolution structure over wide regions by instrumental scanning. The best results are obtained when radio occultation and these other observations are combined.

Bistatic radar observations of the Moon, Venus, and Mars extend and complement Earth-based radar astronomy studies of these objects. For example, the fundamental nature of the lunar surface as a consolidated soil was first demonstrated by a combination of terrestrial radar astronomy and bistatic radar methods. Likewise, determination of the particle sizes in the rings of Saturn was based on a forward scattering experiment for observing the diffraction pattern of the ring particles; refined experiments of this type are planned for Cassini when it reaches Saturn. Similarly, the existence of exotic phase changes in materials at the upper levels of Cytherian mountains was demonstrated by observing variations in polarization from Maxwell Montes with a bistatic scattering experiment conducted with the Magellan spacecraft. Most recently, verification of the typical nature of the Mars Polar Lander target sites on centimeter to decimeter scales was provided by bistatic scattering observations with Mars Global Surveryor.

Radio tracking studies of gravity are uniquely suited to determine the interior structure of planets, in those cases for which the appropriate geometrical conditions can be obtained. To date, the intense radiation field of Jupiter's magnetosphere and the hazard of planetary rings at Saturn and Uranus have prevented close

approaches to these planets by spacecraft, thereby limiting the utility of this technique at the outer planets. While in these cases the best information to date is obtained by classical methods, suggested missions that would fly beneath the radiation belts of Jupiter, say, hold considerable promise for solving the puzzle of that planet's interior organization. When practical, spacecraft methods are superior in all instances for determination of total system mass, the internal distribution of mass of various bodies, and the masses of individual satellites.

2.3 Technique

Radio science instrumentation combines equipment on the ground with on-board spacecraft hardware required to create and maintain a highly stable and precise radio link. Most commonly, two-way radio signals have been generated on the ground and transmitted 'uplink' through the large antennas of the NASA Deep Space Network. These transmissions are received by the spacecraft transponder, shifted in frequency, and then re-transmitted 'downlink' to the Earth where they are received either at the original site or at a second site, possibly located on another continent. Transponder design is such that the frequency of the downlink signal is coherently related to the received uplink frequency by a known integer ratio. Because the downlink signal frequency is derived precisely from that of the uplink, it is possible to measure changes in the radio path length by comparison of the received, downlink signal with the ground oscillator that generated the uplink signal originally. An increase in the radio path length decreases the phase of the received downlink signal relative to the ground oscillator, while a decrease in path length has the opposite effect. As hydrogen maser clocks are used for the fundamental frequency reference on the ground, measurement of the downlink phase provides an extremely precise method of determining changes in the round trip propagation time to the spacecraft. A one-hertz difference between the frequencies of the uplink and downlink signals means that the total radio path length is changing at the rate of one wavelength per second; larger or smaller frequency differences correspond to proportionally larger or smaller rates of path length change. Overall, the short term accuracy of the measurement procedure depends on the signal-to-noise ratio achieved and, ultimately, on the stability of the ground station oscillator over the round trip flight time of the radio signals to the spacecraft and back (Eshleman and Tyler 1975; Lipa and Tyler 1979).

On the ground, stations for communication over interplanetary distances are built around the large antennas of 20–100 m diameter. These stations are used primarily for uplink transmission of commands and downlink reception of spacecraft data (Yuen 1983). On spacecraft, however, typical antenna sizes are limited to only a few meters at most, and the transmitted downlink signal power ranges from about 1 to less that 100 W. As mentioned, hydrogen maser atomic clocks are used for the ground station frequency reference, while microwave frequencies in the 2 (S-band) and 8 (X-band) Gigahertz range, corresponding to 12–13 cm and 3–4 cm wavelengths, respectively, are used for the radio signals. Either band can be used separately or both used simultaneously. Use of dual frequencies is advantageous since this permits direct separation of the effects of neutral and ionized gases on the basis of differences in the media dispersive characteristics of the two media at the two frequencies.

Frequency changes as small as about 0.001 hertz can be measured, corresponding to a fractional accuracy in the range of a few parts in 10^{14} (Tyler et al. 1992). In the absence of other effects, this leads to an accuracy in the measurement of spacecraft velocity, for example, in the range of 30 micrometers/second when the 8 gigahertz band is used. Under the best conditions accuracies better than 10 micrometers/second have been achieved. Similar or better accuracies are anticipated for Mars Express. The use of a two-way, uplink/downlink radio path is suitable for study of gravity and for spacecraft navigation purposes. Because it relies on the reception by the spacecraft transponder of an uncorrupted uplink signal, in general the two-way technique can be used reliably only under free-space uplink propagation conditions (Tyler, 1987). The thin atmosphere of Mars introduces relatively little perturbation to the uplink, however. As a result, Mars Express occultation observations can be conducted during periods of occultation immersion when two-way tracking is established prior to the onset of atmospheric effects.

Occultation observations exhibit considerable signal dynamics, with simultaneous variations in signal frequency and amplitude, as well as the presence of near-forward scattering and diffraction when the radio path passes near a planet's surface. In the case of Mars diffraction from the planetary limb is observed on all occasions while near-forward scattering occurs in roughly 80 percent of occultation events.

Observed signals obtained from bistatic scattering experiments are characteristically broadened relative to the illuminating signal as a result of the combination of angular spreading of the waves by the scattering process and the relative motion of the spacecraft and ground station with respect to the planet's surface. Unlike occultation observations, much of the information regarding the surface properties is in the polarization and amplitude of the scattered signal; typically there is no coherent component in the scattered fields.

Thus, both occultation and bistatic scattering observations produce dynamic signals occupying a considerably greater bandwidth than the transmitted illuminating waveform. For this reason, the measurement of these signal characteristics requires capture of the time-sampled waveform at a sufficient sampling rate to avoid frequency aliasing effects. This is accomplished with open-loop receivers pre-programmed to track the expected spectral window. The dynamical characteristics of the occultation and scattered signals preclude reliable use of phase-locked loop techniques for reliable radio occultation measurements.

2.4 Applications to Mars

2.4.1 Atmosphere

Radio occultation studies of atmospheres can be understood in terms of 'geometric' or 'ray' optics refraction of signals traveling between spacecraft and ground stations. In a spatially varying medium wherein the wavelength is very short compared with the scale of variation in refractive index, the direction of propagation of an electromagnetic wave always curves in the direction of increasing refractivity. Consequently, in a spherically symmetric atmosphere with gas refractivity (which is proportional to density) constantly decreasing with height, the radio path remains in a plane and bends about the center of the system. The degree of bending depends on the strength of the refractivity variation. This simple model approximates a real atmosphere and is useful for understanding the basic phenomena of radio occultation. This is also true for ionosphere, with the exception that refractivity profiles are not monotonic with altitude in this case.

The geometry is illustrated in Figure 2.4-1, where the atmosphere is represented by the refractivity as a function of radius from the center, $\mu(\rho)$, and the bending can be described in terms of a bending angle, α, and a ray asymptote, a. The variation of the bending angle, ray asymptote, and refractivity are linked elegantly through an Abel transform relationship (Fjeldbo and Eshleman 1971); viz.,

$$\alpha(a) = -2a \int_{\rho=\rho_0}^{\rho=\infty} \frac{1}{\mu} \frac{\partial \mu}{\partial \rho} \frac{\partial \rho}{\left[(\mu r)^2 - a^2\right]^{1/2}} \tag{2-1}$$

where $\rho_0 = a/\mu(\rho_0)$, from Bouguer's Rule, is the ray periapse, and

$$\mu(\rho_{01}) = \exp\left\{-\frac{1}{\pi} \int_{a=a_1}^{a=\infty} \ln\left\{\frac{a}{a_1} + \left[\left(\frac{a}{a_1}\right)^2 - 1\right]^{1/2}\right\} \frac{d\alpha}{da} da\right\} \tag{2-2}$$

with $\rho_{01} = a_1/\mu(\rho_{01})$. In this last expression, a_1 represents the asymptotic miss distance for a ray whose radius of closest approach is ρ_{01}. Thus, for spherical atmospheres, if $\alpha(a)$ is known, then the corresponding refractivity profile can be found exactly. For non-spherical geometry alternative numerical solutions are available.

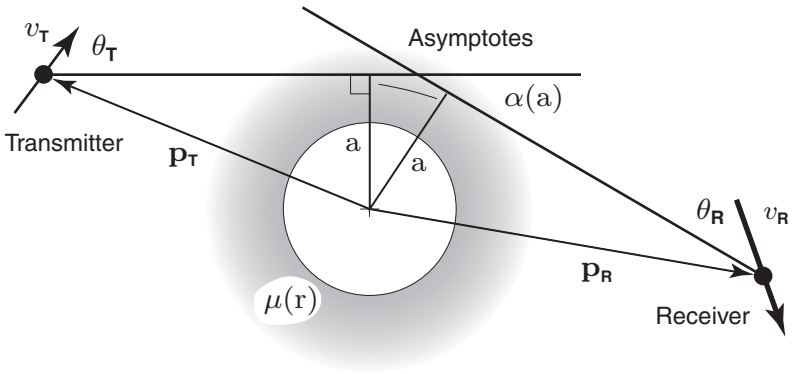

Figure 2.4-1: Occultation ray path geometry. Signals passing between spacecraft and Earth are refracted by a planetary atmosphere. Refraction angle is α. Position and velocity of spacecraft and Earth station are known from tracking data. Angles θ_T $\alpha\nu\delta$ θ_R can be found from the Doppler effect, leading to solution for α and a.

The bending angle and the ray asymptote can be determined accurately by radio occultation measurements to create an experimentally derived table of α versus a, or $\alpha(a)$. This is accomplished as follows: Referring again to Fig.1, the position and velocity of spacecraft with respect to the Earth tracking station and the planet's center can be found from tracking data during periods when the radio path is well-clear of the atmosphere. Given knowledge of the geometry, a measurement of the Doppler shift over the spacecraft-to-ground path is sufficient to find θ and a, from which α then can be determined. It was possible with Voyager to measure α to an accuracy of about 1 x 10^{-8} radians, and equal or better accuracy is expected for Mars Express; the impact parameter a is known typically to about 1 km, and will be known to about 100 m or better for Mars Express. These high levels of measurement accuracy in turn permit determination of an accurate refractivity profile $\mu(\rho)$, as outlined above.

In order to interpret the refractivity in terms of gas parameters, the pressure and temperature are calculated assuming hydrostatic equilibrium, for example, from

$$p(h) = \overline{m}\int_h^\infty g(h')n_t(h')dh' \tag{2-3}$$

and

$$T(h) = \frac{p(h)}{k_B n_t(h)} \tag{2-4}$$

where p and $T(h)$ are the pressure and temperature as a function of height h, respectively, g is gravity, k_B is Boltzmann's constant, $\overline{m}$ is the mean molecular mass, and n_t is the molecular number density. Formal use of these equations requires *a priori* knowledge of the atmospheric composition.

2.4.2 Surface

There are several current mysteries regarding surface processes on Mars that can be addressed by bistatic radar study of the centimeter scale surface morphology, the variation in surface electrical properties, and/or a combination of these characteristics (Simpson 1993). Three examples are (i) the characteristic surface

properties responsible for the virtual absence of backscatter from the 'Stealth' region of the planet (Muhleman et al. 1991), (ii) the nature of the disposition of the polar caps, and (iii) the spatial and time variation of the surficial layers of the surface. With regard to the stealth region, it is important to distinguish between physical mechanisms that reduce the backscatter as a result of re-direction of the incident energy away from the source and those that reduce the backscatter by absorption of the incident energy. This can be determined by observing the oblique scatter to determine the presence or absence of scattered energy in directions other than backscatter; a strong specular lobe would be one possibility. The result will strongly affect the geophysical interpretation and assessment of the stealth region. Second, the physical properties of the polar caps are largely unknown. As examples: Are the frost/ice deposits conformal with the underlying surface or somehow incorporated into the pore spaces? What is the extent of significant frost in winter? Is there a sensible difference between the physical properties of the core deposits and the seasonal deposits? Finally, can changes in the mid-latitude and tropical regions with season or transient events be detected with centimeter-scale radiation?

While such questions also can be addressed by other instruments, only the use of radio wave scattering provides strong coupling to physical structures of centimeter-size scales. As a result, bistatic radar provides an unique tool for study of the Martian surface. The geometry is illustrated in Figure 2.4-2.

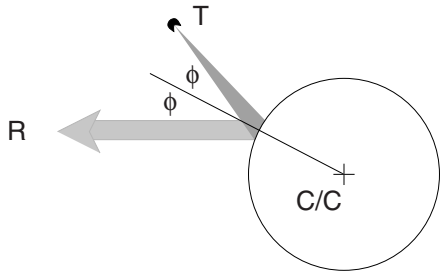

Figure 2.4-2: Bistatic Radar Scattering Geometry. Radio transmissions from an orbiting spacecraft at T are directed towards the surface of Mars. In the experiment shown, the antenna direction is maneuvered so that the location on the surface is such that the angles of incidence and reflection are the same, as indicated. This choice results in a scanning action as the spacecraft source at T moves. An alternative choice is to direct the incident illumination towards a fixed location on the surface so that the angle of incidence is constantly changing, although the angle of reflection and the direction to the receiver on Earth is fixed for short periods of time (minutes). Scanning the surface at the angle of specular reflection (first choice) produces comparative data of areas along the track scanned with a geometry that allows separation of surface electrical properties and gross morphology. Fixed point observations allow observation of the scattering pattern over a range of incident geometries. "C/C" refers to the location of the center of curvature of Mars' surface in the illuminated region.

2.4.3 Gravity

The gravity field of a planet is the result of its mass and depends in detail on the manner in which the mass is distributed. Rapidly rotating planets bulge at the equator as a result of centrifugal forces, for example. Consequently, the associated redistribution of mass to the equatorial plane results in a stronger gravitational acceleration of a spacecraft when it is near the pole than when it is at the same altitude located over the equator. Similarly, variations in the internal distribution of mass, or mass density, are expressed as departures of the external gravitational field from that of a uniform sphere or a stratified spherical distribution. In response to these irregularities in the gravity field, space probes in the vicinity of planetary bodies follow trajectories that differ significantly from the ideal orbits described by Kepler's laws.

Precision two-way radio tracking provides an accurate measurement of spacecraft velocity along the line-of-sight to the tracking station; changes in the line-of-sight velocity can be related to the corresponding gravitational acceleration, thus sensing the mass of a planet or satellite. The utility of the data for study of mass variations is dependent upon the sensitivity of the radio system, the details of the geometry, and the characteristics of the overall spacecraft trajectory. The method is capable of detecting surprisingly small effects - current sensitivities correspond to accelerations of the order of 10^{-6} g, or one-millionth that of Earth's surface gravity. Such data, through the connection between mass and gravitational force, are used to study planetary interiors. From low altitudes, even relatively minor variations in the mass density of surface and near surface features are detectable. For example, a reduction in density of about 0.3 g/cm^3 (or about a 10 percent change in the average Martian crustal density) of a cube of rock 50 km on a side and near the surface is readily measurable.

Combining data from a large number of orbits from the Mariner, Viking, and Mars Global Surveyor missions has allowed construction of a complete gravity map; a current version is shown in Figure 2.4-3. The resolution elements of this map each represent about 2 degrees of arc on the Martian surface. Large scale variations in the strength of gravity correspond to the overall distribution of mass, mostly in the deep interior of Mars, and are relevant to the interpretation of the early history and evolution of the planet. Smaller scale variations, on lateral distances of a few thousand km or less, correspond to mass variations relatively close to the surface. Both large- and small-scale variations must be interpreted in light of the known overall shape of the planet and the variations in the surface elevation since, as in the examples above, topographic variations and variations in mass density can play a similar role in the raw gravity data. Mars Express, as a result of its low periapsis altitude, can improve the present maps by a factor of about 2:1 in linear resolution in areas scanned by the evolution of the orbit.

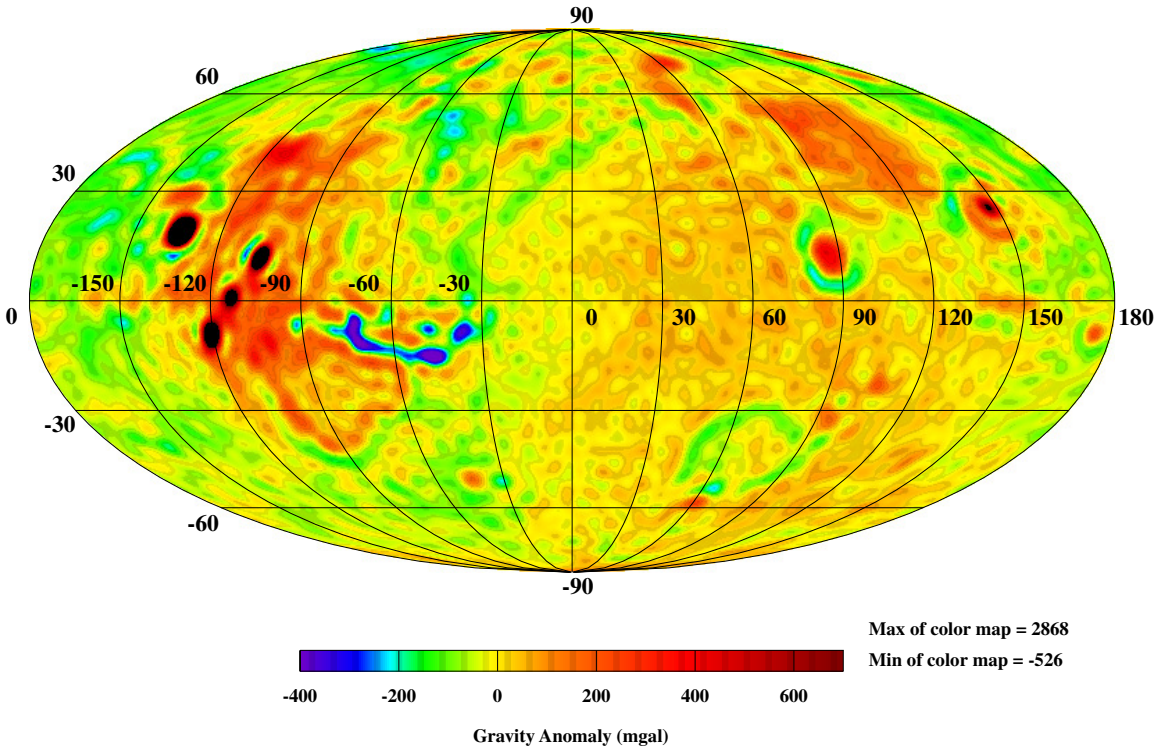

Figure 2.4-3: Gravity Field of Mars. Figure depicts Mars "free-air" gravity anomalies derived from Viking Orbiter 1 & 2, Mariner 9, and Mars Global Surveyor tracking data. The gravity model is a spherical harmonic representation complete to degree and order 75, with horizontal resolution in the range 300–400 km at the surface of Mars. The map shown is a Mollweide projection. The regions of highest elevation on Mars, Tharsis and Olympus Mons volcanoes, show up as very strong positive gravity anomalies. Other weaker, but still prominent positives lie over the Elysium volcanic region, the large Alba volcanic structure, and in the Isidis and Utopia impact basins. The strongest negative anomaly lies over the deep central Vallis Marineris canyons (Tyler et al. 2000).

Page left free

3 Mission Characteristics

3.1 Mission Objectives of the Mars Express Orbiter Radio Science Experiment (MaRS)

3.1.1 Introduction and Overview

As part of the Mars Express Orbiter payload, the Mars Express Orbiter Radio Science experiment (MaRS) will perform the following experiments:

(a) radio sounding of the neutral Martian atmosphere (occultation experiment) to derive vertical density, pressure and temperature profiles as a function of height (height resolution better than 100 meters),
(b) radio sounding of the ionosphere (occultation experiment) to derive vertical ionospheric electron density profiles and to derive a description of the global behavior of the Martian ionosphere through its diurnal and seasonal variations depending also on solar wind conditions,
(c) determination of dielectric and scattering properties of the Martian surface in specific target areas by a bistatic radar experiment,
(d) determination of gravity anomalies in conjunction with simultaneous observations using the camera HRSC as a base for three dimensional (3D) topography for the investigation of the structure and evolution of the Martian crust and lithosphere,
(e) precise determination of the mass of the moon Phobos
(f) radio sounding of the solar corona during the superior conjunction of the planet Mars with the Sun.

The radio links of the spacecraft TT&C subsystem between the orbiter and the Earth will be used for these investigations. A simultaneous and coherent dual-frequency downlink at X-band and S-band via the High Gain Antenna (HGA) is required to separate the contributions from the classical Doppler shift and the dispersive media effects caused by the motion of the spacecraft with respect to the Earth and the propagation of the signals through the dispersive media, respectively.

The experiment relies on the observation of the phase, amplitude, polarisation and propagation times of radio signals transmitted from the spacecraft and received at ground station antennas on Earth. The radio signals are affected by the medium through which the signals propagate (atmospheres, ionospheres, interplanetary medium, solar corona), by the gravitational influence of the planet on the spacecraft and finally by the performance of the various systems involved both on the spacecraft and on ground.

3.1.2 Radio Sounding of the Neutral Atmosphere and Ionosphere

3.1.2.1 Scientific Objectives

The sounding of the Martian atmosphere by radio occultation will contribute to the understanding of the structure of the Martian atmosphere, its circulation and dynamics through the Martian day and seasons. Vertical profiles of density, pressure and temperature with a height resolution better than 100 meters can be derived.

The Martian atmosphere is composed primarily of carbon dioxide with small amounts of molecular nitrogen and argon. The atmospheric surface pressure and temperature is approximately 6 mbar and 220 K and varies largely with time of day, season and topography (Hess et al., 1977). Observations of the vertical structure below 30 km altitude have been made by several spacecraft during occultation. In situ measurements of three atmospheric profiles during the descent of the two Viking landers and Pathfinder are available below 200 km altitude. Local heating of the atmosphere by dust contained in the atmosphere is clearly visible in many occultation temperature profiles.

Radio occultation provides also a measure of the vertical structure of the ionosphere. The fact that the S-band downlink is more sensitive to ionospheric plasma by a factor of $(11/3)^2$ than X-band will provide an averaged large-scale electron density profile as a function of height and planetary latitude with each occultation. Combined with the other information about the ionosphere, it is the goal of the experiment to describe the global behaviour of the Martian ionosphere through the Martian day and seasons including the dependence on the effects of the magnetic field, solar activity and solar wind interaction.

Photochemical processes control the behaviour of the main ionospheric layer of Mars in a manner similar to the terrestrial F layer (Barth et al., 1992). The electron density distribution of a weakly magnetized body like Mars is controlled by solar radiation and the solar wind interaction with the planet. The majority of ionospheric density profiles have gained by occultation experiments of US and Soviet Mars missions. A typical value of the daytime ionospheric peak density is 10^5 el/cm^3 at an altitude of 110 km to 135 km.

The only in situ measurements were provided by the two Viking Landers (Hanson et al., 1977). The dominant ion in the ionosphere was found to be O_2^+ resulting from two ion molecule reactions between $CO_2^+ + O$ and $O^+ + CO_2$, the latter ions were produced by photoionisation. The Martian ionosphere is a Chapman-type layer only to a first order. Some of the ionospheric profiles can be well approximated by a Chapman layer model, however the majority of the available profiles show important departures from the Chapman theory and can only be described by Chapman's theory at a very narrow range about the peak height (Breus et al., 1997). The solar zenith angle dependence and the solar cycle dependence of the peak electron density was found to be different from that expected for Chapman's theory but are very similar to that of Venus (Bauer & Hantsch, 1989).

Recent observations by Mars Global Surveyor (MGS) revealed highly variable and localized magnetic fields. Strong fields at the spacecraft orbit below the ionosphere were observed locally. At other locations, much weaker magnetic fields were found. Therefore, the possibility of a sufficiently strong global magnetic field which participates in the solar wind interaction may no longer be supported. However, only a narrow latitude range was covered by MGS observations at low pericenter altitude during aerobraking. MGS will probably not solve the question of a global magnetic field.

On the other hand, the radio occultation data from Mariner 9 and Viking (Kliore, 1992) indicate the presence of a global magnetic field caused by the ionosphere. With its better resolution (about 100 el/cm^3), Mars Express might answer the question wether there is a global ionosphere supported magnetic field. The height of the ionopause is also not well defined at Mars. At Venus, the ionopause has been defined as that altitude where the electron density falls below 500 el/ cm^3

(Kliore and Luhmann, 1991) while the electron density in the Martian profiles never drops below that limit. Mars Express also has to solve the question of which physical processes define the altitude of the ionopause.

Mars Express occultation egress will always be at nighttime with the opportunity to investigate the nightside ionosphere. Viking could only resolve a nighttime ionosphere in 40% of the measurements which showed also a high variability in shape, peak density and height. The anticipated accuracy of Mars Express will help to solve the question if the nighttime ionosphere is maintained by horizontal transport from the dayside or by impact ionization due to electron precipitation from the tail which should give insights into the direction of the magnetic field on the nightside.

3.1.2.2 Observational Method and anticipated results

3.1.2.2.1 Neutral Atmosphere

Before the spacecraft enters and after the spacecraft exists occultation as seen from the Earth, the radio ray slices through the layers of the ionosphere and neutral atmosphere. The TT&C system operates in the two-way mode which means that the downlink frequencies are derived from the received uplink frequency. Changes in the received radio frequency at a level of 10^{-13} correspond to a change in the angle of refraction of the radio rays by the order of 10^{-8} radians (Tyler, 1987).

The separation of the effects of the ionosphere and the neutral atmosphere on the radio link is feasible by using a dual-frequency downlink and because of fact that the peak height of the ionosphere and the sensible neutral atmosphere are well separated in height.

Atmospheric occultation experiments can be understood in terms of geometric ray optics refraction. Assuming a spherically symmetric atmosphere with gas refractivity decreasing with height, the direction of propagation of an electromagnetic wave bends in the direction of increasing refractivity (Figure 3.1-1). The frequency of the radio signal experiences a Doppler shift (or phase shift) due to the relative motion of transmitter (spacecraft) and receiver on Earth (classical Doppler shift). Because the ray path is deflected or bent by an angle α, this Doppler shift differs from what would have been expected if no atmosphere were present. The bending angle α and the impact parameter ρ_0 (closest approach of the ray path to the planet) are then determined as a function of time from the Doppler shift using precise orbit positions and velocities of the spacecraft relative to Mars.

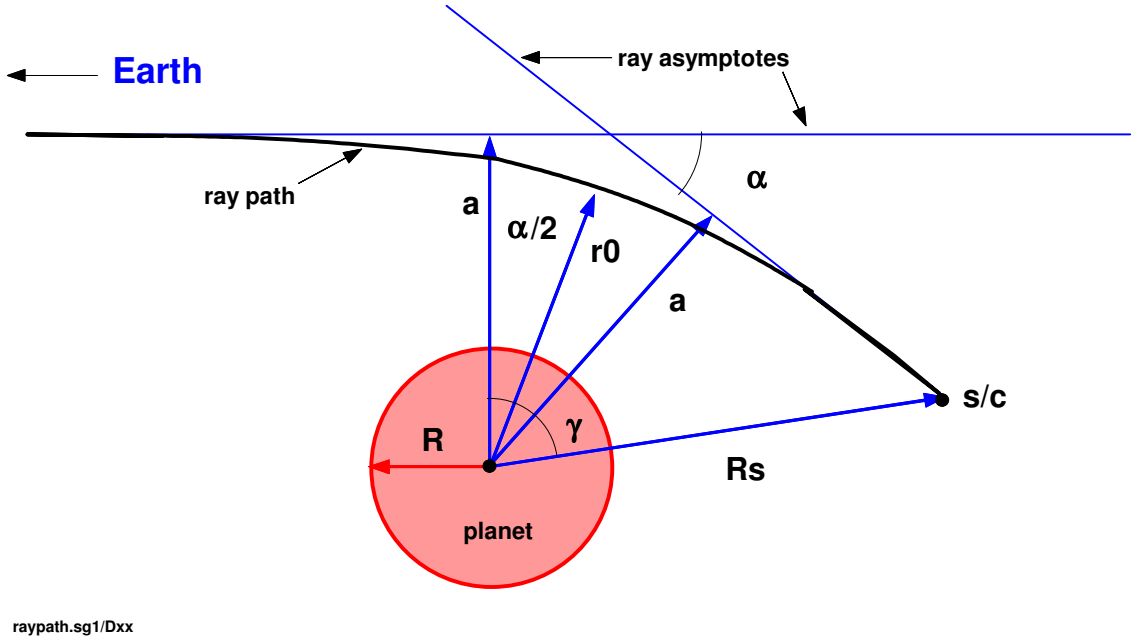

Figure 3.1-1: Radio ray path geometry (idealized and exaggerated) of an occultation experiment. The closest approach of the ray path to the planet is ρ_0, the impact parameter.The ray asymptotes are *a.* Refractive bending of the ray induces a deflection of the ray asymptotes by an angle α.

The atmosphere is sensible at microwaves below an altitude of 30 km. Mars Express would be able to improve this altitude to 50 km due to the high signal-to-noise ratio at X-band (RF power 60 Watts). The effective vertical resolution through use of the Abel transform is determined by the first Fresnel zone radius $(\lambda D)^{1/2}$ which translates to 300 m for X-band and 600 m for S-band radio waves, respectively, (D is the distance from the spacecraft to the closest approach of the ray path to the planet). This resolution is far superior to what can be achieved by other sounding instruments which are limited to typically one atmospheric scale height (order of kilometers).

Marouf et al. (1986) developed a procedure to improve the resolution beyond the natural diffraction limit and applied this procedure to data obtained during the occultation of the Voyager radio signals by Saturns rings. Gresh et al. (1989) applied this procedure to occultation data from the rings of Uranus. This resulted in a resolution of 100 m, about one order of magnitude improvement from the Fresnel diffraction limit. That same technique resulted also in the first direct determination of Triton's surface pressure (Tyler et al., 1989). Karayek & Hinson (1997) applied a similar technique to atmospheres denser than Triton's and succeeded in a resolution of about 40 m for simulated Martian conditions. These works suggest that it is feasible to derive vertical profiles in the Martian atmosphere with a height resolution better than 100 m.

Dust and haze in the atmosphere will not pose a problem to the propagation of the radio carrier waves. However, local heating of the atmosphere by the entrained dust can be revealed from the derived temperature profile. Figure 3.1-2 shows the comparison of a temperature profile derived from a clear atmosphere and a temperature profile which was derived when the locality was engulfed by a major dust storm (Lindal et al., 1979).

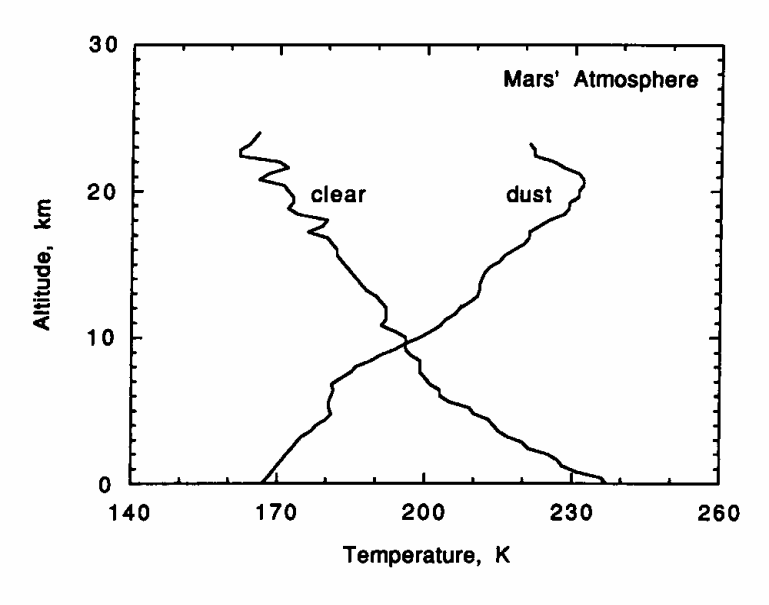

Figure 3.1-2: Temperature profiles derived from Viking occultations for varying dust content in the atmosphere. The profile labeled “dust” was derived from data obtained during the global dust storm of 1977. (Figure taken from Tyler et al., 1992; data were first published by Lindal et al., 1979).

3.1.2.2.2 Ionosphere

Separation of the effects of the ionosphere and the neutral atmosphere on the radio link is feasible by using a dual-frequency downlink and the fact that the peak height of the ionosphere and the sensible neutral atmosphere are well separated in height. This is illustrated in Figure 3.1-3, which shows the refractivity profile derived from Mariner 4 occultation data (profile 6) as a function of height. Negative refractivity represents the ionosphere and is proportional to the electron number density, positive refractivity represents the neutral atmosphere which is linearly related to the mass density of the atmospheric constituents (Fjeldbo & Eshleman, 1968). The refractivity N of free electrons is given by

$$N = -40.31 \cdot 10^6 \, N_e / f^2$$

which allows conversion of refractivity into electron number densities (N_e is the electron density, f is the radio carrier frequency).

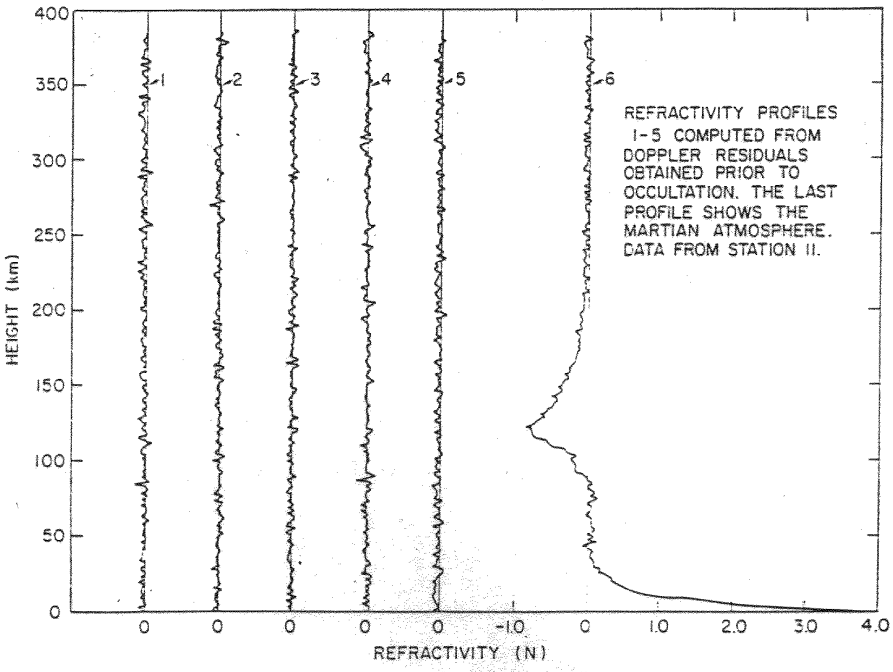

FIG. 4. REFRACTIVITY PROFILES OBTAINED FROM INVERSION OF IMMERSION DOPPLER RESIDUALS.

Figure 3.1-3: Refractivity profiles obtained from the Mariner 4 occultation. The profiles 1 - 5 were taken prior to the occultation and present the zero level after biases and trends due to effects not connected to the Martian atmosphere were removed. Profile 6 shows the refractivity of the Martian atmosphere probed during entry into occultation. Negative refractivity represents the ionosphere, positive the neutral atmosphere (taken from Fjeldbo & Eshleman, 1968).

It is possible to retrieve refractivity profiles separately for the radio carrier frequencies at S-band and X-band. S-band is expected to be more sensitive to the negative refractivity by a factor $(11/3)^2$ compared to X-band while the positive refractivity is essentially independent of the frequency. Given past experiences, X-band results will be limited to the altitude of the ionospheric peak density and peak number density (Tyler et al., 1992) while S-band will yield the entire ionospheric profile from approximately 200 km height down to 90 km. Under favorable conditions it will be possible to investigate the solar wind - magnetic anomalies - ionospheric interaction region.

Computing the differential Doppler from the received S-band and X-band residual Doppler shifts yields the dispersive media effects (electron content) of all ionized media (Martian ionosphere, interplanetary medium, Earth ionosphere) along the path and can be used for calibration, inversion and correction of the classical Doppler shift. The radio ray path spacecraft-Earth will cross through the sensible ionosphere very fast (in the order of minutes) before entering or after exiting occultation. The variation in the Earth ionosphere and the interplanetary medium is assumed to be slow for similar time scales, therefore the observed change in electron content is assumed to be due to and dominated by the Martian ionosphere.

3.1.2.3 Observational strategy

For this kind of observation the radio signals of Mars Express will be analyzed before the spacecraft enters the occultation of the planet as seen from Earth. The HGA will be pointed toward Earth and the spacecraft will operate in the two-way mode.

According to the Mars Express orbit analysis, Earth occultations will occur in distinct seasons. The occultation entry and exits will cover all planetary latitudes of the northern and southern hemisphere.

Occultations will also occur at or close to the pericenter when the instruments are nominally supposed to observe the Martian surface in nadir direction. In this case the HGA will most probably not point toward the Earth. To allow the performance of atmospheric sounding prior and after occultation it is required that radio occultation observations have operational priority.

3.1.3 Determination of the Dielectric Properties of the Surface (Bistatic Radar)

3.1.3.1 Scientific Objectives

The bistatic radar configuration is distinguished from the monostatic by spatial separation of the transmitter (the spacecraft) and the receiver (ground station on Earth). It is a powerful tool in providing information about surface texture (roughness and slope) at scales of the wavelength (in the order cm to meter). Bistatic radar may also be used to determine properties of the surface material, such as dielectric constant, through differential reflection of orthogonal polarizations. The bistatic radar geometry of an orbiting spacecraft is well suited to probing the surface of planets at a variety of latitude, longitude and incidence angles. Bistatic radar experiments have been conducted at the Moon (e.g. Tyler & Howard, 1973; Nozette et al., 1996), Mars (Simpson & Tyler, 1981; Simpson et al., 1984) and Venus (Pettengill et al., 1997; Kolosov et al., 1979).

The objectives of this experiment are focused on the polar regions and caps, the volcanic regions and the famous “Stealth” area west of Tharsis (Muhleman et al., 1991; Edgett et al., 1997). The bistatic geometry is well-suited to probing icy surfaces, which are poorly understood on Mars. The fact that the south residual polar cap on Mars has anomalously high backscatter when viewed from Earth while the northern cap (presumably much more massive) does not stand out is a continuing mystery. The Stealth region, west of Tharsis, is anomalous in the opposite sense; it yields very weak backscatter when probed from Earth. In both cases, the unique geometry of a bistatic experiment offers some hope for better understanding of both the scattering processes and also the underlying surface geology. Selected targets in other areas, such as volcanic plains, will also be studied; despite similar appearance in orbital images, plains do not necessarily have the same radar behavior - again suggesting differences in the underlying surface geology.

3.1.3.2 Method and anticipated results

For a typical downlink bistatic radar experiment the radio signal is transmitted from the spacecraft High Gain Antenna toward the surface and is scattered from the surface. That part of the signal power which is reflected toward Earth is received at the ground station. Optimizing performance of these bistatic radar experiments requires accurate prediction of the orbiter trajectory for the formulation of antenna pointing strategies and prediction of signal parameters such as Doppler shift and

signal amplitude. In a quasi-specular experiment the antenna is then programmed to follow a locus of points for which surface reflection would be specular if Mars were smooth. From the data recorded along these specular point paths, surface roughness can be inferred from Doppler dispersion of the echo signal; the dielectric constant ε of the surface material can be inferred from echo amplitude and/or polarization properties. Dielectric properties of a lunar basin were obtained by measuring the Brewster angle $\tan^2\Phi_B = \varepsilon$ (Tyler, 1968); a Stokes parameter analysis led to detection of a tellurium-like material in Venus highlands (Pettengill et al., 1996).

In a bistatic backscatter experiment, the spacecraft antenna is aimed exactly opposite to the Earth direction, a configuration which is often much easier to implement than dynamically tracking either moving or fixed points. As the antenna beam illuminates regions on the surface, coherent backscatter enhancements will cause ice-covered areas to appear extremely bright. Repeated tracks over the polar region can be used to define the boundaries of icy polar deposits or to monitor their changes as a function of time. The spatial resolution of the measurements is approximately equal to the projection of the HGA beam on the surface. Coherent backscatter enhancements can be sought in the echo amplitude and polarization (Hapke, 1990). Clementine spotlight data suggest the presence of water ice near the lunar South Pole (Nozette et al., 1996).

The radio echo signal is received in the open-loop mode (see below) in two orthogonal polarizations (e.g., LCP, or Left Circular Polarization, and RCP, or Right Circular Polarization), down-converted, sampled, and stored for further processing at home institutions. Figure 3.1-4 shows a typical frequency spectrum of the received radio signal. The direct signal, leaking out from the side lobes of the HGA and which is reduced accordingly in power, is on the right. The echo signal is on the left. It is Doppler shifted relative to the direct signal according to the change in spacecraft-to-surface-to-Earth distance as a function of time; it is broadened according to the roughness of the surface and the motion of the specular point over the surface (Simpson, 1993).

3.1.3.3 Observational strategy

It is required that the High Gain Antenna be pointed toward the surface of Mars. To ensure the maximum signal-to-noise ratio in the echo signal received at Earth, the transmission of the unmodulated X-band carrier at the highest feasible power level is also required. Transmission of linear (or elliptical) polarization has advantages in detecting differential quasi-specular polarization reflections from volcanic plains, while circular (or elliptical) polarization is preferred for spotlight observations of ice deposits.

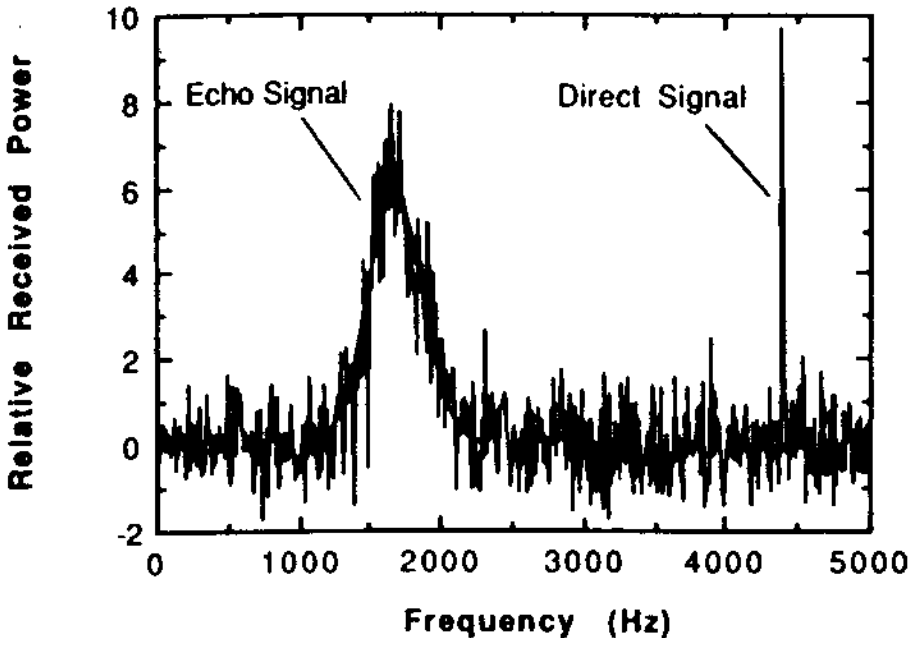

Figure 3.1-4: Typical bistatic radar spectrum showing the separation of the the echo signal from the direct signal leaking out from the HGA side lobes toward the receiver. The broadening of the echo signal is caused by the motion of the specular point over the surface and is proportional to surface roughness (taken from Simpson (1993)).

3.1.4 Gravity Anomalies

3.1.4.1 Scientific Objectives

Two gravity field models of degree and order 50 were derived from radio tracking data of the Viking and Mariner 9 missions (Smith et al., 1993; Konopliv & Sjogren, 1995). The same teams collaborated on derivation of gravity field models of degree and order 60 and higher using the Mars Global Surveyor tracking data (Tyler et al., 2000).

The highly eccentric orbit of Mars Express about the planet is not best suited for a global investigation of the gravity field. The investigation proposed here will focus on specific target areas for the determination of local gravity anomalies. Simultaneous observations of the stereo camera experiment (HRSC) and the radar in the altimeter mode will yield the high resolution three dimensional (3D) topography of the target area. The goal is to combine these data sets (radio science, camera, radar) to study the state and evolution of the Martian crust and lithosphere which yields implications for the tectonic evolution of Mars.

The targets of investigations are the hot spot areas Tharsis and Elysium, large single volcanoes, impact basins and large impact craters, and the highland-lowland boundary. The investigation of impact basins must be seen in the context of similar studies on other planetary bodies including the Earth in the sense of comparative planetology and of studying the impact mechanism which is not fully understood. Studies of the highland-lowland boundary shall contribute to the open question of this dichotomy.

3.1.4.2 Method and anticipated results

Topographic data will provide digital topographic models (DTMs) which in combination with the gravity data are the base for crustal density models. Gravity modelling is demonstrated in Figure 3.1-5 showing a profile across the Tharsis bulge (Janle and Erkul, 1991). The measured line-of-sight (LOS) - freeair anomaly at spacecraft altitudes amounts up to 70 mGal. A complete density model consists of a topographic model (DTM) and a density model of the subsurface structures (e.g. undulations of the crust/mantle boundary, mantle plume). The gravity attraction of the model DTM yields up to 500 mGal which underlines the importance of precise and high resolution topographic data. DTMs are also necessary for bending-stress models of the lithosphere. A schematic of such model is shown in Figure 3.1-6 at the hand of Olympus Mons (Janle and Jannsen, 1986).

The MOLA laser altimeter experiment of MGS provides topographic profiles with a vertical resolution of 10-30 m with along track data points every 300 m and footprints of the shot points of 160 m diameter. The cross distance of the tracks is up to 1.6 km. This allows rather rough DTMs, still sufficient for gravity modelling. More precise DTMs are required for the lithospheric load of bending-stress models in particular for the correlation of the lineament distribution with the topography and calculated stresses. The combination of radar altimeter data and stereo images from the HRSC camera will provide DTMs with a vertical resolution of 12-18 m and a ground resolution of 20-30 m which are perfectly suitable for bending stress models and geologic interpretations of the lineament distribution. Figure 3.1-5 shows a density profile across the Tharsis bulge which demonstrates that such modelling

provides information about the crustal state, i.e. the location of the crust/mantle boundary, the state of isostasy of large volcanoes, and the existence of mantle plumes. The combination of DTMs and gravity models is the base for lithospheric bending-stress models which provides information about the state of the lithosphere (Janle and Jannsen, 1986; van Wees and Cloething, 1994). The example for Olympus Mons in Figure 3.1-6 shows that the topographic load causes a bending of the lithosphere which leads to a crustal thickening below the volcano (Airy root). Because of elastic forces, the isostatic compensation of the topography is achieved partially only (here 54%). The resulting density distribution is consistent with the gravity. The inclusion of the lineament system, which is determined by the stress system from high resolution images is a further boundary condition for the stress calculations, i.e. maximum stresses in Figure 3.1-5 should correlate with the occurrence of lineaments (until now, no such correlation has been found for Olympus Mons which is a paradoxon!). The topographic profile in Figure 3.1-5 leads to the following observations: the load is surrounded by a depression followed by an outer bulge. This has been observed around volcanic islands of hot spots on Earth. Thus the accurate location of topographic features gives a further boundary condition for bending-stress models.

The anticipated accuracy of an X/X-band two-way radio link is in the order of <0.1 mm/s. This translates into an accuracy of gravity accelerations in the order of several mgal depending on the size and extension of the local topographic features (Tyler et al., 1992). For comparison, Viking observations of line-of-sight gravity accelerations over the Tharsis area yielded amplitudes of 50 mgal (Janle & Erkul, 1990).

3.1.4.3 Observational strategy

Gravity information can be obtained at all times when the spacecraft is using the two-way dual-frequency radio link and the spacecraft is close enough to the surface that gravity accelerations significantly affect the spacecraft velocity (pericenter passes). The Earth pointing of the HGA is required to maintain a continuous radio link. The coherent and simultaneous dual-frequency downlink allows extraction of the dispersive effects on the downlink due to the interplanetary medium and the earth ionosphere. Doppler tracking data will be acquired at a rate of one sample per 10 seconds (TBC) and ranging data will be collected at a rate of one point per 10 minutes (TBC).

Velocity contributions induced by attitude control movements of the spacecraft which result in a HGA motion relative to the line-of-sight to Earth may reach several mm/s. Therefore, thruster activities and attitude control commands have to be recorded in order to reconstruct the attitude motion for later correction of derived LOS gravity accelerations.

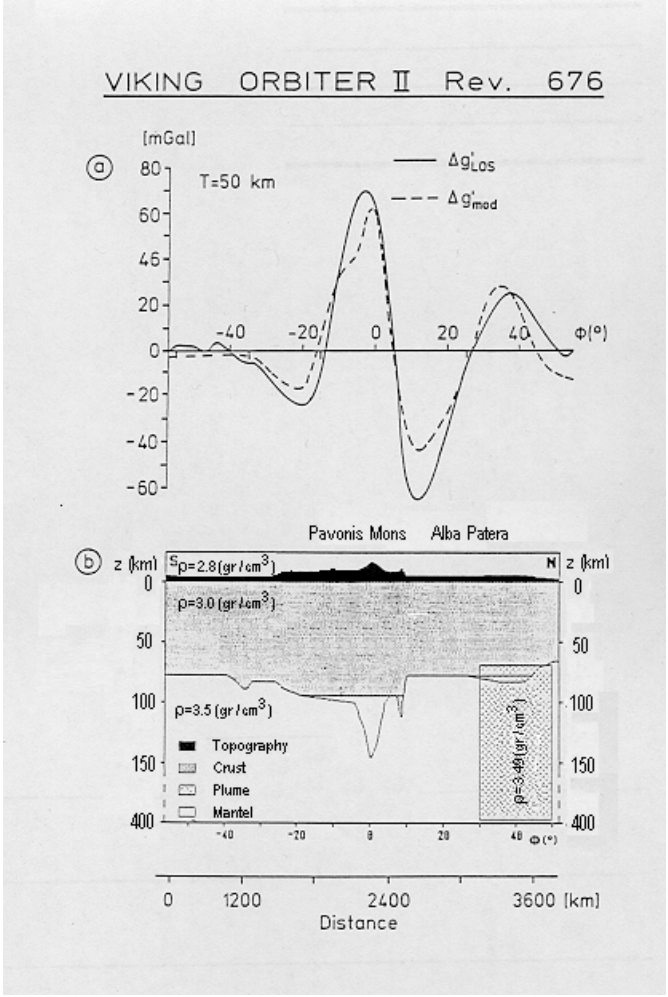

Figure 3.1-5: Pavonis Mons - Alba Patera: Viking Orbiter 2 Rev. 676 .(a) LOS gravity anomalies: Delta g'LOS=LOS-free air anomaly, $\Delta g'_{mod}$=LOS-model gravity of topographic masses and density model below; (b) topography and density depth model with a mean crustal thickness of T=50km. The lower boundary of the dotted area shows the crust/mantle boundary calculated from the topography. Note low density plume below Alba Patera (Janle and Erkul, 1991).

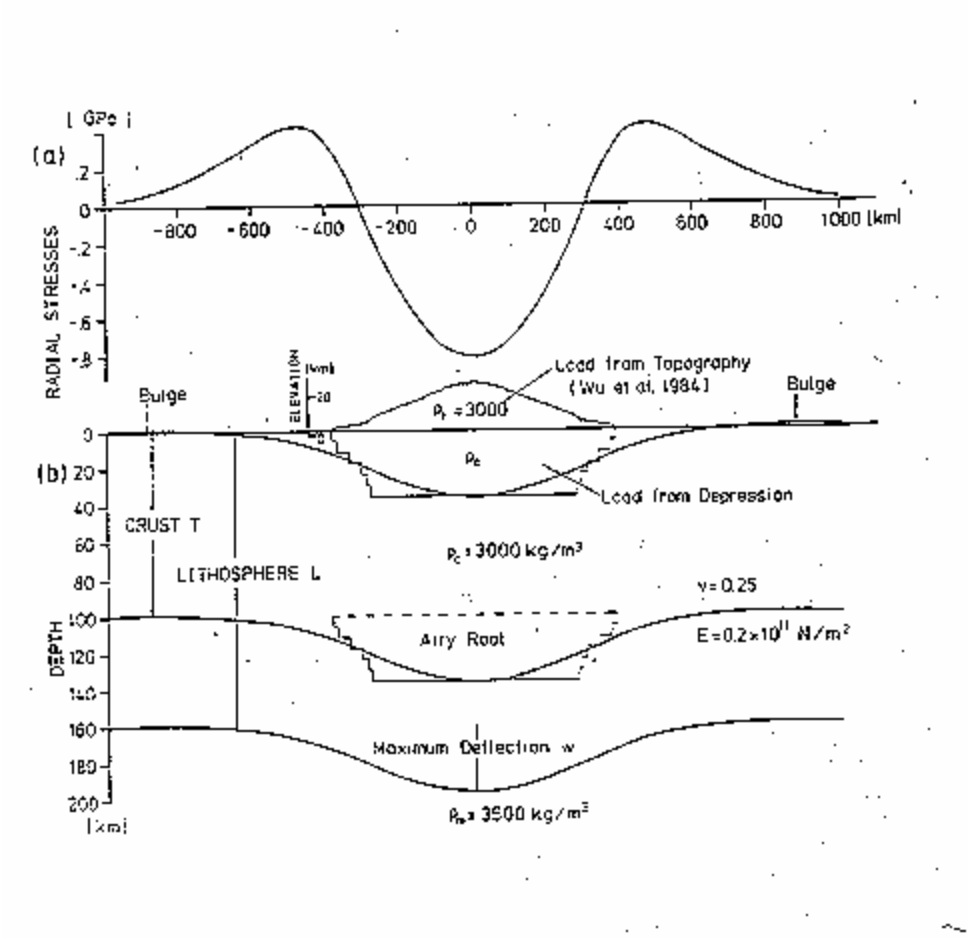

Figure 3.1-6: Example of elastic bending models of the lithosphere with T=100 km (54% compensation) and L=160 km. (a) radial stresses σ_{rr} at the surface, (b) bending model (Janle and Erkul, 1991).

3.1.5 The mass of Phobos

3.1.5.1 Scientific Objectives

The objective is the precise determination of the mass of the moon Phobos and if proven to be feasible also of the low degree spherical harmonics of its gravity field. From the camera observations the shape and volume may be determined and the bulk density of the moon may be derived.

3.1.5.2 Method and anticipated results

The method of close encounter with small bodies is well established. The gravity attraction of the moon Phobos will slightly disturb the trajectory of Mars Express. The difference between predicted trajectory (without Phobos) and the actually observed trajectory will lead to the determination of the attraction forces onto the spacecraft and eventually the GM of the moon.

The spacecraft is operating in the two-way mode TWOD with X-band uplink.

3.1.5.3 Observational strategy

The observations shall be performed each time the spacecraft encounters the moon at closest approach distances of less than 500 km. Because the radius of the moon´s orbit is slightly coinciding with the apocentrums distance of Mars Express, the spacecraft will encounter the moon always at the apocenter point. The times and orbits of these encounters are still TBD.

3.1.6 Radio Sounding of the Solar Corona

3.1.6.1 Scientific Objectives

The planet Mars will move into superior conjunction with the Sun in the fall of 2004 and 2006. Within 10 deg (Figure 3.1-7), the dispersive effects on the radio signals (propagation time, Doppler shift and Doppler noise) are dominated by the solar corona and no reliable results can be gained about the Martian atmosphere and gravity field. It is therefore proposed to use this valuable time for a thorough investigation of the solar corona to derive electron density profiles in the structured corona, solar wind speed, turbulence spectra in the source regions of fast and slow solar wind streams from coronal holes and streamers, respectively, and to detect, identify and describe the spatial and temporal evolution of the shockfronts of coronal mass ejection (Bird et al., 1994; Pätzold et al., 1995; Pätzold et al., 1996; Pätzold et al., 1997; Karl et al., 1997). It is highly desirable to carry out these observations simultaneously with SOHO, if SOHO is still operational in 2004 or other solar space observatories to enhance and compare the observations.

3.1.6.2 Method and anticipated results

The technique of solar corona sounding is well established and has been performed by members of this team during the superior solar conjunctions of the Ulysses (1991, 1995), Magellan (1992), Voyager and Viking spacecraft (Bird et al., 1992; results Bird et al., 1994; Bird et al., 1996; Pätzold et al., 1995; 1996; 1997; Tyler et al., 1977). A two-way radio link and a dual-frequency downlink at S-band and X-band will be used to separate the coronal dispersive effects from the classical Doppler shifts. This two-way link is a powerful tool for the derivation of electron density models from observed electron content when propagation time delay data (ranging) and dispersive Doppler shifts are compared (Pätzold et al., 1997). Furthermore, it is the basis for the derivation of solar wind speed by correlating uplink and downlink signals (Wohlmuth et al., 1997) and a detector for fast outward propagating density enhancement originating from solar events.

3.1.6.3 Observational strategy

The superior solar conjunctions of Mars will occur in mid September 2004 and late October 2006 over the North Pole of the Sun in the plane of sky at an apparent distance to the solar disk of less than three solar radii. It should be emphasized here that the dispersive contributions of the solar corona on the radio link will dominate the classical and dispersive contributions from the Martian gravity field and atmosphere, respectively. The interesting regions for the sounding of the solar corona are within 10 deg elongation on both sides of the solar disk (40 solar radii) in the time frame from mid August to mid October 2004 (Figure 3.1-7) and from September to late November 2006 (Figure 3.1-8).

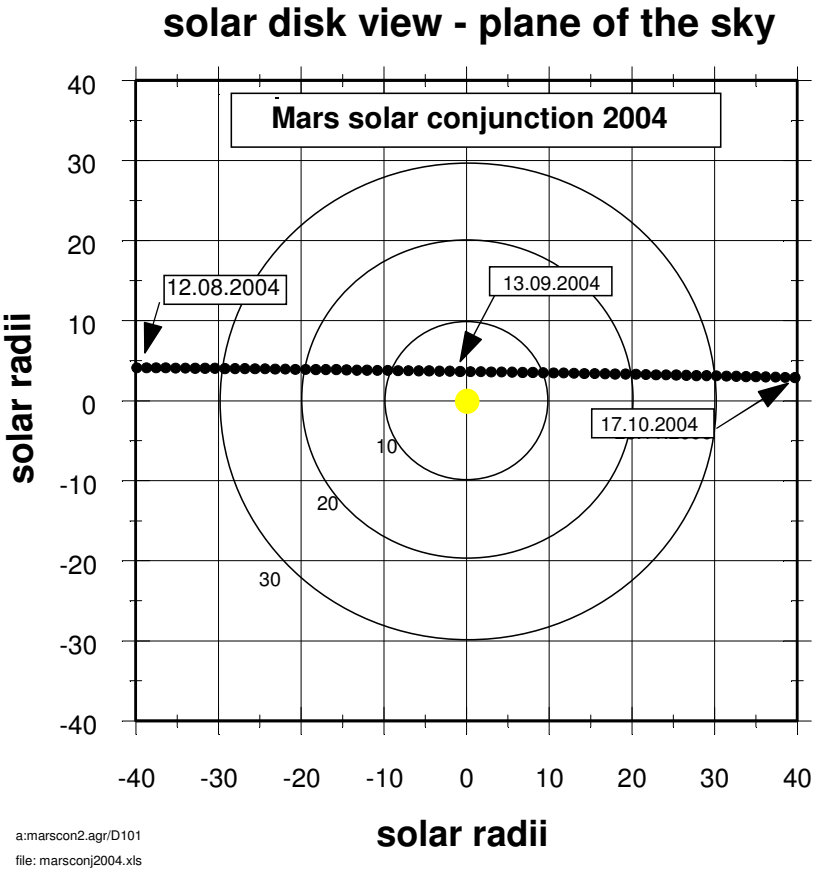

Figure 3.1-7: Superior solar conjunction geometry of planet Mars in the plane-of-sky in 2004. Each circle is one day. Mars is within 40 solar radii (circles mark distances from the solar disk) at both sides of the solar disk from 14 September 2004 to 18 October 2004. Within 12 solar radii, telemetry reception will be degraded. Effectively no telemetry will be received within 4 solar radii. However, an adequate signal-to-noise radio carrier can be received at any time.

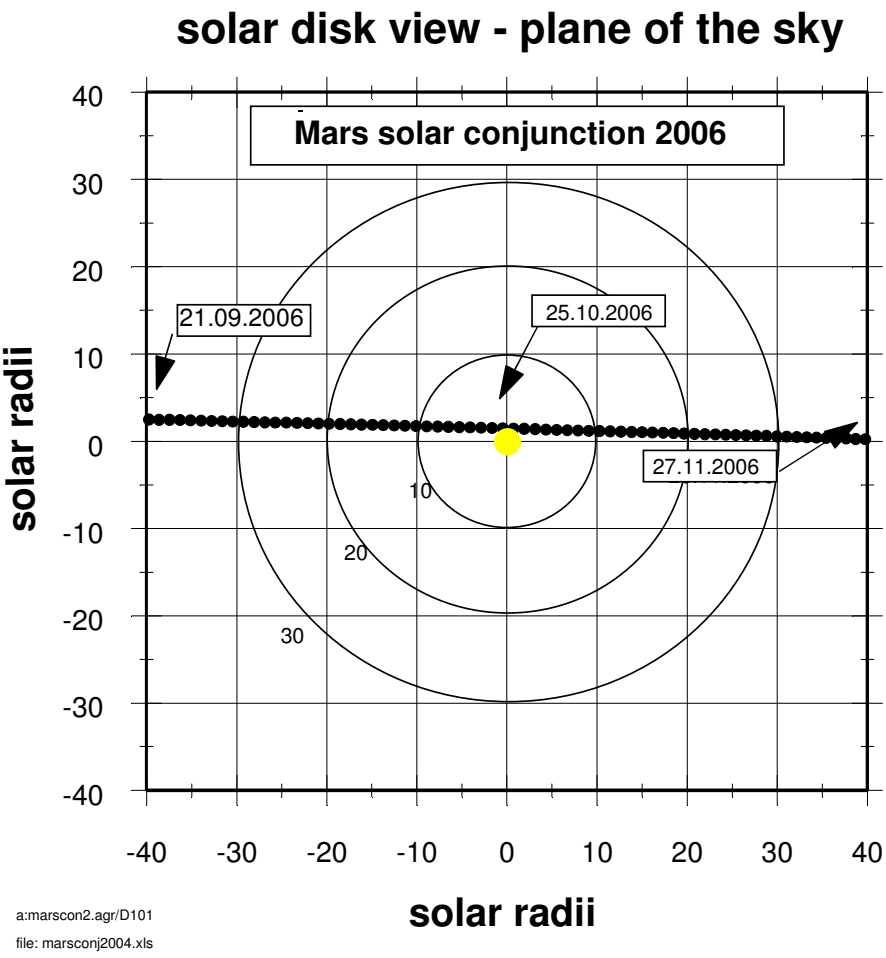

Figure 3.1-8: same as Figure 3.1-7 but for the conjunction in 2006.

3.2 Overview of the Instrument – Space Segment

3.2.1 General

The Mars Express Orbiter Radio Science (MaRS) experiment will make use of the radio link between the orbiter and the ground station(s) on Earth. Frequency, amplitude and polarisation information will be extracted from the radio signal received in the ground station.

3.2.2 Block Diagram of the MEX radio subsystem

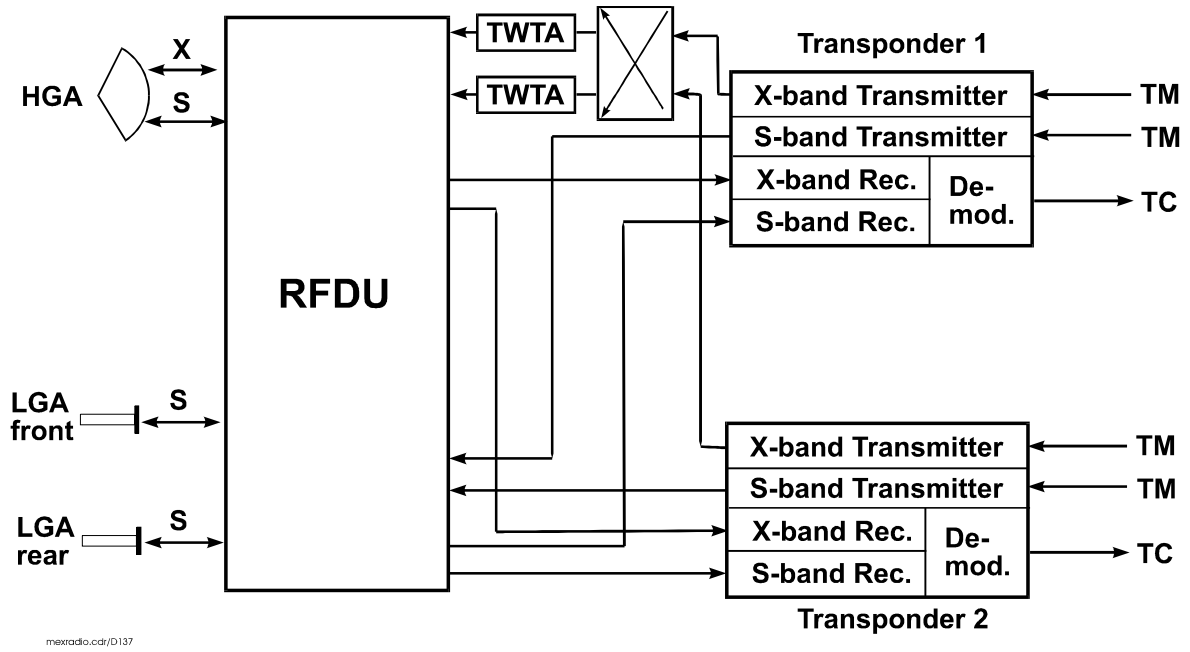

Figure 3.2-1: Principal block diagram of the MEX radio subsystem

The S-band uplink is received via the Low Gain Antennas (LGA) or the High gain Antenna (HGA). In the coherent two-way mode the received frequency is used to derive the downlink frequencies by using the constant transponder ratios 880/221 and 240/221 for X-band and S-band downlink, respectively (Figure 3.2-1).

The X-band uplink is received via the HGA only. In the coherent two-way mode the received frequency is used to derive the downlink frequencies by using the constant transponder ratios 880/749 and 240/749 for X-band and S-band downlink, respectively. An X-band uplink will enhance the performance of the experiment because X-band is less sensitive to the interplanetary plasma along the propagation path.

The simultaneous and phase coherent dual-frequency downlink at X-band and S-band is transmitted via the HGA. The X-band and S-band frequencies are related by a factor of 11/3. If an uplink exists, the downlinks are also coherent with the uplink

by their respective transponding ratios. The dual-frequency downlink is required in order to separate the classical Doppler shift, due to the relative motion of the spacecraft and the ground station, from the dispersive media effects, due to the propagation of the radio waves through the ionosphere and interplanetary medium. It is also required that both frequencies are transmitted via the High Gain Antenna to maximise the signal-to-noise ratio.

3.2.3 Definition of Radio Links

3.2.3.1 Two-way radio link

The two-way dual-frequency radio link (Figure 3.2-2) is used for the occultations, gravity observations and coronal investigations. The radio link benefits from the superior frequency stability of the ground station provided by hydrogen masers.

The dual-frequency downlink at X-band and S-band is used to separate classical and dispersive Doppler shifts and therefore to correct the observed frequency shift by the plasma contribution due to the propagation through the interplanetary medium.

Two-way mode:

- X-band uplink, or
- S-band uplink as requested during solar conjunctions
- simultaneous and coherent S- and X-band downlink via the HGA
- S-band downlink only operational if radio science experiments are performed
- No telemetry modulation at S-band; full RF power on carrier
- No telemetry modulation at X-band; full RF power on carrier
- Periodical ranging at S-band or X-band at begin and end of track ; as requested

3.2.3.2 One-way radio link

The dual-frequency one-way radio link (Figure 3.2.3-1) at X-band and S-band will be used for the bistatic radar observations.

One-way mode:

- simultaneous and coherent S- and X-band downlink via the HGA
- No telemetry modulation at X-band; full RF power on carrier
- No telemetry modulation at S-band; full RF power on carrier
- Downlink frequency controlled by the onboard TCXO

3.2.3.3 Radio Link Budget

Radio Link Budgets were computed for the worst case S/C-Earth distance of 2.5 AU for various scenarios and can be found in detail in section 5.2.

The conclusion is that carrier Doppler and ranging at both frequencies can be received at an acceptable signal-to-noise ratio at the worst case S/C-Earth distance of 2.5 AU using a 35 m ground station.

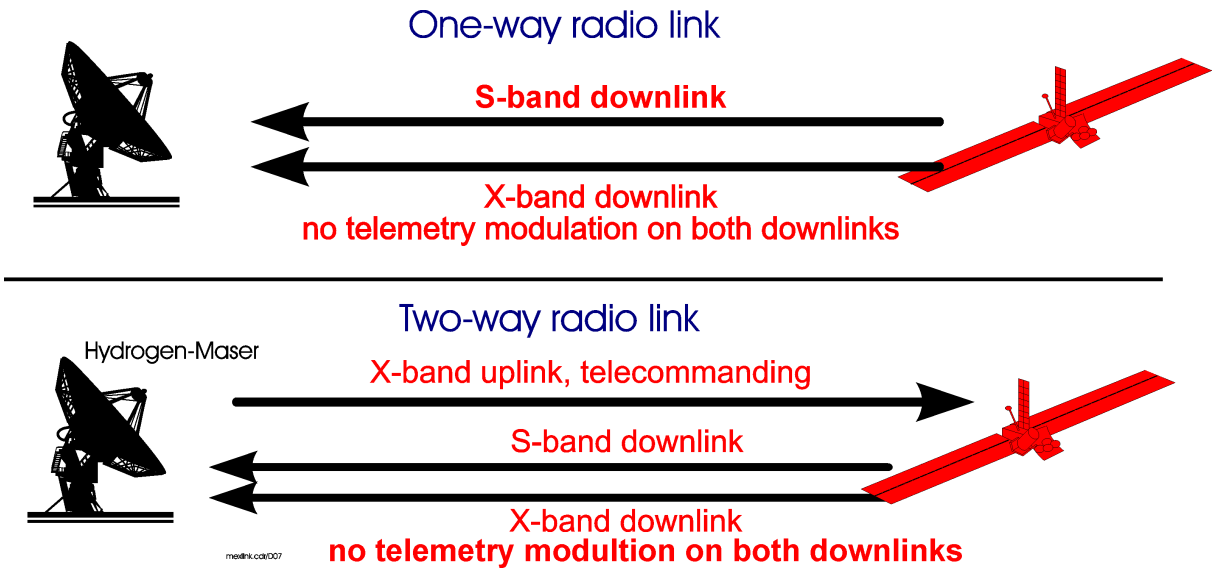

Figure 3.2-2: Proposed radio links between the orbiter and the ground station on Earth. Upper panel: one-way S/X-band downlink for bistatic radar. Lower panel: Two-way radio link where the X-band uplink is transponded back phase coherently in a dual-frequency downlink. The frequency stability is governed by a hydrogen maser located at the ground station.

3.3 Overview of the Instrument – Ground Segment

3.3.1 Overview

Ground stations include antennas, associated equipment and operating systems in the tracking complexes of New Norcia (ESA, 35 m), Australia, and the Deep Space Network (NASA, 34 m and 70 m) in California, Spain and Australia. A tracking pass consists of typically eight to ten hours of visibility. Measurements of the spacecraft range and carrier Doppler shift can be obtained whenever the spacecraft is visible. In the two-way mode the ground station transmits an uplink radio signal at S-band and receives the dual-frequency simultaneous downlink at X-band and S-band. The information about signal amplitude, received frequency and polarization is extracted and stored as a function of ground receive time.

3.3.2 Ground stations

3.3.2.1 European Ground Stations

ESA will install a new 35 m ground station at its complex in New Norcia, Australia. This station will most probably be operable in 2003. The current station baseline calls for an X-band or S-band uplink and a dual-frequency downlink at S-band and X-band capability. The station equipment which will partly be adjusted to the requirements of the Rosetta Radio Science Investigations (RSI) experiment are compliant with the requirements of the Mars Express radio science experiment.

3.3.2.2 Deep Space Network

The DSN ground stations provide uplinks at S-band or X-band and a full suite of radio science equipment used for most NASA missions.

It should be emphasized that the feasibility of the two-way measurements do not depend on the uplink frequency. The two data types, closed-loop and open-loop, can be generated simultaneously regardless of the radio link configuration, one-way or two-way.

The open-loop equipment is capable of receiving one frequency in two polarizations (LCP and RCP) or two frequencies in one polarization (LCP or RCP). The reception of two frequencies in two polarization (four channels) is only possible at the 70-m ground stations.

3.3.3 Ground Station Capabilities

The following required ground station capabilities are supported by the new IFMS system at New Norcia and the DSN:

1. X-band uplink transmission
2. S-band uplink transmission
3. S-band downlink reception
4. X-band downlink reception
5. S,X-band downlink simultaneous reception
6. Doppler sample rates: 1000, 100, 10, 1, 0.1 samples/sec. (to be selected by MaRS)
7. X/S ranging
8. X/X ranging
9. S/X ranging
10. S/S ranging
11. X/S and X/X simultaneous ranging (DSN only)
12. S/S and S/X simultaneous ranging (DSN only)
13. ranging sample rates: 1..120 sec., 1 sec. steps
14. Storage of Doppler frequencies and range values in a defined data format :

	description
IFMS	GRST-TTC-GS-ICD-0518-TOSG
DSN	TRK 2-34 0159-Science

15. Monitoring and recording of S, X-band AGC, sample rates 60, 10, 1, 0.1 samples/s
16. Determination and monitoring of receiving system performance (e.g. T_{system}) during MaRS operations

    The following requirement can only be supported by an "open-loop" equivalent system whose specifications are currently under definition by the Rosetta radio science experiment (RSI) in cooperation with ESOC. The realization of an open-loop system is subject to modifications of and/or additions to the IFMS. That would lead towards building an RSI IFMS extension. Specifications of an RSI Open-loop System will be described in the "RSI Open-loop System Specifications" document which is under preparation.

17. Digitally recording of RHC and LHC signals at S-band and X-band

3.3.3.1 Ground Station Frequency Reference Source

A Hydrogen maser frequency standard has frequency stability in the order of 10^{-15} . This stability is required for precise two-way tracking in order to achieve velocity accuracy better than 0.1 mm/s at one second integration time.

3.3.3.2 Further Equipment: IFMS

Specifications of an RSI Open-loop System is described in “IFMS User Requirement Document” (MEX-MRS-IGM-RS-3014). MaRS requirements are compliant to RSI requirements.

The modifications of the IFMS and the realization of an open-loop system in New Norcia are ongoing work. Any progress in the development and integration will be integrated into the MaRS User Manual.

3.3.4 Ground Station Configurations

For bistatic radar there will be no uplink to MEX and the antenna and the receiving system should be configured for best sensitivity.
Open-loop receiving system sampling rate and filters are chosen to capture expected echo bandwidth and carrier if possible.
Monitor system temperature on all receiving channels.

3.4 Data Products

3.4.1 Data types

3.4.1.1 Closed-loop data

Closed-loop data acquisition is done with a phase-locked loop receiver at the ground station. Two-way Doppler shifts are extracted by comparing each measure of the downlink carrier frequency from the phase-locked loop with a reference from the ground station frequency reference source, e.g. a hydrogen maser with a frequency stability in the order of 10^{-15} to 10^{-16} . Because this frequency reference source is also used for the generation of the uplink carrier, the accuracy of the frequency determination is as good as the reference source. The Doppler integration time needed to achieve a certain signal to noise ratio controls the time between successive frequency determinations. The amplitude of the radio signal is estimated by the Automatic Gain Control (AGC).

3.4.1.2 Open-loop data

Open-loop data recording is done by filtering and down-converting the received radio carrier signal to baseband where it is A/D converted and stored for subsequent analysis. The open-loop receiver is tuned by a local oscillator. The frequency of the local oscillator is given by the best available estimate of the carrier frequency transmitted by the spacecraft and applying Doppler corrections due to the relative s/c-to-Earth motion.
For Bistatic Radar not the carrier, but the echo signal is important. The echo is converted to baseband and sampled. The local oscillator must track the echo frequency (not the carrier) although the echo signal sometimes depends on the carrier.

3.4.2 Data required from ESOC

3.4.2.1 Observation data from New Norcia

The radio science observation data are recorded in the ground station by the IFMS systems. Depending on the ground station configuration up to three IFMS may record radio science data.

The Radio Science IFMS is an integral part of the receiving system at the ESA ground station. Its configuration has to fulfill the requirements of the Radio Science experiments, it can however serve also as a complementary and redundant unit for ESA´s prime receiving units.

The following tables show the likely configuration scenarios for the IFMS system when Radio Science experiments will be conducted in OL mode. All Doppler and ranging measurements must be performed by the standard ESA IFMS units with two downlink frequencies (TWOD) in order to allow compensation for the ionospheric/interplanetary TEC contribution.

In all cases requiring the Radio Science IFMS in OL mode operation, no telemetry modulation shall be applied to the downlink carrier analysed by the Radio Science IFMS in order to preserve spectral cleanliness as much as possible.

Also, as a highly desirable option, scenarios are suggested which require in addition to the Radio Science IFMS either IFMS A or IFMS B in OL configuration.

3.4.2.1.1 IFMS Configurations

As agreed with ESOC the three IFMS in New Norcia are configured as:

- IFMS A: controls uplink; could be at either X- or S-band (S-band for Solar Conjunction). Two channels of closed-loop reception are possible; these could be any two of the four XR, XL, SR and SL combinations. If XR/XL is selected, then the IFMS computes “polarization”.
- IFMS B: is backup for IFMS A; MaRS can specify its configuration on request (tbc)
- IFMS RS: MaRS can specify the configuration

IFMS configurations for the various radio links are listed in Section 4.2.

3.4.2.1.2 IFMS Data files

Closed-loop data:

Data type	Received X-band Doppler Received S-band Doppler X-band signal amplitude S-band signal amplitude X-band ranging S-band ranging Polarization	Hz Hz dBm dBm s s deg
Sample rate	To be selected by MaRS	s^{-1}

Open-loop data:

Data type	Received X-band voltage samples Or Received S-band voltage samples	V V
Sample rate	To be selected by MaRS	s^{-1}

The following data files from each operating IFMS at the New Norcia 35 m ground station are requested:

IFMS_NNNN_sss_YYYY_DOY_dk_dt_hhmmss_xxxx

Identifier	Explanation	options
NNNN	Ground station ID	NN12 = New Norcia Redu = Redu
sss	spacecraft acronym	MEX
YYYY	Year	
DOY	Day of year	
dk	Data kind	OP = operational CL = calibration TS = test
dt	Data type	D1 = Doppler 1 D2 = Doppler 2 RG = ranging MT = meteo
hhmmss	Start time in hours, minutes, seconds	
xxxx	Data set sequence ID	Starting with 0001

3.4.2.2 Observation data from the DSN

3.4.2.2.1 DSMS Tracking System Data Archival Data (TRK-2-34)
TBD

3.4.2.2.2 Radio Science Receiver Data (RSR)
TBD

3.4.2.3 Auxiliary Data

Data required	Timing	Data source	Freq.	Sampling	Accuracy (Required)
Major S/C events (Orbit Manoeuvres, Eclipse etc)	Planned and Predicted	Ground	Monthly	Event related	Highest feasible
Long range Orbit Prediction	Predict (a) gravity field GM (b) gravity field 10x10 (c) gravity field 50x50	Ground	Monthly	1 sample/min.	Highest feasible
Near Term Orbit Prediction	Predict (a) gravity field GM (b) gravity field 10x10 (c) gravity field 50x50	Ground	Weekly	1 sample/min.	Highest feasible
Quick look Orbit Estimation	Post-obs	Tracking Data	Once in 2 days	1 sample/sec.	Highest feasible
Precision Orbit Estimation	Post-obs	Tracking Data	Once in 2 weeks	1 sample/sec.	Highest feasible
Predicted Attitude Quarternions representation in both s/c orbiting ref.system and inertial reference system	Predict	Ground	Event related	1 sample/min.	Highest feasible
Reconstituted Attitude (Attitude and Rates) Quarternions representation in both s/c orbiting ref.system And inertial reference system	Post-obs.	S/C Data + Ground	Event related	1 sample/sec.	Highest feasible

Data required	Timing	Data source	Freq.	Sampling	Accuracy (Required)
Rotation Angle of solar arrays (SA) with respect to S/C frame of reference	Post–obs.	S/C Data	Weekly	1 sample/min	Highest feasible
Pericentre 'TICK'	Predict	Ground	Weekly	Every Orbit	Highest feasible
	Post-obs	Tracking Data	daily	Every Orbit	Highest feasible
Orbit Time Period	Predict	Ground	Weekly	Every Orbit	Highest feasible
	Post-obs	Tracking Data	daily	Every Orbit	Highest feasible
Thruster Firing Times (Start Time & Duration)	Predict & Post-obs.	Ground & S/C	Event related	Every Manoeuvre	millisec
Sun Zenith Angle (Over Pericentre)	Predict	Ground	Weekly		Highest feasible
Times of Earth Occultation Entry and Exit	Predict	Ground	Weekly	Each Earth occultation	seconds
Spacecraft Position at Earth occultation entry and exit	Predict	Ground	Weekly	Each Earth occultation	Highest feasible
	Post-obs.	Tracking Ground	daily	Each Earth occultation	Highest feasible
Longitude & Latitude of occultation entry and exit	Predict	Ground	Weekly	Each Earth occultation	Arc minutes
	Post-obs.	Ground	daily	Each Earth occultation	Arc minutes

Data required	Timing	Data source	Freq.	Sampling	Accuracy (Required)
Solar Zenith Angle at Earth occultation entry and exit	Predict	Ground	Weekly	Each Earth occultation	Arc minutes
	Post-obs	Ground	daily	Each Earth occultation	Arc minutes
Duration of Earth Occultation	Predict	Ground	Weekly	Each Earth occultation	seconds
Spacecraft position as subsatellite point	Predict	Ground	weekly	Event related (approved pericenter pass for gravity)	Highest feasible
	Post-obs.	Tracking & Ground	Daily	Event related (approved pericenter pass for gravity)	Highest feasible
HGA pointing direction Angle wrt NADIR (for gravity)	Post-obs	Ground + S/C	Each event	1 sample/sec	Arc minutes
Angle wrt Earth direction (for bistatic radar)	Post-obs	Ground + S/C	Each event	1 sample/sec	Arc minutes
Quarternions representation in both s/c orbiting ref. System and inertial reference system	Post-obs	Ground + S/C	Each event	1 sample/sec	Arc minutes

3.4.2.4 Housekeeping Data

To be specified

3.4.3 Data Volume

Estimate of the data volume (order of magnitude numbers):

closed-loop:

IFMS	**Calculation (bytes)**	**One hour data recording @ 1 second sampling time**
Overhead		18 kBytes
Ranging	110 x number of samples /hour	396 kBytes
Doppler	220 x number of samples/hour	792 kBytes
Meteo	100 x number of samples/hour	6 kbytes (1 min sampling time)

DSN ATDF	**Calculation (bytes)**	**One hour data recording @ 1 second sampling time**
Ranging Doppler	288 x number of samples/hour	1036 kBytes

Open-loop:

IFMS	**Calculation (bytes)**	**Event volume**
Occultation	6 bytes*5000 samples/s	54 Mbyte/30 minutes
Bistatic radar	6 bytes*50000 samples/s	2160 Mbyte/2 hours
Solar corona	6 bytes*5000 samples/s	648 Mbyte/6 hours

DSN ODR	**Calculation (bytes)**	**Event volume (tracking pass)**
Occultations	0.5 Mbytes / minute	15 Mbytes total (duration 2x 15 minutes)
Bistatic radar	12.5 Mbytes / minute	750 Mbytes total (duration 1 hour)
Solar corona	0.5 Mbytes / minute	195 Mbytes total (6.5 hours)

3.4.4 End-to-end performance

A Doppler error analysis was performed for the Rosetta RSI experiment. The following is an excerpt from RO-RSI-IGM-TN-3057.

3.4.4.1 Discussion of Doppler noise sources

When evaluating error sources one has to analyze both ground station and space segment contributions and cannot concentrate only on the transponder quantization error.

Thermal contribution: Taking a 1 second integration interval, assuming a H2 Maser reference frequency source we obtain an r.m.s. velocity error due to thermal noise contribution of

$$\sigma_v = \frac{c\sqrt{\frac{2BN_0}{C}}}{4\pi f_d T} \qquad (3\text{-}1)$$

Assuming the noise band of the ground station PLL receiver, C/N_o the total carrier to noise power spectral density ratio, T the integration time, f_d the nominal downlink frequency and the c the speed of light in vacuum.

It is well justified to assume that the uplink *C/N* dominates over the downlink *C/N*, hence it is the downlink *C/N* which enters into equation (3-1). For S-Band we obtain with an estimated C/N_o 23 dBHz at the ground station (3 AU), 1 sec integration time *and 2B = 1 Hz* loop bandwidth a velocity error of:

0.8 mm/s.

We are correspondingly better at X- band due to an improved C/N_o .

Taking the totally accumulated phase error (thermal noise, NCO ground station quantization error, reference frequency instability and path delay instability at the New Norcia ground station, ref. [5,6], we receive at a corresponding velocity error of (naturally depending critically on link quality):

1 mm/s for S-band and 0.3 mm/s for X-band

Additional noise sources are now given by the onboard transponder NCO quantization error noise contribution. The implementation of the NCO (32 bit word) will lead to a quantization error in frequency of 3mHz r.m.s. (applicable as well for S- as for X-band) corresponding to a velocity error of:

0.4 mm/s for S-band and 0.1 mm/s for X-band

Assuming an incremental error of $d = 2\pi/2048$ in phase (12 bit word) and a uniform error distribution we obtain a variance of that error of

$$\frac{d}{\sqrt{12}} = 0.88 \text{ mrad r.m.s.}$$

This error contributes in the following way to the velocity error:

$$\sigma_v = \frac{c\sqrt{2}\sigma_\varphi}{4\pi f_d T} \qquad (3\text{-}2)$$

resulting in

0.01 mm/s for S-band and 0.004 mm/s for X-band.

On the basis of r.s.s. we obtain on the basis of a H2 maser at the ground station for an integration time of 1 second a

total velocity error: 1.1 mm/s for S-band and 0.32 mm/s for X-band

3.4.4.2 Summary of error sources:

Error source	Velocity error σ_v	
	S-band	X-band
Total phase error (thermal and ground station contribution)	1.0 mm/s	0.3 mm/s
Transponder quantization error in frequency	0.4 mm/s	0.1 mm/s
Transponder quantization error in phase	0.01 mm/s	0.004 mm/s
Total error (coherent mode)	**1.1 mm/s**	**0.32 mm/s**

These Doppler errors are assumed for an integration time of 1 second and are comparable to those already observed from past missions. Considerable improvements can be achieved using longer integration times.

3.4.4.3 Doppler accuracy for longer integration times

For integration times longer than one second, this scales as

$$\Delta v_{total}(\Delta t) = \Delta v_{totalerror}\sqrt{\frac{1}{\Delta t}}$$

for both frequencies, where Δt is the integration time and $\Delta v_{totalerror}$ is the velocity error at S-band or X-band at one second.

Figure 3.4-1 shows the expected Doppler noise as a function of integration time between 1 second and 1000 seconds. The integration times which will be used for the different gravity applications are marked.

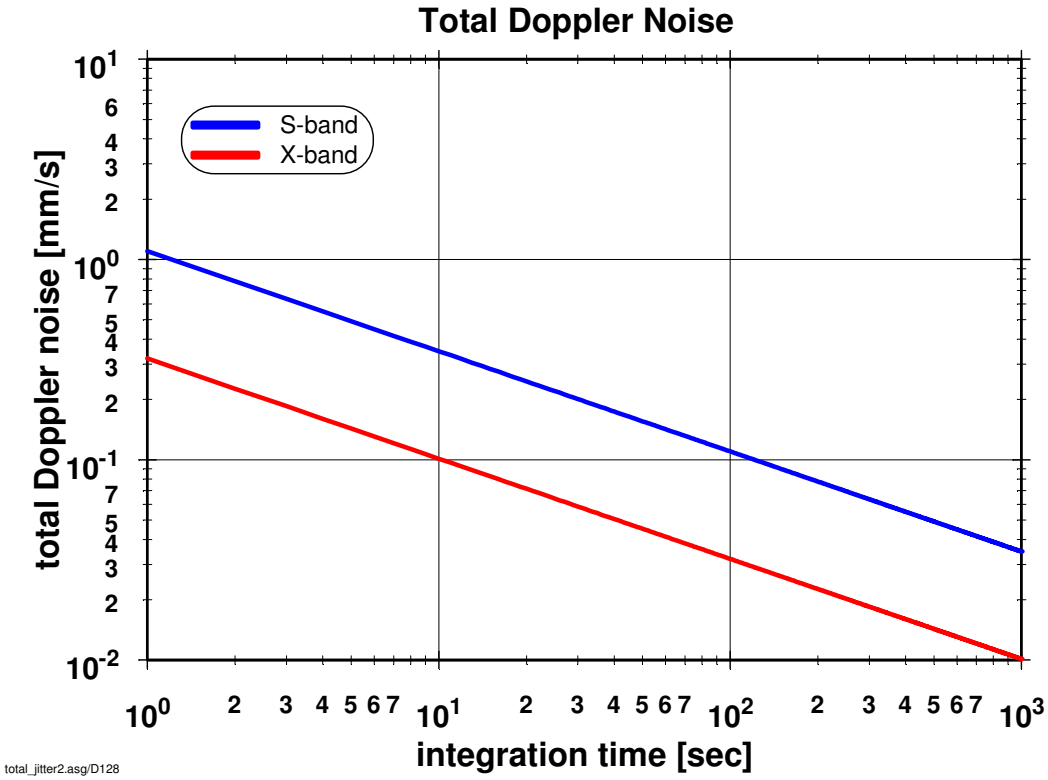

Figure 3.4-1: Expected total Doppler noise

4 Experiment Operations

4.1.1 Overview of Experiment Observation Modes

4.1.1.1 Science Operations

Radio science operations can only be requested when ground station coverage is available. Ground station visibility will be correlated with spacecraft orbits using request files as defined in section 6.1. Radio science ops requests will focus on those orbits which are covered by ground station availability.

4.1.1.1.1 Radio Sounding of the Atmosphere and Ionosphere

The sounding of neutral and ionized atmosphere is performed before the spacecraft enters occultation by the planet. The High Gain Antenna (HGA) is pointed toward the Earth an adequate time (approx. 10 to 15 minutes) before entering occultation. The radio link is two-way dual-frequency downlink (TWOD) with unmodulated carriers. The radio link performs a vertical swath through the atmosphere from an altitude of approximately 500 km to the surface.

4.1.1.1.2 Gravity Field

Orbit perturbations by the Martian gravity field can be extracted from precise two-way dual-frequency radio tracking (TWOD) during pericenter passes. For this configuration, the HGA is pointed toward the Earth.

4.1.1.1.3 Bistatic Radar

The HGA is pointed toward the surface of Mars and one-way signals without modulation (full power on carrier) are transmitted (ONED). Several passes above specific targets are requested. The experiment can be performed even at apocenter distance but with low SNR. It is recommended that one of the DSN ground stations be used for recording of the echo signals because of their higher SNR;only 70-m DSN stations can capture all four echo signals in ONED mode.

4.1.1.1.4 Phobos

In orbits having close encounters with the Mars moon Phobos (distance to Phobos < 500 km), the spacecraft and ground station are configured in the two-way mode TWOD. The HGA is pointed toward the Earth.

4.1.1.1.5 Solar Corona

From mid August to mid October 2004 and again in 2006, Mars is within 10° elongation about the solar disk in the plane-of-sky. The operational radio link for the sounding of the solar corona is the two-way dual-frequency radio link (TWOD) whenever the spacecraft is tracked for data return.

4.2 Definitions and Configurations

4.2.1 Definition of Radio Links

Definition of the radio links (Figure 3.2-2) is:

Two-way mode:

- X-band uplink
- S-band uplink as requested by MaRS during solar conjunctions
- simultaneous and coherent S- and X-band downlink via the HGA
- S-band downlink only operational if radio science experiments are performed
- No telemetry modulation at S-band (TBC); full RF power on carrier
- No telemetry modulation at X-band (TBC); full RF power on carrier
- Periodical simultaneous ranging at S-band or X-band at begin and end of track

One-way mode:

- X-band downlink via the HGA
- S-band downlink via the HGA
- simultaneous and coherent S- and X-band downlink via the HGA
- No telemetry modulation at X-band; full RF power on carrier
- No telemetry modulation at S-band; full RF power on carrier

4.2.2 Space Segment Configurations

The space segment configurations ONES, ONED, TWOS, and TWOD are defined according to Table 4.2-1.

Table 4.2-1: Space Segment Configuration

Exp.Mode Space Segment	**Acronym**	**Additional Power (W)**	**Functional Use**
One-way single downlink X-band	ONES (X)	60W	BSR to NNO (not so good for roughness)
One-way single downlink S-band	ONES (S)	5W	BSR to NNO (may be better for roughness)
One-way dual-frequency D/L	ONED	60W X 5W S	BSR to DSN (preferred configuration) BSR to NNO (if reflectivity is less important) Occultations (exit backup)[1]
Two-way dual-frequency D/L S-band uplink	TWOS (S-up)	60W X 5W S	Solar corona (preferred configuration)
Two-way dual-frequency D/L X-band uplink	TWOD (X-up)	60W X 5W S	Occultations (preferred) Gravity[2] Phobos Solar corona (backup)

[1] To be used only if TWOD (X-up) lock time is too large compared to the occultation exit time
[2] TWOD for gravity preferred

4.2.3 Ground Segment Configurations

Table 4.2-2: Ground Segment Configuration

Ground Configuration		Spacecraft Configuration	IFMS A		IFMS B		IFMS RS	DSN	Functional Use
			U/L	D/L	U/L	D/L			
ONES(X)		ONES(X)	-	XR-CL	-	XR-CL	XR-CL X-OL(?)	XR-CL X-OL(?)	BSR to NNO
ONES(S)		ONES(S)	-	SR-CL	-	SR-CL	SR-CL S-OL(?)	SR-CL S-OL(?)	BSR to NNO
ONED70	ONED 34S?X?	ONED	-	SR-CL XR-CL?	-	SR-CL XR-CL?	XR-CL SR-CL?	SR-CL XR-CL?	BSR, OCC (exit backup)
							S?-OL X?-OL	S?-OL X?-OL	34/35m: Polarizations to be chosen for each observation; probably same for each BSR band; always R for OCC
								SR-CL XR-CL S-OL(?) X-OL(?)	70m: XR,XL,SR,SLreceived in OL for BSR; XR and SR only for OCC
TWODS70	TWDOD34	TWOD(S-up)	S	SR-CL XR-CL?	-	SR-CL XR-CL?	XR-CL SR-CL?	SR-CL XR-CL	Solar Conjunctions (preferred)
							SR-OL XR-OL	SR-OL XR-OL	34/35m
								S-OL? X-OL	70m
TWODX70		TWOD(X-up)	X	XR-CL SR-CL	-	XR-CL SR-CL	SR-CL XR-CL	SR-CL XR-CL	OCC (preferred),GRA, PNO,SCP (backup)
							SR-OL XR-OL	SR-OL XR-OL	34/35m
								SL-OL XL-OL	70m, SCP only

4.2.4 Operational Constraints to other experiments

Mars operations will constrain and impact the operations of other experiments or limit the telemetry return.

When MaRS operations are scheduled, operational priority is required. Full power on the RF carrier (no telemetry modulation) is required to maximize the received SNR. HGA Earth pointing for most of the science objectives is required which will not allow simultaneous Nadir observations.

Table 4.2-3 summarizes these constraints.

Table 4.2-3: Impact of radio science observations on other experiments

<table>
<tr><td></td><td colspan="4">Science Objectives</td></tr>
<tr><td></td><td colspan="2">Sounding of atmosphere and ionosphere (occultations)</td><td>Gravity</td><td>Bistatic radar</td><td>Solar corona</td></tr>
<tr><td>Baselined nominal orbit phase</td><td>Communication phase</td><td>Observation phase</td><td>Observation phase</td><td>Communication phase</td><td>Communication Phase</td></tr>
<tr><td>Required HGA pointing direction</td><td>Earth</td><td>Earth</td><td>Earth</td><td>Surface</td><td>Earth</td></tr>
<tr><td>Duration</td><td colspan="2">10 – 15 min
before going into occultation and/or after exiting occultation</td><td>20 - 30 min</td><td>1-4 hours
Depends on ground coverage during track</td><td>6.5 hours</td></tr>
<tr><td>Pointing baseline?</td><td>OK (default)</td><td>NO
Design goal</td><td>NO
Design goal</td><td>NO
Design goal</td><td>OK (default)</td></tr>
<tr><td rowspan="2">Impact on other exp.</td><td colspan="2">unmodulated carrier => no telemetry transmission</td><td>unmodulated carrier => no telemetry transmission</td><td>unmodulated carrier => no telemetry transmission</td><td>low bit rate telemetry</td></tr>
<tr><td></td><td>No NADIR pointing</td><td>No NADIR pointing</td><td></td><td></td></tr>
<tr><td rowspan="3">Requested number of observations</td><td colspan="2">If S/C is going into occultation</td><td rowspan="2">TBD
depends on ground coverage dawn/dusk pericenters feasible</td><td>Average one per week</td><td rowspan="2">Every tracking pass from mid September to mid November 2004
Same in 2006</td></tr>
<tr><td>Each orbit</td><td>1 per sol</td><td></td></tr>
<tr><td colspan="3"></td><td>No daylight/nighttime constraints</td></tr>
<tr><td colspan="5">to be correlated with ground station visibility</td></tr>
</table>

Z:\mars_rs\files\ops_constraints.doc

4.2.5 HGA Pointing Requirements

4.2.5.1 Overview

MaRS requires specific HGA pointing directions which are not baselined but considered as spacecraft design goals.

HGA Earth pointing is required for

- Atmosphere & ionosphere sounding (occultation experiment)
- Gravity anomalies
- Phobos
- Solar corona sounding

HGA surface pointing is required for

- Bistatic radar

Table 4.2-4 describes the MaRS pointing requirements as a deviation from the baselined nominal pointing during the different orbit phases.

Table 4.2-4: MaRS Pointing requirements; deviations from nominal pointing directions

Science Objective		**Baselined Nominal Pointing Phase**	**MaRS required HGA Pointing**
Atmosphere Ionosphere (occultation experiment)	Occultation occurs during observation phase (pericenter pass)	Observation phase (Nadir)	Earth pointing
	Occultation occurs during communication phase	Communication phase (HGA Earth pointing)	Earth pointing (compliant)
Gravity anomalies	Performed during observation phase (pericenter pass)	Observation phase (Nadir)	Earth pointing
Phobos	Probably exclusively during apocenter passes	Communication phase (HGA Earth pointing)	Earth pointing (compliant)
Bistatic radar		Communication phase (HGA Earth pointing)	Surface pointing
Solar Corona		Communication phase (HGA Earth pointing)	Earth pointing (compliant)

4.2.5.2 Detailed description of required HGA pointing

4.2.5.2.1 Occultations

Table 4.2-5: HGA Pointing during Occultations

Space Segment		
Occultation entry is during	Observation phase	Communication phase
Baseline HGA pointing	Nadir for instruments Somewhere for HGA	Earth
Required HGA pointing	Earth	
MaRS space segment configuration	TWOD (entry phase) ONED (exit phase) Coherent	
Uplink frequency	X-band (entry phase) No uplink (exit phase)	
Downlink frequency	S-band and X-band simultaneous	
Additional power	S-band DC power (TBD)	
Carrier modulation	No (full power on carrier)	
Begin of measurement	10 – 15 min before occultation (altitude 500 km) 10 –15 min after leaving occultation (altitude 500 km)	
Number of measurements	Each occultation during ground station visibility Exact time and number of occultations is TBD	
Ground Segment		
MaRS ground segment configuration	See Table 5.3-1	
Data products	**closed-loop**	**open-loop**
	S & X Doppler	S & X open-loop samples
	S & X AGC	
	Auxiliary data	

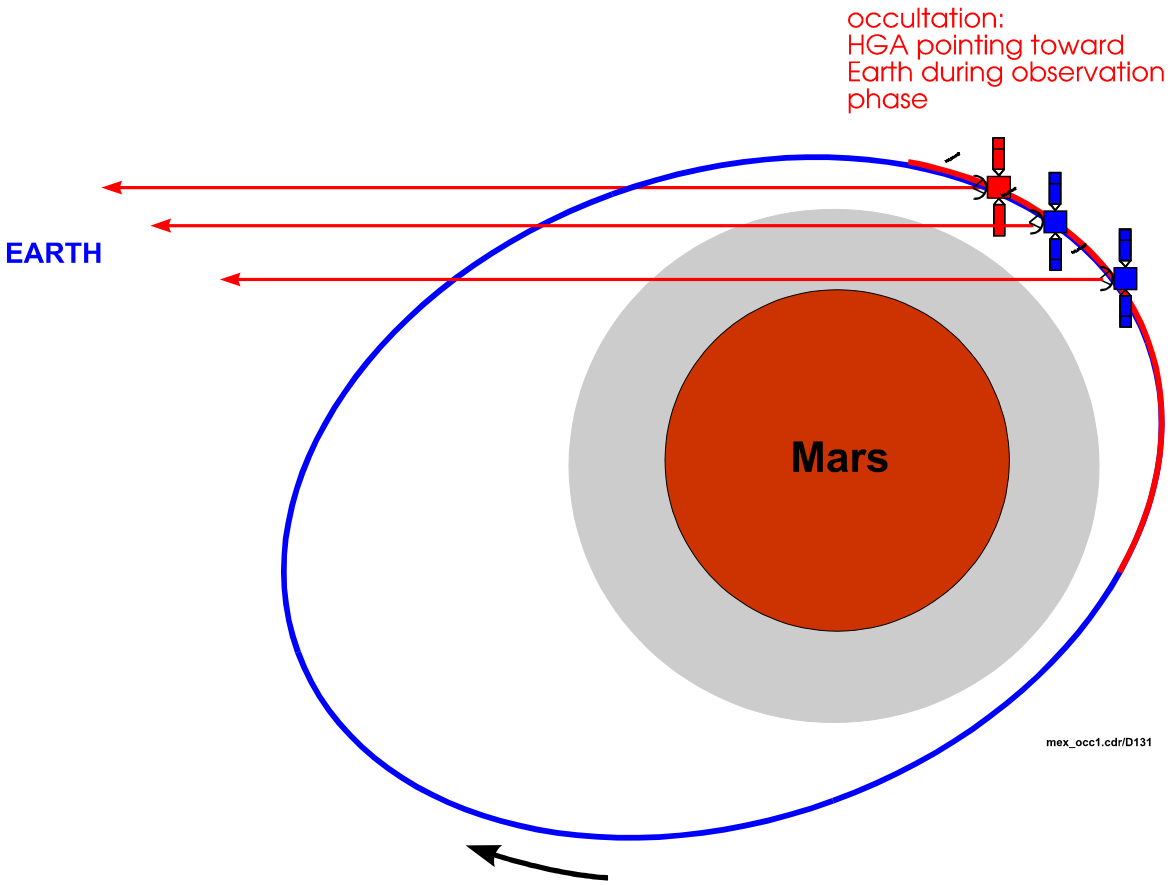

Figure 4.2-1: in-orbit pointing configuration for the sounding of the atmosphere and ionosphere in the case that occultation entry is during the nominal observation phase (near pericenter). 10 to 15 minutes prior to occultation the HGA is pointed toward the Earth.

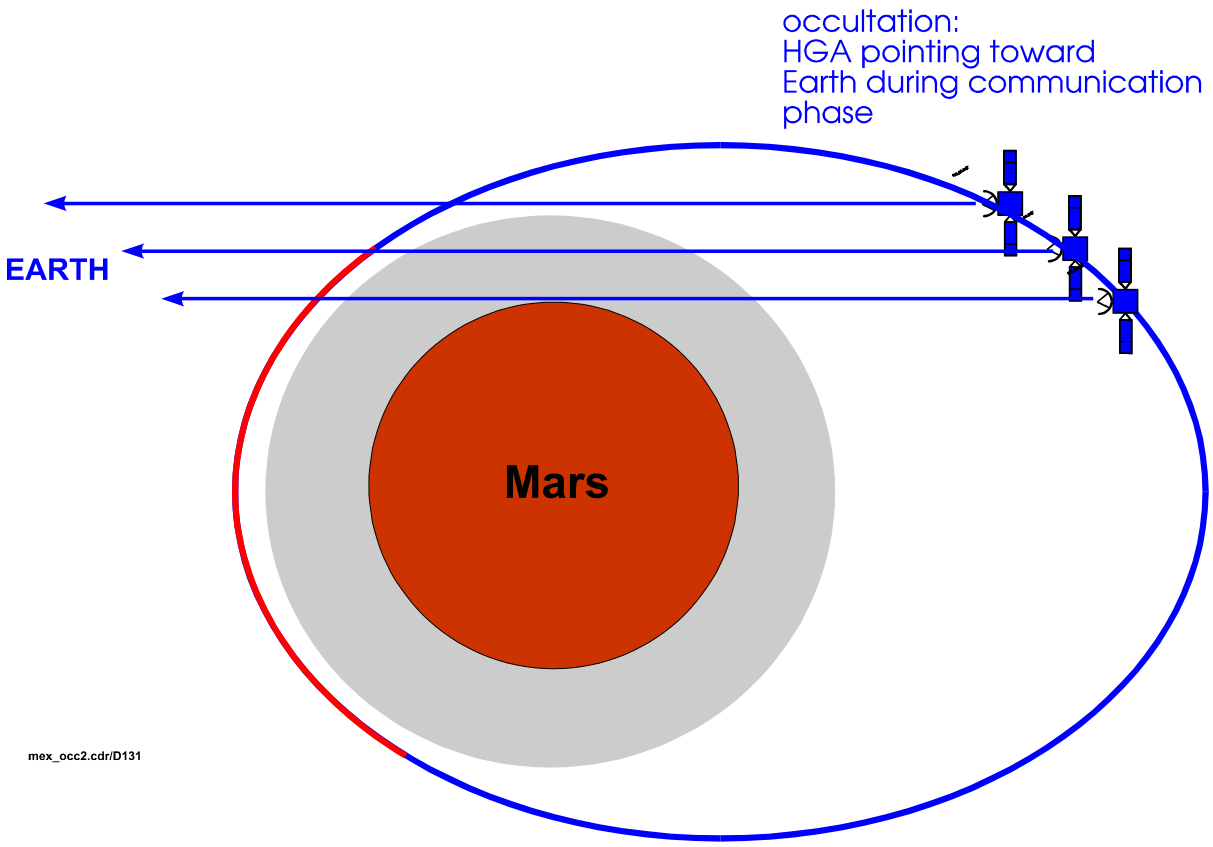

Figure 4.2-2: : in-orbit pointing configuration for the sounding of the atmosphere and ionosphere in the case that occultation entry is during the nominal communication..

4.2.5.2.2 Bistatic Radar

In this mode the HGA is always pointing

1) to a pre-defined target point (see Figure 4.2-3)
2) to illuminate the specular point as it moves across the surface (see Figure 4.2-4)
3) in an inertially fixed position(see Figure 4.2-5)

while the Earth is located in the same half-space as the target area on Mars. The measurements will be performed during the communication phase around apocentre. Each measurement will last for 2 hours at total.

Table 4.2-6: Bistatic radar pointing

Space Segment		
Performed during	Observation phase	Communication phase
Baseline HGA pointing	Nadir for instruments Somewhere for HGA	Earth
Required HGA pointing	Predefined HGA toward surface	
MaRS space segment configuration	ONED	
Uplink frequency	No uplink	
Downlink frequency	X-band and S-band simultaneous	
Additional power	S-band DC power	
Carrier modulation	No (full power on carriers)	
time of measurement	Up to 4 hours	
Number of measurements	TBD (Average one per week)	
Ground Segment		
MaRS ground segment configuration	See Table 5.3-3	
Data products	**Closed-loop**	**ONES-OL**
	None required except TCXO frequency estimates/ predicts and T_{sys}	X-band & S-band open-loop samples up to 4 channels total
	Auxiliary data	

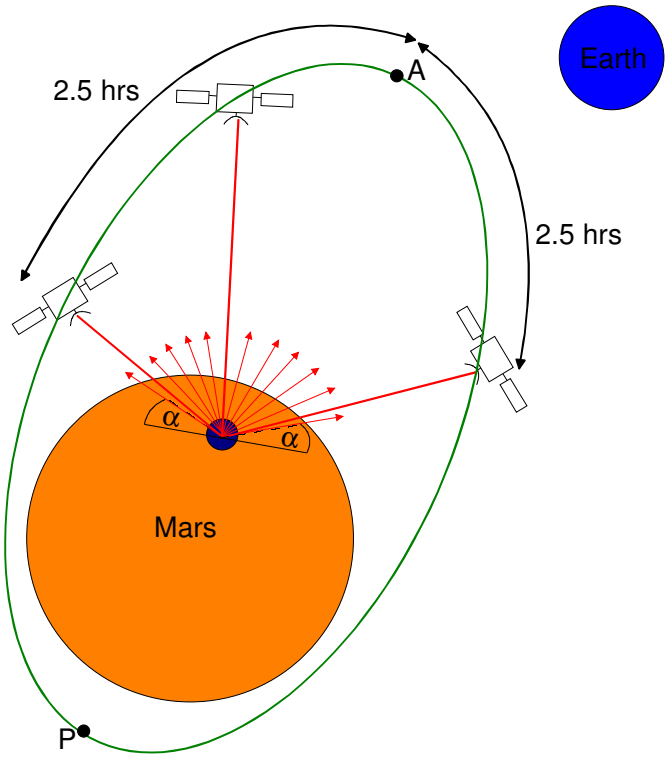

Figure 4.2-3: 1st in-orbit pointing configuration for the bistatic radar experiment. In this mode the HGA is always pointing to a pre-defined target point

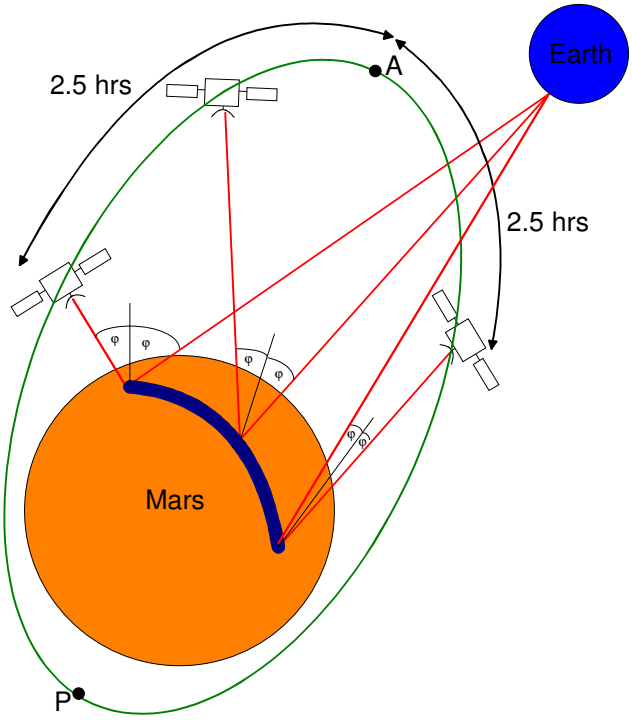

Figure 4.2-4: : 2nd in-orbit pointing configuration for the bistatic radar experiment. In this mode the HGA is always pointing to illuminate the specular point as it moves across the surface

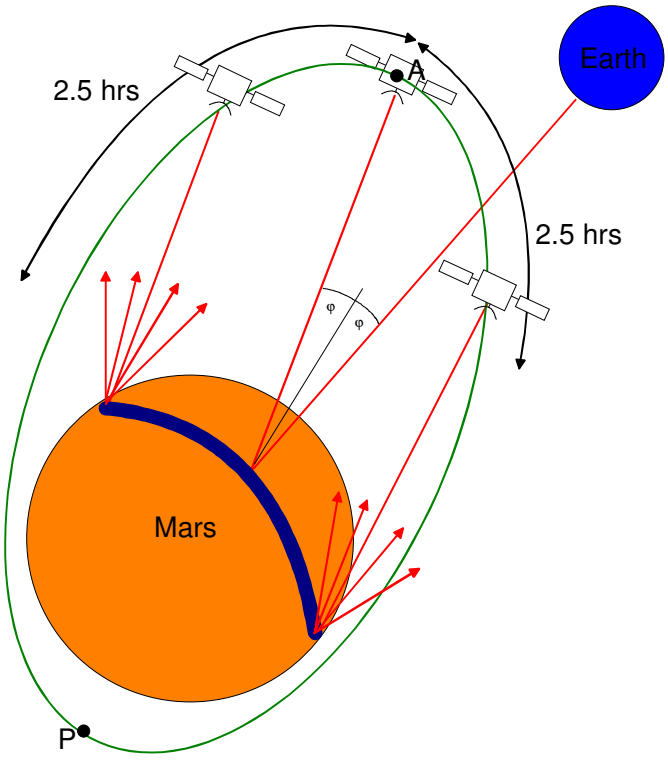

Figure 4.2-5: 3rd in-orbit pointing configuration for the bistatic radar experiment. In this mode the HGA is always pointing in an inertially fixed position

4.2.5.2.3 Gravity

Table 4.2-7: Gravity anomalies HGA pointing

Space Segment		
Performed during	Observation phase	
Baseline HGA pointing	Nadir for instruments Somewhere for HGA	
Required HGA pointing	Earth	
MaRS space segment configuration	TWOD Coherent	
Uplink frequency	X-band	
Downlink frequency	S-band and X-band simultaneous	
Additional power	S-band DC power (TBD)	
Carrier modulation	No (full power on carriers)	
Begin of measurement	20 – 30 min during pericenter pass (TBC)	
Number of measurements	TBD number of pericenter passes over selected target areas during ground station visibility (TBD) Pericenter passes at dawn/dusk feasible	
Ground Segment		
MaRS ground segment configuration	See Table 5.3-4	
	TWOD-CL	**TWOD-OL**

Data products	S & X Doppler (phase for DSN)	-
	S & X AGC	-
	Auxiliary data	

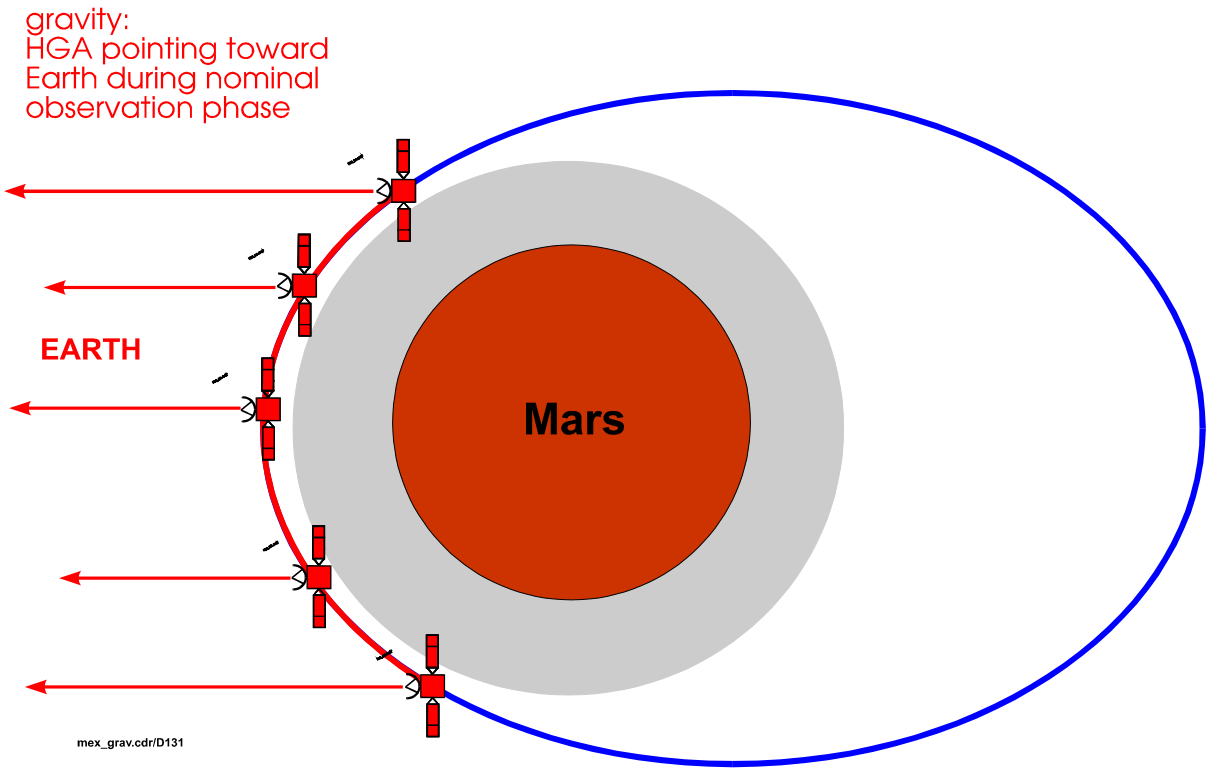

Figure 4.2-6: In-orbit pointing configuration for the gravity observations. The whole nominal observation phase is devoted to gravity observations. The HGA pointing direction for the entire phase is toward the Earth.

4.2.5.2.4 Phobos

Table 4.2-8: Phobos HGA pointing

Space Segment		
Performed during	communication phase	
Baseline HGA pointing	Earth	
Required HGA pointing	Earth	
MaRS space segment configuration	TWOD Coherent	
Uplink frequency	X-band	
Downlink frequency	S-band and X-band simultaneous	
Additional power	S-band DC power (TBD)	
Carrier modulation	No (full power on carriers)	
Begin of measurement	TBD	
Number of measurements	TBD	
Ground Segment		
MaRS ground segment configuration	See Table 5.3-2	
Data products	**TWOD-CL**	**TWOD-OL**
	S & X Doppler (phase for DSN)	-
	S & X AGC	-
	Auxiliary data	

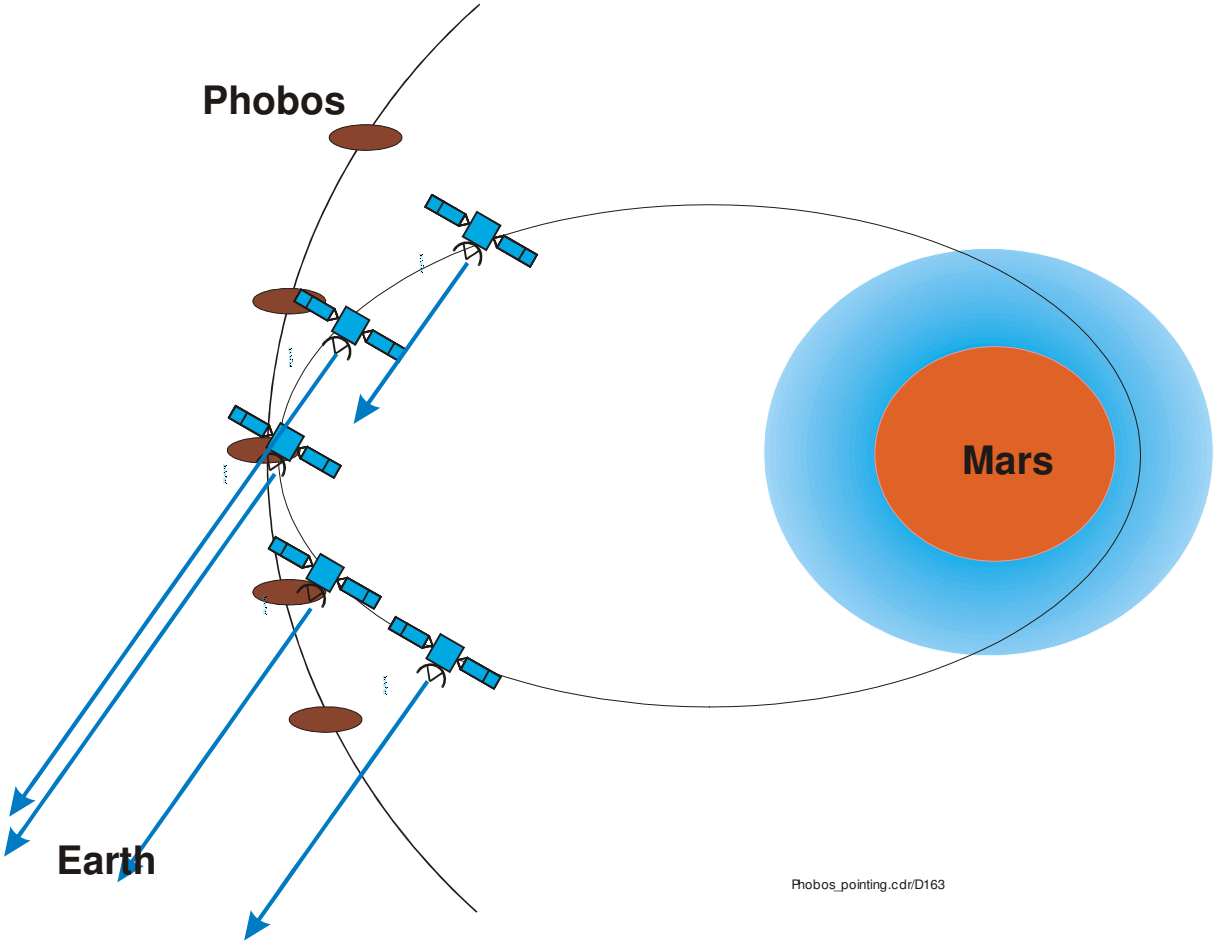

Figure 4.2-7: In orbit configuration for close Phobos encounters. HGA pointing is toward the Earth.

4.2.5.2.5 Solar Corona

Table 4.2-9: Solar Corona sounding HGA pointing

Space Segment		
Performed during	Communication phase	
Baseline HGA pointing	Earth	
Required HGA pointing	Earth	
MaRS space segment configuration	TWOD Coherent	
Uplink frequency	S-band	
Downlink frequency	S-band and X-band simultaneous	
Additional power	S-band DC power (TBD)	
Carrier modulation	at low bitrate	
Begin of measurement	14 August 2004 TBC (first solar conjunction) 21 September 2006 TBC (second solar conjunction)	
Number of measurements	Each day for 60 days during ground station visibility for each conjunction	
Ground Segment		
MaRS ground segment configuration	TWOD-CL (IFMS closed-loop) TWOD-OL (open-loop)	
Data products	**TWOD-CL**	**TWOD-OL**
	S & X Doppler	S & X open-loop samples
	S & X AGC	
	Auxiliary data	

5 Functions

5.1 Functions: Space segment

5.1.1 Design and Functional Description of the RF Subsystem

A Block diagram of the characteristic elements of the Mars Express radio subsystem are shown in Figure 3.2-1.

Mars Express is capable of receiving and transmitting radio signals via two dedicated antenna systems:
1. High Gain Antenna (HGA), a body-fixed parabolic dish of 1.60 m diameter
2. Two Low Gain Antennas (LGA), front and rear, S-band only

The two transponders consist of an S-band and X-band receiver and transmitter each. The spacecraft is capable of receiving one uplink signal at S-band (2100 MHz) via the LGAs, or at either X-band (7100 MHz) or S-band via the HGA. The spacecraft can transmit via the HGA simultaneously two downlink signals at S-band (2300 MHz) and X-band (8400 MHz) or one downlink signal at S-band via the LGAs.

The HGA is the main antenna for receiving telecommands from and transmitting telemetry signals to ground. The LGAs are used during the commissioning phase after launch and for emergency operations.

The S-band uplink is received via the Low Gain Antennas (LGA) or the High gain Antenna (HGA). In the coherent two-way mode the received frequency is used to derive the downlink frequencies by using the constant transponder ratios 880/221 and 240/221 for X-band and S-band downlink, respectively.

The X-band uplink is received via the HGA only. In the coherent two-way mode the received frequency is used to derive the downlink frequencies by using the constant transponder ratios 880/749 and 240/749 for X-band and S-band downlink, respectively.

5.2 Radio Link Budgets

The specifications for computing the radio link budget as a function of mission time were taken from the SGICD. One important input parameter is the varying Earth-Mars distance shown in Figure 5.2-1. Parameters used for the radio link budget calculations are listed in Table 5.2-1.

The following important assumptions for the budget tables were made:
- Geocentric distance is 2 AU (varying SNR due to the varying geocentric distance according to Figure 3.2-1 is shown in the Figures 5.2-2 to –3)
- 35 m ground station (New Norcia)

- MPTS receiver in ground station. This will be updated when proper IFMS parameters are available.
- DSN link budgets will be added at the next revision.

The following cases were computed:

1. *MEX radio uplink budget carrier only (section 5.2.2.)*.
2. *MEX downlink budget carrier only (section 5.2.3)*
3. *MEX downlink budget with ranging on both carriers and telemetry modulation on X-band carrier (section 5.2.4)*
4. *MEX downlink budget with telemetry modulation on X-band carrier (section 5.2.5)*

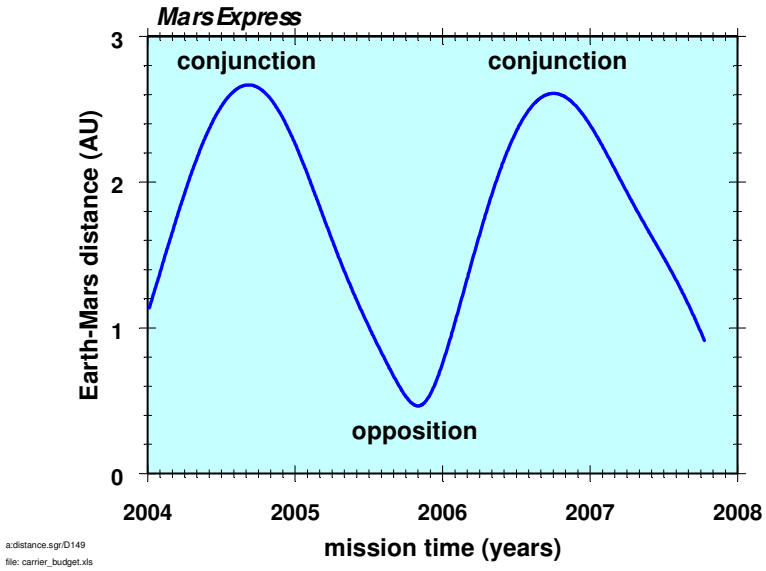

Figure 5.2-1: Earth-Mars distance in AU as a function of mission time. At largest distances of 2.6 AU Mars is in superior solar conjunction and the communication link is also affected by the propagation of the radio signal through the solar corona.

Table 5.2-1: Parameters for Mars Express radio link budget calculation.

Distance Groundstation to Satellite	AU	2,00	2,00
Distance Groundstation to Satellite	m	2,99E+11	2,99E+11
Bitrate Uplink	Bit/s	16	16
Bitrate Downlink	Bit/s	500	32000
Bit Errorrate Uplink		1E-12	1E-12
Required Eb/No Uplink	dB	16,00	16,00
Bit Errorrate Downlink		1E-05	1E-05
Required Eb/No Downlink	dB	9,60	9,60
Ranging Effective Bandwidth	Hz	1E+06	1E+06
Boltzmann-Constant	dBm/K*Hz	-198,60	-198,60
Frequencies Uplink	GHz	2,10	7,10
Frequencies Downlink	GHz	2,30	8,40
Path Loss Uplink	dB	-268,41	-278,99
Path Loss Downlink	dB	-269,20	-280,45
Atmospheric Loss	dB	-0,20	-0,20
Ground-Station Data:			
Antenna Diameter	m	32,00	32,00
Ground Station Antenna Gain Uplink	dBi	53,48	64,06
Ground Station Antenna Gain Downlink	dBi	55,75	67,00
3 dB angle uplink	deg	0,31	0,09
3 dB angle downlink	deg	0,29	0,08
G/T	dBi/K	37,24	49,08
Pointing Loss	dB	-0,10	-0,10
Transmitter Power [W]	W	20000	2000
Transmitter Power [dBmW]	dBmW	73,01	63,01
Ground Station Losses	dB	-0,50	-0,50
Carrier Loop Bandwidth	Hz	3	30
Subcarrier Loop Bandwidth	Hz	10	10
System Noise Temp., clear sky	K	71,0	62,0
System Noise Temp., clear sky	dBK	18,51	17,92
Noise Power Density	dBmW/Hz	-180,09	-180,68
Spacecraft Data:			
Antenna Diameter	m	1,73	1,73
Satellite Antenna Gain Uplink	dBi	28,60	39,18
Satellite Antenna Gain Downlink	dBi	29,56	41,43
3 dB angle uplink	deg		
3 dB angle downlink	deg		
G/T	dBi/K	5,81	14,40
Pointing Loss	dB	0,00	0,00
Transmitter Power	W	5,0	65,0
Transmitter Power	dBmW	36,99	48,13
On-Board Losses	dB	-5,50	-3,00
Carrier Loop Bandwidth	Hz	30	30
Subcarrier Loop Bandwidth	Hz	30	30
System Noise Temp. incl. Sky Noise	K	190	300
Noise Power Density	dBmW/Hz	-175,81	-173,83

5.2.1 MEX radio uplink budget; carrier only

Table 5.2-2: Mars Express radio uplink budget for radio carrier only (no modulation)

	GHz	***2,10***	***7,10***
Transmitter Power [dBmW]	dBmW	73,01	63,01
Ground Station Losses	dB	-0,50	-0,50
Pointing Loss	dB	-0,10	-0,10
Ground Station Antenna Gain Uplink	dBi	53,48	64,06
EIRP	dBmW	**125,89**	**126,47**
Atmospheric Loss	dB	-0,20	-0,20
Path Loss Uplink	dB	-268,41	-278,99
Satellite Antenna Gain Uplink	dBi	28,60	39,18
Pointing Loss	dB	0,00	0,00
On-Board Losses	dB	-5,50	-3,00
Total Received Power	dBmW	**-119,62**	**-116,54**
Noise Power Density	dBmW/Hz	-175,81	-173,83
Available C/No	**dBHz**	**56,19**	**57,29**
Carrier Locking			
Ranging Mod. Index rad pk	rad	0,00	0,00
Modulation Loss	dB	0,00	0,00
Receiver Loss	dB	-1,50	-1,50
Available Carrier Power	dBmW	**-121,12**	**-118,04**
Noise Power Density	dBmW/Hz	-175,81	-173,83
Carrier Loop Bandwidth	dBHz	14,77	14,77
Noise Power in Loop Bandwidth	dBmW	**-161,04**	**-159,06**
Carrier S/N	dB	39,92	41,02
Required S/N	dB	10,00	10,00
Margin Carrier Loop	dB	**29,92**	**31,02**

5.2.2 MEX radio downlink budget; carrier only (no modulation)

Assumptions for Table 5.2-3

- Geocentric distance is 2 AU
- Ground station is 35 m New Norcia
- No ranging modulation on either carrier
- No telemetry modulation on either carrier
- Required S/N is 17 dB

SNR for varying geocentric distances is shown in Figure 5.2-3.

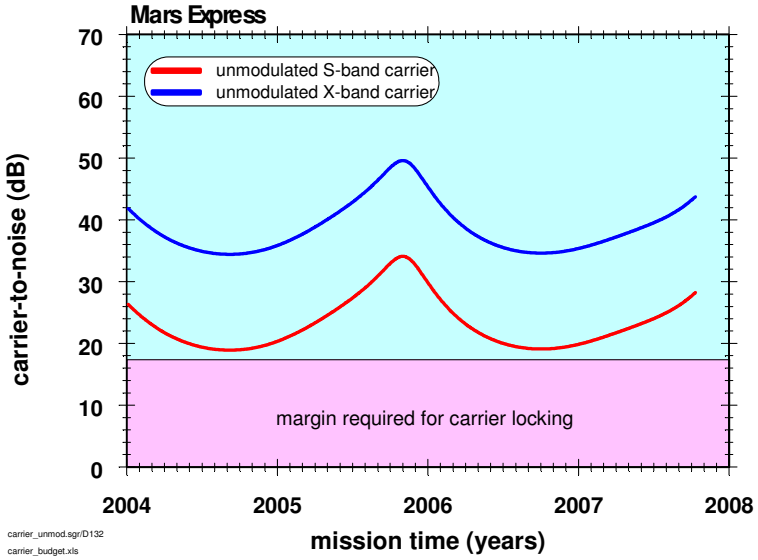

Figure 5.2-2: carrier-to-noise of unmodulated S-band and X-band carriers as a function of mission time

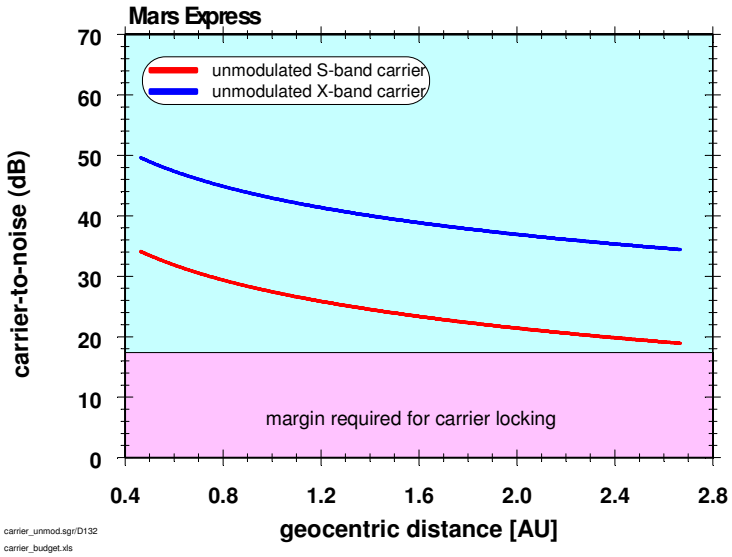

Figure 5.2-3: carrier-to-noise of unmodulated S-band and X-band carriers as a function of geocentric distance

Table 5.2-3: MEX radio downlink budget, carrier only (no modulation)

	GHz	***2,30***	***8,40***
Transmitter Power	dBmW	36,99	48,13
On-Board Losses	dB	-5,50	-3,00
Pointing Loss	dB	0,00	0,00
Satellite Antenna Gain Downlink	dBi	29,56	41,43
EIRP	dBmW	**61,05**	**86,56**
Path Loss Downlink	dB	-269,20	-280,45
Atmospheric Loss	dB	-0,20	-0,20
Ground Station Antenna Gain Downlink	dBi	55,75	67,00
Pointing Loss	dB	-0,10	-0,10
Ground Station Losses	dB	-0,50	-0,50
Total received Power	dBmW	**-153,20**	**-127,69**
Noise Power Density	dBmW/Hz	-180,09	-180,68
Available C/No	**dBHz**	**26,89**	**52,99**
Carrier Locking			
TLM Mod. Index rad pk	rad	0,00	0
Ranging Mod. Index rad pk	rad	0,00	0,00
Noise Mod. Index rad rms	rad	0,00	0,00
Mod. Loss	dB	0,00	0,00
Receiver Loss	dB	-1,50	-1,50
Available Carrier Power	dBmW	**-154,70**	**-129,19**
Noise Power Density	dBmW/Hz	-180,09	-180,68
Carrier Loop Bandwidth	dBHz	4,77	14,77
Noise Power in Loop Bandwidth	dBmW	**-175,32**	**-165,90**
Carrier S/N	dB	20,62	36,72
Required S/N	dB	17,00	17,00
Margin Carrier Loop	dB	**3,62**	**19,72**

5.2.3 MEX radio downlink budget with ranging and telemetry on both carriers

Assumptions for both Table 5.2-4 and Table 5.2-5 are

- Geocentric distance is 2 AU
- Ground station is 35 m New Norcia
- Ranging modulation index is 0.12 radian at X-band and 0.26 radian at S-band
- Telemetry modulation index is 1.0 radian at X-band
- No telemetry modulation at S-band

Table 5.2-4 and Table 5.2-5 give the ranging channel and the data channel, respectively.

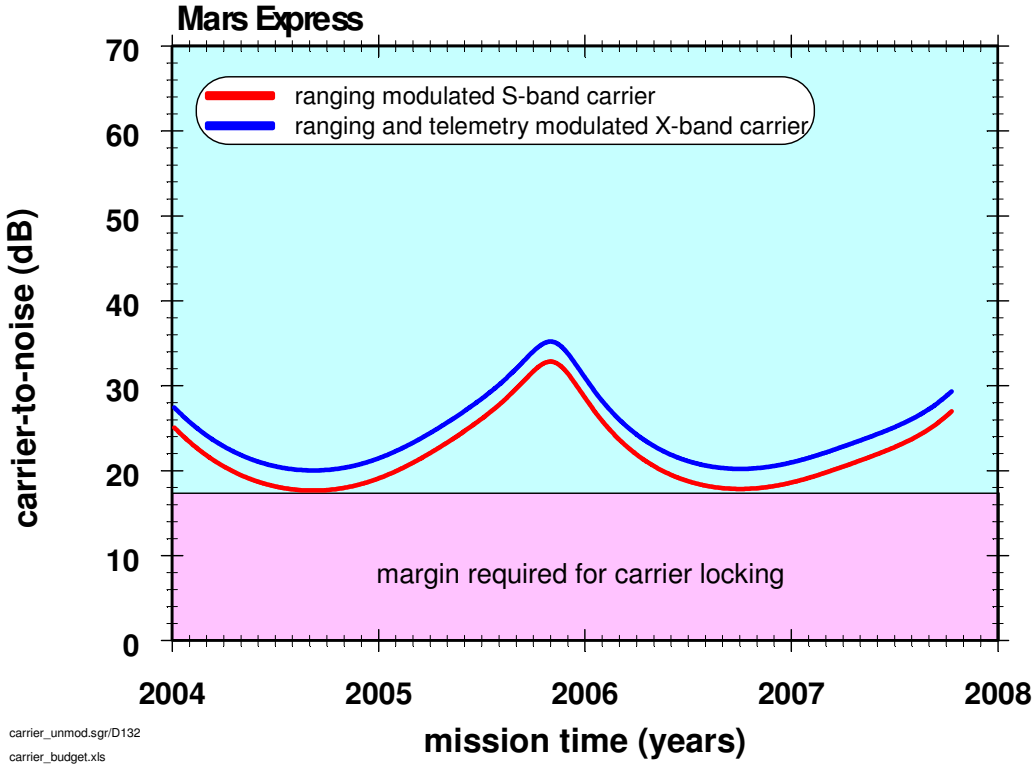

Figure 5.2-4: Carrier-to-noise for modulated X-band and S-band carriers as a function of mission time

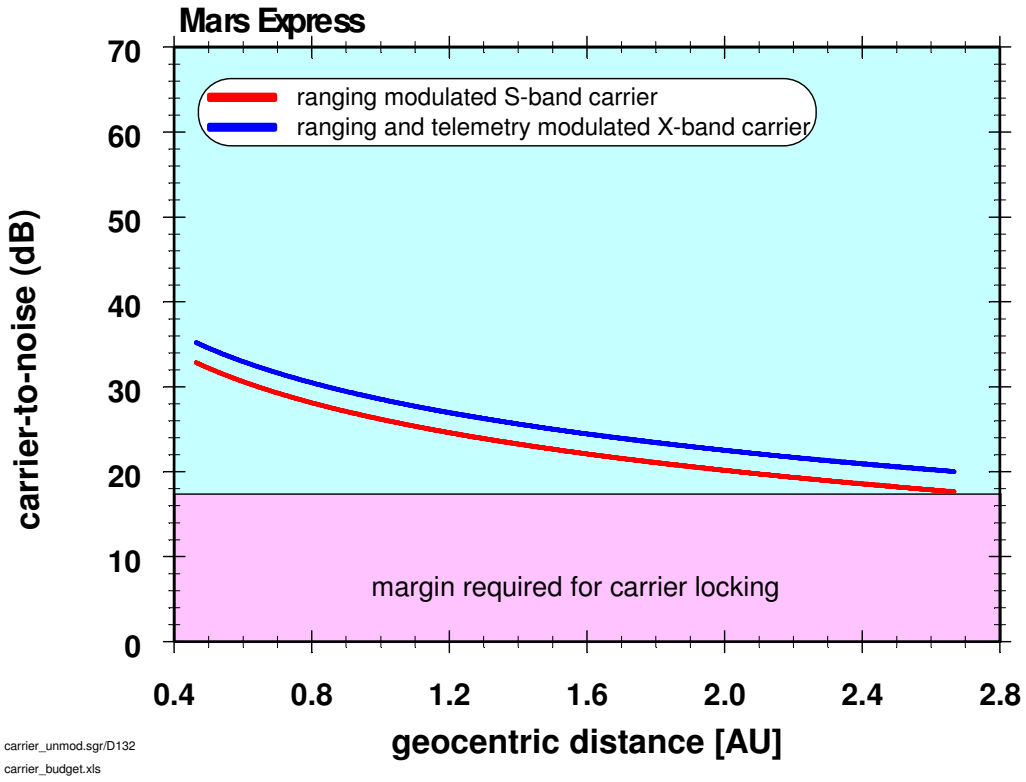

Figure 5.2-5: Carrier-to-noise for modulated X-band and S-band carriers as a function of geocentric distance

Table 5.2-4: MEX radio downlink budget with MPTS ranging on both carriers, telemetry modulation on X-band subcarrier and no modulation on S-band, Ranging channel shown

	GHz		***2,30***	***8,40***
Transmitter Power	dBmW		36,99	48,13
On-Board Losses	dB		-5,50	-3,00
Pointing Loss	dB		0,00	0,00
Satellite Antenna Gain Downlink	dBi		29,56	41,43
EIRP	dBmW		**61,05**	**86,56**
Path Loss Downlink	dB		-269,20	-280,45
Atmospheric Loss	dB		-0,20	-0,20
Ground Station Antenna Gain Downlink	dBi		55,75	67,00
Pointing Loss	dB		-0,10	-0,10
Ground Station Losses	dB		-0,50	-0,50
Total received Power	dBmW		**-153,20**	**-127,69**
Noise Power Density	dBmW/Hz		-180,09	-180,68
Available C/No	**dBHz**		**26,89**	**52,99**
Carrier Locking				
TLM Mod. Index rad pk	rad		0,00	1
Ranging Mod. Index rad pk	rad		0,26	0,12
Noise Mod. Index rad rms	rad		0,46	0,19
Mod. Loss	dB		-1,25	-5,58
Receiver Loss	dB		-1,50	-1,50
Available Carrier Power	dBmW		**-155,95**	**-134,76**
Noise Power Density	dBmW/Hz		-180,09	-180,68
Carrier Loop Bandwidth	dBHz		4,77	14,77
Noise Power in Loop Bandwidth	dBmW		**-175,32**	**-165,90**
Carrier S/N	dB		19,37	31,14
Required S/N	dB		17,00	17,00
Margin Carrier Loop	dB		**2,37**	**14,14**
Ranging Channel				
Modulation Loss	dB		-12,74	-23,65
Degradation	dB		-1,00	-1,00
Available Signal Power	dBmW		**-166,93**	**-152,34**
Noise Power Density	dBmW/Hz		-180,09	-180,68
Ranging Effective Bandwidth	dBHz		60,00	60,00
Noise Power in Bandwidth	dBmW		**-120,09**	**-120,68**
Available S/No	dBHz		13,15	28,34
Required S/No	dBHz		-10,00	-10,00
Margin Ranging	dB		**23,15**	**38,34**

Table 5.2-5: MEX radio downlink budget with MPTS ranging on both carriers, telemetry modulation on X-band subcarrier and no telemetry modulation on S-band, data channel shown

	GHz		***2,30***	***8,40***
Transmitter Power	dBmW		36,99	48,13
On-Board Losses	dB		-5,50	-3,00
Pointing Loss	dB		0,00	0,00
Satellite Antenna Gain Downlink	dBi		29,56	41,43
EIRP	dBmW		**61,05**	**86,56**
Path Loss Downlink	dB		-269,20	-280,45
Atmospheric Loss	dB		-0,20	-0,20
Ground Station Antenna Gain Downlink	dBi		55,75	67,00
Pointing Loss	dB		-0,10	-0,10
Ground Station Losses	dB		-0,50	-0,50
Total received Power	dBmW		**-153,20**	**-127,69**
Noise Power Density	dBmW/Hz		-180,09	-180,68
Available C/No	**dBHz**		**26,89**	**52,99**
Carrier Locking				
TLM Mod. Index rad pk	rad		0	1
Ranging Mod. Index rad pk	rad		0,26	0,12
Noise Mod. Index rad rms	rad		0,46	0,19
Modulation Loss	dB		-1,25	-5,58
Receiver Loss	dB		-1,50	-1,50
Available Carrier Power	dBmW		**-155,95**	**-134,76**
Noise Power Density	dBmW/Hz		-180,09	-180,68
Carrier Loop Bandwidth	dBHz		4,77	14,77
Noise Power in Loop Bandwidth	dBmW		**-175,32**	**-165,90**
Carrier S/N	dB		19,37	31,14
Required S/N	dB		17,00	17,00
Margin Carrier Loop	dB		**2,37**	**14,14**
Data Channel			No Data	
Modulation Loss	dB			-1,73
Degradation	dB			-1,00
Available Signal Power	dBmW			**-130,42**
Noise Power Density	dBmW/Hz			-180,68
Bitrate	dBHz			45,05
Noise Power in Bitrate	dBmW			**-135,62**
Available Eb/No	dB			5,21
Required Eb/No (10E-5)	dB			9,60
Margin Data (no Coding)	dB			**-4,39**
Coding Gain (Convolutional Coding)	dB			4,50
Margin Data (including Coding)	dB			**0,11**

5.2.4 MEX radio downlink budget with telemetry modulation on X-band carrier

Assumption for Table 5.2-1

- Geocentric distance is 2 AU
- Ground station is 35 m New Norcia
- No ranging modulation
- Telemetry modulation index is 1.0 radian at X-band
- No telemetry modulation at S-band

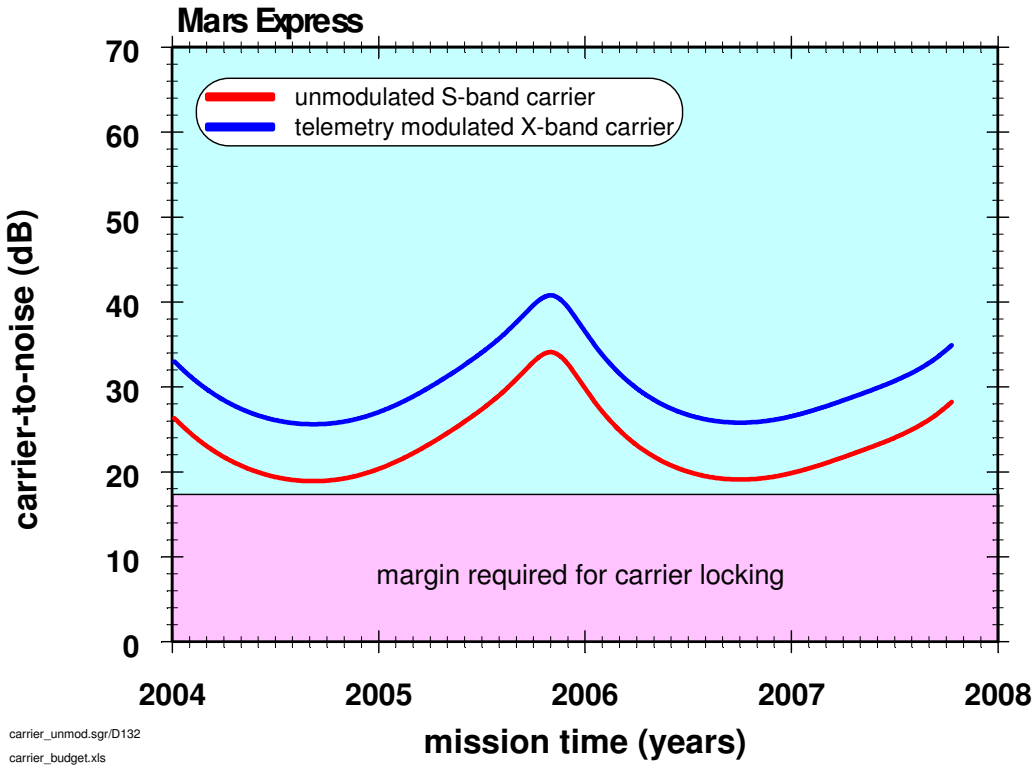

Figure 5.2-6: carrier-to-noise for an unmodulated S-band carrier and telemetry modulated X-band carrier as a function of misison time.

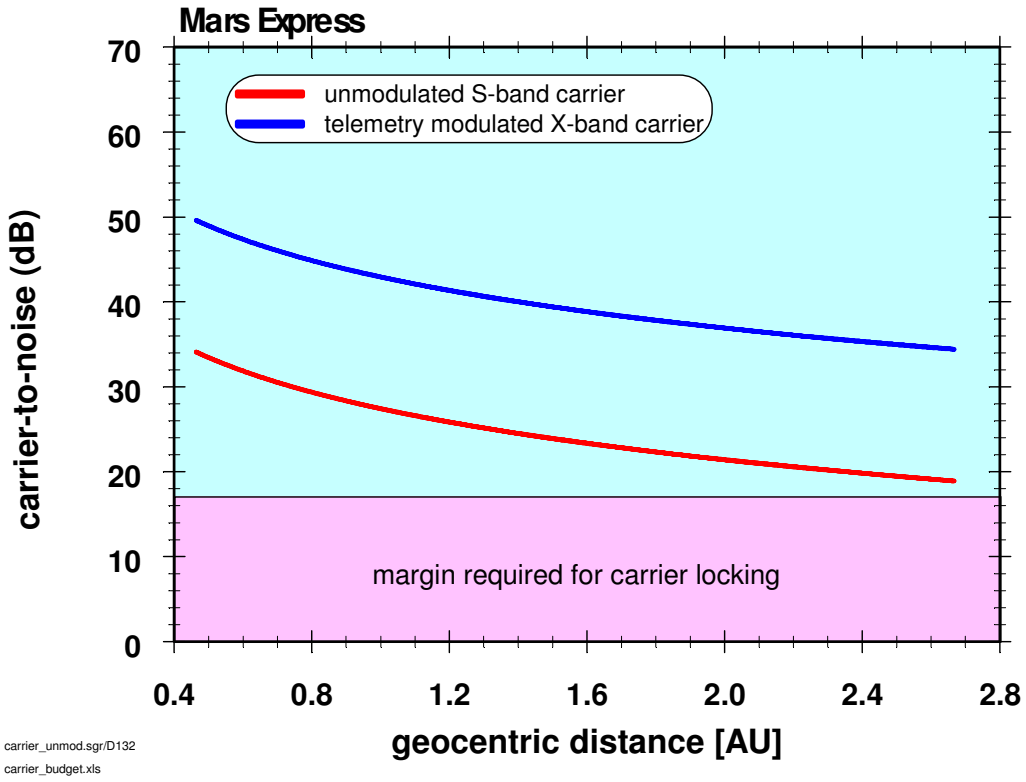

Figure 5.2-7: carrier-to-noise for an unmodulated S-band carrier and telemetry modulated X-band carrier as a function of geocentric distance.

Table 5.2-6: MEX radio downlink budget with telemetry modulation on X-band and no telemetry modulation on S-band. No ranging modulation on both carriers

	GHz		***2,30***	***8,40***
Transmitter Power	dBmW		36,99	48,13
On-Board Losses	dB		-5,50	-3,00
Pointing Loss	dB		0,00	0,00
Satellite Antenna Gain Downlink	dBi		29,56	41,43
EIRP	dBmW		**61,05**	**86,56**
Path Loss Downlink	dB		-269,20	-280,45
Atmospheric Loss	dB		-0,20	-0,20
Ground Station Antenna Gain Downlink	dBi		55,75	67,00
Pointing Loss	dB		-0,10	-0,10
Ground Station Losses	dB		-0,50	-0,50
Total received Power	dBmW		**-153,20**	**-127,69**
Noise Power Density	dBmW/Hz		-180,09	-180,68
Available C/No	**dBHz**		**26,89**	**52,99**
Carrier Locking				
TLM Mod. Index rad pk	rad		0	1,2
Modulation Loss	dB		0,00	-8,82
Receiver Loss	dB		-1,50	-1,50
Available Carrier Power	dBmW		**-154,70**	**-138,00**
Noise Power Density	dBmW/Hz		-180,09	-180,68
Carrier Loop Bandwidth	dBHz		4,77	14,77
Noise Power in Loop Bandwidth	dBmW		**-175,32**	**-165,90**
Carrier S/No	dBHz		25,39	42,67
Carrier S/N	dB		20,62	27,90
Required S/N	dB		17,00	17,00
Margin Carrier Loop	dB		**3,62**	**10,90**
Data Channel			No Data	
Modulation Loss Telemetry	dB			-0,61
Degradation	dB			-1,00
Available Signal Power	dBmW			**-129,30**
Noise Power Density	dBmW/Hz			-180,68
Bitrate	dBHz			45,05
Noise Power in Bitrate	dBmW			**-135,62**
Available Eb/No	dB			6,33
Required Eb/No (10E-5)	dB			9,60
Margin Data (no Coding)	dB			**-3,27**
Coding Gain (Convolutional Coding)	dB			4,50
Margin Data (including Coding)	dB			**1,23**

5.2.5 Bistatic Radar downlink budget

The bistatic radar downlink budget was computed for six cases. Table 5.2-7 to Table 5.2-9 give the received echo power and echo detectability at X-band for an Earth-Mars distance of 0.5 AU, 1.0 AU and 1.5 AU, respectively, when the spacecraft is at four positions (altitudes 250 km, 1,000 km, 5,000 km and 10,000 km) in its orbit. In each case a bistatic backscatter geometry is assumed -- nadir pointing spacecraft antenna and normal incidence on a spherical dielectric surface with Fresnel reflectivity 0.06. For a nominal 0.1 radian (5.7 deg) rms surface roughness, all echoes are beam-limited -- that is, the narrow spacecraft antenna beam fails to illuminate all of the surface that could potentially contribute to the echo (by a factor of over 100 in the first case). In the fifth case (far right column), the rms roughness was reduced to 0.025 radian, and the echo is no longer beam-limited. Detectability is the effective signal-to-noise ratio for a 'yes-no' echo detector based on sampling all 1 Hz frequency bins expected to have an echo once each second. Many additional parameters can affect echo power, such as incidence angle and surface dielectric constant; the values assumed here are conservative.
Table 5.2-10 to Table 5.2-12 repeat the calculations for S-band bistatic radar

5.2.5.1 Bistatic radar link budgets

X-Band MaRS Bistatic Radar 0.5 AU							
constant (pi)	π		3.141593	3.141593	3.141593	3.141593	3.141593
reference frequency	f0	Hz	8.40E+09	8.40E+09	8.40E+09	8.40E+09	8.40E+09
reference wavelength	λ0	m	3.57E-02	3.57E-02	3.57E-02	3.57E-02	3.57E-02
gravitational constant	G		6.67E-11	6.67E-11	6.67E-11	6.67E-11	6.67E-11
Mars mass	M	kg	6.44E+23	6.44E+23	6.44E+23	6.44E+23	6.44E+23
orbit semi-major axis	a	m	9272000	9272000	9272000	9272000	9272000
Mars radius	Rp	m	3397000	3397000	3397000	3397000	3397000
rms surface roughness	ζ	rad	0.1	0.1	0.1	0.1	0.025
Earth-Mars distance	∈	AU	0.50				
Earth-Mars distance	Rr	m	7.48E+10	7.48E+10	7.48E+10	7.48E+10	7.48E+10
operating frequency	f	Hz	8.40E+09	8.40E+09	8.40E+09	8.40E+09	8.40E+09
operating wavelength	λ	m	3.57E-02	3.57E-02	3.57E-02	3.57E-02	3.57E-02
transmit power	Pt	dBm	48.13	48.13	48.13	48.13	48.13
HGA gain	Gt	dB	41.43	41.43	41.43	41.43	41.43
HGA HPHBW		rad	0.0133	0.0133	0.0133	0.0133	0.0133
EIRP		dBm	89.56	89.56	89.56	89.56	89.56
altitude	h	m	250000	1000000	5000000	10000000	10000000
radial distance	r	m	3647000	4397000	8397000	13397000	13397000
space loss to Mars		dB	-142.23	-143.86	-149.47	-153.53	-153.53
perfect sphere RCS	σ	dB	141.04	139.83	137.56	136.77	136.77
spacecraft velocity	v	m/s	4350.11	3860.76	2366.06	1334.11	1334.11
specular point velocity	V	m/s	4051.92	2982.72	957.19	338.28	338.28
Fjeldbo bandwidth	BW f	Hz	37782.54	27812.69	8925.41	3154.36	788.59
beam-limited bandwidth	BW a	Hz	3245.70	2880.59	1765.36	995.41	995.41
HGA footprint (diameter)	L	m	6661.8	26647.1	133235.5	266471.0	266471.0
beam-limiting reduction		dB	-21.32	-19.70	-14.08	-10.02	0.00
Fresnel reflectivity	ρ	dB	-12.22	-12.22	-12.22	-12.22	-12.22
space loss to Earth		dB	-228.47	-228.47	-228.47	-228.47	-228.47
receive gain	Gr	dB	74.20	74.20	74.20	74.20	74.20
gain to aperture factor		dB	-39.94	-39.94	-39.94	-39.94	-39.94

receive aperture	Ar	dB	34.26	34.26	34.26	34.26	34.26
echo received power	Pr	dBm	-139.38	-140.58	-142.86	-143.64	-133.63
system temperature	Tsys	K	30.00	30.00	30.00	30.00	30.00
echo received power density		**dBm/Hz**	**-174.49**	**-175.18**	**-175.33**	**-173.62**	**-162.59**
noise power density	**Pn**	**dBm/Hz**	**-183.83**	**-183.83**	**-183.83**	**-183.83**	**-183.83**
direct signal received power	Pd	dBm	-104.65	-104.65	-104.65	-104.65	-104.65
direct signal SNR	SNR0	dB	79.18	79.18	79.18	79.18	79.18
echo SNR per bin		**dB**	**9.34**	**8.65**	**8.50**	**10.21**	**21.24**
echo detectability (1 sec)		**dB**	**26.90**	**25.95**	**24.74**	**25.20**	**35.72**

Table 5.2-7: Bistatic radar Link Budget for Earth-Mars distance of 0.5 AU

X-Band MaRS Bistatic Radar 1 AU

constant (pi)	π		3.141593	3.141593	3.141593	3.141593	3.141593
reference frequency	f0	Hz	8.40E+09	8.40E+09	8.40E+09	8.40E+09	8.40E+09
reference wavelength	λ0	m	3.57E-02	3.57E-02	3.57E-02	3.57E-02	3.57E-02
gravitational constant	G		6.67E-11	6.67E-11	6.67E-11	6.67E-11	6.67E-11
Mars mass	M	kg	6.44E+23	6.44E+23	6.44E+23	6.44E+23	6.44E+23
orbit semi-major axis	a	m	9272000	9272000	9272000	9272000	9272000
Mars radius	Rp	m	3397000	3397000	3397000	3397000	3397000
rms surface roughness	ζ	rad	0.1	0.1	0.1	0.1	0.025
Earth-Mars distance	$\in$	AU	1.00				
Earth-Mars distance	Rr	m	1.50E+11	1.50E+11	1.50E+11	1.50E+11	1.50E+11
operating frequency	f	Hz	8.40E+09	8.40E+09	8.40E+09	8.40E+09	8.40E+09
operating wavelength	λ	m	3.57E-02	3.57E-02	3.57E-02	3.57E-02	3.57E-02
transmit power	Pt	dBm	48.13	48.13	48.13	48.13	48.13
HGA gain	Gt	dB	41.43	41.43	41.43	41.43	41.43
HGA HPHBW		rad	0.0133	0.0133	0.0133	0.0133	0.0133
ERP		dBm	89.56	89.56	89.56	89.56	89.56
altitude	h	m	250000	1000000	5000000	10000000	10000000
radial distance	r	m	3647000	4397000	8397000	13397000	13397000
space loss to Mars		dB	-142.23	-143.86	-149.47	-153.53	-153.53
perfect sphere RCS	σ	dB	141.04	139.83	137.56	136.77	136.77
spacecraft velocity	v	m/s	4350.11	3860.76	2366.06	1334.11	1334.11

specular point velocity	V	m/s	4051.92	2982.72	957.19	338.28	338.28
Fjeldbo bandwidth	BWf	Hz	37782.54	27812.69	8925.41	3154.36	788.59
beam-limited bandwidth	BWa	Hz	3245.70	2880.59	1765.36	995.41	995.41
HGA footprint (diameter)	L	m	6661.8	26647.1	133235.5	266471.0	266471.0
beam-limiting reduction		dB	-21.32	-19.70	-14.08	-10.02	0.00
Fresnel reflectivity	ρ	dB	-12.22	-12.22	-12.22	-12.22	-12.22
space loss to Earth		dB	-234.49	-234.49	-234.49	-234.49	-234.49
receive gain	Gr	dB	74.20	74.20	74.20	74.20	74.20
gain to aperture factor		dB	-39.94	-39.94	-39.94	-39.94	-39.94
receive aperture	Ar	dB	34.26	34.26	34.26	34.26	34.26
echo received power	Pr	dBm	-145.40	-146.60	-148.88	-149.66	-139.65
system temperature	Tsys	K	30.00	30.00	30.00	30.00	30.00
echo received power density		**dBm/Hz**	**-180.51**	**-181.20**	**-181.35**	**-179.64**	**-168.61**
noise power density	**Pn**	**dBm/Hz**	**-183.83**	**-183.83**	**-183.83**	**-183.83**	**-183.83**
direct signal received power	Pd	dBm	-110.67	-110.67	-110.67	-110.67	-110.67
direct signal SNR	SNR0	dB	73.16	73.16	73.16	73.16	73.16
echo SNR per bin		**dB**	**3.32**	**2.63**	**2.48**	**4.19**	**15.22**
echo detectability (1 sec)		**dB**	**20.88**	**19.93**	**18.72**	**19.18**	**29.70**

Table 5.2-8: same as Table 5.2-7 for an Earth-Mars distance of 1.0 AU

X-Band MaRS Bistatic Radar 1.5 AU

constant (pi)	π		3.141593	3.141593	3.141593	3.141593	3.141593
reference frequency	f0	Hz	8.40E+09	8.40E+09	8.40E+09	8.40E+09	8.40E+09
reference wavelength	λ0	m	3.57E-02	3.57E-02	3.57E-02	3.57E-02	3.57E-02
gravitational constant	G		6.67E-11	6.67E-11	6.67E-11	6.67E-11	6.67E-11
Mars mass	M	kg	6.44E+23	6.44E+23	6.44E+23	6.44E+23	6.44E+23
orbit semi-major axis	a	m	9272000	9272000	9272000	9272000	9272000
Mars radius	Rp	m	3397000	3397000	3397000	3397000	3397000
rms surface roughness	ζ	rad	0.1	0.1	0.1	0.1	0.025
Earth-Mars distance	∈	AU	1.50				
Earth-Mars distance	Rr	m	2.24E+11	2.24E+11	2.24E+11	2.24E+11	2.24E+11
operating frequency	f	Hz	8.40E+09	8.40E+09	8.40E+09	8.40E+09	8.40E+09
operating wavelength	λ	m	3.57E-02	3.57E-02	3.57E-02	3.57E-02	3.57E-02
transmit power	Pt	dBm	48.13	48.13	48.13	48.13	48.13
HGA gain	Gt	dB	41.43	41.43	41.43	41.43	41.43
HGA HPHBW		rad	0.0133	0.0133	0.0133	0.0133	0.0133
ERP		dBm	89.56	89.56	89.56	89.56	89.56
altitude	h	m	250000	1000000	5000000	10000000	10000000
radial distance	r	m	3647000	4397000	8397000	13397000	13397000
space loss to Mars		dB	-142.23	-143.86	-149.47	-153.53	-153.53
perfect sphere RCS	σ	dB	141.04	139.83	137.56	136.77	136.77
spacecraft velocity	v	m/s	4350.11	3860.76	2366.06	1334.11	1334.11
specular point velocity	V	m/s	4051.92	2982.72	957.19	338.28	338.28
Fjeldbo bandwidth	BWf	Hz	37782.54	27812.69	8925.41	3154.36	788.59
beam-limited bandwidth	BWa	Hz	3245.70	2880.59	1765.36	995.41	995.41
HGA footprint (diameter)	L	m	6661.8	26647.1	133235.5	266471.0	266471.0
beam-limiting reduction		dB	-21.32	-19.70	-14.08	-10.02	0.00
Fresnel reflectivity	ρ	dB	-12.22	-12.22	-12.22	-12.22	-12.22
space loss to Earth		dB	-238.01	-238.01	-238.01	-238.01	-238.01
receive gain	Gr	dB	74.20	74.20	74.20	74.20	74.20
gain to aperture factor		dB	-39.94	-39.94	-39.94	-39.94	-39.94
receive aperture	Ar	dB	34.26	34.26	34.26	34.26	34.26

echo received power	Pr	dBm	-148.92	-150.12	-152.40	-153.19	-143.17
system temperature	Tsys	K	30.00	30.00	30.00	30.00	30.00
echo received power density		**dBm/Hz**	**-184.03**	**-184.72**	**-184.87**	**-183.17**	**-172.14**
noise power density	**Pn**	**dBm/Hz**	**-183.83**	**-183.83**	**-183.83**	**-183.83**	**-183.83**
direct signal received power	Pd	dBm	-114.19	-114.19	-114.19	-114.19	-114.19
direct signal SNR	SNR0	dB	69.64	69.64	69.64	69.64	69.64
echo SNR per bin		**dB**	**-0.20**	**-0.89**	**-1.04**	**0.66**	**11.69**
echo detectability (1 sec)		**dB**	**17.35**	**16.41**	**15.20**	**15.65**	**26.18**

Table 5.2-9 same as Table 5.2-7 for an Earth-Mars distance of 1.5 AU

S-Band MaRS Bistatic Radar at 0.5 AU

constant (pi)	π		3.141593	3.141593	3.141593	3.141593	3.141593
reference frequency	f0	Hz	8.40E+09	8.40E+09	8.40E+09	8.40E+09	8.40E+09
reference wavelength	λ0	m	3.57E-02	3.57E-02	3.57E-02	3.57E-02	3.57E-02
gravitational constant	G		6.67E-11	6.67E-11	6.67E-11	6.67E-11	6.67E-11
Mars mass	M	kg	6.44E+23	6.44E+23	6.44E+23	6.44E+23	6.44E+23
orbit semi-major axis	a	m	9272000	9272000	9272000	9272000	9272000
Mars radius	Rp	m	3397000	3397000	3397000	3397000	3397000
rms surface roughness	ζ	rad	0.1	0.1	0.1	0.1	0.025
Earth-Mars distance	∈	AU	0.50				
Earth-Mars distance	Rr	m	7.48E+10	7.48E+10	7.48E+10	7.48E+10	7.48E+10
operating frequency	f	Hz	2.30E+09	2.30E+09	2.30E+09	2.30E+09	2.30E+09
operating wavelength	λ	m	1.30E-01	1.30E-01	1.30E-01	1.30E-01	1.30E-01
transmit power	Pt	dBm	36.99	36.99	36.99	36.99	36.99
HGA gain	Gt	dB	29.56	29.56	29.56	29.56	29.56
HGA HPHBW		rad	0.0523	0.0523	0.0523	0.0523	0.0523
EIRP		dBm	66.55	66.55	66.55	66.55	66.55
altitude	h	m	250000	1000000	5000000	10000000	10000000
radial distance	r	m	3647000	4397000	8397000	13397000	13397000
space loss to Mars		dB	-142.23	-143.86	-149.47	-153.53	-153.53
perfect sphere RCS	σ	dB	141.04	139.83	137.56	136.77	136.77
spacecraft velocity	v	m/s	4350.11	3860.76	2366.06	1334.11	1334.11
specular point velocity	V	m/s	4051.92	2982.72	957.19	338.28	338.28
Fjeldbo bandwidth	BW f	Hz	10345.22	7615.38	2443.86	863.69	215.92
beam-limited bandwidth	BW a	Hz	3485.44	3093.35	1895.76	1068.93	1068.93
HGA footprint (diameter)	L	m	26127.0	104508.1	522540.4	1045080.8	1045080.8
beam-limiting reduction		dB	-9.45	-7.83	-2.21	0.00	0.00
Fresnel reflectivity	ρ	dB	-12.22	-12.22	-12.22	-12.22	-12.22
space loss to Earth		dB	-228.47	-228.47	-228.47	-228.47	-228.47

receive gain	Gr	dB	62.95	62.95	62.95	62.95	62.95
gain to aperture factor		dB	-28.68	-28.68	-28.68	-28.68	-28.68
receive aperture	Ar	dB	34.26	34.26	34.26	34.26	34.26
echo received power	Pr	dBm	-150.52	-151.72	-154.00	-156.64	-156.64
system temperature	Tsys	K	30.00	30.00	30.00	30.00	30.00
echo received power density		**dBm/Hz**	**-185.94**	**-186.62**	**-186.78**	**-186.00**	**-179.98**
noise power density	**Pn**	**dBm/Hz**	**-183.83**	**-183.83**	**-183.83**	**-183.83**	**-183.83**
direct signal received power	Pd	dBm	-127.66	-127.66	-127.66	-127.66	-127.66
direct signal SNR	SNR0	dB	56.17	56.17	56.17	56.17	56.17
echo SNR per bin		**dB**	**-2.11**	**-2.79**	**-2.95**	**-2.17**	**3.85**
echo detectability (1 sec)		**dB**	**15.60**	**14.66**	**13.44**	**12.51**	**15.52**

Table 5.2-10: same as Table 5.2-7 for an Earth-Mars distance of 1.0 AU

S-Band MaRS Bistatic Radar at 1 AU

constant (pi)	π		3.141593	3.141593	3.141593	3.141593	3.141593
reference frequency	f0	Hz	8.40E+09	8.40E+09	8.40E+09	8.40E+09	8.40E+09
reference wavelength	λ0	m	3.57E-02	3.57E-02	3.57E-02	3.57E-02	3.57E-02
gravitational constant	G		6.67E-11	6.67E-11	6.67E-11	6.67E-11	6.67E-11
Mars mass	M	kg	6.44E+23	6.44E+23	6.44E+23	6.44E+23	6.44E+23
orbit semi-major axis	a	m	9272000	9272000	9272000	9272000	9272000
Mars radius	Rp	m	3397000	3397000	3397000	3397000	3397000
rms surface roughness	ζ	rad	0.1	0.1	0.1	0.1	0.025
Earth-Mars distance	$\in$	AU	1.00				
Earth-Mars distance	Rr	m	1.50E+11	1.50E+11	1.50E+11	1.50E+11	1.50E+11
operating frequency	f	Hz	2.30E+09	2.30E+09	2.30E+09	2.30E+09	2.30E+09
operating wavelength	λ	m	1.30E-01	1.30E-01	1.30E-01	1.30E-01	1.30E-01
transmit power	Pt	dBm	36.99	36.99	36.99	36.99	36.99
HGA gain	Gt	dB	29.56	29.56	29.56	29.56	29.56
HGA HPHBW		rad	0.0523	0.0523	0.0523	0.0523	0.0523
EIRP		dBm	66.55	66.55	66.55	66.55	66.55
altitude	h	m	250000	1000000	5000000	10000000	10000000
radial distance	r	m	3647000	4397000	8397000	13397000	13397000
space loss to Mars		dB	-142.23	-143.86	-149.47	-153.53	-153.53
perfect sphere RCS	σ	dB	141.04	139.83	137.56	136.77	136.77
spacecraft velocity	v	m/s	4350.11	3860.76	2366.06	1334.11	1334.11
specular point velocity	V	m/s	4051.92	2982.72	957.19	338.28	338.28
Fjeldbo bandwidth	BW f	Hz	10345.22	7615.38	2443.86	863.69	215.92
beam-limited bandwidth	BW a	Hz	3485.44	3093.35	1895.76	1068.93	1068.93
HGA footprint (diameter)	L	m	26127.0	104508.1	522540.4	1045080.8	1045080.8
beam-limiting reduction		dB	-9.45	-7.83	-2.21	0.00	0.00
Fresnel reflectivity	ρ	dB	-12.22	-12.22	-12.22	-12.22	-12.22
space loss to Earth		dB	-234.49	-234.49	-234.49	-234.49	-234.49

receive gain	Gr	dB	62.95	62.95	62.95	62.95	62.95
gain to aperture factor		dB	-28.68	-28.68	-28.68	-28.68	-28.68
receive aperture	Ar	dB	34.26	34.26	34.26	34.26	34.26
echo received power	Pr	dBm	-156.54	-157.74	-160.02	-162.66	-162.66
system temperature	Tsys	K	30.00	30.00	30.00	30.00	30.00
echo received power density		**dBm/Hz**	**-191.96**	**-192.65**	**-192.80**	**-192.02**	**-186.00**
noise power density	**Pn**	**dBm/Hz**	**-183.83**	**-183.83**	**-183.83**	**-183.83**	**-183.83**
direct signal received power	Pd	dBm	-133.68	-133.68	-133.68	-133.68	-133.68
direct signal SNR	SNR0	dB	50.15	50.15	50.15	50.15	50.15
echo SNR per bin		**dB**	**-8.13**	**-8.82**	**-8.97**	**-8.19**	**-2.17**
echo detectability (1 sec)		**dB**	**9.58**	**8.64**	**7.42**	**6.49**	**9.50**

Table 5.2-11: same as Table 5.2-7 for an Earth-Mars distance of 1.0 AU

S-Band MaRS Bistatic Radar at 1.5 AU							
constant (pi)	π		3.141593	3.141593	3.141593	3.141593	3.141593
reference frequency	f0	Hz	8.40E+09	8.40E+09	8.40E+09	8.40E+09	8.40E+09
reference wavelength	λ0	m	3.57E-02	3.57E-02	3.57E-02	3.57E-02	3.57E-02
gravitational constant	G		6.67E-11	6.67E-11	6.67E-11	6.67E-11	6.67E-11
Mars mass	M	kg	6.44E+23	6.44E+23	6.44E+23	6.44E+23	6.44E+23
orbit semi-major axis	a	m	9272000	9272000	9272000	9272000	9272000
Mars radius	Rp	m	3397000	3397000	3397000	3397000	3397000
rms surface roughness	ζ	rad	0.1	0.1	0.1	0.1	0.025
Earth-Mars distance	$\in$	AU	1.50				
Earth-Mars distance	Rr	m	2.24E+11	2.24E+11	2.24E+11	2.24E+11	2.24E+11
operating frequency	f	Hz	2.30E+09	2.30E+09	2.30E+09	2.30E+09	2.30E+09
operating wavelength	λ	m	1.30E-01	1.30E-01	1.30E-01	1.30E-01	1.30E-01
transmit power	Pt	dBm	36.99	36.99	36.99	36.99	36.99
HGA gain	Gt	dB	29.56	29.56	29.56	29.56	29.56
HGA HPHBW		rad	0.0523	0.0523	0.0523	0.0523	0.0523
EIRP		dBm	66.55	66.55	66.55	66.55	66.55

altitude	h	m	250000	1000000	5000000	10000000	10000000
radialdistance	r	m	3647000	4397000	8397000	13397000	13397000
space loss to Mars		dB	-142.23	-143.86	-149.47	-153.53	-153.53
perfect sphere RCS	σ	dB	141.04	139.83	137.56	136.77	136.77
spacecraft velocity	v	m/s	4350.11	3860.76	2366.06	1334.11	1334.11
specular point velocity	V	m/s	4051.92	2982.72	957.19	338.28	338.28
Fjeldbo bandwidth	BW f	Hz	10345.22	7615.38	2443.86	863.69	215.92
beam-limited bandwidth	BW a	Hz	3485.44	3093.35	1895.76	1068.93	1068.93
HGA footprint (diameter)	L	m	26127.0	1045081	5225404	10450808	10450808
beam-limiting reduction		dB	-9.45	-7.83	-2.21	0.00	0.00
Fresnel reflectivity	ρ	dB	-12.22	-12.22	-12.22	-12.22	-12.22
space loss to Earth		dB	-238.01	-238.01	-238.01	-238.01	-238.01
receive gain	Gr	dB	62.95	62.95	62.95	62.95	62.95
gain to aperture factor		dB	-28.68	-28.68	-28.68	-28.68	-28.68
receive aperture	Ar	dB	34.26	34.26	34.26	34.26	34.26
echo received power	Pr	dBm	-160.06	-161.26	-163.54	-166.18	-166.18
system temperature	Tsys	K	30.00	30.00	30.00	30.00	30.00
echo received power density		**DBm/Hz**	**-195.48**	**-196.17**	**-196.32**	**-195.54**	**-189.52**
noise power density	**Pn**	**DBm/Hz**	**-183.83**	**-183.83**	**-183.83**	**-183.83**	**-183.83**
direct signal received power	Pd	dBm	-137.20	-137.20	-137.20	-137.20	-137.20
direct signal SNR	SNR0	dB	46.63	46.63	46.63	46.63	46.63
echo SNR per bin		**dB**	**-11.65**	**-12.34**	**-12.49**	**-11.71**	**-5.69**
echo detectability (1 sec)		**dB**	**6.06**	**5.12**	**3.90**	**2.97**	**5.98**

Table 5.2-12: same as Table 5.2-7 for an Earth-Mars distance of 1.0 AU

5.3 Functions: Ground Segment

5.3.1 New Norcia Ground Station

5.3.1.1 Overview IFMS

The New Norcia ground station, Australia, is equipped with two standard (operational) IFMSs and a third IFMS unit dedicated to the Radio Science observations
The dedicated Radio Science IFMS has to fulfill the requirements of the Radio Science experiments; it can however serve also as a complementary and redundant unit for ESA´s prime IFMS receiving units.

5.3.1.2 System Description

Each IFMS provides the following functions (MEX-MRS-IGM-RS-3014):

1. Two polarizations can be analyzed by one IFMS
2. Two downlink carriers at S-band and X-band can be received simultaneously, only one carrier will be modulated with telemetry
3. One, alternatively also two downlink carriers modulated with ranging signals can be received
4. Radio science open-loop measurements will be carried out simultaneously at S- and X-band[3]

The IFMS block diagram is shown in Figure 5.3-1. The configuration change from standard CL configuration to OL configuration will not involve any hardware changes. A schematic including the digital signal processing part relevant for MaRS is shown in Figure 5.3-3.

[3] There is the certain risk that there is no G/S equipment redundancy when performing radio science observations. The IFMS can quickly be reconfigured in the case of problems, so that that risk can be tolerated.

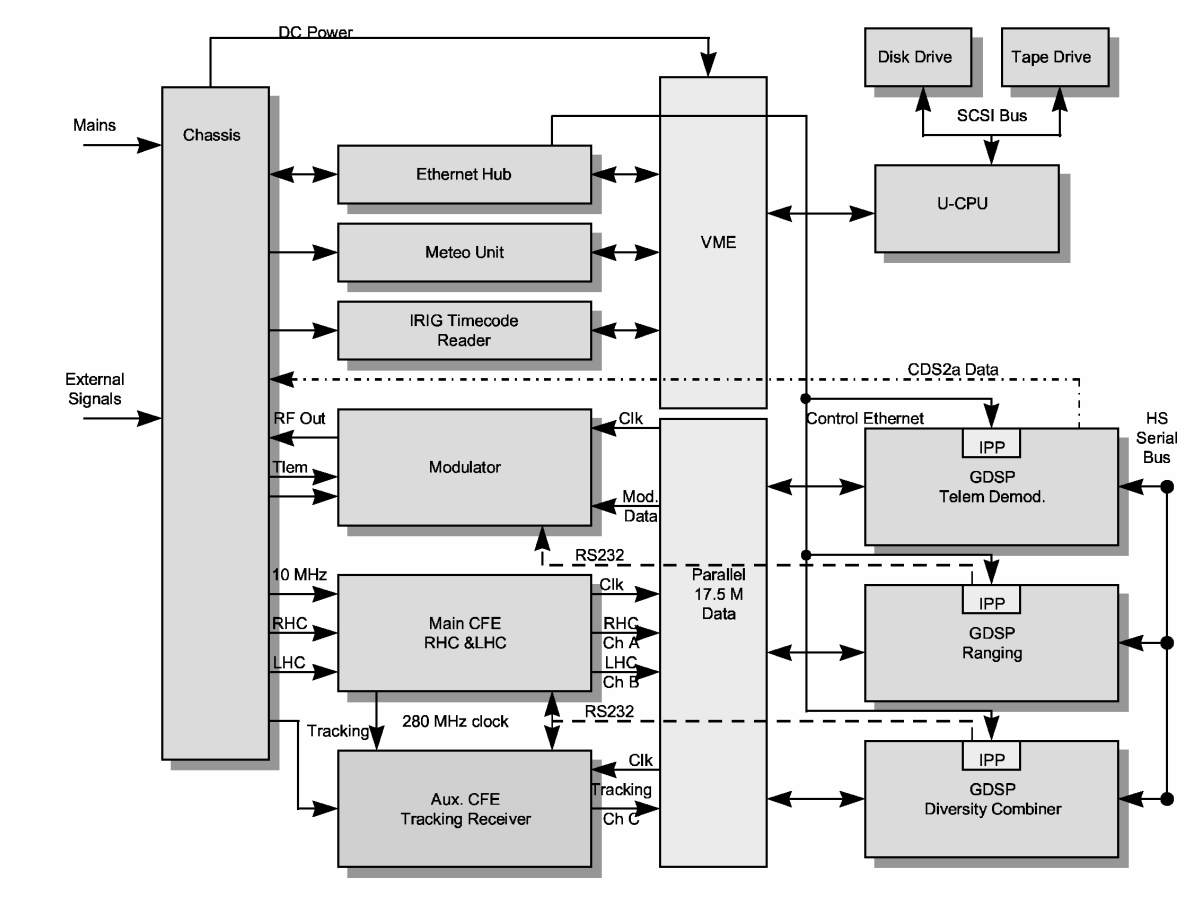

Figure 5.3-1: IFMS block diagram

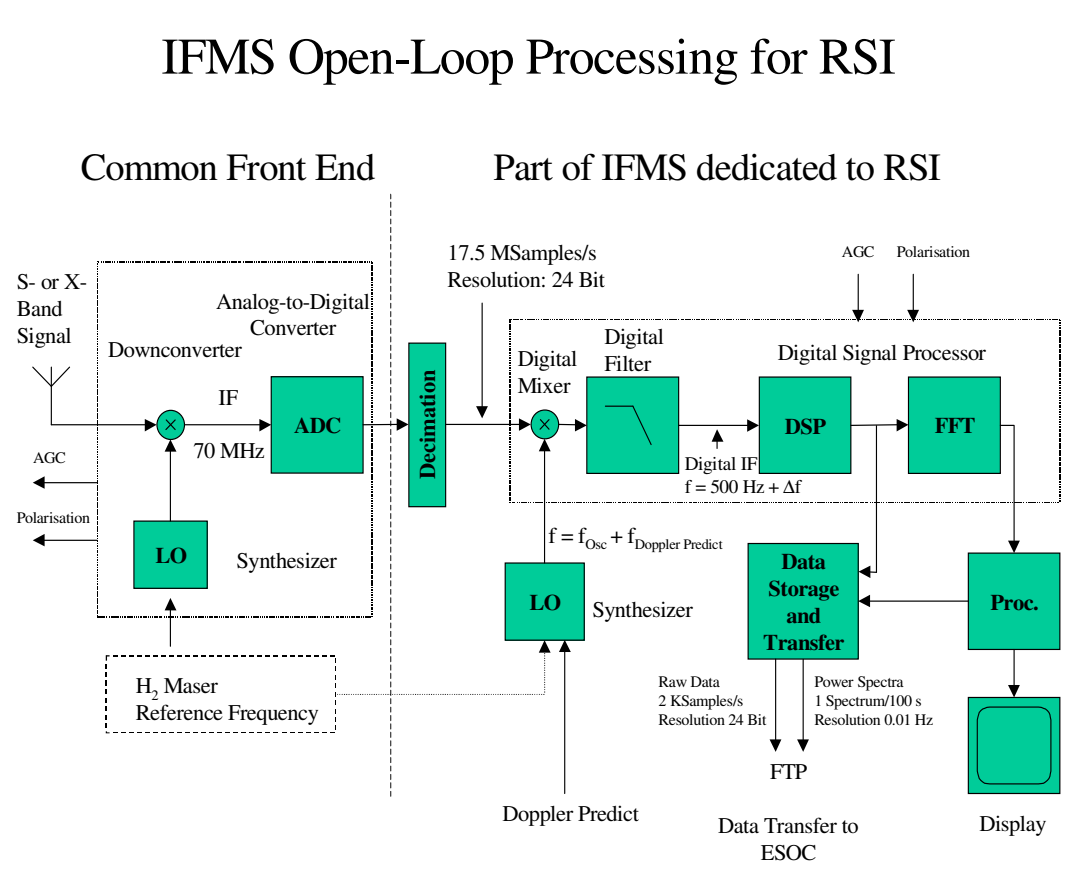

Figure 5.3-2: IFMS Open-Loop Digital Data Processing Part for Mars

It is assumed that the IFMS input is operates on a 17.5 Msps 24-bit complex baseband stream (containing 12 bit words each for the I and Q channels) which results from filtering and decimating the 280 Msps 8-bit stream output by the Common Front End (CFE) Analogue to Digital converter. These channels are provided for both RCP and LCP polarisations.

The Radio Science raw data can be directly transferred to a mass storage device and/or processed by a Fast Fourier routine.

Data transfer rates from the DSP to Data Storage (disk) is presently limited to 10 samples/s. Data Transfer to ESOC can be done via FTP with a rate of 2 ksps.

The Doppler predict has to be accurate enough to allow carrier signal analysis in the desired narrow frequency band.

The internally generated raw data stream consists of I and Q signals which are distributed on 12 parallel bits each for both left- and right-hand polarized signals. Since the rate with which these signals can be transfered to stable storage is limited to 10 samples/s, the I and Q signals could be routed via a V11 balanced interface to a data dump and processing device (“PC” configured for MaRS/RSI, see alsoFigure 5.3-3) in order to obtain higher data rates. Here, the absolute maximum data rate is limited to 10 Mb/s. However, much lower data rates will be more likely for MaRS and RSI.

The incoming signals will be further processed in a diversity combiner providing the combined output together with an estimate for the electrical phase angle (MEX-MRS-IGM-RS-3014).

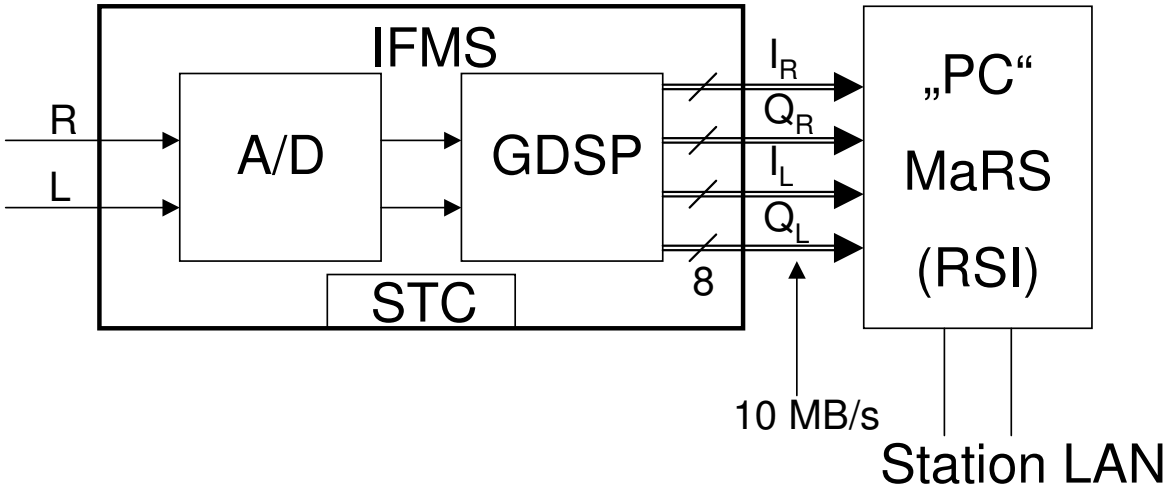

Figure 5.3-3: Alternative capture of high sample rates from IFMS

MaRS requires both the preservation of raw data for later data retrieval and the near real time data processing and conversion. These requests are further specified in section 6.1.

5.3.1.3 IFMS Configurations

The following tables show the likely configuration scenarios for the IFMS system when Radio Science experiments are conducted in OL mode. All Doppler and ranging measurements must be performed by the standard ESA IFMS units with two downlink frequencies (TWOD) in order to allow compensation for the ionospheric/interplanetary TEC contribution.

The listed scenarios show that for all cases requiring the Radio Science IFMS in OL mode operation, no telemetry modulation shall be applied to the downlink carrier analysed by the Radio Science IFMS in order to preserve spectral cleanliness as much as possible.

Also, as a highly desirable option, scenarios are suggested which require in addition to the Radio Science IFMS either IFMS A or IFMS B in OL configuration.

Table 5.3-1: IFMS receiver system scenario 1

Functional use: MaRS occultations (atmosphere/ionosphere sounding, ingress)

Scenario1	**IFMS A**	**IFMS B**	**Radio Science IFMS**
Uplink Frequency	X	-	-
Downlink frequency	X	X	S
Telemetry modulation	Off	Off	Off
Receiver Loop	CL	CL	OL
Observational parameters	Doppler, Ranging AGC Meteo	Doppler AGC	Amplitudes LHC/RHC

Table 5.3-2: IFMS receiver system scenario 2

Functional use: MaRS solar corona sounding

Scenario 2	IFMS A	IFMS B	Radio Science IFMS
Uplink Frequency	S	-	-
Downlink frequency	S	S	X
Telemetry modulation	Off (TBC)	Off (TBC)	Off (TBC)
Receiver Loop	CL	CL	CL
Observational parameters	Doppler, Ranging AGC Meteo	Doppler AGC	Doppler ranging AGC

Table 5.3-3: IFMS receiver system scenario 3

Functional use: MaRS occultations (atmosphere/ionosphere sounding, egress)

Scenario 3	IFMS A	IFMS B	Radio Science IFMS
Uplink Frequency	-	-	-
Downlink frequency	X	S	S
Telemetry modulation	Off	Off	Off
Receiver Loop	CL	CL	OL
Observational parameters	Doppler AGC Meteo	Doppler AGC	Amplitudes LHC/RHC

Table 5.3-4: IFMS receiver system scenario 4

Functional use: MaRS planetary gravity field, Phobos

Scenario 4	IFMS A	IFMS B	Radio Science IFMS
Uplink frequency	X	-	-
Downlink frequency	X	X	S
Telemetry modulation	Off	Off	Off
Receiver loop	CL	CL	CL
Observational parameters	Doppler, Ranging AGC Meteo	Doppler AGC	Doppler, Ranging AGC

Table 5.3-5: IFMS receiver system scenario 5

Functional use: MaRS Bistatic Radar

Scenario 5	**IFMS A**	**IFMS B**	**Radio Science IFMS**
Uplink Frequency	-	-	-
Downlink frequency	X	S	S or X or both
Telemetry modulation	Off	Off	Off
Receiver Loop	CL	CL	CL + OL
Observational parameters	AGC f_c	AGC f_c	AGC f_c Voltage samples

5.3.2 Deep Space Network

5.3.2.1 Overview

Three Deep Space Communications Complexes (DSCCs) (near Barstow, CA; Canberra, Australia; and Madrid, Spain) comprise the DSN tracking network. Each complex is equipped with several antennas [including at least one each 70-m, 34-m High Efficiency (HEF), and 34-m Beam WaveGuide (BWG)], associated electronics, and operational systems. Primary activity at each complex is radiation of commands to and reception of telemetry data from active spacecraft. Transmission and reception is possible in several radio-frequency bands, the most common being S-band (nominally a frequency of 2100-2300 MHz or a wavelength of 14.2-13.0 cm) and X-band (7100-8500 MHz or 4.2-3.5 cm). Transmitter output powers of up to 400 kW are available

Ground stations have the ability to transmit coded and uncoded waveforms which can be echoed by distant spacecraft. Analysis of the received coding allows navigators to determine the distance to the spacecraft; analysis of Doppler shift on the carrier signal allows estimation of the line-of-sight spacecraft velocity. Range and Doppler measurements are used to calculate the spacecraft trajectory and to infer gravity fields of objects near the spacecraft.

Ground stations can record spacecraft signals that have propagated through or been scattered from target media.

The Deep Space Network is managed by the Jet Propulsion Laboratory of the California Institute of Technology for the U.S. National Aeronautics and Space Administration.

For more information on the Deep Space Network and its use in radio science see reports by Asmar & Renzetti (1993), Asmar & Herrera (1993), and Asmar et al (1995). For design specifications on DSN subsystems see [DSN810-5].

5.3.2.2 DSN Radio Science Equipment

The Deep Space Communications Complexes (DSCCs) are an integral part of Radio Science instrumentation, along with the spacecraft Radio Frequency Subsystem. Their system performance directly determines the degree of success of Radio Science investigations, and their system calibration determines the degree of accuracy in the results of the experiments. The following paragraphs describe the functions performed by the individual subsystems of a DSCC. This material has been adapted from Asmar & Herrera (1993) and [JPLD-14027]; for additional information, consult [DSN810-5]. Each DSCC includes a set of antennas, a Signal Processing Center (SPC), and communication links to the Jet Propulsion Laboratory (JPL). The general configuration is illustrated in Figure 5.3-4; antennas (Deep Space Stations, or DSS -- a term carried over from earlier times when antennas were individually instrumented) are also listed in the figure.

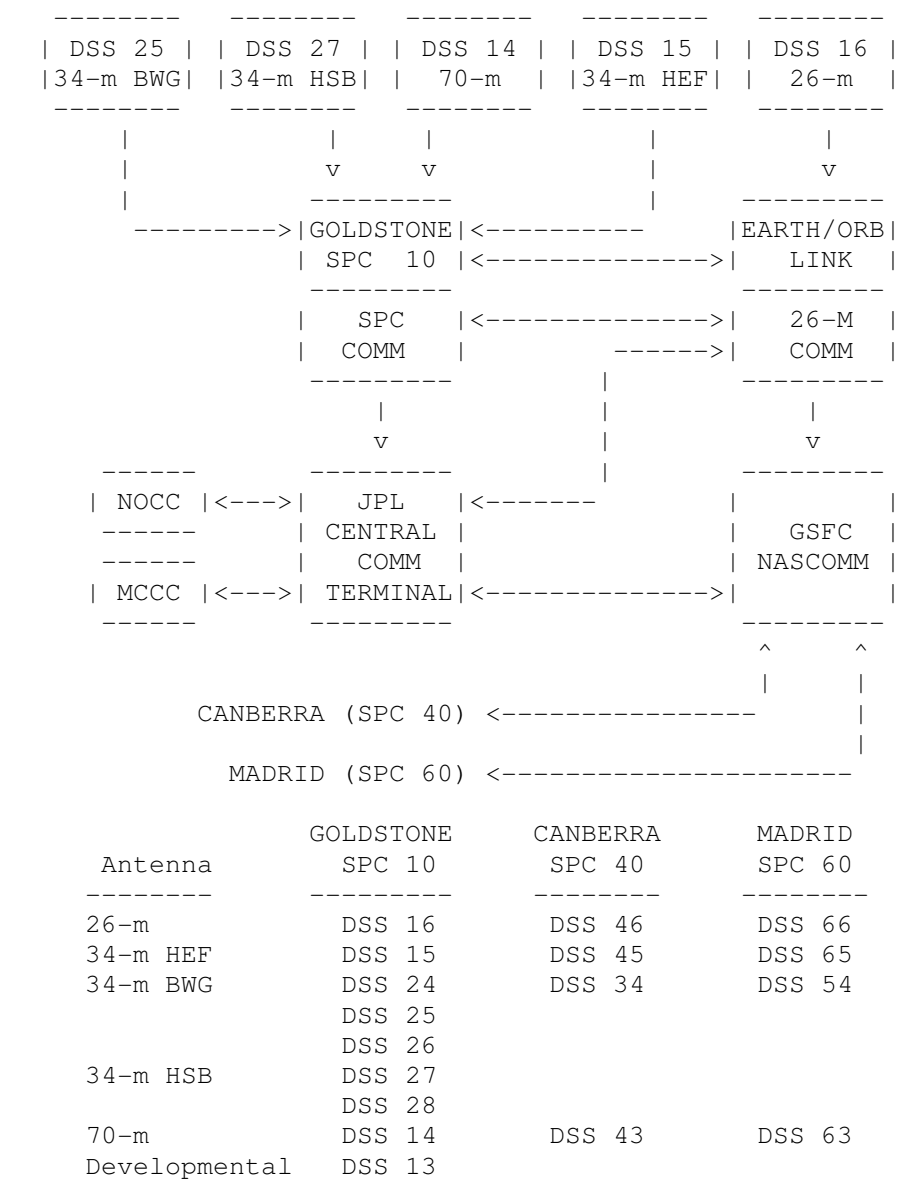

Antenna	GOLDSTONE SPC 10	CANBERRA SPC 40	MADRID SPC 60
26-m	DSS 16	DSS 46	DSS 66
34-m HEF	DSS 15	DSS 45	DSS 65
34-m BWG	DSS 24	DSS 34	DSS 54
	DSS 25		
	DSS 26		
34-m HSB	DSS 27		
	DSS 28		
70-m	DSS 14	DSS 43	DSS 63
Developmental	DSS 13		

Figure 5.3-4: DSN Network

Subsystem interconnections at each DSCC are shown in figure Figure 5.3-5, and they are described in the sections that follow. The Monitor and Control Subsystem is connected to all other subsystems; the Test Support Subsystem can be.

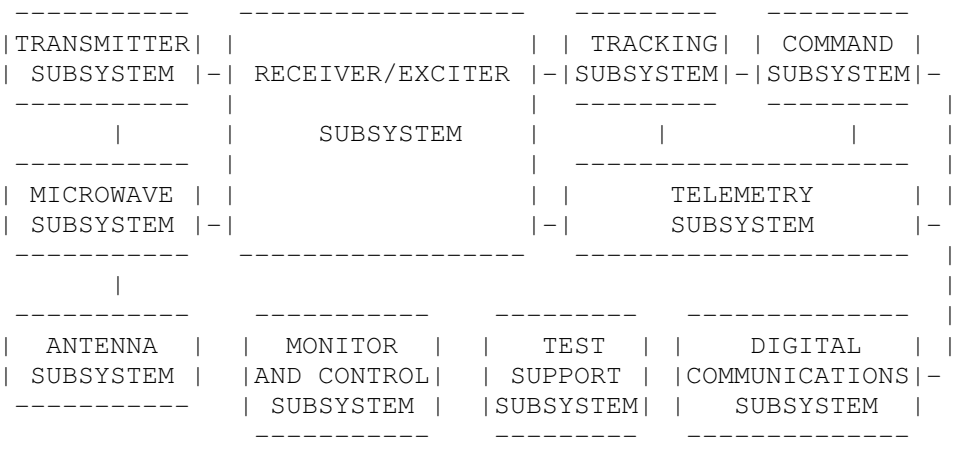

Figure 5.3-5: DSN subsystem schematics

5.3.2.2.1 DSCC Monitor and Control Subsystem

The DSCC Monitor and Control Subsystem (DMC) is part of the Monitor and Control System (MON) which also includes the ground communications Central Communications Terminal and the Network Operations Control Center (NOCC) Monitor and Control Subsystem. The DMC is the center of activity at a DSCC. The DMC receives and archives most of the information from the NOCC needed by the various DSCC subsystems during their operation. Control of most of the DSCC subsystems, as well as the handling and displaying of any responses to control directives and configuration and status information received from each of the subsystems, is done through the DMC. The effect of this is to centralize the control, display, and archiving functions necessary to operate a DSCC. Communication among the various subsystems is done using a Local Area Network (LAN) hooked up to each subsystem via a network interface unit (NIU).

DMC operations are divided into two separate areas: the Complex Monitor and Control (CMC) and the Link Monitor and Control (LMC). The primary purpose of the CMC processor for Radio Science support is to receive and store all predict sets transmitted from NOCC such as Radio Science, antenna pointing, tracking, receiver, and uplink predict sets and then, at a later time, to distribute them to the appropriate subsystems via the LAN. Those predict sets can be stored in the CMC for a maximum of three days under normal conditions. The CMC also receives, processes, and displays event/alarm messages; maintains an operator log; and produces tape labels for the DSP. Assignment and configuration of the LMCs is done through the CMC; to a limited degree the CMC can perform some of the functions performed by the LMC. There are two CMCs (one on-line and one backup) and three LMCs at each DSCC The backup CMC can function as an additional LMC if necessary.

The LMC processor provides the operator interface for monitor and control of a link -- a group of equipment required to support a spacecraft pass. For Radio Science, a link might include the DSCC Spectrum Processing Subsystem (DSP) (which, in turn, can control the SSI), or the Tracking Subsystem. The LMC also maintains an operator log which includes operator directives and subsystem responses. One important Radio Science specific function that the LMC performs is

receipt and transmission of the system temperature and signal level data from the PPM for display at the LMC console and for inclusion in Monitor blocks. These blocks are recorded on magnetic tape as well as appearing in the Mission Control and Computing Center (MCCC) displays. The LMC is required to operate without interruption for the duration of the Radio Science data acquisition period.

The Area Routing Assembly (ARA), which is part of the Digital Communications Subsystem, controls all data communication between the stations and JPL. The ARA receives all required data and status messages from the LMC/CMC and can record them to tape as well as transmit them to JPL via data lines. The ARA also receives predicts and other data from JPL and passes them on to the CMC.

5.3.2.2.2 DSCC Open-Loop Receiver (RIV)

The open loop receiver block diagram shown in Figure 5.3-6 is for the RIV system at 70-m and 34-m HEF and BWG antenna sites. Input signals at both S- and X-band are mixed to approximately 300 MHz by fixed-frequency local oscillators near the antenna feed. Based on a tuning prediction file, the POCA controls the DANA synthesizer, the output of which (after multiplication) mixes the 300 MHz IF to 50 MHz for amplification. These signals in turn are down converted and passed through additional filters until they yield output with bandwidths up to 45 kHz. The Output is digitally sampled and either written to magnetic tape or electronically transferred for further analysis.

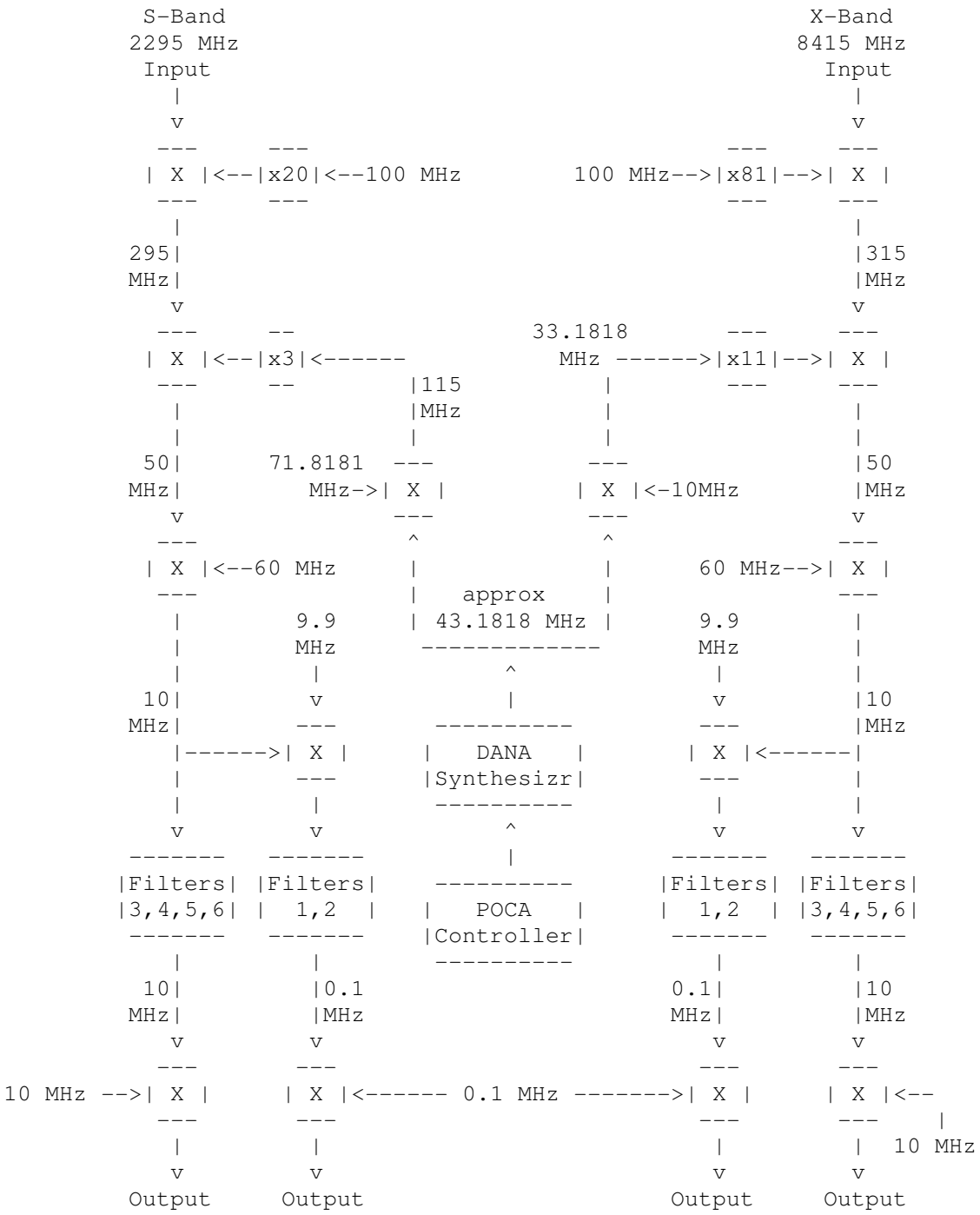

Figure 5.3-6: DSN open loop receiver block diagram

Reconstruction of the antenna frequency from the frequency of the signal in the recorded data can be achieved through use of one of the following formulas. Filters are defined below.

FS_{ant}=3*SYN+1.95*10^9+3*(790/11)*10^6+F_{rec} (Filter 4)
=3*SYN+1.95*10^9+3*(790/11)*10^6-F_{samp}+F_{rec} (Filters 1-3,5,6)

FX_{ant}=11*SYN + 7.940*10^9 + F_{samp} - F_{rec} (Filter 4)
=11*SYN + 7.940*10^9 - 3*F_{samp} + F_{rec} (Filters 1,2,3,6)

where FS_{ant},FX_{ant} are the antenna frequencies of the incoming signals at S and X bands, respectively, SYN is the output frequency of the DANA synthesizer, commonly labeled the readback POCA frequency on data tapes, F_{samp} is the effective sampling rate of the digital samples, and F_{rec} is the apparent signal frequency in a spectrum reconstructed from the digital samples.

NB: For many of the filter choices (see below) the Output is that of a bandpass filter. The sampling rates in the table below are sufficient for the bandwidth but not the absolute maximum frequency, and aliasing results. The reconstruction expressions above are appropriate ONLY when the sample rate shown in the tables below is used.

5.3.2.3 Operational Modes - DSN

- DSCC Antenna Mechanical Subsystem
  Pointing of DSCC antennas may be carried out in several ways. For details see the subsection 'DSCC Antenna Mechanical Subsystem' in the 'Subsystem' section. Binary pointing is the preferred mode for tracking spacecraft; pointing predicts are provided, and the antenna simply follows those. With CONSCAN, the antenna scans conically about the optimum pointing direction, using closed-loop receiver signal strength estimates as feedback. In planetary mode, the system interpolates from three (slowly changing) RA-DEC target coordinates; this is 'blind' pointing since there is no feedback from a detected signal. In sidereal mode, the antenna tracks a fixed point on the celestial sphere. In 'precision' mode, the antenna pointing is adjusted using an optical feedback system. It is possible on most antennas to freeze z-axis motion of the subreflector to minimize phase changes in the received signal.

- DSCC Receiver-Exciter Subsystem
  The diplexer in the signal path between the transmitter and the feed horns on all antennas may be configured so that it is out of the received signal path in order to improve the signal-to-noise ratio in the receiver system. This is known as the 'listen-only' or 'bypass' mode.

- Closed-Loop vs. Open-Loop Reception
  Radio Science data can be collected in two modes: closed-loop, in which a phase-locked loop receiver tracks the spacecraft signal, or open-loop, in which a receiver samples and records a band within which the desired signal presumably resides. Closed-loop data are collected using Closed-Loop Receivers, and open-loop data are collected using Open-Loop Receivers in conjunction with the DSCC Spectrum Processing Subsystem (DSP). See the Subsystems section for further information.

- Closed-Loop Receiver AGC Loop
  The closed-loop receiver AGC loop can be configured to one of three settings: narrow, medium, or wide. Ordinarily it is configured so that expected signal amplitude changes are accommodated with minimum distortion. The loop bandwidth is ordinarily configured so that expected phase changes can be accommodated while maintaining the best possible loop SNR.

- Coherent vs. Non-Coherent Operation
  The frequency of the signal transmitted from the spacecraft can generally be controlled in two ways -- by locking to a signal received from a ground station or by locking to an on-board oscillator. These are known as the coherent (or 'two-way') and non-coherent ('one-way') modes, respectively. Mode selection is made at the spacecraft, based on commands received from the ground. When operating in the coherent mode, the transponder carrier frequency is derived from the received uplink carrier frequency with a 'turn-around ratio' typically of 240/221. In the non-coherent mode, the downlink carrier frequency is derived from the spacecraft on-board crystal-controlled oscillator. Either closed-loop or open-loop receivers (or both) can be used with either spacecraft frequency reference mode. Closed-loop reception in two-way mode is usually preferred for routine tracking. Occasionally the spacecraft operates coherently while two ground stations receive the 'downlink' signal; this is sometimes known as the 'three-way' mode.

- DSCC Spectrum Processing Subsystem (DSP)
  The DSP can operate in four sampling modes with from 1 to 4 input signals. Input channels are assigned to ADC inputs during DSP configuration. Modes and sampling rates are summarized in the tables below:

Mode	Analog-to-Digital Operation
1	4 signals, each sampled by a single ADC
2	1 signal, sampled sequentially by 4 ADCs
3	2 signals, each sampled sequentially by 2 ADCs
4	2 signals, the first sampled by ADC #1 and the second sampled sequentially at 3 times the rate by ADCs #2-4

Table 5.3-6: DSN operational modes

8-bit Samples Sampling Rates (samples/sec per ADC)	12-bit Samples Sampling Rates (samples/sec per ADC)
50000	
31250	
25000	
15625	
12500	
10000	10000
6250	
5000	5000
4000	
3125	
2500	
	2000
1250	
1000	1000
500	
400	
250	
200	200

Table 5.3-7: DSN sampling rates

Input to each ADC is identified in header records by a Signal Channel Number (J1 - J4). Nominal channel assignments are shown below.

Signal Channel Number	Receiver Channel
J1	X-RCP
J2	S-RCP
J3	X-LCP
J4	S-LCP

Table 5.3-8: DSN Channel assignments

5.3.2.4 Interface DSN/ESOC

TBD

6 MaRS Interface with Ground

6.1 Submission of Operation Procedure Requests

The following section is identical to MEX-RAL-TN-0026:
During Radio Science (MaRS) data-taking periods the ground station will measure properties of the MEX radio signal from which scientific results can be derived. To do this the ground station and the spacecraft must be specially configured (type of observation, RF band, modulation etc.) in response to requests from the MaRS PI team. This section specifies the format and procedures for delivery of these requests (MaRS configuration data files) from the PI team to POS. On receipt of these requests POS will ingest them into its planning database for later delivery to ESOC.

The Mission Planning Concept [CONCEPT] requires that the Radio Science Observation Requests are delivered to ESOC as part of the Medium Term Planning (MTP) cycle. For convenience these data will be included as special records of the main MTP product from POS to ESOC, namely the pointing request (PTR) file. Thus each four-week block of Radio Science configuration data must be ready for delivery to ESOC before the deadline for delivery of the PTR for that period, so as not to delay a critical product delivery for the whole payload. POS will provide a delivery schedule, and MTP numbering convention, on PosWeb.

6.1.1 MaRS configuration data file specification

6.1.1.1 File formats

The MaRS configuration data shall be delivered to POS using the same format that the Radio Science team use for the equivalent instrument on Rosetta – namely the Instrument Timeline (ITL) format [ITL]. These are ASCII files that specify the initial state and subsequent timeline of the radio science configuration for a given period.

6.1.1.2 Naming convention

MaRS configuration data files shall use lower-case names of the form mars_mmm_vv.itl where mmm is the number of the MTP period and v is a sequential version number, e.g. the first delivery with observations starting in MTP 11 will have name mars_011_01.itl. If a MaRS request were to span an MTP boundary, it should be considered as part of the earlier period (but as general rule science operations across MTP boundaries are discouraged).

6.1.1.3 Scope

The observation requests within an ITL file shall replace any previous requests that overlap with the time range of the new ITL file. This time range shall start with the first action in the ITL and end with the last action in the ITL file.

6.1.1.4 File delivery mechanism

MaRS configuration data files shall be delivered by zipped email attachment to the POS operator pos_ops@rl.ac.uk. There shall be a single zipped attachment file but this may contain an arbitrary number of ITL files. These files will be handled independently so they do not have to be contiguous and may span more than more MTP period. The zip file name shall be a lower case name of form mars_xxxx.zip, where xxxx is a sequential reference number.

6.1.2 Procedures for configuration file delivery

6.1.2.1 Contact points

POS. The contact point for POS handling of MaRS configuration data files shall be the POS operator, email address pos_ops@rl.ac.uk. An email to this address will be forwarded to all members of the POS operations group so that it can be handled by the duty operator.
MaRS. The MaRS PI shall declare a contact point for their handling of MaRS configuration data files. This may be an explicit group of people or an alias for that group. This contact point may be changed as necessary by email to pos_ops@rl.ac.uk and confirmation of its receipt by POS.

6.1.2.2 File ingestion

The MaRS team shall deliver configuration data files using the email mechanism described above (add cross-ref). On receipt of this email the POS operator shall copy the zip file to the appropriate directory in the POS operational system and execute software to unpack the ITL files and ingest them into the POS planning database. On completion of the ingestion process, the operator shall send an email to the MaRS contact point to report receipt of the configuration data files and the status of the ingestion process. The report shall include the name of the zip file and of the unpacked ITL files; it shall indicate whether or not each ITL file was successfully ingested. In the case that ingestion fails the POS operator shall provide information on the failure as appropriate to the circumstances of the failure.

The operator will aim to process the configuration data file delivery within 4 working hours of its receipt at POS. Thus, if the MaRS contact point does not receive an email report from the POS Operator within that time, it should contact POS to determine if there is a problem. It is strongly recommended that emails used to deliver configuration data files should include the options to request automatic delivery and read receipts.

6.1.2.3 Schedule of activities

The deadline for delivery of MaRS configuration data to POS is that all data for a particular four-weekly MTP cycle must be delivered to POS in time to be processed ahead of the deadline for delivery of the PTR for that period to ESOC. The latter deadlines will be determined according to the algorithms specified in the Mission

Planning Concept [CONCEPT]. The specific time of the PTR deadline for each MTP cycle will be made available via POSweb together with the execution time range covered by that cycle. To allow time for processing, the MaRS configuration data must be delivered before this deadline. For initial operations, a value of 2 working days will be used for this lead time. This will be reviewed after a few months of operations to set a value in accord with the experience gained.

The POS operator will liase with the MaRS contact point during the week prior to each PTR deadline to ensure that all MaRS configuration data are delivered in time for the deadline. Configuration data will not be accepted after the deadline unless specially approved (and on a case-by-case basis) by the POS Project Manager and ESOC Spacecraft Operations Manager.

The MaRS team shall use this schedule to build, and revise, the overall timeline of MaRS operations in conveniently-sized segments. That size shall be determined, from time to time, by discussion between MaRS and POS in order to optimise their joint workload.

6.1.2.4 Validation of the data

It is assumed that the MaRS configuration data files will be validated by the MaRS team before delivery to POS. Thus POS will not undertake any explicit validation on these files, but will simply ingest them and convert the data into the format required by ESOC [ESOC-ICD]. These processes require parsing of the ITL records into data fields and manipulation of those fields. Any errors detected by this conversion will be reported to the MaRS contact point.

The details of the conversion process are an internal POS process and thus outside the scope of the present document. POS will document the conversion process in a separate technical note [TN26] and make this available for review by the MaRS team and by ESOC.

POS will also provide the MaRS team with visibility of (a) the ingested ITL data (via a POSweb access to the database) and (b) the configuration data delivered to ESOC (via the general PI access to copies of the PTR files delivered to ESOC).

6.2 Structure of Operation Procedure Request

Radio Science Operations are requested by Operations Requests in a syntax compatible with the EPS software tool (cf. SOP-RSSD-SP-002). In addition to this syntax, requests are preceeded by the lines
'BEGIN'
'TYPE = RADIO SCIENCE'
and followed by the line
'END'.
A detailed description of Action and Module specifications will follow in the next issue of this manual.
In general, procedure requests will look as follows:

```
CCCCCCCCCCCCCCCCCCCCCCCCCCCCCCCCCCCCCCCCCCCCCCCC
C Radio Science Request Example
CCCCCCCCCCCCCCCCCCCCCCCCCCCCCCCCCCCCCCCCCCCCCCCC
C comment lines starting with C
C
BEGIN
C Specify S/C TTC configuration
TYPE = RADIO SCIENCE
<EPS-compatible request lines>
END
```

6.2.1 EPS syntax

6.2.1.1 Request handling

The experiment planning system EPS uses a CONFIGURATION FILE (*.cfg) to determine how to handle operations requests. In the configuration file, the parameters CHECK_GLOBAL_<variable> usually do not need to be changed. Desired output files like errors, conflicts, power are given. Names of variables are generally self-explanatory. The most important output file options are MODULE_STATES, which gives an ASCII configuration table of RSI modes almost identical to flight operations procedure tables. The option CONFLICTS must be included to identify possible misconfigurations of the telemetry system. If given, EPS will write all conflicts defined in the CONSTRAINTS section of the EDF to a file.

```
# Filename: rsi.cfg
#
# Author:  Axel Hagermann
# Date:    28 August 2002
#
# (c) ESA/Estec
#
# Description: This is an EPS configuration file for RSI.
#
# $Id: config.example,v 1.2 2002/02/28 17:28:02 rosetta Exp $
#
# $Log: config.example,v $
# Revision 1.0  2002/08/28 rsi
# Initial revision
#
#
#Command_line: "-t 10 -s 120 -d 0"
#

Setting: CHECK_GLOBAL_ACTION FALSE
Setting: CHECK_GLOBAL_PARAM  FALSE
Setting: CHECK_GLOBAL_UNIT   FALSE
```

```
#
Output_files: POWER_AVG POWER_PEAK POWER_LOW MODULE_STATES
MS_CHANGES\
        ACTIONS TIMELINE CONFLICTS
#
```

6.2.1.2 Definition of request formats

Operations request formats are defined in an experiment definition file (rsi.edf). Configurations of the experiment are defined as MODULES with various STATES (i.e. module USO_state can have the states MUTE and ACTIVE. Module states are changed by pre-defined ACTIONS (e.g. the action USO_UP powers the USO on. ACTIONS can also be used to set PARAMETERS (e.g. the parameter UL (=uplink) can have the values <X>, <S> and <_> for X-band, S-band and no request respectively. A MODE comprises several module states. For example, the mode ONEWAY containes all individual module settings for a one-way radio link. Therefore, changing an instrument mode by an action will result in changing all module states defined in the mode. CONSTRAINTS can be inserted e.g. to prevent conflicts between modules states. In the case of RSI e.g., the use of IFMS A is heavily constrained. EDF- and ITL-files for RSI and MaRS are identical with the following exceptions:

- The ‚Experiment name' variable is RSI or MRS respectively
- For MaRS, USO configuration is not possible, therefore USO-related items have no effect on the experiment

In the EDF as well as in the ITL, predefined experiment modes can be selected (cf. the following file). These modes can be selected in the ITL, but alternatively all settings can be made in ‚DEFAULT' configuration (recommended).
In general, all entries in the EDF file are self-explanatory. Comments are marked by a hash <#> sign.
The RSI experiment definition file v.09. is quoted below for reference.

```
#
# Filename: rsi.edf
# Change record: ##################################
# Author: Axel Hagermann
# version 0.9
# Date: 28-Aug-2002
# Changes: Sampling rate definitions made, templates deleted,
#
# added a few more comments
#
#
# based on experiment.template
# Authors: Axel Hagermann & Raymond Hoofs
# Date: 28-Jun-2002
#
# Authors:  Peter van der Plas & Raymond Hoofs
# Date:     5 October 1999
```

```
#
# (c) ESA/Estec
#
# $Id: experiment.template,v 1.15 2002/02/22 14:21:06 rosetta Exp $
#
#
# <Experiments start here...>
#
Nr_of_experiments: 1
#
Experiment: RSI "Rosetta Radio Science Investigations"
#
# <Global properties start here...>
#
Global_actions: TM_bitrate \
        COHERENCY_ON COHERENCY_OFF \
        SC_LINK \
        USO_ACT USO_MUTE USO_UP \
        TM_ON TM_OFF \
        IFMS_A_Configure IFMS_B_Configure IFMS_RS_Configure  \
        TRACKMODE \
        WAIT
Global_constraints: CHECK_TM_ON CHECK_IFMS_A_ACTION  \
        CHECK_TCXO
#
#
# <Modules start here...>
### Module definitions on S/C side ###################################
#
  Module: Coherency "Up/downlink coherency definition"
  Module_level: LEVEL1
  Sub_modules:
  Nr_of_module_states: 2
        Module_state: TWO_ "TWOx Configuration, i.e. coherency on"
        Module_state: ONE_ "ONEx Configuration, i.e. coherency off"
#
  Module: SC_TRSP "S/C transponder downlink definition"
  Module_level: LEVEL1
  Sub_modules:
  Nr_of_module_states: 3
        Module_state: S_x "X-Band D/L (default)"
        MS_power: 0 [Watts]
        Module_state: S_s "S-Band D/L"
        MS_power: 25 [Watts]
        Module_state: D_xs "Dual D/L"
        MS_power: 25 [Watts]
#
  Module: USO_pwr "USO Power"
  Module_level: LEVEL1
```

```
  Sub_modules:
  Nr_of_module_states: 3
        Module_state: ON "On"
        MS_power: 3 [Watts]
        Module_state: OFF "Off"
        MS_power: 0 [Watts]
        Module_state: HEAT "Heating"
        MS_power: 7.5 [Watts]
#
  Module: USO_state "USO State"
  Module_level: LEVEL1
  Sub_modules:
  Nr_of_module_states: 2
        Module_state: MUTE "Mute"
        Module_state: ACTIVE "Active"
#
  Module: TCXO_state "TCXO State"
  Module_level: LEVEL1
  Sub_modules:
  Nr_of_module_states: 2
        Module_state:  MUTE "Mute"
        Module_state: ACTIVE "Active"
#
  Module: TM_modulation "Telemetry modulation"
  Module_level: LEVEL1
  Sub_modules:
  Nr_of_module_states: 2
        Module_state: ON "TM On"
        Module_state: OFF "TM Off"
#
  Module: TM_fsc "Telemetry subcarrier"
  Module_level: LEVEL1
  Sub_modules:
  Nr_of_module_states: 2
        Module_state: 262 "262144 Hz subcarrier"
        Module_state: 8 "8192 Hz subcarrier"
#
  Module: TM_N "Subcarrier/Trans. symbol rate ratio"
  Module_level: LEVEL1
  Sub_modules:
  Nr_of_module_states: 6
        Module_state: 5 "N=5"
        Module_state: 6 "N=6"
        Module_state: 8 "N=8"
        Module_state: 10 "N=10"
        Module_state: 12 "N=12"
        Module_state: 16 "N=16"
        #etc...
### Module definition G/S side ###################################
```

```
  Module: IFMS_A_UL "IFMS A Uplink"
  Module_level: LEVEL1
  Sub_modules:
  Nr_of_module_states: 3
        Module_state: X "X-Band uplink"
        Module_state: S "S-Band uplink"
        Module_state: _ "No request"
#
  Module: IFMS_A_DL "IFMS A Downlink"
  Module_level: LEVEL1
  Sub_modules:
  Nr_of_module_states: 5
        Module_state: X_CL "X-Band closed-loop"
        Module_state: S_CL "S-Band closed-loop"
        Module_state: X_OL "X-Band open-loop"
        Module_state: S_OL "S-Band open-loop"
        Module_state: _    "No request"
#
  Module: IFMS_B_UL "IFMS B Uplink"
  Module_level: LEVEL1
  Sub_modules:
  Nr_of_module_states: 3
        Module_state: X "X-Band uplink"
        Module_state: S "S-Band uplink"
        Module_state: _ "No request"
#
  Module: IFMS_B_DL "IFMS B Downlink"
  Module_level: LEVEL1
  Sub_modules:
  Nr_of_module_states: 5
        Module_state: X_CL "X-Band closed-loop"
        Module_state: S_CL "S-Band closed-loop"
        Module_state: X_OL "X-Band open-loop"
        Module_state: S_OL "S-Band open-loop"
        Module_state: _    "No request"
#
  Module: IFMS_RS_DL "IFMS RS Downlink"
  Module_level: LEVEL1
  Sub_modules:
  Nr_of_module_states: 5
        Module_state: X_CL "X-Band closed-loop"
        Module_state: S_CL "S-Band closed-loop"
        Module_state: X_OL "X-Band open-loop"
        Module_state: S_OL "S-Band open-loop"
        Module_state: _    "No request"
#
  Module: TRACKMODE "Tracking mode"
  Module_level: LEVEL1
  Sub_modules:
```

```
  Nr_of_module_states: 3
        Module_state: DOPPLER "Doppler only"
        Module_state: DOP_RNG "Simultaneous Doppler and Range"
        Module_state: RANGE   "Ranging only"

# Set sampling rate for IFMS ############################
  Module: SAMPLING_OL "IFMS sampling rate open-loop (1/sec)"
  Module_level: LEVEL2
  Sub_modules:
  Nr_of_module_states: 6
        Module_state: 1000 "from here, Open-loop only"
        Module_state: 2000
        Module_state: 5000
        Module_state: 10000
        Module_state: 20000
        Module_state: 50000
  Module: SAMPLING_B "IFMS sampling rate closed-loop (1/sec)"
  Module_level: LEVEL2
  Sub_modules:
  Nr_of_module_states: 3
        Module_state: 1 "1 sample/sec"
        Module_state: 10
        Module_state: 100

# <Modes start here...>
#
#Nr_of_modes: <p>
 Mode: MODE "Dummy mode"

 Mode: DEFAULT "Dummy mode"

 Mode: STDCONF "Standard configuration"
  Module_states: \
        Coherency TWO_ \
        SC_TRSP S_x \
        USO_state MUTE \
        TCXO_state ACTIVE \
        TM_modulation ON \
        IFMS_A_UL X \
        IFMS_A_DL X_CL \
        IFMS_B_UL _ \
        IFMS_B_DL _ \
        IFMS_RS_DL _

 Mode: ONEWAY "Standard ONES configuration"
  Module_states: \
        Coherency ONE_ \
        USO_state ACTIVE \
        TCXO_state MUTE \
```

```
        TM_modulation ON \
        IFMS_A_UL X \
        IFMS_A_DL X_CL \
        IFMS_B_UL _ \
        IFMS_B_DL _ \
        IFMS_RS_DL _

  Mode: TWOWAY "Standard TWOS configuration"
   Module_states: \
        Coherency TWO_ \
        TM_modulation ON \
        IFMS_A_UL X \
        IFMS_A_DL X_CL \
        IFMS_B_UL _ \
        IFMS_B_DL _ \
        IFMS_RS_DL _

#########################################################################
# <Parameters start here...>

#
#Nr_of_parameters: <q>
   Parameter: FSCFREQ "Subcarrier frequency"
   Raw_type: INT
   Parameter_value: 262
   Parameter_update: MSP 262
   Parameter_value: 8
   Parameter_update: MSP 8
#
   Parameter: UL "Uplink"
        Eng_type: TEXT
        Default_value: _
        Parameter_value: _
        Parameter_update: MSP _
        Parameter_value: X
        Parameter_update: MSP X
        Parameter_value: S
        Parameter_update: MSP S
#
  Parameter: DL "Downlink"
        Eng_type: TEXT
        Default_value: _
        Parameter_value: _
        Parameter_update: MSP _
        Parameter_value: X_CL
        Parameter_update: MSP X_CL
        Parameter_value: S_CL
        Parameter_update: MSP S_CL
        Parameter_value: X_OL
```

```
        Parameter_update: MSP X_OL
        Parameter_value: S_OL
        Parameter_update: MSP S_OL
#
  Parameter: SCLINK "S/C Transponder D/L mode"
        Eng_type: TEXT
        Default_value: S_x
        Parameter_value: S_x
        Parameter_update: MSP S_x
        Parameter_value: S_s
        Parameter_update: MSP S_s
        Parameter_value: D_xs
        Parameter_update: MSP D_xs
#
  Parameter: TRKMOD
        Eng_type: TEXT
        Default_value: DOPPLER
        Parameter_value: DOPPLER
        Parameter_update: MSP DOPPLER
        Parameter_value: DOP_RNG
        Parameter_update: MSP DOP_RNG
        Parameter_value: RANGE
        Parameter_update: MSP RANGE

   Parameter: NRATIO "Symbol rate ratio"
   Raw_type: INT

Parameter: WAITTIME "Wait duration parameter"
   Eng_type: REAL
   Default_value: 1.0 [secs]
   Unit: secs
   Eng_limits: 1.0 3600.0 [secs]
   Resource: DURATION

Parameter: SAMPRATE "Sampling rate"
        Raw_type: INT
#
#
#########################################################################
###
# <Actions start here...>
### Action definitions ############################
# USO-related
#
   Action: USO_UP "Bring the USO up: Heat for 20 min, then goto standby"
        Action_level: LEVEL1
        Duration: 20 [minutes]
        Run_type: RELATIVE
        Run_actions:        00:00:00 uso_heat \
```

```
                    00:20:00 uso_on
#
  Action: uso_heat "Heat the USO"
          Action_level: LEVEL2
          Update_when_ready: MS USO_pwr HEAT
#
  Action: uso_on "USO is up"
          Action_level: LEVEL2
          Update_when_ready: MS USO_pwr ON
#
  Action: USO_OFF "Power the USO off"
        Action_level: LEVEL1
        Update_when_ready: MS USO_pwr OFF
        Action_constraints: CHECK_TCXO
#
  Action: USO_ACT "Switch USO to ACTIVE mode"
        Action_level: LEVEL1
        Update_when_ready: \
        MS USO_state ACTIVE \
        MS TCXO_state MUTE
        Action_constraints: CHECK_TM_ON
#
  Action: USO_MUTE "Mute USO, unmute TCXO"
        Action_level: LEVEL1
        Update_when_ready: \
        MS TCXO_state ACTIVE \
        MS USO_state MUTE
        Action_constraints: CHECK_TM_ON
#
  Action: COHERENCY_ON "Go to Two-way mode"
        Action_level: LEVEL1
        Update_when_ready: \
        MS Coherency TWO_

#
  Action: COHERENCY_OFF "Go to One-way mode"
        Action_level: LEVEL1
        Update_when_ready: \
        MS Coherency ONE_


  Action: SC_LINK "S/C Transponder D/L mode"
        Action_level: LEVEL1
        Action_parameters: SCLINK
        Update_when_ready: \
        MSP SC_TRSP SCLINK

#
# Telemetry related ##########################################
```

```
#
  Action: TM_OFF "Switch telemetry modulation OFF"
        Action_level: LEVEL1
        Update_when_ready: MS TM_modulation OFF
#
  Action: TM_ON "Switch telemetry modulation ON"
        Action_level: LEVEL2
        Update_when_ready: MS TM_modulation ON
#
  Action: TM_Bitrate "Select Telemetry subcarrier & bitrate ratio"
        Action_level: LEVEL2
        Action_parameters: FSCFREQ NRATIO
        Update_when_ready: \
        MSP TM_fsc FSCFREQ \
        MSP TM_N NRATIO
#
  Action: IFMS_A_Configure "Configure IFMS A"
        Action_level: LEVEL1
        Action_parameters: UL DL
        Duration: 1 #"Duration is a dummy, but needed to raise the error flag"
        Update_when_ready: \
        MSP IFMS_A_UL UL \
        MSP IFMS_A_DL DL
#       Action_constraints: CHECK_IFMS_A_ACTION
#
  Action: IFMS_B_Configure "Configure IFMS B"
        Action_level: LEVEL1
        Action_parameters: UL DL
        Update_when_ready: \
        MSP IFMS_B_UL UL \
        MSP IFMS_B_DL DL
#
  Action: IFMS_RS_Configure "Configure Radio Science IFMS"
        Action_level: LEVEL1
        Action_parameters: DL
        Update_when_ready: \
        MSP IFMS_RS_DL DL
#
  Action: WAIT "Wait a while"
        Action_level: LEVEL2
        Action_parameters: WAITTIME
#
  Action: TRACKMODE "Set tracking mode (Doppler/Range)"
        Action_level: LEVEL1
        Action_parameters: TRKMOD
        Update_when_ready: \
        MSP TRACKMODE TRKMOD
#
  Action: SET_SAMPLING_OL "Set sampling rate for open-loop recording"
```

```
        Action_level: LEVEL1
        Action_parameters: SAMPRATE
        Update_when_ready: \
        MSP SAMPLING_OL SAMPRATE
#
  Action: SET_SAMPLING_CL "Set sampling rate for closed-loop recording"
        Action_level: LEVEL1
        Action_parameters: SAMPRATE
        Update_when_ready: \
        MSP SAMPLING_CL SAMPRATE
#
################################################
# <Constraints start here...>

   Constraint: CHECK_TM_ON "Warn when telemetry is OFF"
        Constraint_type: TIME
        Severity: WARNING
        Condition: MS NOT TM_modulation ON
#
   Constraint: CHECK_IFMS_A_ACTION "WATCH OUT! RSI IS TRYING TO MESS
WITH IFMS A!"
        Constraint_type: TIME
        Severity: WARNING
        Condition: ACTION IS IFMS_A_Configure
#
   Constraint: CHECK_TCXO "TCXO is inactive"
        Constraint_type: TIME
        Severity: ERROR
        Condition: MS NOT TCXO_state ACTIVE
#
# Additional Check for IFMS A, can be called anytime
#   Constraint: CHECK_IFMS_A_CONFIG "Is IFMS A in standard configuration?"
#        Constraint_type:
#        Severity: INFO
#        Condition:  MS NOT IFMS_A_DL X_CL
#AND (MS IS IFMS_A_UL X OR MS IS IFMS_A_UL _)
```

NB: Care must be taken to escape line-breaks within a single syntactic option with a backslash <\>

6.2.1.3 Issuing of requests

The actual operations request is performed in the instrument-timeline file (rsi.itl). Here the actions defined in the EDF are called. Subsequently module states are changed as defined in the EDF. In the first lines, it must include a start and stop time and the initial module states. The actual requests are then entered in the syntax:
<timetag> <experiment> <action>

where <timetag> can be any epoch as specified in the EPS user manual. For valid epoch identifiers, see also the rosetta event definition file issued with the respective EPS release. For most operations requests, the experiment name is „RSI“. For pointing requests, „PTR“ is used as experiment identifier. <action> is the action defined in the EDF to be executed. Note that ACTION PARAMETERS are included in brackets. An example of an ITL:

```
#
# Filename: input.example
#
# Author: Peter van der Plas
# Date:   10 January 2000
#
# (c) ESA/Estec
#
# Description: This is an example input timeline file.
#
# $Id: input.example,v 1.7 2002/02/22 14:23:42 rosetta Exp $
#
# $Log: input.example,v $
# Revision 1.7  2002/02/22 14:23:42  rosetta
# SEPARATION parameter has relative time value.
#
# Revision 1.6  2002/02/19 16:13:41  rosetta
# Added step numbers and source file info message.
#
# Revision 1.5  2001/07/11 13:00:21  rosetta
# Updated to be compatible with the CRID issue B1.
# New implementation of parameters, also on events.
# New timing functionality and include file layout.
# PTR information can now be embedded in the ITL.
#
# Revision 1.4  2000/10/31 17:20:35  rosetta
# Removed all simulator state references.
# Added the Start_timeline and Stop_timeline keywords.
# Added the Event_time keyword.
# Updated the use of arguments.
# Direct DEFAULT updates are allowed now.
# Include files can now be scheduled on events.
#
# Revision 1.3  2000/03/13 19:33:25  rosetta
# Changed implementation of modules
# Added module power an data rate
# Added module level and sub-modules
# Changed action type to action level
# Various minor changes and document updates
#
# Revision 1.2  2000/02/21 16:51:54  rosetta
# Added use of include files and delta time values.
```

```
# More detailed description of arguments, labels and values.
#
# Revision 1.1  2000/01/10 12:30:17  rosetta
# Initial revision
#
#
Version: 00001
#
Ref_date: 21-February-2011
#
Start_time: 00:00:00
End_time: 02:00:00
#
Init_MODE: RSI DEFAULT
#
Init_MS: RSI USO_pwr OFF
#Init_MS: RSI TM_N 10
Init_MS:      RSI Coherency TWO_
Init_MS:      RSI SC_TRSP S_x
Init_MS:      RSI USO_state MUTE
Init_MS:      RSI TCXO_state ACTIVE
Init_MS:      RSI TM_modulation ON
Init_MS:      RSI IFMS_A_UL X
Init_MS:      RSI IFMS_A_DL X_CL
Init_MS:      RSI IFMS_B_UL _
Init_MS:      RSI IFMS_B_DL _
Init_MS:      RSI IFMS_RS_DL _

#
#000_00:10:00   RSI   DEFAULT      TM_bitrate ( \
#                                  FSCFREQ = 8 \
#                                  NRATIO = 6 )

#000_00:00:00      RSI   DEFAULT
000_00:20:00       RSI   DEFAULT   USO_UP
000_00:30:00       RSI   DEFAULT   COHERENCY_OFF
000_00:35:00       RSI   DEFAULT   TM_OFF
000_00:50:00       RSI   DEFAULT   IFMS_B_Configure (UL=X  DL=X_CL )
000_01:00:00       RSI   DEFAULT   USO_ACT
000_01:05:00       RSI   DEFAULT   USO_MUTE
000_01:10:00       RSI   DEFAULT   COHERENCY_OFF
000_01:15:00       RSI   DEFAULT   SC_LINK (SCLINK = D_xs)
000_01:20:00       RSI   DEFAULT   IFMS_A_Configure (UL=S DL=S_CL)
000_01:30:00       RSI   DEFAULT          TRACKMODE
(TRKMOD=DOP_RNG)
000_01:40:00       PTR   NADIR      ( OBJECT_TO_BE_POINTED = HGA \
                         OBJECT = EARTH )
```

6.3 Data Retrieval

IFMS and auxiliary data will be made available on the DDS at ESOC as soon as feasible after the tracking pass depending on the data transfer time from New Norcia to ESOC.

6.4 Interface JPL/MaRS

Radio science data observed and recorded at the DSN ground stations will be collected and organized by the Multimission Radio Science Group at JPL and Stanford and forwarded to Cologne for further processing.

7 MaRS Operational Procedures

7.1 General Overview

MaRS has defined the following operational procedures.

7.1.1 TVT Tracking Verification Test

Purpose:	Verify operation of radio-science equipment and determine radio link quality
S/C Configuration:	TWOS; TWOD ONES; ONED
Ground Seg. Config.:	TWOS-CL; TWOD-OL ONES-CL; ONES-OL ONED-CL; ONED-OL ONES-POL; ONED-POL
Execution:	Commissioning phase (after launch and at Mars arrival)
Requirements:	No S/C orbit correction or thruster activity within TVT

7.1.2 GRA Gravity Mapping of Anomalies

Purpose:	Detect Mars Local Gravity Field Anomalies
S/C Configuration:	TWOD[4]
Ground Seg. Config.:	TWOD-CL
Execution:	during nominal observation phase (pericenter passes)
Requirements:	HGA Earth pointing No S/C orbit correction within GMA Minimum thruster activity and logging of thruster activity

7.1.3 OCC Occultation Procedures

Purpose:	sounding of neutral and ionized atmosphere prior entering occultation and after exiting occultation
S/C Configuration:	TWOD when entering occultation ONED when exiting occultation
Ground Seg. Config.:	TWOD-CL when entering occultation TWOD-OL when entering occultation ONED-OL when exiting occultation ONED-CL when exiting occultation
Execution:	prior to occultation entry and occultation exit
Constraint:	executed once per sol if occultation entry is within nominal observation phase

[4] TWOS acceptable in case of power problems

	executed every orbit if occultation entry is within nominal communication phase
	execution must be correlated with ground station visibility
Requirements:	switch to TWOD configuration TBD minutes prior to occultation entry
	No telemetry modulation at both downlinks
	No orbit correction or thruster activity within OCP

7.1.4 PHO Phobos encounter procedure

Purpose:	Phobos mass determination
S/C Configuration:	TWOD[5]
Ground Seg. Config.:	TWOD-CL
Execution:	during nominal communication phase (apocenter passes) if distance to Phobos is less than 500 km
Requirements:	HGA Earth pointing
	No S/C orbit correction within PHO
	no thruster activity

7.1.5 BSR Bistatic Radar procedure

Purpose:	Mars surface properties
S/C Configuration:	ONED
Ground Seg. Config.:	ONED-OL; ONED-POL
Execution:	As targets are available under good observing conditions; once per week
Requirements:	Pointing of HGA toward the planetary surface
	Recording of RHC and LHC radio signals at the ground station (selection TBD)
	No orbit correction or thruster activity during BSR
	No uplink to MEX
	No telemetry

7.1.6 SCP Solar Conjunction Procedures

Purpose:	Radio sounding of the solar corona
S/C Configuration:	TWOD; S-band uplink
Ground Seg. Config.:	TWOD-CL; TWOD-OL (TBC)
Execution:	
	in Fall 2004
	in Fall 2006
	Executed during nominal communication phase
Requirements:	Daily tracking passes
	S-band uplink

[5] TWOS acceptable in case of power problems

7.2 Detailed Description of Science Operations

7.3 MaRS Science Operations Priorities

MaRS science operations are event or target oriented operations.

7.3.1 Event oriented operations

Event driven operations result from specific astronomical constellation alignments of the Earth, Mars, Sun, Phobos and the spacecraft. These are:

1. Earth occultations in six occultation seasons distributed over the prime and extended mission (for details see section 7.4)
2. Superior solar conjunctions in two conjunction seasons in late summer 2004 and 2006 (for details see section 7.8)
3. Phobos flybys at distances less than 400 km (for details see section 7.7)

7.3.2 Target oriented operations

Gravity measurements and Bistatic Radar are target oriented operations. Target lists are given in

1. Gravity: section 7.5
2. Bistatic radar: section 7.6

7.3.3 Operational ranking

1. Solar conjunctions

Justification: the corona will dominate all propagation effects on the radio carrier link. There is no hope to extract effects from the atmosphere or the gravity field during conjunctions.

2. Phobos flyby:

Justification: Phobos flybys will occur about apocenter. Flybys within 400 km are rare events and have priority above all other operations.

3. Occultations

Justification: the sounding of the atmosphere/ionosphere is the prime objective of MaRS. Two occultations per sol shall be covered when occultation entry/exit is outside of +/- 60 deg true anomaly; one occultation per sol shall be covered when occultation entry/exit is within +/- 60 deg true anomaly.

4. Gravity and Bistatic Radar

Justification: depending on ground track coverage at pericenter or apocenter, respectively.

Figure 7.3-1 shows a decision diagram for MaRS operations.

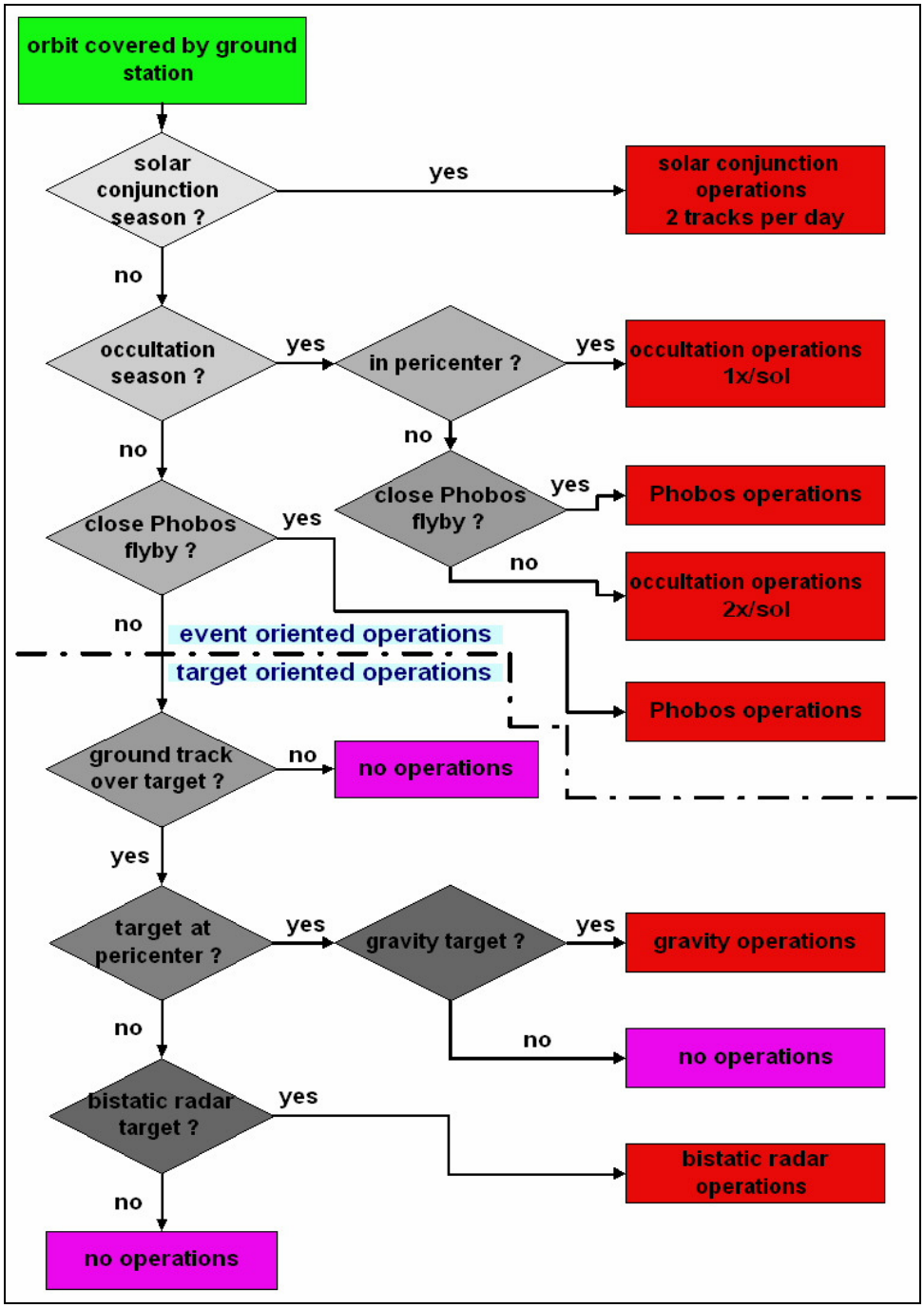

Figure 7.3-1: A decision flow chart for MaRS science operations

page left free

7.4 Occultations: Neutral and Ionized Atmosphere

7.4.1 Description

Occultation observations will provide a measure of the vertical structure of the atmosphere and ionosphere of Mars. Density, temperature and pressure profiles will be derived from the Doppler recordings during the occultation ingress and egress phase.

7.4.2 Measurement Technique

Before the spacecraft is entering occultation as seen from the Earth, the radio ray slices through the layers of the ionosphere and neutral atmosphere. The TT&C system is operating in the two-way mode. Changes in the received radio frequency to an accuracy of 10^{-13} correspond to a detection of a change in the angle of refraction of radio rays in occultation experiments on the order of 10^{-8} radians.

With Viking the atmosphere was sensible at microwaves below an altitude of 30 km. Mars Express would be able to improve this altitude to 50 km due to the high signal-to-noise ratio at X-band (RF power 60 Watts). The effective vertical resolution through use of the Abel transform is determined by the first Fresnel zone radius $(\lambda D)^{1/2}$ which translates to 300 m for X-band and 600 m for S-band radio waves, respectively, (D is the distance of the spacecraft to the closest approach of the ray path to the planet). This resolution is far superior than what can be achieved by other sounding instruments which are limited to typically one atmospheric scale height (order of kilometers).

7.4.3 Operations

7.4.3.1 Configuration

Operations will be conducted using a coherent simultaneous dual-frequency two-way tracking link prior to occultation entry. When leaving occultation the spacecraft is configured as ONED. A dual-frequency downlink is mandatory for the separation of ionospheric and interplanetary plasma effects from the classical Doppler shift. Open loop tracking is requested to analyse high temporal variations.

Table 7.4-1: Configurations for atmospheric and ionospheric sounding

S/C configuration	TWOD entry phase ONED exit phase		
Ground segment configuration		up	down
NNO	IFMS A	X	X-CL
	IFMS B		X-CL
	IFMS RS		S-CL S-OL RCP X-OL RCP
DSN 34-m	Closed-loop	X	X-CL
			S-CL
	Open-loop		X-OL RCP
			S-OL RCP
Telemetry modulation	OFF		
MaRS operational procedure	OCP-DFLT OCO-Peri		

7.4.3.2 HGA Pointing

The HGA is pointed toward the Earth.

7.4.3.3 Operations Timeline (Sequence-of-events SOE)

For this kind of observation, the radio signals of Mars Express will be observed before the spacecraft enters occultation and after leaving occultation. The HGA is pointed toward the Earth and the spacecraft operates in the two-way mode when entering occultation and in the one-way mode when leaving occultation.

Detailed timelines and sequence of events are given in section 8.

7.4.3.4 Number of occultations

Table 7.4-2: Occultation seasons as a function of MEX orbit number

Occultation season			Start orbit	Stop orbit	number of orbits
Acronym	**Start date**	**Stop date**			
OCC1****	29.03.04	12.08.04	283	728	445
OCC2	17.12.04	11.02.05	1118	1291	173
OCC3	02.04.05	29.05.05	Tbd	Tbd	Tbd
OCC4	21.07.05	06.05.06	Tbd	Tbd	Tbd
OCC5	08.09.06	22.11.06	Tbd	Tbd	Tbd
OCC6	26.04.07	01.06.07	Tbd	Tbd	Tbd

****** occultation season OCC1 ends nominally with orbit 788 but is cut short due to the first solar conjunction season which starts with orbit 729.**

Table 7.4-2 and Table 7.4-3 list the start and stop dates of the occultation seasons OCP1 to OCP6 over the mission time, the number of orbits when occultations occur and the maximal number of requested orbits when occultations can be observed from Earth. The latter depends crucially on ground station visibility and availability.

ESA ground station New Norcia:

Table 7.4-3: Occultation seasons as a function of mission time

ground station NEW NORCIA					
Occultation season			Number of days	Number of orbits	number of requested orbits[6]
Acronym	**Start date**	**Stop date**			
OCC1	29.03.04	12.08.04	136	445	214
OCC2	17.12.04	11.02.05	56	179	94
OCC3	02.04.05	29.05.05	57	182	Tbd
OCC4	21.07.05	06.05.06	289	924	Tbd
OCC5	08.09.06	22.11.06	75	240	Tbd
OCC6	26.04.07	01.06.07	36	115	tbd

[6] For one ground station

NASA Deep Space Network:

Table 7.4-4: Occultation sequences as a function of mission time

DSN ground station complex MADRID or GOLDSTONE					
Occultation season			Number of days	Number of orbits	number of requested orbits[7]
Acronym	Start date	Stop date			
OCC1	29.03.04	12.08.04	136	445	100
OCC2	17.12.04	11.02.05	56	179	60
OCC3	02.04.05	29.05.05	57	182	Tbd
OCC4	21.07.05	06.05.06	289	924	Tbd
OCC5	08.09.06	22.11.06	75	240	Tbd
OCC6	26.04.07	01.06.07	36	115	tbd

7.4.3.5 Duration of occultations

Figure 7.4-1 shows the duration of the occultation as a function of mission time.

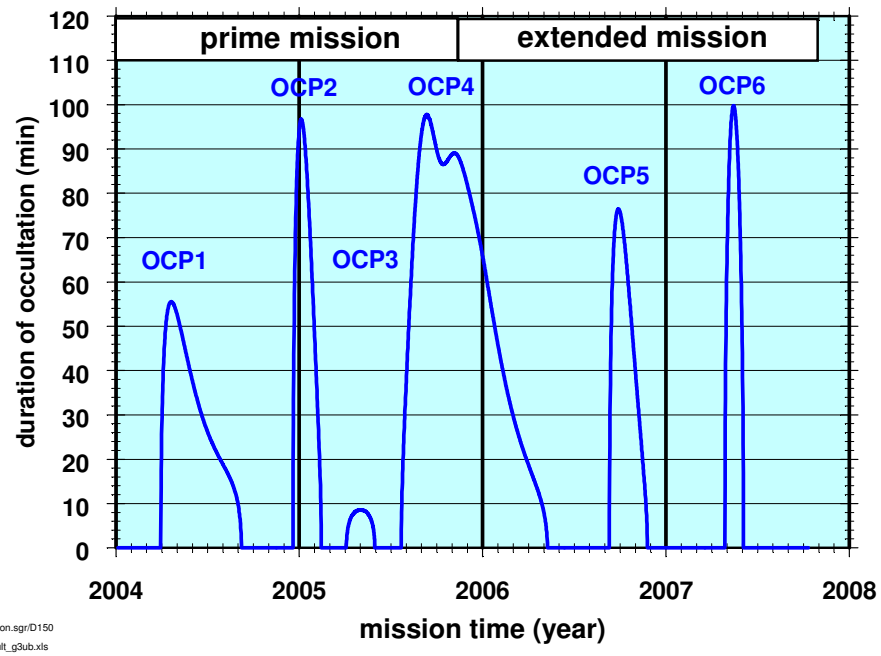

Figure 7.4-1: Duration of occultations

[7] For one ground station

7.4.3.6 Occultation entry and exit

Figure 7.4-1: Duration of occultations, Figure 7.4-2: Occultation entries with respect to pericenter (hours) and Figure 7.4-3 show the entry into occultation and the exit with respect to the pericenter in hours and true anomaly, respectively.

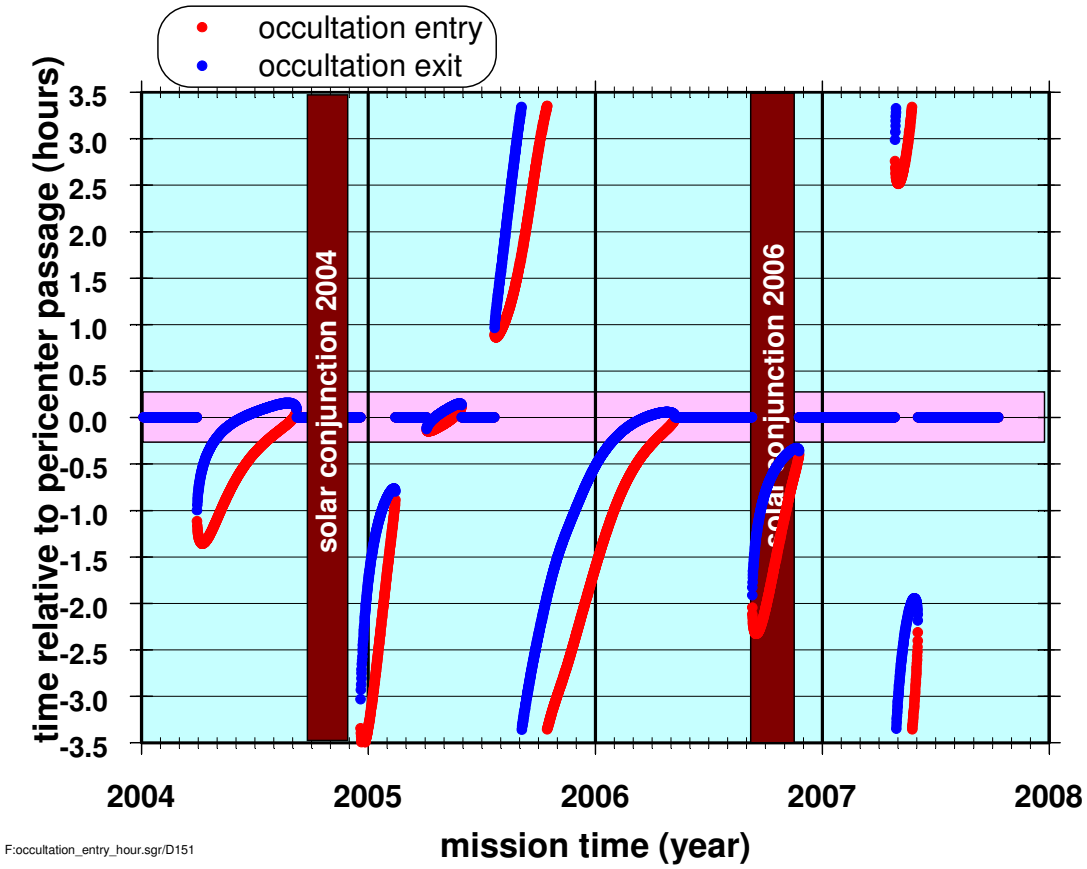

Figure 7.4-2: Occultation entries with respect to pericenter (hours)

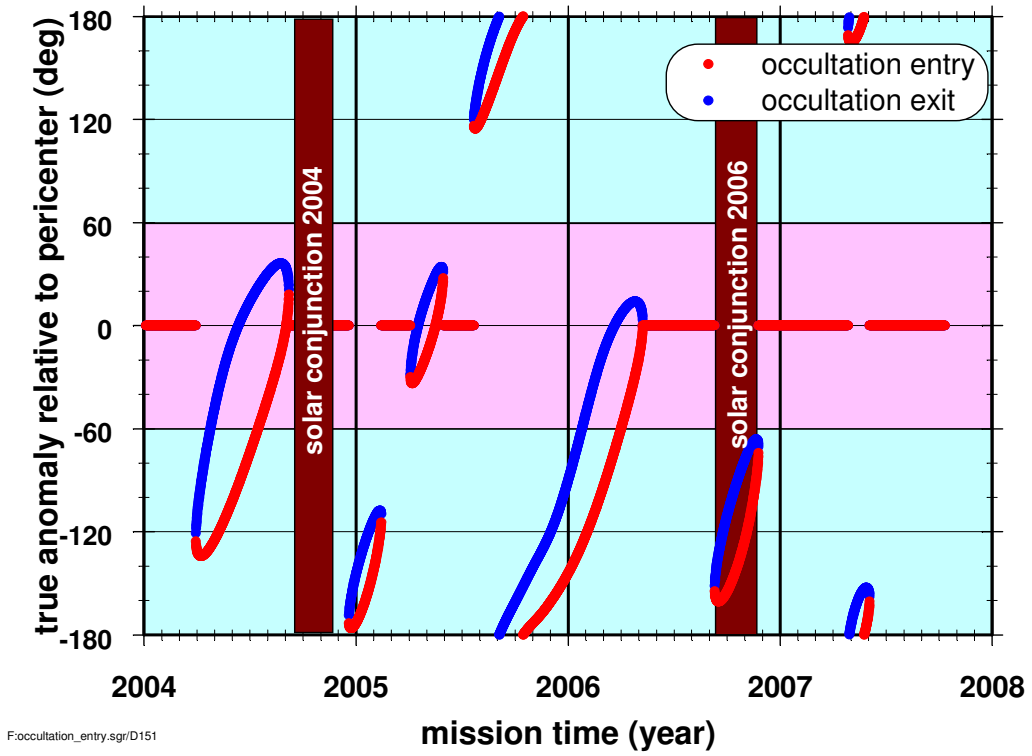

Figure 7.4-3: occultation entries with respect to pericenter (true anomaly). The pink area marks the true anomaly when the spacecraft is considered to be in nadir pointing. The dark red areas mark the time of the two solar conjunctions.

7.4.3.7 Constraints

According to the Mars Express orbit analysis, Earth occultations will occur in distinct seasons. The occultation entry and exits will cover all planetary latitudes of the northern and southern hemisphere. When the true anomalies of the occultation entry and exits are far from the orbital pericenter the Earth pointing of the HGA is assumed.

It is also likely that the occultations occur at or close to the pericenter and that the instruments are observing the Martian surface in nadir direction. In this case the HGA will not point toward the Earth. To allow the performance of atmospheric sounding prior to (and after) occultation, it is required that radio occultation observations have operational priority at least once per sol correlated with ground station visibility. Therefore, occultations which occur during pericenter passes are only requested to be observed from New Norcia, and additional occultation observations from the DSN stations are only requested outside pericenter passes.

Any spacecraft orbit correction maneuvers must not be performed within the operation period. Furthermore, spacecraft attitude thruster activities should be avoided or kept at a minimum. In case of thruster activities, a logging of relevant thrust parameters has to be performed.

7.4.4 Data

7.4.4.1 Mission Products

New Norcia Ground Station:

Table 7.4-5: IFMS Data products

Receiver	Frequency band	Data products
IFMS A (closed-loop)	X	Doppler ranging meteo
IFMS B (closed-loop)	X	Doppler
IFMS RS (closed-loop)	S	Doppler ranging
IFMS RS (open-loop)	S X	Voltage samples RHC Voltage samples RHC

Deep Space Network:

Table 7.4-6: DSN Data products

Receiver	Frequency band	Data products	Data file type
closed-loop	X	phase	TRK-2-34
	S	phase	
open-loop	X	Voltage samples	
	S	Voltage samples	RSR

7.4.4.2 Accuracy

The accuracy of the derived atmospheric surface values, the receiver system temperature, EIRP and Earth- Mars distance is governed by the stability of the frequency reference source. A stability of 10^{-13} at one second integration time is required to achieve the goals.

7.4.4.3 Sample Rate

Table 7.4-7: Occultations: sample rate

Closed-loop	10 samples / second
Open-loop	5000 samples / second 2500 Hz bandwidth
Auxiliary data	TBD

7.4.4.4 Data Volume

Table 7.4-8: Occultations: Data volume

	Data Volume
Closed-loop IFMS DSN	 2100 kByte per frequency; entry phase 2000 kByte per frequency; exit phase 260 kByte per frequency; both phases
Open-loop IFMS DSN	 54 Mbyte, both phases 15,000 kByte entry and exit phase
Auxiliary data	TBD
Ground station meteo	Already contained in IFMS figure

7.4.4.5 Availability

TBD

7.4.5 Detailed description of occultation seasons

7.4.5.1 OCC-1

7.4.5.1.1 Coordinates of occultation footpoints

tbd

7.4.5.1.2 Latitudinal coverage

tbd

7.4.5.1.3 List of requested orbits OCC1

VERY PRELIMINARY! Contains ALL ground stations!

				start	stop		
orbit #	attitude	instrument	Experiment	relative to pericenter		pointing	ground station
283	FIX	MaRS	OCC	-65.69	-55.69	ERT	MAD
283	FIX	MaRS	OCC	-47.19	-37.19	ERT	MAD
284	FIX	MaRS	OCC	-68.59	-58.59	ERT	GST(MAD)
284	FIX	MaRS	OCC	-44.09	-34.09	ERT	GST(MAD)
285	FIX	MaRS	OCC	-70.35	-60.35	ERT	NNO
285	FIX	MaRS	OCC	-42.35	-32.35	ERT	NNO
286	FIX	MaRS	OCC	-71.67	-61.67	ERT	MAD
286	FIX	MaRS	OCC	-40.67	-30.67	ERT	MAD
287	FIX	MaRS	OCC	-72.47	-62.47	ERT	GST(MAD)
287	FIX	MaRS	OCC	-38.47	-28.47	ERT	GST(MAD)
288	FIX	MaRS	OCC	-73.72	-63.72	ERT	NNO
288	FIX	MaRS	OCC	-37.72	-27.72	ERT	NNO
289	FIX	MaRS	OCC	-74.61	-64.61	ERT	NNO
289	FIX	MaRS	OCC	-36.11	-26.11	ERT	NNO
290	FIX	MaRS	OCC	-74.92	-64.92	ERT	GST(MAD)
290	FIX	MaRS	OCC	-34.92	-24.92	ERT	GST(MAD)
291	FIX	MaRS	OCC	-75.81	-65.81	ERT	NNO
291	FIX	MaRS	OCC	-34.30	-24.30	ERT	NNO
292	FIX	MaRS	OCC	-76.26	-66.26	ERT	NNO
292	FIX	MaRS	OCC	-33.26	-23.26	ERT	NNO
293	FIX	MaRS	OCC	-76.14	-66.14	ERT	GST(MAD)
293	FIX	MaRS	OCC	-32.14	-22.14	ERT	GST(MAD)
294	FIX	MaRS	OCC	-77.13	-67.13	ERT	GST
294	FIX	MaRS	OCC	-31.13	-21.13	ERT	GST
295	FIX	MaRS	OCC	-77.53	-67.53	ERT	NNO
295	FIX	MaRS	OCC	-30.52	-20.52	ERT	NNO
296	FIX	MaRS	OCC	-77.39	-67.39	ERT	GST(MAD)
296	FIX	MaRS	OCC	-29.39	-19.39	ERT	GST(MAD)
297	FIX	MaRS	OCC	-77.82	-67.82	ERT	GST
297	FIX	MaRS	OCC	-28.82	-18.82	ERT	GST
298	FIX	MaRS	OCC	-78.11	-68.11	ERT	NNO
298	FIX	MaRS	OCC	-28.11	-18.11	ERT	NNO
299	FIX	MaRS	OCC	-78.45	-68.45	ERT	MAD
299	FIX	MaRS	OCC	-27.45	-17.45	ERT	GST(MAD)
300	FIX	MaRS	OCC	-78.28	-68.28	ERT	GST
300	FIX	MaRS	OCC	-26.28	-16.28	ERT	GST
301	FIX	MaRS	OCC	-79.05	-69.05	ERT	NNO
301	FIX	MaRS	OCC	-26.05	-16.05	ERT	NNO
302	FIX	MaRS	OCC	-78.95	-68.95	ERT	MAD
302	FIX	MaRS	OCC	-25.45	-15.45	ERT	MAD
303	FIX	MaRS	OCC	-78.78	-68.78	ERT	GST(MAD)
303	FIX	MaRS	OCC	-24.27	-14.27	ERT	GST(MAD)
304	FIX	MaRS	OCC	-79.16	-69.16	ERT	NNO

304	FIX	MaRS	OCC	-24.16	-14.16	ERT	NNO
305	FIX	MaRS	OCC	-79.63	-69.63	ERT	MAD
305	FIX	MaRS	OCC	-23.63	-13.63	ERT	MAD
306	FIX	MaRS	OCC	-79.03	-69.03	ERT	GST(MAD)
306	FIX	MaRS	OCC	-23.02	-13.02	ERT	GST(MAD)
307	FIX	MaRS	OCC	-79.53	-69.53	ERT	NNO
307	FIX	MaRS	OCC	-22.53	-12.53	ERT	NNO
308	FIX	MaRS	OCC	-79.45	-69.45	ERT	MAD
308	FIX	MaRS	OCC	-21.95	-11.95	ERT	MAD
309	FIX	MaRS	OCC	-79.34	-69.34	ERT	GST(MAD)
309	FIX	MaRS	OCC	-21.34	-11.34	ERT	GST(MAD)
310	FIX	MaRS	OCC	-79.30	-69.30	ERT	NNO
310	FIX	MaRS	OCC	-20.80	-10.80	ERT	NNO
311	FIX	MaRS	OCC	-79.62	-69.62	ERT	NNO
311	FIX	MaRS	OCC	-20.62	-10.62	ERT	NNO
312	FIX	MaRS	OCC	-79.49	-69.49	ERT	GST(MAD)
312	FIX	MaRS	OCC	-19.99	-9.99	ERT	GST(MAD)
313	FIX	MaRS	OCC	-79.34	-69.34	ERT	GST
313	FIX	MaRS	OCC	-19.34	-9.34	ERT	GST
314	FIX	MaRS	OCC	-79.63	-69.63	ERT	NNO
314	FIX	MaRS	OCC	-19.13	-9.13	ERT	NNO
315	FIX	MaRS	OCC	-79.55	-69.55	ERT	GST(MAD)
315	FIX	MaRS	OCC	-19.05	-9.05	ERT	GST(MAD)
316	FIX	MaRS	OCC	-78.90	-68.90	ERT	GST
316	FIX	MaRS	OCC	-17.90	-7.90	ERT	GST
317	FIX	MaRS	OCC	-79.30	-69.30	ERT	NNO
317	FIX	MaRS	OCC	-17.80	-7.80	ERT	NNO
318	FIX	MaRS	OCC	-79.29	-69.29	ERT	MAD
318	FIX	MaRS	OCC	-17.29	-7.29	ERT	GST(MAD)
319	FIX	MaRS	OCC	-78.70	-68.70	ERT	GST
319	FIX	MaRS	OCC	-16.70	-6.70	ERT	GST
320	FIX	MaRS	OCC	-78.72	-68.72	ERT	NNO
320	FIX	MaRS	OCC	-16.72	-6.72	ERT	NNO
321	FIX	MaRS	OCC	-78.67	-68.67	ERT	MAD
321	FIX	MaRS	OCC	-16.17	-6.17	ERT	MAD
322	FIX	MaRS	OCC	-78.58	-68.58	ERT	GST(MAD)
322	FIX	MaRS	OCC	-15.58	-5.58	ERT	GST(MAD)
323	FIX	MaRS	OCC	-78.57	-68.57	ERT	NNO
323	FIX	MaRS	OCC	-15.57	-5.57	ERT	NNO
324	FIX	MaRS	OCC	-78.42	-68.42	ERT	MAD
324	FIX	MaRS	OCC	-14.92	-4.92	ERT	MAD
325	FIX	MaRS	OCC	-78.31	-68.31	ERT	GST(MAD)
325	FIX	MaRS	OCC	-14.81	-4.81	ERT	GST(MAD)
326	FIX	MaRS	OCC	-78.19	-68.19	ERT	NNO
326	FIX	MaRS	OCC	-14.19	-4.19	ERT	NNO
327	FIX	MaRS	OCC	-78.01	-68.01	ERT	MAD
327	FIX	MaRS	OCC	-14.00	-4.00	ERT	MAD
328	FIX	MaRS	OCC	-77.94	-67.94	ERT	GST(MAD)
328	FIX	MaRS	OCC	-13.94	-3.94	ERT	GST(MAD)
329	FIX	MaRS	OCC	-77.30	-67.30	ERT	NNO
329	FIX	MaRS	OCC	-13.30	-3.30	ERT	NNO

330	FIX	MaRS	OCC	-77.71	-67.71	ERT	NNO
330	FIX	MaRS	OCC	-13.21	-3.21	ERT	NNO
331	FIX	MaRS	OCC	-77.22	-67.22	ERT	GST(MAD)
331	FIX	MaRS	OCC	-12.71	-2.71	ERT	GST(MAD)
332	FIX	MaRS	OCC	-77.14	-67.14	ERT	GST
332	FIX	MaRS	OCC	-12.13	-2.13	ERT	NNO
333	FIX	MaRS	OCC	-77.17	-67.17	ERT	NNO
333	FIX	MaRS	OCC	-12.17	-2.17	ERT	NNO
334	FIX	MaRS	OCC	-76.64	-66.64	ERT	GST(MAD)
334	FIX	MaRS	OCC	-11.63	-1.63	ERT	GST(MAD)
335	FIX	MaRS	OCC	-76.56	-66.56	ERT	GST
335	FIX	MaRS	OCC	-11.56	-1.56	ERT	GST
336	FIX	MaRS	OCC	-76.07	-66.07	ERT	NNO
336	FIX	MaRS	OCC	-11.07	-1.07	ERT	NNO
337	FIX	MaRS	OCC	-75.94	-65.94	ERT	GST(MAD)
337	FIX	MaRS	OCC	-10.94	-0.94	ERT	GST(MAD)
338	FIX	MaRS	OCC	-75.85	-65.85	ERT	GST
338	FIX	MaRS	OCC	-10.85	-0.85	ERT	GST
339	FIX	MaRS	OCC	-75.75	-65.75	ERT	NNO
339	FIX	MaRS	OCC	-10.25	-0.25	ERT	NNO
340	FIX	MaRS	OCC	-75.57	-65.57	ERT	MAD
340	FIX	MaRS	OCC	-10.07	-0.07	ERT	MAD
341	FIX	MaRS	OCC	-75.51	-65.51	ERT	GST
341	FIX	MaRS	OCC	-10.01	-0.01	ERT	GST
342	FIX	MaRS	OCC	-74.87	-64.87	ERT	NNO
342	FIX	MaRS	OCC	-9.37	0.63	ERT	NNO
343	FIX	MaRS	OCC	-74.77	-64.77	ERT	MAD
343	FIX	MaRS	OCC	-9.27	0.73	ERT	MAD
344	FIX	MaRS	OCC	-74.78	-64.78	ERT	GST(MAD)
344	FIX	MaRS	OCC	-9.27	0.73	ERT	GST(MAD)
345	FIX	MaRS	OCC	-74.19	-64.19	ERT	NNO
345	FIX	MaRS	OCC	-8.69	1.31	ERT	NNO
346	FIX	MaRS	OCC	-74.22	-64.22	ERT	MAD
346	FIX	MaRS	OCC	-8.22	1.78	ERT	MAD
347	FIX	MaRS	OCC	-73.69	-63.69	ERT	GST(MAD)
347	FIX	MaRS	OCC	-8.19	1.81	ERT	GST(MAD)
348	FIX	MaRS	OCC	-73.63	-63.63	ERT	NNO
348	FIX	MaRS	OCC	-7.62	2.38	ERT	NNO
349	FIX	MaRS	OCC	-73.14	-63.14	ERT	NNO
349	FIX	MaRS	OCC	-7.64	2.36	ERT	NNO
350	FIX	MaRS	OCC	-73.03	-63.03	ERT	GST(MAD)
350	FIX	MaRS	OCC	-7.53	2.47	ERT	GST(MAD)
351	FIX	MaRS	OCC	-72.94	-62.94	ERT	GST
351	FIX	MaRS	OCC	-6.94	3.06	ERT	NNO
352	FIX	MaRS	OCC	-72.35	-62.35	ERT	NNO
352	FIX	MaRS	OCC	-6.85	3.15	ERT	NNO
353	FIX	MaRS	OCC	-72.18	-62.18	ERT	GST(MAD)
353	FIX	MaRS	OCC	-6.68	3.32	ERT	GST(MAD)
354	FIX	MaRS	OCC	-72.12	-62.12	ERT	GST
354	FIX	MaRS	OCC	-6.62	3.38	ERT	GST
355	FIX	MaRS	OCC	-71.48	-61.48	ERT	NNO

355	FIX	MaRS	OCC	-5.98	4.02	ERT	NNO
356	FIX	MaRS	OCC	-71.38	-61.38	ERT	GST(MAD)
356	FIX	MaRS	OCC	-5.88	4.12	ERT	GST(MAD)
357	FIX	MaRS	OCC	-71.38	-61.38	ERT	GST
357	FIX	MaRS	OCC	-5.88	4.12	ERT	GST
358	FIX	MaRS	OCC	-70.79	-60.79	ERT	NNO
358	FIX	MaRS	OCC	-5.29	4.71	ERT	NNO
359	FIX	MaRS	OCC	-70.82	-60.82	ERT	MAD
359	FIX	MaRS	OCC	-5.31	4.69	ERT	MAD
360	FIX	MaRS	OCC	-70.29	-60.29	ERT	GST
360	FIX	MaRS	OCC	-5.29	4.71	ERT	GST
361	FIX	MaRS	OCC	-69.73	-59.73	ERT	NNO
361	FIX	MaRS	OCC	-4.73	5.27	ERT	NNO
362	FIX	MaRS	OCC	-69.76	-59.76	ERT	MAD
362	FIX	MaRS	OCC	-4.76	5.24	ERT	MAD
363	FIX	MaRS	OCC	-69.65	-59.65	ERT	GST(MAD)
363	FIX	MaRS	OCC	-4.65	5.35	ERT	GST(MAD)
364	FIX	MaRS	OCC	-69.08	-59.08	ERT	NNO
364	FIX	MaRS	OCC	-4.07	5.93	ERT	NNO
365	FIX	MaRS	OCC	-69.00	-59.00	ERT	MAD
365	FIX	MaRS	OCC	-4.00	6.00	ERT	MAD
366	FIX	MaRS	OCC	-68.83	-58.83	ERT	GST(MAD)
366	FIX	MaRS	OCC	-3.83	6.17	ERT	GST(MAD)
367	FIX	MaRS	OCC	-68.27	-58.27	ERT	NNO
367	FIX	MaRS	OCC	-3.77	6.23	ERT	NNO
368	FIX	MaRS	OCC	-67.64	-57.64	ERT	NNO
368	FIX	MaRS	OCC	-3.14	6.86	ERT	NNO
369	FIX	MaRS	OCC	-67.53	-57.53	ERT	GST(MAD)
369	FIX	MaRS	OCC	-3.53	6.47	ERT	GST(MAD)
370	FIX	MaRS	OCC	-67.53	-57.53	ERT	GST
370	FIX	MaRS	OCC	-3.02	6.98	ERT	NNO
371	FIX	MaRS	OCC	-66.93	-56.93	ERT	NNO
371	FIX	MaRS	OCC	-2.93	7.07	ERT	NNO
372	FIX	MaRS	OCC	-66.95	-56.95	ERT	GST(MAD)
372	FIX	MaRS	OCC	-2.95	7.05	ERT	GST(MAD)
373	FIX	MaRS	OCC	-66.43	-56.43	ERT	GST
373	FIX	MaRS	OCC	-2.43	7.57	ERT	GST
374	FIX	MaRS	OCC	-66.37	-56.37	ERT	NNO
374	FIX	MaRS	OCC	-2.37	7.63	ERT	NNO
375	FIX	MaRS	OCC	-65.91	-55.91	ERT	GST(MAD)
375	FIX	MaRS	OCC	-1.91	8.09	ERT	GST(MAD)
376	FIX	MaRS	OCC	-65.81	-55.81	ERT	GST
376	FIX	MaRS	OCC	-1.81	8.19	ERT	GST
377	FIX	MaRS	OCC	-65.25	-55.25	ERT	NNO
377	FIX	MaRS	OCC	-1.74	8.26	ERT	NNO
378	FIX	MaRS	OCC	-65.18	-55.18	ERT	MAD
378	FIX	MaRS	OCC	-1.68	8.32	ERT	GST(MAD)
379	FIX	MaRS	OCC	-65.02	-55.02	ERT	GST
379	FIX	MaRS	OCC	-1.52	8.48	ERT	GST
380	FIX	MaRS	OCC	-64.47	-54.47	ERT	NNO
380	FIX	MaRS	OCC	-1.46	8.54	ERT	NNO

381	FIX	MaRS	OCC	-63.84	-53.84	ERT	MAD
381	FIX	MaRS	OCC	-0.83	9.17	ERT	MAD
382	FIX	MaRS	OCC	-63.72	-53.72	ERT	GST(MAD)
382	FIX	MaRS	OCC	-0.72	9.28	ERT	GST(MAD)
383	FIX	MaRS	OCC	-63.71	-53.71	ERT	NNO
383	FIX	MaRS	OCC	-0.71	9.29	ERT	NNO
384	FIX	MaRS	OCC	-63.12	-53.12	ERT	MAD
384	FIX	MaRS	OCC	-0.12	9.88	ERT	MAD
385	FIX	MaRS	OCC	-63.13	-53.13	ERT	GST(MAD)
385	FIX	MaRS	OCC	-0.63	9.37	ERT	GST(MAD)
386	FIX	MaRS	OCC	-62.62	-52.62	ERT	NNO
386	FIX	MaRS	OCC	-0.11	9.89	ERT	NNO
387	FIX	MaRS	OCC	-62.05	-52.05	ERT	NNO
387	FIX	MaRS	OCC	-0.05	9.95	ERT	NNO
388	FIX	MaRS	OCC	-62.10	-52.10	ERT	GST(MAD)
388	FIX	MaRS	OCC	-0.10	9.90	ERT	GST(MAD)
389	FIX	MaRS	OCC	-62.01	-52.01	ERT	NNO
389	FIX	MaRS	OCC	0.49	10.49	ERT	NNO
390	FIX	MaRS	OCC	-61.45	-51.45	ERT	NNO
390	FIX	MaRS	OCC	0.55	10.55	ERT	NNO
391	FIX	MaRS	OCC	-60.90	-50.90	ERT	GST(MAD)
391	FIX	MaRS	OCC	0.60	10.60	ERT	GST(MAD)
392	FIX	MaRS	OCC	-60.75	-50.75	ERT	GST
392	FIX	MaRS	OCC	0.75	10.75	ERT	GST
393	FIX	MaRS	OCC	-60.70	-50.70	ERT	NNO
393	FIX	MaRS	OCC	0.81	10.81	ERT	NNO
394	FIX	MaRS	OCC	-60.07	-50.07	ERT	GST(MAD)
394	FIX	MaRS	OCC	1.43	11.43	ERT	GST(MAD)
395	FIX	MaRS	OCC	-59.95	-49.95	ERT	GST
395	FIX	MaRS	OCC	1.05	11.05	ERT	GST
396	FIX	MaRS	OCC	-59.94	-49.94	ERT	NNO
396	FIX	MaRS	OCC	1.56	11.56	ERT	NNO
397	FIX	MaRS	OCC	-59.34	-49.34	ERT	MAD
397	FIX	MaRS	OCC	1.66	11.66	ERT	GST(MAD)
398	FIX	MaRS	OCC	-58.84	-48.84	ERT	GST
398	FIX	MaRS	OCC	1.66	11.66	ERT	GST
399	FIX	MaRS	OCC	-58.83	-48.83	ERT	NNO
399	FIX	MaRS	OCC	1.67	11.67	ERT	NNO
400	FIX	MaRS	OCC	-58.27	-48.27	ERT	MAD
400	FIX	MaRS	OCC	2.23	12.23	ERT	MAD
401	FIX	MaRS	OCC	-58.32	-48.32	ERT	GST(MAD)
401	FIX	MaRS	OCC	2.18	12.18	ERT	GST(MAD)
402	FIX	MaRS	OCC	-57.74	-47.74	ERT	NNO
402	FIX	MaRS	OCC	2.26	12.26	ERT	NNO
403	FIX	MaRS	OCC	-57.69	-47.69	ERT	MAD
403	FIX	MaRS	OCC	2.31	12.31	ERT	MAD
404	FIX	MaRS	OCC	-57.15	-47.15	ERT	GST(MAD)
404	FIX	MaRS	OCC	2.85	12.85	ERT	GST(MAD)
405	FIX	MaRS	OCC	-57.01	-47.01	ERT	NNO
405	FIX	MaRS	OCC	2.99	12.99	ERT	NNO
406	FIX	MaRS	OCC	-56.46	-46.46	ERT	MAD

406	FIX	MaRS	OCC	3.04	13.04	ERT	MAD
407	FIX	MaRS	OCC	-56.34	-46.34	ERT	GST(MAD)
407	FIX	MaRS	OCC	3.16	13.16	ERT	GST(MAD)
408	FIX	MaRS	OCC	-56.21	-46.21	ERT	NNO
408	FIX	MaRS	OCC	3.29	13.29	ERT	NNO
409	FIX	MaRS	OCC	-55.70	-45.70	ERT	NNO
409	FIX	MaRS	OCC	3.30	13.30	ERT	NNO
410	FIX	MaRS	OCC	-55.09	-45.09	ERT	GST(MAD)
410	FIX	MaRS	OCC	3.41	13.41	ERT	GST(MAD)
411	FIX	MaRS	OCC	-55.09	-45.09	ERT	GST
411	FIX	MaRS	OCC	3.41	13.41	ERT	GST
412	FIX	MaRS	OCC	-55.07	-45.07	ERT	NNO
412	FIX	MaRS	OCC	3.93	13.93	ERT	NNO
413	FIX	MaRS	OCC	-54.51	-44.51	ERT	GST(MAD)
413	FIX	MaRS	OCC	3.99	13.99	ERT	GST(MAD)
414	FIX	MaRS	OCC	-54.07	-44.07	ERT	GST
414	FIX	MaRS	OCC	3.94	13.94	ERT	GST
415	FIX	MaRS	OCC	-54.00	-44.00	ERT	NNO
415	FIX	MaRS	OCC	4.00	14.00	ERT	NNO
416	FIX	MaRS	OCC	-53.45	-43.45	ERT	MAD
416	FIX	MaRS	OCC	4.55	14.55	ERT	GST(MAD)
417	FIX	MaRS	OCC	-53.43	-43.43	ERT	GST
417	FIX	MaRS	OCC	4.58	14.58	ERT	GST
418	FIX	MaRS	OCC	-53.29	-43.29	ERT	NNO
418	FIX	MaRS	OCC	4.71	14.71	ERT	NNO
419	FIX	MaRS	OCC	-52.74	-42.74	ERT	MAD
419	FIX	MaRS	OCC	4.76	14.76	ERT	MAD
420	FIX	MaRS	OCC	-52.63	-42.63	ERT	GST(MAD)
420	FIX	MaRS	OCC	4.88	14.88	ERT	GST(MAD)
421	FIX	MaRS	OCC	-52.00	-42.00	ERT	NNO
421	FIX	MaRS	OCC	5.00	15.00	ERT	NNO
422	FIX	MaRS	OCC	-51.98	-41.98	ERT	MAD
422	FIX	MaRS	OCC	5.02	15.02	ERT	MAD
423	FIX	MaRS	OCC	-51.37	-41.37	ERT	GST(MAD)
423	FIX	MaRS	OCC	5.13	15.13	ERT	GST(MAD)
424	FIX	MaRS	OCC	-51.35	-41.35	ERT	NNO
424	FIX	MaRS	OCC	5.15	15.15	ERT	NNO
425	FIX	MaRS	OCC	-50.84	-40.84	ERT	MAD
425	FIX	MaRS	OCC	5.66	15.66	ERT	MAD
426	FIX	MaRS	OCC	-50.77	-40.77	ERT	GST(MAD)
426	FIX	MaRS	OCC	5.73	15.73	ERT	GST(MAD)
427	FIX	MaRS	OCC	-50.33	-40.33	ERT	NNO
427	FIX	MaRS	OCC	5.67	15.67	ERT	NNO
428	FIX	MaRS	OCC	-50.27	-40.27	ERT	NNO
428	FIX	MaRS	OCC	5.73	15.73	ERT	NNO
429	FIX	MaRS	OCC	-49.73	-39.73	ERT	GST(MAD)
429	FIX	MaRS	OCC	6.28	16.28	ERT	GST(MAD)
430	FIX	MaRS	OCC	-49.71	-39.71	ERT	GST
430	FIX	MaRS	OCC	6.29	16.29	ERT	NNO
431	FIX	MaRS	OCC	-49.08	-39.08	ERT	NNO
431	FIX	MaRS	OCC	6.42	16.42	ERT	NNO

432	FIX	MaRS	OCC	-49.04	-39.04	ERT	GST(MAD)
432	FIX	MaRS	OCC	6.46	16.46	ERT	GST(MAD)
433	FIX	MaRS	OCC	-48.43	-38.43	ERT	GST
433	FIX	MaRS	OCC	6.57	16.57	ERT	GST
434	FIX	MaRS	OCC	-48.30	-38.30	ERT	NNO
434	FIX	MaRS	OCC	6.70	16.70	ERT	NNO
435	FIX	MaRS	OCC	-48.28	-38.28	ERT	GST(MAD)
435	FIX	MaRS	OCC	6.72	16.72	ERT	GST(MAD)
436	FIX	MaRS	OCC	-47.66	-37.66	ERT	GST
436	FIX	MaRS	OCC	6.84	16.84	ERT	GST
437	FIX	MaRS	OCC	-47.64	-37.64	ERT	NNO
437	FIX	MaRS	OCC	6.86	16.86	ERT	NNO
438	FIX	MaRS	OCC	-47.12	-37.12	ERT	MAD
438	FIX	MaRS	OCC	6.88	16.88	ERT	MAD
439	FIX	MaRS	OCC	-47.05	-37.05	ERT	GST
439	FIX	MaRS	OCC	7.45	17.45	ERT	GST
440	FIX	MaRS	OCC	-46.61	-36.61	ERT	NNO
440	FIX	MaRS	OCC	7.39	17.39	ERT	NNO
441	FIX	MaRS	OCC	-46.55	-36.55	ERT	MAD
441	FIX	MaRS	OCC	7.45	17.45	ERT	MAD
442	FIX	MaRS	OCC	-46.01	-36.01	ERT	GST(MAD)
442	FIX	MaRS	OCC	7.49	17.49	ERT	GST(MAD)
443	FIX	MaRS	OCC	-46.01	-36.01	ERT	NNO
443	FIX	MaRS	OCC	7.49	17.49	ERT	NNO
444	FIX	MaRS	OCC	-45.39	-35.39	ERT	MAD
444	FIX	MaRS	OCC	7.61	17.61	ERT	MAD
445	FIX	MaRS	OCC	-45.35	-35.35	ERT	GST(MAD)
445	FIX	MaRS	OCC	8.15	18.15	ERT	GST(MAD)
446	FIX	MaRS	OCC	-45.25	-35.25	ERT	NNO
446	FIX	MaRS	OCC	8.25	18.25	ERT	NNO
447	FIX	MaRS	OCC	-44.61	-34.61	ERT	NNO
447	FIX	MaRS	OCC	7.89	17.89	ERT	NNO
448	FIX	MaRS	OCC	-44.59	-34.59	ERT	GST(MAD)
448	FIX	MaRS	OCC	8.41	18.41	ERT	GST(MAD)
449	FIX	MaRS	OCC	-43.97	-33.97	ERT	GST
449	FIX	MaRS	OCC	8.53	18.53	ERT	NNO
450	FIX	MaRS	OCC	-43.93	-33.93	ERT	NNO
450	FIX	MaRS	OCC	8.57	18.57	ERT	NNO
451	FIX	MaRS	OCC	-43.91	-33.91	ERT	GST(MAD)
451	FIX	MaRS	OCC	8.59	18.59	ERT	GST(MAD)
452	FIX	MaRS	OCC	-43.34	-33.34	ERT	GST
452	FIX	MaRS	OCC	8.66	18.66	ERT	GST
453	FIX	MaRS	OCC	-43.39	-33.39	ERT	NNO
453	FIX	MaRS	OCC	8.61	18.61	ERT	NNO
454	FIX	MaRS	OCC	-42.84	-32.84	ERT	GST(MAD)
454	FIX	MaRS	OCC	9.16	19.16	ERT	GST(MAD)
455	FIX	MaRS	OCC	-42.80	-32.80	ERT	GST
455	FIX	MaRS	OCC	9.20	19.20	ERT	GST
456	FIX	MaRS	OCC	-42.31	-32.31	ERT	NNO
456	FIX	MaRS	OCC	9.19	19.19	ERT	NNO
457	FIX	MaRS	OCC	-42.20	-32.20	ERT	MAD

457	FIX	MaRS	OCC	9.30	19.30	ERT	MAD
458	FIX	MaRS	OCC	-41.67	-31.67	ERT	GST
458	FIX	MaRS	OCC	9.33	19.33	ERT	GST
459	FIX	MaRS	OCC	-41.57	-31.57	ERT	NNO
459	FIX	MaRS	OCC	9.43	19.43	ERT	NNO
460	FIX	MaRS	OCC	-41.44	-31.44	ERT	MAD
460	FIX	MaRS	OCC	9.57	19.57	ERT	MAD
461	FIX	MaRS	OCC	-40.91	-30.91	ERT	GST(MAD)
461	FIX	MaRS	OCC	9.59	19.59	ERT	GST(MAD)
462	FIX	MaRS	OCC	-40.78	-30.78	ERT	NNO
462	FIX	MaRS	OCC	9.72	19.72	ERT	NNO
463	FIX	MaRS	OCC	-40.73	-30.73	ERT	MAD
463	FIX	MaRS	OCC	9.77	19.77	ERT	MAD
464	FIX	MaRS	OCC	-40.21	-30.21	ERT	GST(MAD)
464	FIX	MaRS	OCC	9.79	19.79	ERT	GST(MAD)
465	FIX	MaRS	OCC	-40.13	-30.13	ERT	NNO
465	FIX	MaRS	OCC	10.37	20.37	ERT	NNO
466	FIX	MaRS	OCC	-39.68	-29.68	ERT	NNO
466	FIX	MaRS	OCC	10.32	20.32	ERT	NNO
467	FIX	MaRS	OCC	-39.64	-29.64	ERT	GST(MAD)
467	FIX	MaRS	OCC	10.37	20.37	ERT	GST(MAD)
468	FIX	MaRS	OCC	-39.10	-29.10	ERT	GST
468	FIX	MaRS	OCC	10.40	20.40	ERT	NNO
469	FIX	MaRS	OCC	-39.12	-29.12	ERT	NNO
469	FIX	MaRS	OCC	10.38	20.38	ERT	NNO
470	FIX	MaRS	OCC	-38.51	-28.51	ERT	GST(MAD)
470	FIX	MaRS	OCC	10.49	20.49	ERT	GST(MAD)
471	FIX	MaRS	OCC	-38.48	-28.48	ERT	GST
471	FIX	MaRS	OCC	10.52	20.52	ERT	GST
472	FIX	MaRS	OCC	-38.39	-28.39	ERT	NNO
472	FIX	MaRS	OCC	10.61	20.61	ERT	NNO
473	FIX	MaRS	OCC	-37.76	-27.76	ERT	GST(MAD)
473	FIX	MaRS	OCC	10.74	20.74	ERT	GST(MAD)
474	FIX	MaRS	OCC	-37.73	-27.73	ERT	GST
474	FIX	MaRS	OCC	10.77	20.77	ERT	GST
475	FIX	MaRS	OCC	-37.60	-27.60	ERT	NNO
475	FIX	MaRS	OCC	10.90	20.90	ERT	NNO
476	FIX	MaRS	OCC	-37.54	-27.54	ERT	MAD
476	FIX	MaRS	OCC	10.96	20.96	ERT	GST(MAD)
477	FIX	MaRS	OCC	-37.02	-27.02	ERT	GST
477	FIX	MaRS	OCC	11.49	21.49	ERT	GST
478	FIX	MaRS	OCC	-36.93	-26.93	ERT	NNO
478	FIX	MaRS	OCC	11.57	21.57	ERT	NNO
479	FIX	MaRS	OCC	-36.48	-26.48	ERT	MAD
479	FIX	MaRS	OCC	11.52	21.52	ERT	MAD
480	FIX	MaRS	OCC	-36.43	-26.43	ERT	GST(MAD)
480	FIX	MaRS	OCC	11.57	21.57	ERT	GST(MAD)
481	FIX	MaRS	OCC	-35.90	-25.90	ERT	NNO
481	FIX	MaRS	OCC	11.60	21.60	ERT	NNO
482	FIX	MaRS	OCC	-35.93	-25.93	ERT	MAD
482	FIX	MaRS	OCC	11.57	21.57	ERT	MAD

483	FIX	MaRS	OCC	-35.33	-25.33	ERT	GST(MAD)
483	FIX	MaRS	OCC	11.67	21.67	ERT	GST(MAD)
484	FIX	MaRS	OCC	-35.30	-25.30	ERT	NNO
484	FIX	MaRS	OCC	11.70	21.70	ERT	NNO
485	FIX	MaRS	OCC	-35.22	-25.22	ERT	NNO
485	FIX	MaRS	OCC	11.78	21.78	ERT	NNO
486	FIX	MaRS	OCC	-34.59	-24.59	ERT	GST(MAD)
486	FIX	MaRS	OCC	11.91	21.91	ERT	GST(MAD)
487	FIX	MaRS	OCC	-34.55	-24.55	ERT	NNO
487	FIX	MaRS	OCC	11.95	21.95	ERT	NNO
488	FIX	MaRS	OCC	-34.42	-24.42	ERT	NNO
488	FIX	MaRS	OCC	12.08	22.08	ERT	NNO
489	FIX	MaRS	OCC	-34.35	-24.35	ERT	GST(MAD)
489	FIX	MaRS	OCC	12.15	22.15	ERT	GST(MAD)
490	FIX	MaRS	OCC	-33.82	-23.82	ERT	GST
490	FIX	MaRS	OCC	12.68	22.68	ERT	GST
491	FIX	MaRS	OCC	-33.73	-23.73	ERT	NNO
491	FIX	MaRS	OCC	12.77	22.77	ERT	NNO
492	FIX	MaRS	OCC	-33.27	-23.27	ERT	GST(MAD)
492	FIX	MaRS	OCC	12.73	22.73	ERT	GST(MAD)
493	FIX	MaRS	OCC	-33.23	-23.23	ERT	GST
493	FIX	MaRS	OCC	12.77	22.77	ERT	GST
494	FIX	MaRS	OCC	-32.69	-22.69	ERT	NNO
494	FIX	MaRS	OCC	12.81	22.81	ERT	NNO
495	FIX	MaRS	OCC	-32.73	-22.73	ERT	MAD
495	FIX	MaRS	OCC	12.77	22.77	ERT	GST(MAD)
496	FIX	MaRS	OCC	-32.64	-22.64	ERT	GST
496	FIX	MaRS	OCC	12.86	22.86	ERT	GST
497	FIX	MaRS	OCC	-32.12	-22.12	ERT	NNO
497	FIX	MaRS	OCC	12.88	22.88	ERT	NNO
498	FIX	MaRS	OCC	-32.05	-22.05	ERT	MAD
498	FIX	MaRS	OCC	12.95	22.95	ERT	MAD
499	FIX	MaRS	OCC	-31.92	-21.92	ERT	GST(MAD)
499	FIX	MaRS	OCC	13.08	23.08	ERT	GST(MAD)
500	FIX	MaRS	OCC	-31.38	-21.38	ERT	NNO
500	FIX	MaRS	OCC	13.12	23.12	ERT	NNO
501	FIX	MaRS	OCC	-31.25	-21.25	ERT	MAD
501	FIX	MaRS	OCC	13.25	23.25	ERT	MAD
502	FIX	MaRS	OCC	-31.17	-21.17	ERT	GST(MAD)
502	FIX	MaRS	OCC	13.33	23.33	ERT	GST(MAD)
503	FIX	MaRS	OCC	-30.64	-20.64	ERT	NNO
503	FIX	MaRS	OCC	13.86	23.86	ERT	NNO
504	FIX	MaRS	OCC	-30.54	-20.54	ERT	NNO
504	FIX	MaRS	OCC	13.96	23.96	ERT	NNO
505	FIX	MaRS	OCC	-30.57	-20.57	ERT	GST(MAD)
505	FIX	MaRS	OCC	13.93	23.93	ERT	GST(MAD)
506	FIX	MaRS	OCC	-30.03	-20.03	ERT	NNO
506	FIX	MaRS	OCC	13.97	23.97	ERT	NNO
507	FIX	MaRS	OCC	-29.99	-19.99	ERT	NNO
507	FIX	MaRS	OCC	14.01	24.01	ERT	NNO
508	FIX	MaRS	OCC	-30.04	-20.04	ERT	GST(MAD)

508	FIX	MaRS	OCC	13.96	23.96	ERT	GST(MAD)
509	FIX	MaRS	OCC	-29.46	-19.46	ERT	GST
509	FIX	MaRS	OCC	14.04	24.04	ERT	GST
510	FIX	MaRS	OCC	-29.45	-19.45	ERT	NNO
510	FIX	MaRS	OCC	14.06	24.06	ERT	NNO
511	FIX	MaRS	OCC	-29.38	-19.38	ERT	GST(MAD)
511	FIX	MaRS	OCC	14.12	24.12	ERT	GST(MAD)
512	FIX	MaRS	OCC	-28.75	-18.75	ERT	GST
512	FIX	MaRS	OCC	14.25	24.25	ERT	GST
513	FIX	MaRS	OCC	-28.72	-18.72	ERT	NNO
513	FIX	MaRS	OCC	14.28	24.28	ERT	NNO
514	FIX	MaRS	OCC	-28.58	-18.58	ERT	MAD
514	FIX	MaRS	OCC	14.42	24.42	ERT	GST(MAD)
515	FIX	MaRS	OCC	-28.50	-18.50	ERT	GST
515	FIX	MaRS	OCC	14.51	24.51	ERT	GST
516	FIX	MaRS	OCC	-27.96	-17.96	ERT	NNO
516	FIX	MaRS	OCC	14.54	24.54	ERT	NNO
517	FIX	MaRS	OCC	-27.85	-17.85	ERT	MAD
517	FIX	MaRS	OCC	14.65	24.65	ERT	MAD
518	FIX	MaRS	OCC	-27.88	-17.88	ERT	GST(MAD)
518	FIX	MaRS	OCC	14.62	24.62	ERT	GST(MAD)
519	FIX	MaRS	OCC	-27.34	-17.34	ERT	NNO
519	FIX	MaRS	OCC	470.14	480.14	ERT	NNO
520	FIX	MaRS	OCC	-27.30	-17.30	ERT	MAD
520	FIX	MaRS	OCC	470.18	480.18	ERT	MAD
521	FIX	MaRS	OCC	-27.35	-17.35	ERT	GST(MAD)
521	FIX	MaRS	OCC	470.22	480.22	ERT	GST(MAD)
522	FIX	MaRS	OCC	-26.78	-16.78	ERT	NNO
522	FIX	MaRS	OCC	470.16	480.16	ERT	NNO
523	FIX	MaRS	OCC	-26.77	-16.77	ERT	MAD
523	FIX	MaRS	OCC	470.23	480.23	ERT	MAD
524	FIX	MaRS	OCC	-26.72	-16.72	ERT	GST(MAD)
524	FIX	MaRS	OCC	10.28	20.28	ERT	GST(MAD)
524	FIX	MaRS	OCC	20.78	30.78	ERT	GST(MAD)
524	FIX	MaRS	OCC	470.24	480.24	ERT	GST(MAD)
525	FIX	MaRS	OCC	-26.09	-16.09	ERT	NNO
525	FIX	MaRS	OCC	10.41	20.41	ERT	NNO
525	FIX	MaRS	OCC	20.91	30.91	ERT	NNO
525	FIX	MaRS	OCC	470.29	480.29	ERT	NNO
526	FIX	MaRS	OCC	-26.06	-16.06	ERT	NNO
526	FIX	MaRS	OCC	10.44	20.44	ERT	NNO
526	FIX	MaRS	OCC	20.94	30.94	ERT	NNO
526	FIX	MaRS	OCC	470.42	480.42	ERT	NNO
527	FIX	MaRS	OCC	-25.93	-15.93	ERT	GST(MAD)
527	FIX	MaRS	OCC	10.57	20.57	ERT	GST(MAD)
527	FIX	MaRS	OCC	21.07	31.07	ERT	GST(MAD)
527	FIX	MaRS	OCC	470.45	480.45	ERT	GST(MAD)
528	FIX	MaRS	OCC	-25.83	-15.83	ERT	GST
528	FIX	MaRS	OCC	10.67	20.67	ERT	NNO
528	FIX	MaRS	OCC	21.17	31.17	ERT	NNO
528	FIX	MaRS	OCC	470.59	480.59	ERT	NNO

529	FIX	MaRS	OCC	-25.29	-15.29	ERT	NNO
529	FIX	MaRS	OCC	10.71	20.71	ERT	NNO
529	FIX	MaRS	OCC	21.21	31.21	ERT	NNO
529	FIX	MaRS	OCC	470.68	480.68	ERT	NNO
530	FIX	MaRS	OCC	-25.18	-15.18	ERT	GST(MAD)
530	FIX	MaRS	OCC	10.83	20.83	ERT	GST(MAD)
530	FIX	MaRS	OCC	21.33	31.33	ERT	GST(MAD)
530	FIX	MaRS	OCC	470.73	480.73	ERT	GST(MAD)
531	FIX	MaRS	OCC	-25.19	-15.19	ERT	GST
531	FIX	MaRS	OCC	10.81	20.81	ERT	GST
531	FIX	MaRS	OCC	21.31	31.31	ERT	GST
531	FIX	MaRS	OCC	470.84	480.84	ERT	GST
532	FIX	MaRS	OCC	-24.65	-14.65	ERT	NNO
532	FIX	MaRS	OCC	10.85	20.85	ERT	NNO
532	FIX	MaRS	OCC	21.35	31.35	ERT	NNO
532	FIX	MaRS	OCC	471.32	481.32	ERT	NNO
533	FIX	MaRS	OCC	-24.61	-14.61	ERT	GST(MAD)
533	FIX	MaRS	OCC	10.89	20.89	ERT	GST(MAD)
533	FIX	MaRS	OCC	21.39	31.39	ERT	GST(MAD)
533	FIX	MaRS	OCC	470.86	480.86	ERT	GST(MAD)
534	FIX	MaRS	OCC	-24.67	-14.67	ERT	GST
534	FIX	MaRS	OCC	10.83	20.83	ERT	GST
534	FIX	MaRS	OCC	21.33	31.33	ERT	GST
534	FIX	MaRS	OCC	471.40	481.40	ERT	GST
535	FIX	MaRS	OCC	-24.11	-14.11	ERT	NNO
535	FIX	MaRS	OCC	10.89	20.89	ERT	NNO
535	FIX	MaRS	OCC	21.39	31.39	ERT	NNO
535	FIX	MaRS	OCC	471.34	481.34	ERT	NNO
536	FIX	MaRS	OCC	-24.11	-14.11	ERT	MAD
536	FIX	MaRS	OCC	10.89	20.89	ERT	MAD
536	FIX	MaRS	OCC	21.89	31.89	ERT	MAD
536	FIX	MaRS	OCC	471.40	481.40	ERT	MAD
537	FIX	MaRS	OCC	-24.07	-14.07	ERT	GST
537	FIX	MaRS	OCC	10.93	20.93	ERT	GST
537	FIX	MaRS	OCC	21.93	31.93	ERT	GST
537	FIX	MaRS	OCC	471.40	481.40	ERT	GST
538	FIX	MaRS	OCC	-23.45	-13.45	ERT	NNO
538	FIX	MaRS	OCC	10.55	20.55	ERT	NNO
538	FIX	MaRS	OCC	22.05	32.05	ERT	NNO
538	FIX	MaRS	OCC	471.44	481.44	ERT	NNO
539	FIX	MaRS	OCC	-23.42	-13.42	ERT	MAD
539	FIX	MaRS	OCC	10.58	20.58	ERT	MAD
539	FIX	MaRS	OCC	22.08	32.08	ERT	MAD
539	FIX	MaRS	OCC	471.57	481.57	ERT	MAD
540	FIX	MaRS	OCC	-23.28	-13.28	ERT	GST(MAD)
540	FIX	MaRS	OCC	10.72	20.72	ERT	GST(MAD)
540	FIX	MaRS	OCC	21.72	31.72	ERT	GST(MAD)
540	FIX	MaRS	OCC	471.59	481.59	ERT	GST(MAD)
541	FIX	MaRS	OCC	-23.18	-13.18	ERT	NNO
541	FIX	MaRS	OCC	10.82	20.82	ERT	NNO
541	FIX	MaRS	OCC	21.82	31.82	ERT	NNO

541	FIX	MaRS	OCC	471.73	481.73	ERT	NNO
542	FIX	MaRS	OCC	-22.64	-12.64	ERT	MAD
542	FIX	MaRS	OCC	10.86	20.86	ERT	MAD
542	FIX	MaRS	OCC	21.86	31.86	ERT	MAD
542	FIX	MaRS	OCC	471.83	481.83	ERT	MAD
543	FIX	MaRS	OCC	-22.52	-12.52	ERT	GST(MAD)
543	FIX	MaRS	OCC	10.98	20.98	ERT	GST(MAD)
543	FIX	MaRS	OCC	21.98	31.98	ERT	GST(MAD)
543	FIX	MaRS	OCC	471.88	481.88	ERT	GST(MAD)
544	FIX	MaRS	OCC	-22.53	-12.53	ERT	NNO
544	FIX	MaRS	OCC	10.97	20.97	ERT	NNO
544	FIX	MaRS	OCC	22.47	32.47	ERT	NNO
544	FIX	MaRS	OCC	472.00	482.00	ERT	NNO
545	FIX	MaRS	OCC	-21.99	-11.99	ERT	NNO
545	FIX	MaRS	OCC	11.01	21.01	ERT	NNO
545	FIX	MaRS	OCC	22.51	32.51	ERT	NNO
545	FIX	MaRS	OCC	471.99	481.99	ERT	NNO
546	FIX	MaRS	OCC	-21.95	-11.95	ERT	GST(MAD)
546	FIX	MaRS	OCC	11.06	21.06	ERT	GST(MAD)
546	FIX	MaRS	OCC	22.56	32.56	ERT	GST(MAD)
546	FIX	MaRS	OCC	472.03	482.03	ERT	GST(MAD)
547	FIX	MaRS	OCC	-22.01	-12.01	ERT	GST
547	FIX	MaRS	OCC	10.99	20.99	ERT	NNO
547	FIX	MaRS	OCC	22.49	32.49	ERT	NNO
547	FIX	MaRS	OCC	472.07	482.07	ERT	NNO
548	FIX	MaRS	OCC	-21.46	-11.46	ERT	NNO
548	FIX	MaRS	OCC	11.04	21.04	ERT	NNO
548	FIX	MaRS	OCC	22.54	32.54	ERT	NNO
548	FIX	MaRS	OCC	472.50	482.50	ERT	NNO
549	FIX	MaRS	OCC	-21.46	-11.46	ERT	GST(MAD)
549	FIX	MaRS	OCC	11.04	21.04	ERT	GST(MAD)
549	FIX	MaRS	OCC	22.54	32.54	ERT	GST(MAD)
549	FIX	MaRS	OCC	472.56	482.56	ERT	GST(MAD)
550	FIX	MaRS	OCC	-21.43	-11.43	ERT	GST
550	FIX	MaRS	OCC	11.07	21.07	ERT	GST
550	FIX	MaRS	OCC	22.57	32.57	ERT	GST
550	FIX	MaRS	OCC	472.55	482.55	ERT	GST
551	FIX	MaRS	OCC	-20.82	-10.82	ERT	NNO
551	FIX	MaRS	OCC	10.68	20.68	ERT	NNO
551	FIX	MaRS	OCC	22.68	32.68	ERT	NNO
551	FIX	MaRS	OCC	472.58	482.58	ERT	NNO
552	FIX	MaRS	OCC	-20.79	-10.79	ERT	GST(MAD)
552	FIX	MaRS	OCC	10.71	20.71	ERT	GST(MAD)
552	FIX	MaRS	OCC	22.71	32.71	ERT	GST(MAD)
552	FIX	MaRS	OCC	472.70	482.70	ERT	GST(MAD)
553	FIX	MaRS	OCC	-20.66	-10.66	ERT	GST
553	FIX	MaRS	OCC	10.84	20.84	ERT	GST
553	FIX	MaRS	OCC	22.84	32.84	ERT	GST
553	FIX	MaRS	OCC	472.72	482.72	ERT	GST
554	FIX	MaRS	OCC	-20.56	-10.56	ERT	NNO
554	FIX	MaRS	OCC	10.95	20.95	ERT	NNO

554	FIX	MaRS	OCC	22.95	32.95	ERT	NNO
554	FIX	MaRS	OCC	472.85	482.85	ERT	NNO
555	FIX	MaRS	OCC	-20.51	-10.51	ERT	MAD
555	FIX	MaRS	OCC	10.99	20.99	ERT	MAD
555	FIX	MaRS	OCC	22.99	32.99	ERT	MAD
555	FIX	MaRS	OCC	472.96	482.96	ERT	MAD
556	FIX	MaRS	OCC	-20.38	-10.38	ERT	GST
556	FIX	MaRS	OCC	11.12	21.12	ERT	GST
556	FIX	MaRS	OCC	23.12	33.12	ERT	GST
556	FIX	MaRS	OCC	473.00	483.00	ERT	GST
557	FIX	MaRS	OCC	-19.89	-9.89	ERT	NNO
557	FIX	MaRS	OCC	11.12	21.12	ERT	NNO
557	FIX	MaRS	OCC	23.12	33.12	ERT	NNO
557	FIX	MaRS	OCC	473.13	483.13	ERT	NNO
558	FIX	MaRS	OCC	-19.85	-9.85	ERT	MAD
558	FIX	MaRS	OCC	11.16	21.16	ERT	MAD
558	FIX	MaRS	OCC	23.16	33.16	ERT	MAD
558	FIX	MaRS	OCC	473.13	483.13	ERT	MAD
559	FIX	MaRS	OCC	-19.80	-9.80	ERT	GST(MAD)
559	FIX	MaRS	OCC	11.20	21.20	ERT	GST(MAD)
559	FIX	MaRS	OCC	23.20	33.20	ERT	GST(MAD)
559	FIX	MaRS	OCC	473.17	483.17	ERT	GST(MAD)
560	FIX	MaRS	OCC	-19.37	-9.37	ERT	NNO
560	FIX	MaRS	OCC	11.13	21.13	ERT	NNO
560	FIX	MaRS	OCC	23.13	33.13	ERT	NNO
560	FIX	MaRS	OCC	473.21	483.21	ERT	NNO
561	FIX	MaRS	OCC	-19.33	-9.33	ERT	MAD
561	FIX	MaRS	OCC	11.18	21.18	ERT	MAD
561	FIX	MaRS	OCC	23.18	33.18	ERT	MAD
561	FIX	MaRS	OCC	473.64	483.64	ERT	MAD
562	FIX	MaRS	OCC	-18.84	-8.84	ERT	GST(MAD)
562	FIX	MaRS	OCC	11.16	21.16	ERT	GST(MAD)
562	FIX	MaRS	OCC	23.66	33.66	ERT	GST(MAD)
562	FIX	MaRS	OCC	473.69	483.69	ERT	GST(MAD)
563	FIX	MaRS	OCC	-18.82	-8.82	ERT	NNO
563	FIX	MaRS	OCC	11.18	21.18	ERT	NNO
563	FIX	MaRS	OCC	23.68	33.68	ERT	NNO
563	FIX	MaRS	OCC	473.18	483.18	ERT	NNO
564	FIX	MaRS	OCC	-18.71	-8.71	ERT	NNO
564	FIX	MaRS	OCC	10.79	20.79	ERT	NNO
564	FIX	MaRS	OCC	23.79	33.79	ERT	NNO
564	FIX	MaRS	OCC	473.69	483.69	ERT	NNO
565	FIX	MaRS	OCC	-18.70	-8.70	ERT	GST(MAD)
565	FIX	MaRS	OCC	10.81	20.81	ERT	GST(MAD)
565	FIX	MaRS	OCC	23.81	33.81	ERT	GST(MAD)
565	FIX	MaRS	OCC	473.80	483.80	ERT	GST(MAD)
566	FIX	MaRS	OCC	-18.57	-8.57	ERT	NNO
566	FIX	MaRS	OCC	10.93	20.93	ERT	NNO
566	FIX	MaRS	OCC	23.43	33.43	ERT	NNO
566	FIX	MaRS	OCC	473.32	483.32	ERT	NNO
567	FIX	MaRS	OCC	-18.46	-8.46	ERT	NNO

567	FIX	MaRS	OCC	11.04	21.04	ERT	NNO
567	FIX	MaRS	OCC	23.54	33.54	ERT	NNO
567	FIX	MaRS	OCC	473.44	483.44	ERT	NNO
568	FIX	MaRS	OCC	-17.91	-7.91	ERT	GST(MAD)
568	FIX	MaRS	OCC	11.09	21.09	ERT	GST(MAD)
568	FIX	MaRS	OCC	23.59	33.59	ERT	GST(MAD)
568	FIX	MaRS	OCC	474.05	484.05	ERT	GST(MAD)
569	FIX	MaRS	OCC	-17.78	-7.78	ERT	GST
569	FIX	MaRS	OCC	11.22	21.22	ERT	GST
569	FIX	MaRS	OCC	23.72	33.72	ERT	GST
569	FIX	MaRS	OCC	473.60	483.60	ERT	GST
570	FIX	MaRS	OCC	-17.77	-7.77	ERT	NNO
570	FIX	MaRS	OCC	11.23	21.23	ERT	NNO
570	FIX	MaRS	OCC	23.73	33.73	ERT	NNO
570	FIX	MaRS	OCC	473.73	483.73	ERT	NNO
571	FIX	MaRS	OCC	-17.23	-7.23	ERT	GST(MAD)
571	FIX	MaRS	OCC	11.27	21.27	ERT	GST(MAD)
571	FIX	MaRS	OCC	23.77	33.77	ERT	GST(MAD)
571	FIX	MaRS	OCC	474.24	484.24	ERT	GST(MAD)
572	FIX	MaRS	OCC	-17.18	-7.18	ERT	GST
572	FIX	MaRS	OCC	11.32	21.32	ERT	GST
572	FIX	MaRS	OCC	23.82	33.82	ERT	GST
572	FIX	MaRS	OCC	474.28	484.28	ERT	GST
573	FIX	MaRS	OCC	-17.26	-7.26	ERT	NNO
573	FIX	MaRS	OCC	11.24	21.24	ERT	NNO
573	FIX	MaRS	OCC	24.24	34.24	ERT	NNO
573	FIX	MaRS	OCC	474.33	484.33	ERT	NNO
574	FIX	MaRS	OCC	-16.72	-6.72	ERT	MAD
574	FIX	MaRS	OCC	11.28	21.28	ERT	MAD
574	FIX	MaRS	OCC	24.28	34.28	ERT	MAD
574	FIX	MaRS	OCC	474.25	484.25	ERT	MAD
575	FIX	MaRS	OCC	-16.74	-6.74	ERT	GST
575	FIX	MaRS	OCC	11.26	21.26	ERT	GST
575	FIX	MaRS	OCC	24.26	34.26	ERT	GST
575	FIX	MaRS	OCC	474.29	484.29	ERT	GST
576	FIX	MaRS	OCC	-16.74	-6.74	ERT	NNO
576	FIX	MaRS	OCC	11.26	21.26	ERT	NNO
576	FIX	MaRS	OCC	24.26	34.26	ERT	NNO
576	FIX	MaRS	OCC	474.27	484.27	ERT	NNO
577	FIX	MaRS	OCC	-16.14	-6.14	ERT	MAD
577	FIX	MaRS	OCC	11.36	21.36	ERT	MAD
577	FIX	MaRS	OCC	24.36	34.36	ERT	MAD
577	FIX	MaRS	OCC	474.77	484.77	ERT	MAD
578	FIX	MaRS	OCC	-16.13	-6.13	ERT	GST(MAD)
578	FIX	MaRS	OCC	11.37	21.37	ERT	GST(MAD)
578	FIX	MaRS	OCC	24.37	34.37	ERT	GST(MAD)
578	FIX	MaRS	OCC	474.87	484.87	ERT	GST(MAD)
579	FIX	MaRS	OCC	-16.01	-6.01	ERT	NNO
579	FIX	MaRS	OCC	10.99	20.99	ERT	NNO
579	FIX	MaRS	OCC	24.49	34.49	ERT	NNO
579	FIX	MaRS	OCC	474.38	484.38	ERT	NNO

580	FIX	MaRS	OCC	-15.89	-5.89	ERT	MAD
580	FIX	MaRS	OCC	11.11	21.11	ERT	MAD
580	FIX	MaRS	OCC	24.61	34.61	ERT	MAD
580	FIX	MaRS	OCC	474.50	484.50	ERT	MAD
581	FIX	MaRS	OCC	-15.85	-5.85	ERT	GST(MAD)
581	FIX	MaRS	OCC	11.15	21.15	ERT	GST(MAD)
581	FIX	MaRS	OCC	24.65	34.65	ERT	GST(MAD)
581	FIX	MaRS	OCC	475.12	485.12	ERT	GST(MAD)
582	FIX	MaRS	OCC	-15.71	-5.71	ERT	NNO
582	FIX	MaRS	OCC	11.29	21.29	ERT	NNO
582	FIX	MaRS	OCC	24.79	34.79	ERT	NNO
582	FIX	MaRS	OCC	474.66	484.66	ERT	NNO
583	FIX	MaRS	OCC	-15.69	-5.69	ERT	NNO
583	FIX	MaRS	OCC	11.31	21.31	ERT	NNO
583	FIX	MaRS	OCC	24.81	34.81	ERT	NNO
583	FIX	MaRS	OCC	474.80	484.80	ERT	NNO
584	FIX	MaRS	OCC	-15.15	-5.15	ERT	GST(MAD)
584	FIX	MaRS	OCC	11.35	21.35	ERT	GST(MAD)
584	FIX	MaRS	OCC	24.85	34.85	ERT	GST(MAD)
584	FIX	MaRS	OCC	475.32	485.32	ERT	GST(MAD)
585	FIX	MaRS	OCC	-15.09	-5.09	ERT	NNO
585	FIX	MaRS	OCC	11.41	21.41	ERT	NNO
585	FIX	MaRS	OCC	24.91	34.91	ERT	NNO
585	FIX	MaRS	OCC	474.86	484.86	ERT	NNO
586	FIX	MaRS	OCC	-15.16	-5.16	ERT	NNO
586	FIX	MaRS	OCC	11.34	21.34	ERT	NNO
586	FIX	MaRS	OCC	24.84	34.84	ERT	NNO
586	FIX	MaRS	OCC	475.42	485.42	ERT	NNO
587	FIX	MaRS	OCC	-14.61	-4.61	ERT	GST(MAD)
587	FIX	MaRS	OCC	11.39	21.39	ERT	GST(MAD)
587	FIX	MaRS	OCC	24.89	34.89	ERT	GST(MAD)
587	FIX	MaRS	OCC	475.35	485.35	ERT	GST(MAD)
588	FIX	MaRS	OCC	-14.63	-4.63	ERT	GST
588	FIX	MaRS	OCC	11.38	21.38	ERT	GST
588	FIX	MaRS	OCC	24.88	34.88	ERT	GST
588	FIX	MaRS	OCC	475.40	485.40	ERT	GST
589	FIX	MaRS	OCC	-14.62	-4.62	ERT	NNO
589	FIX	MaRS	OCC	11.38	21.38	ERT	NNO
589	FIX	MaRS	OCC	24.88	34.88	ERT	NNO
589	FIX	MaRS	OCC	475.39	485.39	ERT	NNO
590	FIX	MaRS	OCC	-14.02	-4.02	ERT	GST(MAD)
590	FIX	MaRS	OCC	11.48	21.48	ERT	GST(MAD)
590	FIX	MaRS	OCC	24.98	34.98	ERT	GST(MAD)
590	FIX	MaRS	OCC	475.39	485.39	ERT	GST(MAD)
591	FIX	MaRS	OCC	-14.00	-4.00	ERT	GST
591	FIX	MaRS	OCC	11.50	21.50	ERT	GST
591	FIX	MaRS	OCC	25.00	35.00	ERT	GST
591	FIX	MaRS	OCC	475.49	485.49	ERT	GST
592	FIX	MaRS	OCC	-13.88	-3.88	ERT	NNO
592	FIX	MaRS	OCC	11.12	21.12	ERT	NNO
592	FIX	MaRS	OCC	25.12	35.12	ERT	NNO

592	FIX	MaRS	OCC	475.51	485.51	ERT	NNO
593	FIX	MaRS	OCC	-13.74	-3.74	ERT	MAD
593	FIX	MaRS	OCC	11.26	21.26	ERT	MAD
593	FIX	MaRS	OCC	25.26	35.26	ERT	GST(MAD)
593	FIX	MaRS	OCC	475.63	485.63	ERT	MAD
594	FIX	MaRS	OCC	-13.68	-3.68	ERT	GST
594	FIX	MaRS	OCC	11.33	21.33	ERT	GST
594	FIX	MaRS	OCC	25.33	35.33	ERT	GST
594	FIX	MaRS	OCC	475.77	485.77	ERT	GST
595	FIX	MaRS	OCC	-13.51	-3.51	ERT	NNO
595	FIX	MaRS	OCC	11.49	21.49	ERT	NNO
595	FIX	MaRS	OCC	25.49	35.49	ERT	NNO
595	FIX	MaRS	OCC	475.84	485.84	ERT	NNO
596	FIX	MaRS	OCC	-13.46	-3.46	ERT	MAD
596	FIX	MaRS	OCC	11.54	21.54	ERT	MAD
596	FIX	MaRS	OCC	25.54	35.54	ERT	MAD
596	FIX	MaRS	OCC	476.00	486.00	ERT	MAD
597	FIX	MaRS	OCC	-12.89	-2.89	ERT	GST(MAD)
597	FIX	MaRS	OCC	11.61	21.61	ERT	GST(MAD)
597	FIX	MaRS	OCC	25.61	35.61	ERT	GST(MAD)
597	FIX	MaRS	OCC	476.05	486.05	ERT	GST(MAD)
598	FIX	MaRS	OCC	-12.80	-2.80	ERT	NNO
598	FIX	MaRS	OCC	25.70	35.70	ERT	NNO
599	FIX	MaRS	OCC	-12.85	-2.85	ERT	MAD
599	FIX	MaRS	OCC	11.65	21.65	ERT	MAD
599	FIX	MaRS	OCC	25.65	35.65	ERT	MAD
599	FIX	MaRS	OCC	476.21	486.21	ERT	MAD
600	FIX	MaRS	OCC	-12.29	-2.29	ERT	GST(MAD)
600	FIX	MaRS	OCC	25.71	35.71	ERT	GST(MAD)
601	FIX	MaRS	OCC	-12.28	-2.28	ERT	NNO
601	FIX	MaRS	OCC	25.72	35.72	ERT	NNO
602	FIX	MaRS	OCC	-12.26	-2.26	ERT	NNO
602	FIX	MaRS	OCC	25.74	35.74	ERT	NNO
603	FIX	MaRS	OCC	-12.13	-2.13	ERT	GST(MAD)
603	FIX	MaRS	OCC	25.87	35.87	ERT	GST(MAD)
604	FIX	MaRS	OCC	-12.10	-2.10	ERT	NNO
604	FIX	MaRS	OCC	25.90	35.90	ERT	NNO
605	FIX	MaRS	OCC	-11.95	-1.95	ERT	NNO
605	FIX	MaRS	OCC	26.05	36.05	ERT	NNO
606	FIX	MaRS	OCC	-11.79	-1.79	ERT	GST(MAD)
606	FIX	MaRS	OCC	26.21	36.21	ERT	GST(MAD)
607	FIX	MaRS	OCC	-11.69	-1.69	ERT	GST
607	FIX	MaRS	OCC	26.31	36.31	ERT	NNO
608	FIX	MaRS	OCC	-11.50	-1.50	ERT	NNO
608	FIX	MaRS	OCC	26.00	36.00	ERT	NNO
609	FIX	MaRS	OCC	-11.42	-1.42	ERT	GST(MAD)
609	FIX	MaRS	OCC	26.08	36.08	ERT	GST(MAD)
610	FIX	MaRS	OCC	-10.82	-0.82	ERT	GST
610	FIX	MaRS	OCC	26.18	36.18	ERT	GST
611	FIX	MaRS	OCC	-11.20	-1.20	ERT	NNO
611	FIX	MaRS	OCC	26.30	36.30	ERT	NNO

612	FIX	MaRS	OCC	-10.73	-0.73	ERT	MAD
612	FIX	MaRS	OCC	26.27	36.27	ERT	MAD(GST)
613	FIX	MaRS	OCC	-10.64	-0.64	ERT	GST
613	FIX	MaRS	OCC	26.36	36.36	ERT	GST
614	FIX	MaRS	OCC	-10.61	-0.61	ERT	NNO
614	FIX	MaRS	OCC	26.39	36.39	ERT	NNO
615	FIX	MaRS	OCC	-10.58	-0.58	ERT	MAD
615	FIX	MaRS	OCC	26.42	36.42	ERT	MAD
616	FIX	MaRS	OCC	-9.95	0.05	ERT	GST
616	FIX	MaRS	OCC	26.55	36.55	ERT	GST
617	FIX	MaRS	OCC	-9.89	0.11	ERT	NNO
617	FIX	MaRS	OCC	26.61	36.61	ERT	NNO
618	FIX	MaRS	OCC	-9.73	0.27	ERT	MAD
618	FIX	MaRS	OCC	26.77	36.77	ERT	MAD
619	FIX	MaRS	OCC	-9.55	0.45	ERT	GST(MAD)
619	FIX	MaRS	OCC	26.95	36.95	ERT	GST(MAD)
620	FIX	MaRS	OCC	-9.44	0.56	ERT	NNO
620	FIX	MaRS	OCC	27.06	37.06	ERT	NNO
621	FIX	MaRS	OCC	-9.73	0.27	ERT	NNO
621	FIX	MaRS	OCC	26.77	36.77	ERT	NNO
622	FIX	MaRS	OCC	-9.62	0.38	ERT	GST(MAD)
622	FIX	MaRS	OCC	26.88	36.88	ERT	GST(MAD)
623	FIX	MaRS	OCC	-8.99	1.01	ERT	NNO
623	FIX	MaRS	OCC	27.01	37.01	ERT	NNO
624	FIX	MaRS	OCC	-8.85	1.15	ERT	NNO
624	FIX	MaRS	OCC	27.15	37.15	ERT	NNO
625	FIX	MaRS	OCC	-8.86	1.14	ERT	GST(MAD)
625	FIX	MaRS	OCC	27.14	37.14	ERT	GST(MAD)
626	FIX	MaRS	OCC	-8.26	1.74	ERT	GST
626	FIX	MaRS	OCC	27.24	37.24	ERT	NNO
627	FIX	MaRS	OCC	-8.71	1.29	ERT	NNO
627	FIX	MaRS	OCC	27.29	37.29	ERT	NNO
628	FIX	MaRS	OCC	-8.67	1.33	ERT	GST(MAD)
628	FIX	MaRS	OCC	27.33	37.33	ERT	GST(MAD)
629	FIX	MaRS	OCC	-8.02	1.98	ERT	GST
629	FIX	MaRS	OCC	27.48	37.48	ERT	GST
630	FIX	MaRS	OCC	-7.95	2.05	ERT	NNO
630	FIX	MaRS	OCC	27.55	37.55	ERT	NNO
631	FIX	MaRS	OCC	-8.27	1.73	ERT	MAD
631	FIX	MaRS	OCC	27.23	37.23	ERT	GST(MAD)
632	FIX	MaRS	OCC	-8.07	1.93	ERT	GST
632	FIX	MaRS	OCC	27.43	37.43	ERT	GST
633	FIX	MaRS	OCC	-7.43	2.57	ERT	NNO
633	FIX	MaRS	OCC	27.57	37.57	ERT	NNO
634	FIX	MaRS	OCC	-7.69	2.31	ERT	MAD
634	FIX	MaRS	OCC	27.81	37.81	ERT	MAD
635	FIX	MaRS	OCC	-7.55	2.45	ERT	GST
635	FIX	MaRS	OCC	27.45	37.45	ERT	GST
636	FIX	MaRS	OCC	-6.90	3.10	ERT	NNO
636	FIX	MaRS	OCC	27.60	37.60	ERT	NNO
637	FIX	MaRS	OCC	-7.23	2.77	ERT	MAD

637	FIX	MaRS	OCC	27.77	37.77	ERT	MAD
638	FIX	MaRS	OCC	-7.22	2.78	ERT	GST(MAD)
638	FIX	MaRS	OCC	27.78	37.78	ERT	GST(MAD)
639	FIX	MaRS	OCC	-6.60	3.40	ERT	NNO
639	FIX	MaRS	OCC	27.90	37.90	ERT	NNO
640	FIX	MaRS	OCC	-6.54	3.46	ERT	MAD
640	FIX	MaRS	OCC	27.96	37.96	ERT	MAD
641	FIX	MaRS	OCC	-6.50	3.50	ERT	GST(MAD)
641	FIX	MaRS	OCC	28.00	38.00	ERT	GST(MAD)
642	FIX	MaRS	OCC	-6.34	3.66	ERT	NNO
642	FIX	MaRS	OCC	28.16	38.16	ERT	NNO
643	FIX	MaRS	OCC	-6.26	3.74	ERT	NNO
643	FIX	MaRS	OCC	28.24	38.24	ERT	NNO
644	FIX	MaRS	OCC	-6.08	3.92	ERT	GST(MAD)
644	FIX	MaRS	OCC	27.92	37.92	ERT	GST(MAD)
645	FIX	MaRS	OCC	-5.86	4.14	ERT	NNO
645	FIX	MaRS	OCC	28.14	38.14	ERT	NNO
646	FIX	MaRS	OCC	-5.71	4.29	ERT	NNO
646	FIX	MaRS	OCC	28.30	38.30	ERT	NNO
647	FIX	MaRS	OCC	-5.95	4.05	ERT	GST(MAD)
647	FIX	MaRS	OCC	28.05	38.05	ERT	GST(MAD)
648	FIX	MaRS	OCC	-5.78	4.22	ERT	GST
648	FIX	MaRS	OCC	28.22	38.22	ERT	GST
649	FIX	MaRS	OCC	-5.11	4.89	ERT	NNO
649	FIX	MaRS	OCC	28.39	38.39	ERT	NNO
650	FIX	MaRS	OCC	-5.42	4.58	ERT	GST(MAD)
650	FIX	MaRS	OCC	28.58	38.58	ERT	GST(MAD)
651	FIX	MaRS	OCC	-5.38	4.62	ERT	GST
651	FIX	MaRS	OCC	28.62	38.62	ERT	GST
652	FIX	MaRS	OCC	-4.75	5.25	ERT	NNO
652	FIX	MaRS	OCC	28.25	38.25	ERT	NNO
653	FIX	MaRS	OCC	-4.67	5.33	ERT	MAD
653	FIX	MaRS	OCC	28.33	38.33	ERT	MAD
654	FIX	MaRS	OCC	-4.62	5.38	ERT	GST
654	FIX	MaRS	OCC	28.38	38.38	ERT	GST
655	FIX	MaRS	OCC	-4.46	5.54	ERT	NNO
655	FIX	MaRS	OCC	28.54	38.54	ERT	NNO
656	FIX	MaRS	OCC	-4.37	5.63	ERT	MAD
656	FIX	MaRS	OCC	28.63	38.63	ERT	MAD
657	FIX	MaRS	OCC	-4.18	5.82	ERT	GST(MAD)
657	FIX	MaRS	OCC	28.82	38.82	ERT	GST(MAD)
658	FIX	MaRS	OCC	-3.94	6.06	ERT	NNO
658	FIX	MaRS	OCC	28.56	38.56	ERT	NNO
659	FIX	MaRS	OCC	-3.78	6.22	ERT	MAD
659	FIX	MaRS	OCC	28.72	38.72	ERT	MAD
660	FIX	MaRS	OCC	-4.00	6.00	ERT	GST(MAD)
660	FIX	MaRS	OCC	29.00	39.00	ERT	GST(MAD)
661	FIX	MaRS	OCC	-3.81	6.19	ERT	NNO
661	FIX	MaRS	OCC	28.69	38.69	ERT	NNO
662	FIX	MaRS	OCC	-3.62	6.38	ERT	NNO
662	FIX	MaRS	OCC	28.88	38.88	ERT	NNO

663	FIX	MaRS	OCC	-3.41	6.59	ERT	GST(MAD)
663	FIX	MaRS	OCC	29.09	39.09	ERT	GST(MAD)
664	FIX	MaRS	OCC	-3.35	6.65	ERT	NNO
664	FIX	MaRS	OCC	29.15	39.15	ERT	NNO
665	FIX	MaRS	OCC	-2.71	7.29	ERT	NNO
665	FIX	MaRS	OCC	29.29	39.29	ERT	NNO
666	FIX	MaRS	OCC	-3.11	6.89	ERT	GST(MAD)
666	FIX	MaRS	OCC	28.89	38.89	ERT	GST(MAD)
667	FIX	MaRS	OCC	-3.05	6.95	ERT	GST
667	FIX	MaRS	OCC	28.95	38.95	ERT	GST
668	FIX	MaRS	OCC	-2.38	7.62	ERT	NNO
668	FIX	MaRS	OCC	29.12	39.12	ERT	NNO
669	FIX	MaRS	OCC	-2.79	7.21	ERT	GST(MAD)
669	FIX	MaRS	OCC	29.21	39.21	ERT	GST(MAD)
670	FIX	MaRS	OCC	-2.59	7.41	ERT	GST
670	FIX	MaRS	OCC	29.41	39.41	ERT	GST
671	FIX	MaRS	OCC	-2.35	7.65	ERT	NNO
671	FIX	MaRS	OCC	29.15	39.15	ERT	NNO
672	FIX	MaRS	OCC	-2.17	7.83	ERT	MAD
672	FIX	MaRS	OCC	29.33	39.33	ERT	MAD
673	FIX	MaRS	OCC	-2.38	7.62	ERT	GST
673	FIX	MaRS	OCC	29.62	39.62	ERT	GST
674	FIX	MaRS	OCC	-2.17	7.83	ERT	NNO
674	FIX	MaRS	OCC	29.34	39.34	ERT	NNO
675	FIX	MaRS	OCC	-1.46	8.54	ERT	MAD
675	FIX	MaRS	OCC	29.54	39.54	ERT	MAD
676	FIX	MaRS	OCC	-1.73	8.27	ERT	GST(MAD)
676	FIX	MaRS	OCC	29.77	39.77	ERT	GST(MAD)
677	FIX	MaRS	OCC	-1.65	8.35	ERT	NNO
677	FIX	MaRS	OCC	29.85	39.85	ERT	NNO
678	FIX	MaRS	OCC	-1.00	9.00	ERT	MAD
678	FIX	MaRS	OCC	29.50	39.50	ERT	MAD
679	FIX	MaRS	OCC	-1.39	8.61	ERT	GST(MAD)
679	FIX	MaRS	OCC	29.61	39.61	ERT	GST(MAD)
680	FIX	MaRS	OCC	-1.32	8.68	ERT	NNO
680	FIX	MaRS	OCC	29.68	39.68	ERT	NNO
681	FIX	MaRS	OCC	-0.65	9.35	ERT	NNO
681	FIX	MaRS	OCC	29.85	39.85	ERT	NNO
682	FIX	MaRS	OCC	-1.05	8.95	ERT	GST(MAD)
682	FIX	MaRS	OCC	29.95	39.95	ERT	GST(MAD)
683	FIX	MaRS	OCC	-0.85	9.15	ERT	NNO
683	FIX	MaRS	OCC	29.65	39.65	ERT	NNO
684	FIX	MaRS	OCC	-0.59	9.41	ERT	NNO
684	FIX	MaRS	OCC	29.91	39.91	ERT	NNO
685	FIX	MaRS	OCC	-0.40	9.60	ERT	GST(MAD)
685	FIX	MaRS	OCC	30.10	40.10	ERT	GST(MAD)
686	FIX	MaRS	OCC	-0.60	9.40	ERT	GST
686	FIX	MaRS	OCC	29.90	39.90	ERT	GST
687	FIX	MaRS	OCC	-0.36	9.64	ERT	NNO
687	FIX	MaRS	OCC	30.14	40.14	ERT	NNO
688	FIX	MaRS	OCC	-0.14	9.86	ERT	GST(MAD)

688	FIX	MaRS	OCC	29.86	39.86	ERT	GST(MAD)
689	FIX	MaRS	OCC	0.11	10.11	ERT	GST
689	FIX	MaRS	OCC	30.11	40.11	ERT	GST
690	FIX	MaRS	OCC	0.20	10.20	ERT	NNO
690	FIX	MaRS	OCC	30.20	40.20	ERT	NNO
691	FIX	MaRS	OCC	0.37	10.37	ERT	MAD
691	FIX	MaRS	OCC	30.37	40.37	ERT	MAD
692	FIX	MaRS	OCC	0.49	10.49	ERT	GST
692	FIX	MaRS	OCC	29.99	39.99	ERT	GST
693	FIX	MaRS	OCC	0.56	10.56	ERT	NNO
693	FIX	MaRS	OCC	30.06	40.06	ERT	NNO
694	FIX	MaRS	OCC	0.74	10.74	ERT	MAD
694	FIX	MaRS	OCC	30.24	40.24	ERT	MAD
695	FIX	MaRS	OCC	0.84	10.84	ERT	GST(MAD)
695	FIX	MaRS	OCC	30.34	40.34	ERT	GST(MAD)
696	FIX	MaRS	OCC	1.05	11.05	ERT	NNO
696	FIX	MaRS	OCC	30.55	40.55	ERT	NNO
697	FIX	MaRS	OCC	0.81	10.81	ERT	MAD
697	FIX	MaRS	OCC	30.31	40.31	ERT	MAD
698	FIX	MaRS	OCC	1.51	11.51	ERT	GST(MAD)
698	FIX	MaRS	OCC	30.51	40.51	ERT	GST(MAD)
699	FIX	MaRS	OCC	1.33	11.33	ERT	NNO
699	FIX	MaRS	OCC	30.33	40.33	ERT	NNO
700	FIX	MaRS	OCC	1.08	11.08	ERT	NNO
700	FIX	MaRS	OCC	30.58	40.58	ERT	NNO
701	FIX	MaRS	OCC	1.82	11.82	ERT	GST(MAD)
701	FIX	MaRS	OCC	30.32	40.32	ERT	GST(MAD)
702	FIX	MaRS	OCC	1.59	11.59	ERT	NNO
702	FIX	MaRS	OCC	30.59	40.59	ERT	NNO
703	FIX	MaRS	OCC	1.70	11.70	ERT	NNO
703	FIX	MaRS	OCC	30.70	40.70	ERT	NNO
704	FIX	MaRS	OCC	2.38	12.38	ERT	GST(MAD)
704	FIX	MaRS	OCC	30.38	40.38	ERT	GST(MAD)
705	FIX	MaRS	OCC	2.01	12.01	ERT	GST
705	FIX	MaRS	OCC	30.51	40.51	ERT	NNO
706	FIX	MaRS	OCC	2.08	12.08	ERT	NNO
706	FIX	MaRS	OCC	30.58	40.58	ERT	NNO
707	FIX	MaRS	OCC	2.76	12.76	ERT	MAD(GST)
707	FIX	MaRS	OCC	30.77	40.77	ERT	GST(MAD)
708	FIX	MaRS	OCC	2.37	12.37	ERT	GST
708	FIX	MaRS	OCC	30.87	40.87	ERT	GST
709	FIX	MaRS	OCC	2.58	12.58	ERT	NNO
709	FIX	MaRS	OCC	30.58	40.58	ERT	NNO
710	FIX	MaRS	OCC	2.85	12.85	ERT	MAD
710	FIX	MaRS	OCC	30.85	40.85	ERT	MAD
711	FIX	MaRS	OCC	3.05	13.05	ERT	GST
711	FIX	MaRS	OCC	31.05	41.05	ERT	GST
712	FIX	MaRS	OCC	2.88	12.88	ERT	NNO
712	FIX	MaRS	OCC	30.88	40.88	ERT	NNO
713	FIX	MaRS	OCC	3.15	13.15	ERT	MAD
713	FIX	MaRS	OCC	30.65	40.65	ERT	MAD

714	FIX	MaRS	OCC	3.40	13.40	ERT	GST
714	FIX	MaRS	OCC	30.90	40.90	ERT	GST
715	FIX	MaRS	OCC	3.18	13.18	ERT	NNO
715	FIX	MaRS	OCC	31.18	41.18	ERT	NNO
716	FIX	MaRS	OCC	3.31	13.31	ERT	MAD
716	FIX	MaRS	OCC	30.81	40.81	ERT	MAD
717	FIX	MaRS	OCC	4.00	14.00	ERT	GST(MAD)
717	FIX	MaRS	OCC	31.00	41.00	ERT	GST(MAD)
718	FIX	MaRS	OCC	3.65	13.65	ERT	NNO
718	FIX	MaRS	OCC	31.15	41.15	ERT	NNO
719	FIX	MaRS	OCC	4.22	14.22	ERT	NNO
719	FIX	MaRS	OCC	31.22	41.22	ERT	NNO
720	FIX	MaRS	OCC	4.41	14.41	ERT	GST(MAD)
720	FIX	MaRS	OCC	30.91	40.91	ERT	GST(MAD)
721	FIX	MaRS	OCC	4.52	14.52	ERT	NNO
721	FIX	MaRS	OCC	31.02	41.02	ERT	NNO
722	FIX	MaRS	OCC	4.23	14.23	ERT	NNO
722	FIX	MaRS	OCC	31.23	41.23	ERT	NNO
723	FIX	MaRS	OCC	4.50	14.50	ERT	GST(MAD)
723	FIX	MaRS	OCC	31.00	41.00	ERT	GST(MAD)
724	FIX	MaRS	OCC	4.71	14.71	ERT	GST
724	FIX	MaRS	OCC	31.21	41.21	ERT	NNO
725	FIX	MaRS	OCC	4.54	14.54	ERT	NNO
725	FIX	MaRS	OCC	31.04	41.04	ERT	NNO
726	FIX	MaRS	OCC	4.83	14.83	ERT	GST(MAD)
726	FIX	MaRS	OCC	31.33	41.33	ERT	GST(MAD)
727	FIX	MaRS	OCC	5.09	15.09	ERT	GST
727	FIX	MaRS	OCC	31.09	41.09	ERT	GST
728	FIX	MaRS	OCC	4.89	14.89	ERT	NNO
728	FIX	MaRS	OCC	31.39	41.39	ERT	NNO
729	FIX	MaRS	OCC	5.03	15.03	ERT	MAD

7.4.5.2 OCC-2

7.4.5.2.1 Coordinates of occultation footpoints

tbd

7.4.5.2.2 Latitudinal coverage

tbd

7.4.5.2.3 List of requested orbits OCC2

VERY PRELIMINARY! Contains ALL ground stations!

				start	stop		
orbit #	attitude	instrument	Experiment	relative to pericenter		pointing	ground station
1118	FIX	MaRS	OCC	-192.71	-182.71	ERT	NNO
1118	FIX	MaRS	OCC	-162.71	-152.71	ERT	NNO
1119	FIX	MaRS	OCC	-196.38	-186.38	ERT	GST(MAD)
1119	FIX	MaRS	OCC	-157.38	-147.38	ERT	GST(MAD)
1120	FIX	MaRS	OCC	-197.54	-187.54	ERT	NNO
1120	FIX	MaRS	OCC	-153.04	-143.04	ERT	NNO
1121	FIX	MaRS	OCC	-199.67	-189.67	ERT	NNO
1121	FIX	MaRS	OCC	-149.67	-139.67	ERT	NNO
1122	FIX	MaRS	OCC	-199.99	-189.99	ERT	GST(MAD)
1122	FIX	MaRS	OCC	-145.99	-135.99	ERT	GST(MAD)
1123	FIX	MaRS	OCC	-200.74	-190.74	ERT	NNO
1123	FIX	MaRS	OCC	-142.74	-132.74	ERT	NNO
1124	FIX	MaRS	OCC	-202.07	-192.07	ERT	NNO
1124	FIX	MaRS	OCC	-140.57	-130.57	ERT	NNO
1125	FIX	MaRS	OCC	-202.00	-192.00	ERT	MAD
1125	FIX	MaRS	OCC	-137.50	-127.50	ERT	MAD
1126	FIX	MaRS	OCC	-202.82	-192.82	ERT	GST
1126	FIX	MaRS	OCC	-135.32	-125.32	ERT	NNO
1127	FIX	MaRS	OCC	-203.25	-193.25	ERT	NNO
1127	FIX	MaRS	OCC	-132.75	-122.75	ERT	NNO
1128	FIX	MaRS	OCC	-203.04	-193.04	ERT	MAD
1128	FIX	MaRS	OCC	-130.04	-120.04	ERT	MAD
1129	FIX	MaRS	OCC	-204.26	-194.26	ERT	GST
1129	FIX	MaRS	OCC	-128.76	-118.76	ERT	GST
1130	FIX	MaRS	OCC	-203.54	-193.54	ERT	NNO
1130	FIX	MaRS	OCC	-126.04	-116.04	ERT	NNO
1131	FIX	MaRS	OCC	-203.67	-193.67	ERT	MAD
1131	FIX	MaRS	OCC	-124.17	-114.17	ERT	MAD
1132	FIX	MaRS	OCC	-203.85	-193.85	ERT	GST
1132	FIX	MaRS	OCC	-122.35	-112.35	ERT	GST
1133	FIX	MaRS	OCC	-203.01	-193.01	ERT	NNO
1133	FIX	MaRS	OCC	-120.02	-110.02	ERT	NNO
1134	FIX	MaRS	OCC	-203.64	-193.64	ERT	MAD
1134	FIX	MaRS	OCC	-118.64	-108.64	ERT	MAD
1135	FIX	MaRS	OCC	-202.96	-192.96	ERT	GST
1135	FIX	MaRS	OCC	-116.46	-106.46	ERT	GST
1136	FIX	MaRS	OCC	-202.71	-192.71	ERT	NNO
1136	FIX	MaRS	OCC	-114.72	-104.72	ERT	NNO
1137	FIX	MaRS	OCC	-203.04	-193.04	ERT	NNO
1137	FIX	MaRS	OCC	-113.54	-103.54	ERT	NNO
1138	FIX	MaRS	OCC	-201.97	-191.97	ERT	GST
1138	FIX	MaRS	OCC	-110.97	-100.97	ERT	GST

1139	FIX	MaRS	OCC	-202.30	-192.30	ERT	NNO
1139	FIX	MaRS	OCC	-109.80	-99.80	ERT	NNO
1140	FIX	MaRS	OCC	-201.72	-191.72	ERT	NNO
1140	FIX	MaRS	OCC	-108.73	-98.73	ERT	NNO
1141	FIX	MaRS	OCC	-201.03	-191.03	ERT	GST(MAD)
1141	FIX	MaRS	OCC	-106.54	-96.54	ERT	GST(MAD)
1142	FIX	MaRS	OCC	-201.26	-191.26	ERT	NNO
1142	FIX	MaRS	OCC	-105.77	-95.77	ERT	NNO
1143	FIX	MaRS	OCC	-200.56	-190.56	ERT	NNO
1143	FIX	MaRS	OCC	-104.06	-94.06	ERT	NNO
1144	FIX	MaRS	OCC	-200.20	-190.20	ERT	MAD
1144	FIX	MaRS	OCC	-102.70	-92.70	ERT	GST(MAD)
1145	FIX	MaRS	OCC	-199.88	-189.88	ERT	GST
1145	FIX	MaRS	OCC	-101.39	-91.39	ERT	NNO
1146	FIX	MaRS	OCC	-198.56	-188.56	ERT	NNO
1146	FIX	MaRS	OCC	-99.56	-89.56	ERT	NNO
1147	FIX	MaRS	OCC	-198.69	-188.69	ERT	MAD
1147	FIX	MaRS	OCC	-98.69	-88.69	ERT	MAD
1148	FIX	MaRS	OCC	-198.00	-188.00	ERT	GST
1148	FIX	MaRS	OCC	-97.01	-87.01	ERT	NNO
1149	FIX	MaRS	OCC	-196.76	-186.76	ERT	NNO
1149	FIX	MaRS	OCC	-95.26	-85.26	ERT	NNO
1150	FIX	MaRS	OCC	-196.58	-186.58	ERT	MAD
1150	FIX	MaRS	OCC	-95.09	-85.09	ERT	MAD
1151	FIX	MaRS	OCC	-195.52	-185.52	ERT	GST
1151	FIX	MaRS	OCC	-93.02	-83.02	ERT	GST
1152	FIX	MaRS	OCC	-195.35	-185.35	ERT	NNO
1152	FIX	MaRS	OCC	-92.35	-82.35	ERT	NNO
1153	FIX	MaRS	OCC	-194.78	-184.78	ERT	MAD
1153	FIX	MaRS	OCC	-91.29	-81.29	ERT	MAD
1154	FIX	MaRS	OCC	-193.60	-183.60	ERT	GST
1154	FIX	MaRS	OCC	-89.61	-79.61	ERT	GST
1155	FIX	MaRS	OCC	-193.85	-183.85	ERT	NNO
1155	FIX	MaRS	OCC	-89.35	-79.35	ERT	NNO
1156	FIX	MaRS	OCC	-192.66	-182.66	ERT	NNO
1156	FIX	MaRS	OCC	-87.66	-77.66	ERT	NNO
1157	FIX	MaRS	OCC	-191.81	-181.81	ERT	GST
1157	FIX	MaRS	OCC	-86.82	-76.82	ERT	GST
1158	FIX	MaRS	OCC	-191.50	-181.50	ERT	NNO
1158	FIX	MaRS	OCC	-86.01	-76.01	ERT	NNO
1159	FIX	MaRS	OCC	-190.19	-180.19	ERT	NNO
1159	FIX	MaRS	OCC	-84.20	-74.20	ERT	NNO
1160	FIX	MaRS	OCC	-189.83	-179.83	ERT	GST(MAD)
1160	FIX	MaRS	OCC	-83.83	-73.83	ERT	GST(MAD)
1161	FIX	MaRS	OCC	-189.14	-179.14	ERT	NNO
1161	FIX	MaRS	OCC	-82.65	-72.65	ERT	NNO
1162	FIX	MaRS	OCC	-187.90	-177.90	ERT	NNO
1162	FIX	MaRS	OCC	-81.40	-71.40	ERT	NNO
1163	FIX	MaRS	OCC	-187.72	-177.72	ERT	MAD
1163	FIX	MaRS	OCC	-80.72	-70.72	ERT	GST(MAD)
1164	FIX	MaRS	OCC	-186.15	-176.15	ERT	NNO

1164	FIX	MaRS	OCC	-79.16	-69.16	ERT	NNO
1165	FIX	MaRS	OCC	-185.49	-175.49	ERT	NNO
1165	FIX	MaRS	OCC	-78.49	-68.49	ERT	NNO
1166	FIX	MaRS	OCC	-184.93	-174.93	ERT	MAD
1166	FIX	MaRS	OCC	-77.93	-67.93	ERT	MAD
1167	FIX	MaRS	OCC	-183.76	-173.76	ERT	GST
1167	FIX	MaRS	OCC	-76.26	-66.26	ERT	NNO
1168	FIX	MaRS	OCC	-183.51	-173.51	ERT	NNO
1168	FIX	MaRS	OCC	-76.52	-66.52	ERT	NNO
1169	FIX	MaRS	OCC	-182.34	-172.34	ERT	MAD
1169	FIX	MaRS	OCC	-75.34	-65.34	ERT	MAD
1170	FIX	MaRS	OCC	-181.51	-171.51	ERT	GST
1170	FIX	MaRS	OCC	-74.51	-64.51	ERT	GST
1171	FIX	MaRS	OCC	-181.22	-171.22	ERT	NNO
1171	FIX	MaRS	OCC	-74.22	-64.22	ERT	NNO
1172	FIX	MaRS	OCC	-179.42	-169.42	ERT	MAD
1172	FIX	MaRS	OCC	-72.42	-62.42	ERT	MAD
1173	FIX	MaRS	OCC	-179.06	-169.06	ERT	GST
1173	FIX	MaRS	OCC	-72.06	-62.06	ERT	GST
1174	FIX	MaRS	OCC	-177.88	-167.88	ERT	NNO
1174	FIX	MaRS	OCC	-71.38	-61.38	ERT	NNO
1175	FIX	MaRS	OCC	-176.63	-166.63	ERT	NNO
1175	FIX	MaRS	OCC	-70.14	-60.14	ERT	NNO
1176	FIX	MaRS	OCC	-175.95	-165.95	ERT	GST
1176	FIX	MaRS	OCC	-69.96	-59.96	ERT	GST
1177	FIX	MaRS	OCC	-174.39	-164.39	ERT	NNO
1177	FIX	MaRS	OCC	-68.40	-58.40	ERT	NNO
1178	FIX	MaRS	OCC	-174.23	-164.23	ERT	NNO
1178	FIX	MaRS	OCC	-68.23	-58.23	ERT	NNO
1179	FIX	MaRS	OCC	-173.18	-163.18	ERT	GST
1179	FIX	MaRS	OCC	-67.68	-57.68	ERT	GST
1180	FIX	MaRS	OCC	-172.02	-162.02	ERT	NNO
1180	FIX	MaRS	OCC	-66.02	-56.02	ERT	NNO
1181	FIX	MaRS	OCC	-171.29	-161.29	ERT	NNO
1181	FIX	MaRS	OCC	-66.29	-56.29	ERT	NNO
1182	FIX	MaRS	OCC	-170.13	-160.13	ERT	MAD
1182	FIX	MaRS	OCC	-65.13	-55.13	ERT	GST(MAD)
1183	FIX	MaRS	OCC	-169.32	-159.32	ERT	NNO
1183	FIX	MaRS	OCC	-64.82	-54.82	ERT	NNO
1184	FIX	MaRS	OCC	-168.53	-158.53	ERT	NNO
1184	FIX	MaRS	OCC	-64.54	-54.54	ERT	NNO
1185	FIX	MaRS	OCC	-167.24	-157.24	ERT	MAD
1185	FIX	MaRS	OCC	-63.25	-53.25	ERT	GST(MAD)
1186	FIX	MaRS	OCC	-166.40	-156.40	ERT	GST
1186	FIX	MaRS	OCC	-62.90	-52.90	ERT	NNO
1187	FIX	MaRS	OCC	-165.22	-155.22	ERT	NNO
1187	FIX	MaRS	OCC	-62.22	-52.22	ERT	NNO
1188	FIX	MaRS	OCC	-163.98	-153.98	ERT	MAD
1188	FIX	MaRS	OCC	-60.98	-50.98	ERT	MAD
1189	FIX	MaRS	OCC	-163.29	-153.29	ERT	GST
1189	FIX	MaRS	OCC	-61.30	-51.30	ERT	GST

1190	FIX	MaRS	OCC	-161.74	-151.74	ERT	NNO
1190	FIX	MaRS	OCC	-59.74	-49.74	ERT	NNO
1191	FIX	MaRS	OCC	-161.08	-151.08	ERT	MAD
1191	FIX	MaRS	OCC	-59.58	-49.58	ERT	MAD
1192	FIX	MaRS	OCC	-160.53	-150.53	ERT	GST
1192	FIX	MaRS	OCC	-59.04	-49.04	ERT	GST
1193	FIX	MaRS	OCC	-158.89	-148.89	ERT	NNO
1193	FIX	MaRS	OCC	-57.90	-47.90	ERT	NNO
1194	FIX	MaRS	OCC	-158.17	-148.17	ERT	MAD
1194	FIX	MaRS	OCC	-58.18	-48.18	ERT	MAD
1195	FIX	MaRS	OCC	-157.03	-147.03	ERT	GST
1195	FIX	MaRS	OCC	-57.03	-47.03	ERT	GST
1196	FIX	MaRS	OCC	-156.23	-146.23	ERT	NNO
1196	FIX	MaRS	OCC	-56.73	-46.73	ERT	NNO
1197	FIX	MaRS	OCC	-155.46	-145.46	ERT	NNO
1197	FIX	MaRS	OCC	-56.96	-46.96	ERT	NNO
1198	FIX	MaRS	OCC	-153.68	-143.68	ERT	GST
1198	FIX	MaRS	OCC	-55.19	-45.19	ERT	GST
1199	FIX	MaRS	OCC	-152.84	-142.84	ERT	NNO
1199	FIX	MaRS	OCC	-55.35	-45.35	ERT	NNO
1200	FIX	MaRS	OCC	-151.67	-141.67	ERT	NNO
1200	FIX	MaRS	OCC	-55.17	-45.17	ERT	NNO
1201	FIX	MaRS	OCC	-150.43	-140.43	ERT	GST(MAD)
1201	FIX	MaRS	OCC	-53.94	-43.94	ERT	GST(MAD)
1202	FIX	MaRS	OCC	-149.75	-139.75	ERT	NNO
1202	FIX	MaRS	OCC	-53.75	-43.75	ERT	NNO
1203	FIX	MaRS	OCC	-148.20	-138.20	ERT	NNO
1203	FIX	MaRS	OCC	-52.70	-42.70	ERT	NNO
1204	FIX	MaRS	OCC	-147.04	-137.04	ERT	MAD
1204	FIX	MaRS	OCC	-52.55	-42.55	ERT	GST(MAD)
1205	FIX	MaRS	OCC	-146.50	-136.50	ERT	NNO
1205	FIX	MaRS	OCC	-52.51	-42.51	ERT	NNO
1206	FIX	MaRS	OCC	-144.88	-134.88	ERT	NNO
1206	FIX	MaRS	OCC	-51.38	-41.38	ERT	NNO
1207	FIX	MaRS	OCC	-144.17	-134.17	ERT	MAD
1207	FIX	MaRS	OCC	-51.67	-41.67	ERT	MAD
1208	FIX	MaRS	OCC	-143.05	-133.05	ERT	GST
1208	FIX	MaRS	OCC	-50.55	-40.55	ERT	NNO
1209	FIX	MaRS	OCC	-141.76	-131.76	ERT	NNO
1209	FIX	MaRS	OCC	-50.27	-40.27	ERT	NNO
1210	FIX	MaRS	OCC	-141.50	-131.50	ERT	MAD
1210	FIX	MaRS	OCC	-50.50	-40.50	ERT	MAD
1211	FIX	MaRS	OCC	-139.24	-129.24	ERT	GST
1211	FIX	MaRS	OCC	-49.25	-39.25	ERT	GST
1212	FIX	MaRS	OCC	-138.91	-128.91	ERT	NNO
1212	FIX	MaRS	OCC	-49.42	-39.42	ERT	NNO
1213	FIX	MaRS	OCC	-137.74	-127.74	ERT	MAD
1213	FIX	MaRS	OCC	-48.74	-38.74	ERT	MAD
1214	FIX	MaRS	OCC	-136.01	-126.01	ERT	GST
1214	FIX	MaRS	OCC	-48.02	-38.02	ERT	GST
1215	FIX	MaRS	OCC	-135.33	-125.33	ERT	NNO

1215	FIX	MaRS	OCC	-48.34	-38.34	ERT	NNO
1216	FIX	MaRS	OCC	-133.79	-123.79	ERT	NNO
1216	FIX	MaRS	OCC	-47.29	-37.29	ERT	NNO
1217	FIX	MaRS	OCC	-132.64	-122.64	ERT	GST
1217	FIX	MaRS	OCC	-46.64	-36.64	ERT	GST
1218	FIX	MaRS	OCC	-132.10	-122.10	ERT	NNO
1218	FIX	MaRS	OCC	-46.61	-36.61	ERT	NNO
1219	FIX	MaRS	OCC	-130.49	-120.49	ERT	NNO
1219	FIX	MaRS	OCC	-45.99	-35.99	ERT	NNO
1220	FIX	MaRS	OCC	-129.80	-119.80	ERT	GST(MAD)
1220	FIX	MaRS	OCC	-46.30	-36.30	ERT	GST(MAD)
1221	FIX	MaRS	OCC	-128.69	-118.69	ERT	NNO
1221	FIX	MaRS	OCC	-45.69	-35.69	ERT	NNO
1222	FIX	MaRS	OCC	-127.43	-117.43	ERT	NNO
1222	FIX	MaRS	OCC	-44.93	-34.93	ERT	NNO
1223	FIX	MaRS	OCC	-126.68	-116.68	ERT	MAD
1223	FIX	MaRS	OCC	-45.18	-35.18	ERT	GST(MAD)
1224	FIX	MaRS	OCC	-124.94	-114.94	ERT	NNO
1224	FIX	MaRS	OCC	-43.94	-33.94	ERT	NNO
1225	FIX	MaRS	OCC	-124.12	-114.12	ERT	NNO
1225	FIX	MaRS	OCC	-44.62	-34.62	ERT	NNO
1226	FIX	MaRS	OCC	-123.45	-113.45	ERT	MAD
1226	FIX	MaRS	OCC	-43.95	-33.95	ERT	MAD
1227	FIX	MaRS	OCC	-121.23	-111.23	ERT	GST
1227	FIX	MaRS	OCC	-42.73	-32.73	ERT	NNO
1228	FIX	MaRS	OCC	-121.05	-111.05	ERT	NNO
1228	FIX	MaRS	OCC	-43.56	-33.56	ERT	NNO
1229	FIX	MaRS	OCC	-119.51	-109.51	ERT	MAD
1229	FIX	MaRS	OCC	-42.51	-32.51	ERT	MAD
1230	FIX	MaRS	OCC	-118.37	-108.37	ERT	GST
1230	FIX	MaRS	OCC	-42.37	-32.37	ERT	GST
1231	FIX	MaRS	OCC	-117.34	-107.34	ERT	NNO
1231	FIX	MaRS	OCC	-42.34	-32.34	ERT	NNO
1232	FIX	MaRS	OCC	-115.74	-105.74	ERT	MAD
1232	FIX	MaRS	OCC	-41.24	-31.24	ERT	MAD
1233	FIX	MaRS	OCC	-115.06	-105.06	ERT	GST
1233	FIX	MaRS	OCC	-41.56	-31.56	ERT	GST
1234	FIX	MaRS	OCC	-113.97	-103.97	ERT	NNO
1234	FIX	MaRS	OCC	-40.98	-30.98	ERT	NNO
1235	FIX	MaRS	OCC	-112.73	-102.73	ERT	NNO
1235	FIX	MaRS	OCC	-40.73	-30.73	ERT	NNO
1236	FIX	MaRS	OCC	-111.99	-101.99	ERT	GST
1236	FIX	MaRS	OCC	-41.00	-31.00	ERT	GST
1237	FIX	MaRS	OCC	-110.27	-100.27	ERT	NNO
1237	FIX	MaRS	OCC	-40.27	-30.27	ERT	NNO
1238	FIX	MaRS	OCC	-109.96	-99.96	ERT	NNO
1238	FIX	MaRS	OCC	-40.46	-30.46	ERT	NNO
1239	FIX	MaRS	OCC	-108.80	-98.80	ERT	GST
1239	FIX	MaRS	OCC	-40.30	-30.30	ERT	GST
1240	FIX	MaRS	OCC	-106.58	-96.58	ERT	NNO
1240	FIX	MaRS	OCC	-39.09	-29.09	ERT	NNO

1241	FIX	MaRS	OCC	-106.41	-96.41	ERT	NNO
1241	FIX	MaRS	OCC	-39.41	-29.41	ERT	NNO
1242	FIX	MaRS	OCC	-104.87	-94.87	ERT	MAD
1242	FIX	MaRS	OCC	-38.88	-28.88	ERT	GST(MAD)
1243	FIX	MaRS	OCC	-103.74	-93.74	ERT	NNO
1243	FIX	MaRS	OCC	-38.24	-28.24	ERT	NNO
1244	FIX	MaRS	OCC	-103.21	-93.21	ERT	NNO
1244	FIX	MaRS	OCC	-38.72	-28.72	ERT	NNO
1245	FIX	MaRS	OCC	-101.13	-91.13	ERT	MAD
1245	FIX	MaRS	OCC	-37.63	-27.63	ERT	MAD
1246	FIX	MaRS	OCC	-100.97	-90.97	ERT	GST
1246	FIX	MaRS	OCC	-37.97	-27.97	ERT	NNO
1247	FIX	MaRS	OCC	-99.40	-89.40	ERT	NNO
1247	FIX	MaRS	OCC	-37.90	-27.90	ERT	NNO
1248	FIX	MaRS	OCC	-98.17	-88.17	ERT	MAD
1248	FIX	MaRS	OCC	-37.68	-27.68	ERT	MAD
1249	FIX	MaRS	OCC	-97.96	-87.96	ERT	GST
1249	FIX	MaRS	OCC	-37.96	-27.96	ERT	GST
1250	FIX	MaRS	OCC	-95.75	-85.75	ERT	NNO
1250	FIX	MaRS	OCC	-36.75	-26.75	ERT	NNO
1251	FIX	MaRS	OCC	-95.46	-85.46	ERT	MAD
1251	FIX	MaRS	OCC	-36.96	-26.96	ERT	MAD
1252	FIX	MaRS	OCC	-94.30	-84.30	ERT	GST
1252	FIX	MaRS	OCC	-36.80	-26.80	ERT	GST
1253	FIX	MaRS	OCC	-92.60	-82.60	ERT	NNO
1253	FIX	MaRS	OCC	-36.10	-26.10	ERT	NNO
1254	FIX	MaRS	OCC	-92.43	-82.43	ERT	NNO
1254	FIX	MaRS	OCC	-36.43	-26.43	ERT	NNO
1255	FIX	MaRS	OCC	-90.90	-80.90	ERT	GST
1255	FIX	MaRS	OCC	-35.90	-25.90	ERT	GST
1256	FIX	MaRS	OCC	-89.28	-79.28	ERT	NNO
1256	FIX	MaRS	OCC	-35.28	-25.28	ERT	NNO
1257	FIX	MaRS	OCC	-88.76	-78.76	ERT	NNO
1257	FIX	MaRS	OCC	-35.76	-25.76	ERT	NNO
1258	FIX	MaRS	OCC	-87.19	-77.19	ERT	GST
1258	FIX	MaRS	OCC	-35.19	-25.19	ERT	GST
1259	FIX	MaRS	OCC	-86.54	-76.54	ERT	NNO
1259	FIX	MaRS	OCC	-35.55	-25.55	ERT	NNO
1260	FIX	MaRS	OCC	-85.50	-75.50	ERT	NNO
1260	FIX	MaRS	OCC	-35.00	-25.00	ERT	NNO
1261	FIX	MaRS	OCC	-84.29	-74.29	ERT	GST(MAD)
1261	FIX	MaRS	OCC	-34.79	-24.79	ERT	GST(MAD)
1262	FIX	MaRS	OCC	-83.58	-73.58	ERT	NNO
1262	FIX	MaRS	OCC	-35.09	-25.09	ERT	NNO
1263	FIX	MaRS	OCC	-81.90	-71.90	ERT	NNO
1263	FIX	MaRS	OCC	-34.40	-24.40	ERT	NNO
1264	FIX	MaRS	OCC	-81.62	-71.62	ERT	MAD
1264	FIX	MaRS	OCC	-34.62	-24.62	ERT	MAD
1265	FIX	MaRS	OCC	-80.47	-70.47	ERT	NNO
1265	FIX	MaRS	OCC	-34.97	-24.97	ERT	NNO
1266	FIX	MaRS	OCC	-78.77	-68.77	ERT	NNO

1266	FIX	MaRS	OCC	-33.77	-23.77	ERT	NNO
1267	FIX	MaRS	OCC	-78.60	-68.60	ERT	MAD
1267	FIX	MaRS	OCC	-34.60	-24.60	ERT	MAD
1268	FIX	MaRS	OCC	-77.08	-67.08	ERT	GST
1268	FIX	MaRS	OCC	-34.08	-24.08	ERT	GST
1269	FIX	MaRS	OCC	-75.46	-65.46	ERT	NNO
1269	FIX	MaRS	OCC	-33.46	-23.46	ERT	NNO
1270	FIX	MaRS	OCC	-74.95	-64.95	ERT	MAD
1270	FIX	MaRS	OCC	-33.96	-23.96	ERT	MAD
1271	FIX	MaRS	OCC	-73.41	-63.41	ERT	GST
1271	FIX	MaRS	OCC	-33.41	-23.41	ERT	GST
1272	FIX	MaRS	OCC	-72.78	-62.78	ERT	NNO
1272	FIX	MaRS	OCC	-33.78	-23.78	ERT	NNO
1273	FIX	MaRS	OCC	-71.76	-61.76	ERT	NNO
1273	FIX	MaRS	OCC	-33.76	-23.76	ERT	NNO
1274	FIX	MaRS	OCC	-70.57	-60.57	ERT	GST
1274	FIX	MaRS	OCC	-33.57	-23.57	ERT	GST
1275	FIX	MaRS	OCC	-69.89	-59.89	ERT	NNO
1275	FIX	MaRS	OCC	-33.89	-23.89	ERT	NNO
1276	FIX	MaRS	OCC	-68.22	-58.22	ERT	NNO
1276	FIX	MaRS	OCC	-33.22	-23.22	ERT	NNO
1277	FIX	MaRS	OCC	-67.95	-57.95	ERT	GST
1277	FIX	MaRS	OCC	-33.45	-23.45	ERT	GST
1278	FIX	MaRS	OCC	-66.81	-56.81	ERT	NNO
1278	FIX	MaRS	OCC	-33.81	-23.81	ERT	NNO
1279	FIX	MaRS	OCC	-65.12	-55.12	ERT	NNO
1279	FIX	MaRS	OCC	-32.62	-22.62	ERT	NNO
1280	FIX	MaRS	OCC	-64.45	-54.45	ERT	GST(MAD)
1280	FIX	MaRS	OCC	-33.45	-23.45	ERT	GST(MAD)
1281	FIX	MaRS	OCC	-63.43	-53.43	ERT	NNO
1281	FIX	MaRS	OCC	-32.93	-22.93	ERT	NNO
1282	FIX	MaRS	OCC	-61.82	-51.82	ERT	NNO
1282	FIX	MaRS	OCC	-32.82	-22.82	ERT	NNO
1283	FIX	MaRS	OCC	-61.32	-51.32	ERT	MAD
1283	FIX	MaRS	OCC	-33.32	-23.32	ERT	MAD
1284	FIX	MaRS	OCC	-59.29	-49.29	ERT	NNO
1284	FIX	MaRS	OCC	-33.29	-23.29	ERT	NNO
1285	FIX	MaRS	OCC	-58.68	-48.68	ERT	NNO
1285	FIX	MaRS	OCC	-33.68	-23.68	ERT	NNO
1286	FIX	MaRS	OCC	-57.18	-47.18	ERT	MAD
1286	FIX	MaRS	OCC	-33.68	-23.68	ERT	MAD
1287	FIX	MaRS	OCC	-56.02	-46.02	ERT	GST
1287	FIX	MaRS	OCC	-34.02	-24.02	ERT	GST
1288	FIX	MaRS	OCC	-54.86	-44.86	ERT	NNO
1288	FIX	MaRS	OCC	-34.86	-24.86	ERT	NNO
1289	FIX	MaRS	OCC	-52.71	-42.71	ERT	MAD
1289	FIX	MaRS	OCC	-34.71	-24.71	ERT	MAD
1290	FIX	MaRS	OCC	-51.96	-41.96	ERT	GST
1290	FIX	MaRS	OCC	-35.46	-25.46	ERT	GST
1291	FIX	MaRS	OCC	-49.83	-39.83	ERT	NNO

1291	FIX	MaRS	OCC	-36.83	-26.83	ERT	NNO

7.5 Gravity: Local Anomalies

7.5.1 Description

The highly eccentric orbit of Mars Express about the planet is not best suited for a global investigation of the gravity field. The investigation proposed here will focus on specific target areas for the determination of local gravity anomalies. Simultaneous observations of the stereo camera experiment (HRSC) and the radar in the altimeter mode will yield the high resolution three dimensional (3D) topography of the target area. The goal is to combine these data sets (radio science, camera, radar) to study the state and evolution of the Martian crust and lithosphere which yields implications for the tectonic evolution of Mars.

7.5.2 Measurement Technique

Gravity information can be obtained at all times when the spacecraft is using the two-way dual-frequency radio link and the spacecraft is close enough to the surface that gravity accelerations significantly affect the spacecraft velocity (pericenter passes). The Earth pointing of the HGA is required to maintain a continuous radio link. The coherent and simultaneous dual-frequency downlink allows the extraction of the dispersive effects on the downlink due to the interplanetary medium and the earth ionosphere, in particular if the uplink is operated at S-band. Doppler tracking data will be acquired at a rate of one sample per 10 seconds and ranging data will be collected at a rate of one point per 10 minutes.

Velocity contributions induced by attitude control movements of the spacecraft which result in a HGA motion relative to the line-of-sight to Earth may reach several mm/s. Therefore, thruster activities, attitude control commands and antenna steering commands have to be recorded in order to reconstruct the attitude motion for later correction of derived LOS gravity accelerations.

7.5.3 Targets

Name	Longitude W-/E+	Latitude S-/N+	Radius (km)
Arsia Mons	-121.0	-9.5	500
Pavonis Mons	-112.5	0.5	500
Ascaraeus Mons	-104.0	11.0	500
Olympus Mons	-133.0	18.0	500
Alba Patera	-110.0	40.0	600
Elysium Mons	147.0	25.0	500
Beagle 2 (Isidis)	90.0	10.6	600

Table 7.5-1 Quasi-point targets with a specified radius

Name	**Longitude W-/E+**		**Latitude S-/N+**	
	min	max	min	max
Tharsis Ridge	-100.0	-140.0	-20.0	30.0
Tempe Fossae	-70.0	-90.0	30.0	50.0
Valles Marineris	-40.0	-110.0	-20.0	0.0
Hellas	80.0	50.0	-30.0	-55.0
North Polar Cap	-180.0	180.0	70.0	90.0
South Polar Cap	-180.0	180.0	-70.0	-90.0
Claritas Fossae NW	-100.0	-112.0	-10.0	-30.0
Claritas Fossae SE	-80.0	-100.0	-30.0	-50.0

Table 7.5-2: extended target areas

7.5.4 Operations

7.5.4.1 Configuration

Operations will be conducted using a coherent simultaneous dual-frequency two-way tracking link (TWOD). Coherency of the transponded signal is mandatory for Doppler data acquisition. Dual-frequency operations are mandatory for an a posteriori calibration of ionospheric and interplanetary plasma effects and removal from the Doppler data. Two-way tracking is required to make use of the high-precision ground station frequency reference.

Table 7.5-3: Configurations for the determination of local gravity anomalies

S/C configuration	TWOD		
Ground segment configuration		up	down
	IFMS A	X	X-CL
	IFMS B		X-CL
	IFMS RS		S-CL
Telemetry modulation	OFF		
MaRS operational procedure	GRA		

7.5.4.2 HGA Pointing

The HGA is pointed toward the Earth.

7.5.4.3 Operations Timeline

7.5.4.3.1 Sequence of events

Timeline and sequence of events is given at the end of Section 9.

7.5.4.3.2 Requested Orbits

Table 7.5-4: Gravity observations for the first 1400 orbits:

				start	stop		
orbit #	**attitude**	**instrument**	**Experiment**	**relative to pericenter**		**pointing**	**ground station**
41	FIX	MaRS	GRA	-20.00	20.00	ERT	NNO
70	FIX	MaRS	GRA	-20.00	20.00	ERT	NNO
83	FIX	MaRS	GRA	-20.00	20.00	ERT	NNO
96	FIX	MaRS	GRA	-20.00	20.00	ERT	NNO
114	FIX	MaRS	GRA	-20.00	20.00	ERT	NNO
127	FIX	MaRS	GRA	-20.00	20.00	ERT	NNO
140	FIX	MaRS	GRA	-20.00	20.00	ERT	NNO
177	FIX	MaRS	GRA	-20.00	20.00	ERT	NNO
190	FIX	MaRS	GRA	-20.00	20.00	ERT	NNO
203	FIX	MaRS	GRA	-20.00	20.00	ERT	NNO
216	FIX	MaRS	GRA	-20.00	20.00	ERT	NNO
231	FIX	MaRS	GRA	-20.00	20.00	ERT	NNO
234	FIX	MaRS	GRA	-20.00	20.00	ERT	NNO
244	FIX	MaRS	GRA	-20.00	20.00	ERT	NNO
247	FIX	MaRS	GRA	-20.00	20.00	ERT	NNO
952	FIX	MaRS	GRA	-20.00	20.00	ERT	NNO
955	FIX	MaRS	GRA	-20.00	20.00	ERT	NNO
958	FIX	MaRS	GRA	-20.00	20.00	ERT	NNO
965	FIX	MaRS	GRA	-20.00	20.00	ERT	NNO
968	FIX	MaRS	GRA	-20.00	20.00	ERT	NNO
971	FIX	MaRS	GRA	-20.00	20.00	ERT	NNO
974	FIX	MaRS	GRA	-20.00	20.00	ERT	NNO
978	FIX	MaRS	GRA	-20.00	20.00	ERT	NNO
981	FIX	MaRS	GRA	-20.00	20.00	ERT	NNO
984	FIX	MaRS	GRA	-20.00	20.00	ERT	NNO
987	FIX	MaRS	GRA	-20.00	20.00	ERT	NNO
991	FIX	MaRS	GRA	-20.00	20.00	ERT	NNO
994	FIX	MaRS	GRA	-20.00	20.00	ERT	NNO
1007	FIX	MaRS	GRA	-20.00	20.00	ERT	NNO
1015	FIX	MaRS	GRA	-20.00	20.00	ERT	NNO
1028	FIX	MaRS	GRA	-20.00	20.00	ERT	NNO
1041	FIX	MaRS	GRA	-20.00	20.00	ERT	NNO
1054	FIX	MaRS	GRA	-20.00	20.00	ERT	NNO
1067	FIX	MaRS	GRA	-20.00	20.00	ERT	NNO
1072	FIX	MaRS	GRA	-20.00	20.00	ERT	NNO
1085	FIX	MaRS	GRA	-20.00	20.00	ERT	NNO
1098	FIX	MaRS	GRA	-20.00	20.00	ERT	NNO
1111	FIX	MaRS	GRA	-20.00	20.00	ERT	NNO
1124	FIX	MaRS	GRA	-20.00	20.00	ERT	NNO

7.5.4.4 Constraints

Gravity mapping can be performed during pericenter passes only. HGA Earth pointing is required.

Spacecraft orbit correction maneuvers must not be performed within the operation period. Furthermore, spacecraft attitude thruster activities should be avoided or kept at a minimum. In case of thruster activities, a logging of relevant thrust parameters has to be performed.

7.5.5 Data

7.5.5.1 Mission Products

New Norcia ground station:

Table 7.5-5: Gravity data products

Receiver	Frequency band	Data products
IFMS A (closed-loop)	X	Doppler1 ranging meteo
IFMS B (closed-loop)	X	Doppler2
IFMS RS (closed-loop)	S	Doppler ranging

Deep Space Network:

Table 7.5-6: DSN Data products

Receiver	Frequency band	Data products	Data file type
closed-loop	X	phase	TRK-2-34
	S	phase	
open-loop	-	-	-
	-	-	

7.5.5.2 Accuracy

The accuracy of the X/X- and X/S-Doppler data should be better than 0.3 mm/s (1σ) at 1 second integration time.

7.5.5.3 Sample Rate

Table 7.5-7: Gravity sample rate

Closed-loop	1 samples / 10 second
Open-loop	-
Auxiliary data	TBD

7.5.5.4 Data Volume

Table 7.5-8: Gravity data volume

	Data Volume
Closed-loop IFMS DSN	 615 kByte per frequency 520 kByte per frequency
Open-loop IFMS DSN	 N/A N/A
Auxiliary data	TBD
Ground station meteo	Already contained in IFMS figure

7.5.5.5 Availability

TBD

7.6 Surface (Bistatic Radar)

7.6.1 Description

The bistatic radar configuration is distinguished from the monostatic by spatial separation of the transmitter (the spacecraft) and the receiver (ground station on Earth). It is a powerful tool in providing information about surface texture (roughness and slope) at scales of the radar wavelength (on the order cm to meter). Bistatic radar may also be used to determine properties of the surface material, such as dielectric constant, through differential reflection of orthogonal polarizations (Simpson, 1993). The bistatic radar geometry of an orbiting spacecraft is well suited to probing the surface of planets at a variety of latitude, longitude and incidence angles. Bistatic radar experiments have been conducted at the Moon (e.g. Tyler & Howard, 1973; Nozette et al., 1996; Simpson & Tyler, 1999), Mars (Simpson & Tyler, 1980; 1981; Simpson et al., 1982; 1984) and Venus (Pettengill et al., 1997; Kolosov et al., 1979).

7.6.2 Measurement Technique

For a typical downlink bistatic radar experiment, the radio signal is transmitted from the spacecraft High Gain Antenna (HGA) toward the surface and is scattered from the surface. That part of the signal power which is reflected toward Earth is received at the ground station. Optimizing performance of these bistatic radar experiments requires accurate prediction of the orbiter trajectory for the formulation of antenna pointing strategies and prediction of signal parameters such as Doppler shift and signal amplitude.

In a quasi-specular experiment the antenna is programmed to follow a locus of points for which surface reflection would be specular if Mars were smooth. From the data recorded along these specular point paths, surface roughness can be inferred from Doppler dispersion of the echo signal; the dielectric constant ε of the surface material can be inferred from echo amplitude and/or polarization properties. Dielectric properties of Oceanus Procellarum on the Moon were obtained by measuring the Brewster angle $\tan^2\Phi_B = \varepsilon$ (Tyler, 1968); a Stokes parameter analysis led to detection of a tellurium-like material in Venus highlands (Pettengill et al., 1996).

In a spotlight experiment the antenna is programmed to track a fixed point on the surface, viewed from a variety of angles. When the configuration passes through the backscatter geometry, coherent backscatter enhancements can be sought in the echo amplitude and polarization (Hapke, 1990). Clementine spotlight data suggested the presence of water ice near the lunar South Pole (Nozette et al., 1996) though a second analysis (Simpson and Tyler, 1999) showed no evidence for an enhancement.

In a bistatic backscatter experiment the spacecraft antenna is aimed exactly opposite to the Earth direction, a configuration which is often much easier to implement than

dynamically tracking either moving or fixed points. As the antenna beam illuminates regions on the surface, coherent backscatter enhancements will cause ice-covered areas to appear extremely bright. Repeated tracks over the polar region can be used to define the boundaries of icy polar deposits or to monitor their changes as a function of time. The spatial resolution of the measurements is approximately equal to the projection of the HGA beam onto the surface.

In any of these experimental configurations, the radio echo signal is received in the open-loop mode (see below) in two orthogonal polarizations (e.g., LCP, or Left Circular Polarization, and RCP, or Right Circular Polarization), down-converted, sampled, and stored for further processing at home institutions. Figure 3.1-4 shows a typical frequency spectrum of the received radio signal. The direct signal, leaking out from the side lobes of the HGA and which is reduced accordingly in power, is on the right. The echo signal is on the left. It is Doppler shifted relative to the direct signal according to the change in spacecraft-to-surface-to-Earth distance as a function of time; it is broadened according to the roughness of the surface and the motion of the specular point over the surface (Simpson, 1993).

7.6.3 Targets

The objectives of this experiment are focused on determining electrical and physical properties of the surface in areas such as

1. polar regions and caps,
2. volcanic regions
3. the famous ”stealth” area west of Tharsis (Muhleman et al., 1991; Edgett et al., 1997).
4. high plains south of Valles Marineris
5. landing sites -- new and old

Name	Longitude (W-/E+)	Latitude (S-/N+)
Stealth	-143.5	-2.5
Syrtis Major	70.0	10.0
Residual S. Polar cap	-53.2	-87.4
Syria Sinai Solis	-90.0	-20.0
N Polar Cap	-180.0	90.0
Viking L1	-47.9	22.3
Viking L2	134.5	47.7
Pathfinder	-33.2	19.1
Beagle 2	90.5	11.6

Microwave radar responds to surface texture at scales of the wavelength (cm to m) while the long wave radar on MARSIS responds to structures in the order of hundreds of meters. Therefore MARSIS, HRSC, the infrared spectrometer, and bistatic microwave radar will characterize the surface over a wide range of structural scales. The comparison of radar and high resolution imaging will be useful and highly desirable for deriving relationships among structures in the cm to hundreds of meters range.

The classification ”smooth” or ”rough” is somewhat arbitrary. A surface typically appears rougher as the wavelength becomes shorter (or, sometimes, as the incidence angle becomes smaller). An area reported to be smooth based on MARSIS observations might be classified as extremely rough using the microwave radar. Photogeologists working with HRSC data should have data at these other wavelengths to interpret surface structure properly.

7.6.3.1 Polar regions and caps; icy surfaces

The bistatic geometry is well-suited to probing icy surfaces, which are poorly understood on Mars. The south residual polar cap on Mars has anomalously high radar backscatter when viewed from Earth while the northern cap (presumably much more massive) does not stand out. The opportunity to map the boundaries of the highly reflecting regions in the "bistatic backscatter" configuration (and to monitor their seasonal changes) is unique to the radio science investigation.

Figure 2 shows the surface roughness expressed as rms slope from a Viking 2 "quasi-specular" track in the Martian North Pole region. RMS surface roughness ranges from 1° (smooth) in the polar plains to 6° (moderately rough) in parts of the permanent polar cap.

7.6.3.2 Volcanic Regions

Selected targets in other areas, such as volcanic plains, will also be studied; despite similar appearance in orbital images, plains do not necessarily have the same radar behavior - again suggesting differences in the underlying surface geology. The differences between aa and pahoehoe lava flows, readily apparent at centimeter and meter scales, may not be so clear in images from orbit, for example. Quasi-specular tracks from Viking 2 showed doubling of rms surface roughness near Tritonis Lacus with little or no change in orbital images (Simpson et al., 1984). Bistatic tracks across the vast plains farther north, undifferentiated by topography, may help distinguish their current states based on centimeter-scale roughness and possibly contribute to unraveling their history.

7.6.3.3 The ”Stealth” region

The Stealth region, west of Tharsis, is anomalous in the opposite sense; it yields very weak backscatter when probed from Earth. The unique geometry of a bistatic experiment offers some hope for better understanding of both the scattering processes and also the underlying surface geology.

7.6.3.4 HIGH PLAINS and SEASONAL WATER

Although never confirmed, Earth-based radar data from high plains south of Valles Marineris were interpreted as indicating the presence of seasonal, near-surface, liquid water (S.H. Zisk and P.J. Mouginis-Mark,1980). Reflectivity of this region appeared to increase in southern summer, as one might suspect had permafrost melted. Unfortunately, confirming the discovery would have required additional

measurements when the sub-Earth point returned to latitudes in the vicinity of 20S at a variety of Mars seasons. Telescope time was never allocated for such a campaign, so the question of seasonal water technically remains open, though a number of opposing arguments have been raised since. Quasi-specular bistatic observations do not require that the sub-Earth point lie near 20S -- only that a ground track pass through that region at an interesting Mars season. Enough new data could be obtained by scheduling occasional bistatic radar tracks south of Valles Marineris that the question of liquid water could be addressed independently using Mars Express data alone.

7.6.4 Operations

7.6.4.1 Configuration

Table 7.6-1: Configurations for the determination of the surface properties

S/C configuration	ONED		
Ground segment configuration		up	down
NNO	IFMS A		X-CL
	IFMS B		X-CL
	IFMS RS		S-CL X-OL RCP X-OL LCP
DSN 70-m	Closed-loop		X-CL S-CL
	Open-loop		X-OL RCP X-OL LCP S-OL RCP S-OL LCP
Telemetry modulation	OFF		
MaRS operational procedure	BSR		

7.6.4.2 HGA Pointing

In a quasi-specular experiment the HGA is pre-programmed to follow a locus of points for which surface reflection would be specular if Mars were smooth.

In a spotlight experiment the HGA is pre-programmed to track a fixed point on the surface, viewed from a variety of angles

In a bistatic backscatter experiment the HGA is aimed exactly opposite to the Earth direction (inertial pointing),

7.6.4.3 Operations Timeline

Before depointing, the spacecraft telemetry is turned off, frequency control is switched to the internal (one-way) oscillator, and the new frequency is recorded briefly on the ground. Then the HGA is depointed to the surface.

The sequence-of-events is given in Section 9

7.6.4.4 Constraints

Depointing of the antenna follows a preprogrammed AOCS manoeuver sequence. Command access via the LGA S-band antennas is guaranteed.

No telemetry transmission is feasible during Bistatic Radar Operations since the HGA remains pointed toward the Martian surface. The observations can be performed at any orbit position including apocenter.

A 70-m antenna is required for the polarization channel assignments at the DSN ground stations. In case of a limitation of ground crew shifts, the DSS 43 in Australia is requested since it has approximately the same visibility window as New Norcia.

7.6.5 Data

7.6.5.1 Mission Products

New Norcia Ground Station:

Table 7.6-2: Bistatic radar: data products

Receiver	Frequency band	Data products
IFMS A (closed-loop)	X	Doppler meteo
IFMS B (closed-loop)	X	Doppler
IFMS RS (closed-loop) IFMS-RS (open-loop)	S X X	Doppler Voltage samples RCP Voltage samples LCP

Deep Space Network:

Note: The 70m DSN 43 ground station (Australia) is requested for this procedure

Table 7.6-3: DSN bistatic radar data products

Receiver	Frequency band	Data products	Data file type
closed-loop	X	Phase	TRK-2-34
	S	Phase	
open-loop	X	LCP voltage samples	RSR
	X	RCP voltage samples	
	S	LCP voltage samples	
	S	RCP voltage samples	
	X	LCP system temperature	TBD
	X	RCP system temperature	TBD
	S	LCP system temperature	TBD
	S	RCP system temperature	TBD

7.6.5.2 Accuracy

The required resolution in the frequency spectrum is $\Delta f = 5$ Hz.
The required accuracy for the polarisation angle is 0.1° (TBD).
Sampling should be within +/-1 quantization level over the full range of the analog-to-digital converter.
System temperature should be accurate to +/-0.5K

7.6.5.3 Sample Rate

Table 7.6-4: Bistatic radar: sample rate

Closed-loop	1 per second
Open-loop	50,000 complex samples/second per channel (16-bits I, 16-bits Q) or equivalent (maximum)
Auxiliary data	TBD

7.6.5.4 Data Volume

Table 7.6-5: Bistatic radar: data volume

	Data Volume
Closed-loop IFMS DSN	 N/A N/A
Open-loop IFMS DSN	 2 Gbyte (2 hours) 6 GByte (2 hours)
Auxiliary data	TBD
Ground station meteo	Already contained in IFMS figure

7.6.5.5 Availability

TBD

7.7 Phobos

7.7.1 Description

The scientific objective is the precise determination of the mass and if feasible of the low degree gravity field of the moon Phobos.

7.7.2 Measurement Technique

The mass or the parameter *GM* can be extracted from the two-way Doppler shift.

7.7.3 Operations

7.7.3.1 Configuration

.

Table 7.7-1: Configurations for Phobos mass determination

S/C configuration	TWOD		
Ground segment configuration		up	down
	IFMS A	X	X-CL
	IFMS B		X-CL
	IFMS RS		S-CL
Telemetry modulation	OFF		
MaRS operational procedure	PHO		

7.7.3.2 Operations Timeline

TBD

7.7.3.3 Phobos Encounter Passes

Phobos flyby closer than 400 km for the first 1400 orbits (reference: T. Duxbury, Phobos encounters, 18.02.2003):

Orbit #	Ground station	Date	Closest approach (km)
678	Madrid	2004 Jul 31 12:07:01	181
679	Goldstone or Madrid	2004 Jul 31 19:45:01	362

7.7.3.4 Constraints

TBD

7.7.4 Data

7.7.4.1 Mission Products

New Norcia Ground Station:

Table 7.7-2: IFMS Phobos flyby mission products

Receiver	Frequency band	Data products
IFMS A (closed-loop)	X	Doppler ranging meteo
IFMS B (closed-loop)	X	Doppler
IFMS RS (closed-loop)	S	Doppler ranging

Deep Space Network:

Table 7.7-3: DSN data products

Receiver	Frequency band	Data products	Data file type
closed-loop	X	Phase	TRK-2-34
	S	Phase	
open-loop			

7.7.4.2 Accuracy

TBD

7.7.4.3 Sample Rate

Table 7.7-4: sample rates

Closed-loop	1 sample / second S & X-band Doppler continuous ranging (NNO) ranging sample rate 5 min at DSN
Open-loop	N/A
Auxiliary data	TBD

7.7.4.4 Data Volume

Table 7.7-5: Data volume

	Data Volume per pass
Closed-loop IFMS DSN	 5403 kByte per frequency 6800 kByte per frequency
Open-loop IFMS DSN	 N/A
Auxiliary data	TBD
Ground station meteo	Already contained in IFMS figure

7.7.4.5 Availability

TBD

7.8 Solar Corona

7.8.1 Description

The scientific objectives are the determination of the total electron content of the solar corona, the solar wind speed, the turbulence spectrum, and the identification of coronal mass ejections.

7.8.2 Measurement Technique

The total electron content and its temporal changes, the solar wind speed, and the turbulence spectrum can be derived from measurements of dual-frequency differential group time delay (ranging) and the differential Doppler shift.

7.8.3 Operations

7.8.3.1 Configuration

.

Table 7.8-1: Configurations for the observation of the solar corona

S/C configuration	TWOD		
Ground segment configuration		up	down
NNO	IFMS A	S	X-CL
	IFMS B	-	S-OL
	IFMS RS	-	X-CL
			S-OL RCP
			X-OL RCP
DSN 34m/ 70m	Closed-loop	S	S-CL
			X-CL
	Open-loop	-	S-OL RCP
			X-OL RCP
Telemetry modulation	OFF		
MaRS operational procedure	SCP		

7.8.3.2 Operations Timeline

A daily tracking pass at New Norcia and at one DSN ground station (either Madrid or Goldstone) is requested for the time of solar conjunction when the spacecraft is within 10° elongation about the solar disk in the plane of sky. These measurements can be performed when the spacecraft is tracked for telemetry return. Two 70m

tracking passes are requested when the s/c is within 3° elongation. Detailed timelines and sequence of events are included in Section 9.

7.8.3.3 Solar Conjunction Duration

Table 7.8-2: solar conjunctions as a function of mission time

Solar conjunction			Conjunction Date	Solar offset (minimum)	Number of tracking passes[8]
Acronym	start	stop			
SCP1	12.08.04	17.10.04	13.09.04	4 Rs North Pole	132
SCP2	21.09.06	28.11.06	25.10.06	<2Rs North Pole	136

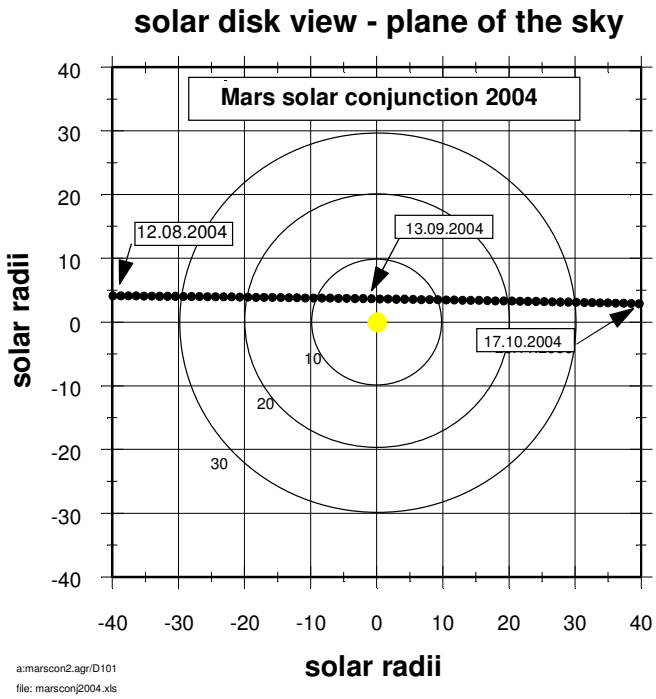

Figure 7.8-1: solar conjunction in 2004 (upper panel). Spacecraft position in the plane of sky for each day at 00:00 UT.

[8] includes one additional DSN ground station pass/day outside 12 solar radii and two 70-m DSN passes (one at DSS 43) inside 12 solar radii.

7.8.3.3.1 First conjunction season 2004

				start	stop		
orbit #	**attitude**	**instrument**	**Experiment**	**relative to pericenter**		**pointing**	**ground station**
729	FIX	MaRS	SCO	31.30	APOCENT	ERT	MAD
730	FIX	MaRS	SCO	APOCENT	-87.35	ERT	MAD(GST)
730	FIX	MaRS	SCO	140.15	APOCENT	ERT	NNO
731	FIX	MaRS	SCO	APOCENT	-99.70	ERT	GST(NNO)
731	FIX	MaRS	SCO	101.30	APOCENT	ERT	MAD
732	FIX	MaRS	SCO	APOCENT	15.97	ERT	MAD(NNO)
732	FIX	MaRS	SCO	31.47	APOCENT	ERT	MAD(GST)
733	FIX	MaRS	SCO	APOCENT	-14.43	ERT	MAD(GST)
733	FIX	MaRS	SCO	31.17	APOCENT	ERT	GST(NNO)
734	FIX	MaRS	SCO	APOCENT	-26.83	ERT	GST(NNO)
734	FIX	MaRS	SCO	176.17	APOCENT	ERT	MAD(NNO)
735	FIX	MaRS	SCO	APOCENT	15.98	ERT	MAD(NNO)
735	FIX	MaRS	SCO	31.48	APOCENT	ERT	MAD(GST)
736	FIX	MaRS	SCO	APOCENT	16.27	ERT	GST(MAD)
736	FIX	MaRS	SCO	31.27	58.67	ERT	MAD(GST)
737	FIX	MaRS	SCO	31.47	46.87	ERT	GST(NNO)
738	FIX	MaRS	SCO	-203.80	16.32	ERT	MAD(NNO)
738	FIX	MaRS	SCO	31.32	APOCENT	ERT	MAD(NNO)
739	FIX	MaRS	SCO	APOCENT	16.62	ERT	GST(MAD)
739	FIX	MaRS	SCO	31.62	132.50	ERT	MAD(GST)
740	FIX	MaRS	SCO	31.38	120.77	ERT	GST(NNO)
741	FIX	MaRS	SCO	-128.42	16.70	ERT	MAD(NNO)
741	FIX	MaRS	SCO	31.20	APOCENT	ERT	MAD(NNO)
742	FIX	MaRS	SCO	APOCENT	16.85	ERT	GST(MAD)
742	FIX	MaRS	SCO	31.35	205.73	ERT	GST(MAD)
743	FIX	MaRS	SCO	31.57	193.95	ERT	GST(NNO)
744	FIX	MaRS	SCO	-53.38	17.25	ERT	MAD(NNO)
744	FIX	MaRS	SCO	31.25	APOCENT	ERT	MAD(NNO)
745	FIX	MaRS	SCO	APOCENT	17.83	ERT	GST(MAD)
745	FIX	MaRS	SCO	31.33	APOCENT	ERT	GST(MAD)
746	FIX	MaRS	SCO	APOCENT	-176.12	ERT	MAD(GST)
746	FIX	MaRS	SCO	31.52	APOCENT	ERT	GST(NNO)
747	FIX	MaRS	SCO	APOCENT	-187.52	ERT	GST(NNO)
747	FIX	MaRS	SCO	31.62	APOCENT	ERT	NNO
748	FIX	MaRS	SCO	APOCENT	17.83	ERT	MAD(NNO)
748	FIX	MaRS	SCO	31.33	APOCENT	ERT	MAD
749	FIX	MaRS	SCO	APOCENT	-103.02	ERT	MAD(GST)
749	FIX	MaRS	SCO	31.62	APOCENT	ERT	GST(NNO)
750	FIX	MaRS	SCO	APOCENT	-114.30	ERT	GST(NNO)
751	FIX	MaRS	SCO	31.18	APOCENT	ERT	MAD(GST)
752	FIX	MaRS	SCO	APOCENT	-29.65	ERT	MAD(GST)
752	FIX	MaRS	SCO	31.50	APOCENT	ERT	GST(NNO)
753	FIX	MaRS	SCO	APOCENT	-40.88	ERT	GST(NNO)
753	FIX	MaRS	SCO	171.12	APOCENT	ERT	MAD(NNO)
754	FIX	MaRS	SCO	APOCENT	18.60	ERT	MAD(NNO)
754	FIX	MaRS	SCO	31.60	APOCENT	ERT	MAD(GST)

755	FIX	MaRS	SCO	APOCENT	18.77	ERT	GST(MAD)
755	FIX	MaRS	SCO	31.27	44.12	ERT	MAD(GST)
756	FIX	MaRS	SCO	31.48	32.83	ERT	GST(NNO)
757	FIX	MaRS	SCO	-208.48	19.17	ERT	MAD(NNO)
757	FIX	MaRS	SCO	31.17	APOCENT	ERT	MAD
758	FIX	MaRS	SCO	APOCENT	19.25	ERT	MAD(GST)
758	FIX	MaRS	SCO	31.25	117.10	ERT	GST(MAD)
759	FIX	MaRS	SCO	31.45	105.78	ERT	GST(NNO)
760	FIX	MaRS	SCO	-133.60	19.57	ERT	MAD(NNO)
760	FIX	MaRS	SCO	31. Jul	APOCENT	ERT	MAD(NNO)
761	FIX	MaRS	SCO	APOCENT	20.28	ERT	GST(MAD)
761	FIX	MaRS	SCO	31.28	190.12	ERT	MAD(GST)
762	FIX	MaRS	SCO	31. Jul	179.40	ERT	GST(NNO)
763	FIX	MaRS	SCO	-58.88	20.28	ERT	MAD(NNO)
763	FIX	MaRS	SCO	31.28	APOCENT	ERT	MAD(NNO)
764	FIX	MaRS	SCO	APOCENT	20.13	ERT	GST(MAD)
764	FIX	MaRS	SCO	31.13	APOCENT	ERT	GST(MAD)
765	FIX	MaRS	SCO	APOCENT	-191.22	ERT	MAD(GST)
767	FIX	MaRS	SCO	31. Aug	APOCENT	ERT	MAD
768	FIX	MaRS	SCO	APOCENT	-117.90	ERT	MAD(GST)
768	FIX	MaRS	SCO	30.77	APOCENT	ERT	GST(NNO)
769	FIX	MaRS	SCO	APOCENT	-128.17	ERT	GST(NNO)
769	FIX	MaRS	SCO	91.33	APOCENT	ERT	MAD(NNO)
770	FIX	MaRS	SCO	APOCENT	21.20	ERT	MAD(NNO)
770	FIX	MaRS	SCO	30.70	APOCENT	ERT	MAD(GST)
771	FIX	MaRS	SCO	APOCENT	-44.90	ERT	MAD(GST)
771	FIX	MaRS	SCO	30.78	APOCENT	ERT	GST(NNO)
772	FIX	MaRS	SCO	APOCENT	-55.20	ERT	GST(NNO)
772	FIX	MaRS	SCO	166.30	APOCENT	ERT	MAD(NNO)
773	FIX	MaRS	SCO	APOCENT	22. Aug	ERT	MAD(NNO)
773	FIX	MaRS	SCO	30.58	APOCENT	ERT	MAD(GST)
774	FIX	MaRS	SCO	APOCENT	22.80	ERT	GST(MAD)
774	FIX	MaRS	SCO	30.80	28.62	ERT	MAD
774	FIX	MaRS	SCO	30.80	APOCENT	ERT	GST
775	FIX	MaRS	SCO	APOCENT	22. Aug	ERT	GST(NNO)
775	FIX	MaRS	SCO	30.58	18.40	ERT	GST
776	FIX	MaRS	SCO	-213.88	22.80	ERT	MAD(NNO)
776	FIX	MaRS	SCO	30.30	APOCENT	ERT	MAD(NNO)
777	FIX	MaRS	SCO	APOCENT	23.17	ERT	GST(MAD)
777	FIX	MaRS	SCO	30.17	101.98	ERT	MAD(GST)
778	FIX	MaRS	SCO	29.98	91.80	ERT	GST(NNO)
779	FIX	MaRS	SCO	-138.40	23.78	ERT	MAD(NNO)
779	FIX	MaRS	SCO	30.28	APOCENT	ERT	MAD(NNO)
780	FIX	MaRS	SCO	APOCENT	23.63	ERT	GST(MAD)
780	FIX	MaRS	SCO	30.13	175.45	ERT	GST(MAD)
781	FIX	MaRS	SCO	29.83	165.15	ERT	GST(NNO)
782	FIX	MaRS	SCO	-63.10	24. Aug	ERT	MAD(NNO)
782	FIX	MaRS	SCO	29.58	APOCENT	ERT	MAD(NNO)
783	FIX	MaRS	SCO	APOCENT	24.28	ERT	GST(MAD)
783	FIX	MaRS	SCO	29.28	APOCENT	ERT	GST(MAD)
784	FIX	MaRS	SCO	APOCENT	-206.32	ERT	MAD(GST)

785	FIX	MaRS	SCO	29. Jul	APOCENT	ERT	NNO
786	FIX	MaRS	SCO	APOCENT	25.67	ERT	MAD(GST)
786	FIX	MaRS	SCO	28.67	APOCENT	ERT	MAD
787	FIX	MaRS	SCO	APOCENT	-133.30	ERT	MAD(GST)
787	FIX	MaRS	SCO	28.38	APOCENT	ERT	GST(NNO)
788	FIX	MaRS	SCO	APOCENT	-143.02	ERT	GST(NNO)
791	FIX	MaRS	SCO	161.40	APOCENT	ERT	MAD
792	FIX	MaRS	SCO	APOCENT	9999.99	ERT	MAD(GST)
793	FIX	MaRS	SCO	APOCENT	13.57	ERT	MAD(GST)
795	FIX	MaRS	SCO	-217.97	APOCENT	ERT	MAD(NNO)
796	FIX	MaRS	SCO	APOCENT	86.75	ERT	MAD(GST)
798	FIX	MaRS	SCO	-142.97	APOCENT	ERT	MAD(NNO)
799	FIX	MaRS	SCO	APOCENT	160.15	ERT	MAD(GST)
801	FIX	MaRS	SCO	-68.37	APOCENT	ERT	MAD(NNO)
802	FIX	MaRS	SCO	APOCENT	9999.99	ERT	MAD(GST)
803	FIX	MaRS	SCO	APOCENT	-221.27	ERT	GST(NNO)
804	FIX	MaRS	SCO	07. Jul	APOCENT	ERT	MAD
805	FIX	MaRS	SCO	APOCENT	9999.99	ERT	MAD(GST)
806	FIX	MaRS	SCO	APOCENT	-147.73	ERT	GST(NNO)
810	FIX	MaRS	SCO	157.07	APOCENT	ERT	MAD(NNO)
811	FIX	MaRS	SCO	APOCENT	9999.99	ERT	MAD(GST)
812	FIX	MaRS	SCO	APOCENT	-1.62	ERT	MAD(GST)
814	FIX	MaRS	SCO	-223.13	APOCENT	ERT	MAD(NNO)
815	FIX	MaRS	SCO	APOCENT	71.60	ERT	MAD(GST)
817	FIX	MaRS	SCO	-147.70	APOCENT	ERT	MAD(NNO)
818	FIX	MaRS	SCO	APOCENT	145.12	ERT	MAD(GST)
820	FIX	MaRS	SCO	-72.25	APOCENT	ERT	MAD(NNO)
821	FIX	MaRS	SCO	APOCENT	218.52	ERT	MAD(GST)
823	FIX	MaRS	SCO	Feb 35	APOCENT	ERT	MAD(NNO)
824	FIX	MaRS	SCO	APOCENT	9999.99	ERT	MAD(GST)
825	FIX	MaRS	SCO	APOCENT	-163.33	ERT	GST(NNO)
826	FIX	MaRS	SCO	77.37	APOCENT	ERT	MAD(NNO)
827	FIX	MaRS	SCO	APOCENT	9999.99	ERT	MAD(GST)
828	FIX	MaRS	SCO	APOCENT	-90.13	ERT	GST(NNO)
829	FIX	MaRS	SCO	152.23	APOCENT	ERT	MAD(NNO)
831	FIX	MaRS	SCO	218.92	APOCENT	ERT	NNO
832	FIX	MaRS	SCO	APOCENT	-24.18	ERT	GST(NNO)
833	FIX	MaRS	SCO	-226.93	APOCENT	ERT	MAD(GST)
834	FIX	MaRS	SCO	APOCENT	56.85	ERT	MAD(GST)
836	FIX	MaRS	SCO	-151.80	APOCENT	ERT	MAD(NNO)
837	FIX	MaRS	SCO	APOCENT	129.88	ERT	MAD(GST)
844	FIX	MaRS	SCO	APOCENT	-177.75	ERT	GST(NNO)
845	FIX	MaRS	SCO	73.17	APOCENT	ERT	MAD(NNO)
846	FIX	MaRS	SCO	APOCENT	9999.99	ERT	MAD(GST)
847	FIX	MaRS	SCO	APOCENT	-104.28	ERT	GST(NNO)
848	FIX	MaRS	SCO	148.47	APOCENT	ERT	MAD(NNO)
849	FIX	MaRS	SCO	APOCENT	9999.99	ERT	MAD(GST)
850	FIX	MaRS	SCO	APOCENT	-31.23	ERT	GST(NNO)
851	FIX	MaRS	SCO	223.38	APOCENT	ERT	MAD(NNO)
852	FIX	MaRS	SCO	APOCENT	9999.99	ERT	MAD(GST)
853	FIX	MaRS	SCO	APOCENT	41.87	ERT	MAD(GST)

858	FIX	MaRS	SCO	-80.95	APOCENT	ERT	MAD(NNO)
859	FIX	MaRS	SCO	APOCENT	188.82	ERT	MAD(GST)
861	FIX	MaRS	SCO	-6.12	APOCENT	ERT	MAD(NNO)
862	FIX	MaRS	SCO	APOCENT	9999.99	ERT	MAD(GST)
863	FIX	MaRS	SCO	APOCENT	-192.80	ERT	GST(NNO)
864	FIX	MaRS	SCO	68.82	APOCENT	ERT	MAD(NNO)
865	FIX	MaRS	SCO	APOCENT	9999.99	ERT	MAD(GST)
866	FIX	MaRS	SCO	APOCENT	-119.72	ERT	GST(NNO)
867	FIX	MaRS	SCO	144.00	APOCENT	ERT	MAD(NNO)
868	FIX	MaRS	SCO	APOCENT	9999.99	ERT	MAD(GST)
869	FIX	MaRS	SCO	APOCENT	-46.28	ERT	GST(NNO)
870	FIX	MaRS	SCO	219.05	APOCENT	ERT	MAD(NNO)
871	FIX	MaRS	SCO	APOCENT	9999.99	ERT	MAD(GST)
872	FIX	MaRS	SCO	APOCENT	27.25	ERT	MAD(GST)
877	FIX	MaRS	SCO	-85.73	APOCENT	ERT	MAD(NNO)
878	FIX	MaRS	SCO	APOCENT	173.45	ERT	MAD(GST)
880	FIX	MaRS	SCO	-10.57	APOCENT	ERT	MAD
881	FIX	MaRS	SCO	APOCENT	9999.99	ERT	MAD(GST)
882	FIX	MaRS	SCO	APOCENT	-207.33	ERT	GST(NNO)
883	FIX	MaRS	SCO	65.00	APOCENT	ERT	MAD
884	FIX	MaRS	SCO	APOCENT	9999.99	ERT	MAD(GST)
885	FIX	MaRS	SCO	APOCENT	-133.78	ERT	GST(NNO)
886	FIX	MaRS	SCO	140.02	APOCENT	ERT	MAD(NNO)
887	FIX	MaRS	SCO	APOCENT	9999.99	ERT	MAD(GST)
888	FIX	MaRS	SCO	APOCENT	-60.57	ERT	GST(NNO)
889	FIX	MaRS	SCO	215.13	APOCENT	ERT	MAD(NNO)
890	FIX	MaRS	SCO	APOCENT	9999.99	ERT	MAD(GST)
891	FIX	MaRS	SCO	APOCENT	Dez 43	ERT	MAD(GST)
893	FIX	MaRS	SCO	-164.58	APOCENT	ERT	MAD(NNO)
894	FIX	MaRS	SCO	APOCENT	85.77	ERT	MAD(GST)
896	FIX	MaRS	SCO	-89.53	APOCENT	ERT	MAD(NNO)
897	FIX	MaRS	SCO	APOCENT	159.40	ERT	MAD(GST)
899	FIX	MaRS	SCO	-13.98	APOCENT	ERT	MAD(NNO)
900	FIX	MaRS	SCO	APOCENT	9999.99	ERT	MAD(GST)
901	FIX	MaRS	SCO	APOCENT	-222.08	ERT	GST(NNO)
905	FIX	MaRS	SCO	135.70	APOCENT	ERT	MAD(NNO)
908	FIX	MaRS	SCO	211.12	APOCENT	ERT	MAD(NNO)
909	FIX	MaRS	SCO	APOCENT	9999.99	ERT	MAD(GST)
910	FIX	MaRS	SCO	APOCENT	-1.62	ERT	MAD(GST)
912	FIX	MaRS	SCO	-167.98	APOCENT	ERT	MAD(NNO)
913	FIX	MaRS	SCO	APOCENT	71.80	ERT	MAD(GST)
915	FIX	MaRS	SCO	-93.35	APOCENT	ERT	MAD(NNO)
916	FIX	MaRS	SCO	APOCENT	144.78	ERT	MAD(GST)

7.8.3.3.2 Second conjunction season 2006

TBD

7.8.3.4 Constraints

Outside of 12 solar radii the tracking of a 34-m ground station is sufficient (New Norcia and DSN). Inside of 12 solar radii, two tracking passes of 70-m DSN ground stations are requested.

7.8.4 Data

7.8.4.1 Mission Products

New Norcia Ground Station:

Table 7.8-3: IFMS solar conjunctions mission products

Receiver	Frequency band	Data products
IFMS A (closed-loop)	X	Doppler1 ranging meteo
IFMS B (closed-loop)	X	Doppler2
IFMS RS (closed-loop)	S	Doppler Ranging
IFMS RS (open-loop)	X S	Voltage samples RCP Voltage samples RCP

Deep Space Network:

Note:One pass is always requested at DSS 43. If the apparent S/C position is inside 12 solar radii, a 70-m ground station is requested.

Table 7.8-4: DSN solar conjunction mission products

Receiver	Frequency band	Data products	Data file type
closed-loop	X	Phase	TRK-2-34
	S	Phase	
open-loop	X	LCP voltage samples	RSR
	X	RCP voltage samples	
	S	LCP voltage samples	
	S	RCP voltage samples	

7.8.4.2 Accuracy

To achieve an accuracy in electron content of 0.005 hexem (5×10^{-13} el/m^2), an accuracy in phase of < 0.02 rad or <1° is required, or a frequency variation of < 2 mHz over the integration period of 1 second.

Ranging or group delay accuracy is required to be better than 5 ns.

7.8.4.3 Sample Rate

Table 7.8-5: sample rates

Closed-loop	1 sample / second S & X-band Doppler 15 minutes ranging at begin and end of track (New Norcia) ranging sample rate 10 min at DSN
Open-loop	5000 samples per second
Auxiliary data	TBD

7.8.4.4 Data Volume

Table 7.8-6: Data volume

	Data Volume per pass
Closed-loop IFMS DSN	 5403 kByte per frequency 6800 kByte per frequency
Open-loop IFMS DSN	 TBD 195,000 kByte
Auxiliary data	TBD
Ground station meteo	Already contained in IFMS figure

7.8.4.5 Availability

TBD

7.9 Tracking Verification Test

7.9.1 Description

A Tracking Verification Tests (TVT) shall be performed after launch during the Commissioning Phase and at Mars arrival. This can be partly done simultaneously with the payload check-out.The purpose of the TVT is the determination and verification of the link quality, Doppler and range accuracy, data recording and retrieval test in the ground station, etc.

7.9.2 Objective

The Tracking Verification Test is an end-to-end test to ensure the proper functioning of the ground station and the S/C.

7.9.3 Operations

On the S/C side, the ONES, ONED, TWOS and TWOD links will be tested in various configurations. On the ground station side, S and X-Band uplinks, Open-loop and and closed-Loop data processing will be tested in various configurations with processing alternating between IFMS A, B and RS to insure a full end-to-end test.

In order to estimate the effect of telemetry modulation of the carrier on Doppler precision steps with “telemetry modulation ON” should be carried out such that Doppler tracking is performed at 262 and 8.2 kHz subcarrier frequency. The MaRS Commissioning Plan is described in detail in MEX-MRS-IGM-PL-3024.

Table 7.9-1: Configurations for the tracking verification test

S/C configuration	TWOD		
Ground segment configuration		up	down
NNO	IFMS A	X	X-CL
	IFMS B		X-CL
	IFMS RS		S-CL
DSN 34m	Closed-loop	X	S-CL
			X-CL
	Open-loop	X	S-OL RCP
			X-OL RCP
Telemetry modulation	OFF		
MaRS operational procedure	TVT-TWOD-X step 1		

S/C configuration	TWOD		
Ground segment configuration		up	down
NNO	IFMS A		X-CL
	IFMS B	X	X-CL
	IFMS RS		S-CL
Telemetry modulation	OFF		
MaRS operational procedure	TVT-TWOD-X (IFMS B) step 2		

S/C configuration	ONES		
Ground segment configuration		up	down
NNO	IFMS A		X-CL
	IFMS B		X-CL
	IFMS RS		X-CL
DSN 70m	Closed-loop		X-CL
	Open-loop		X-OL RCP
			X-OL LCP
Telemetry modulation	OFF		
MaRS operational procedure	TVT-ONES step 4		

S/C configuration	ONED		
Ground segment configuration		up	down
NNO	IFMS A		X-CL
	IFMS B		X-CL
	IFMS RS		S-CL
DSN 70m	Closed-loop		X-CL
			S-CL
	Open-loop		X-OL RCP
			X-OL LCP
			S-OL RCP
			S-OL LCP
Telemetry modulation	OFF		
MaRS operational procedure	TVT-ONED step 5		

S/C configuration	TWOD-S		
Ground segment configuration		up	down
NNO	IFMS A	S	S-CL
	IFMS B		S-CL
	IFMS RS	X	X-CL
DSN 34m	Closed-loop	S	X-CL
			X-CL
	Open-loop	S	X-OL RCP
			S-OL RCP
DSN 70m	Closed-loop	S	X-CL
			S-CL
	Open-loop	S	X-OL RCP
			X-OL LCP
			S-OL RCP
			S-OL LCP
Telemetry modulation	OFF		
MaRS operational procedure	TVT-TWOD-S step 6		

7.9.3.1 Operations Timeline

Tracking verification tests are to be performed regularly during commissioning phase, and prior to Mars arrival. The tracking verification tests constitute of a number of tracking passes, each 6 to 7 hours long. The total tracking verification test may last as long as TBD days.

Detailed timelines are listed in section 8.

7.9.3.2 Constraints

No S/C orbit corrections are to be scheduled within the tracking verification phase. Thruster activities shall be logged.

New Norcia, DSN 34-m and 70-m ground stations are requested.

7.9.4 Data TVT

7.9.4.1 Data Products

New Norcia Ground Station:

Table 7.9-2: IFMS TVT mission products

Receiver	Frequency band	Data products
IFMS A (closed-loop)	X	Doppler1 meteo
IFMS B (closed-loop)	-	
IFMS RS (open-loop)	X	tbd

Receiver	Frequency band	Data products
IFMS A (closed-loop)	X	Doppler1 meteo
IFMS B (open-loop)	S	tbd
IFMS RS (open-loop)	X	tbd

Receiver	Frequency band	Data products
IFMS A (closed-loop)	X	Doppler1 ranging meteo
IFMS B (closed-loop)	-	
IFMS RS (open-loop)	-	-

Receiver	Frequency band	Data products
IFMS A (closed-loop)	X	Doppler1 ranging meteo
IFMS B (closed-loop)	S	Doppler2 ranging
IFMS RS (open-loop)	S	tbd

Deep Space Network:

Table 7.9-3: DSN TVT mission products

Receiver	Frequency band	Data products	Data file type
closed-loop	X	Phase	TRK-2-34
	-	-	
open-loop	X	LCP voltage samples	RSR
	X	RCP voltage samples	
	-	-	
	-	-	

Receiver	Frequency band	Data products	Data file type
closed-loop	X	Phase	TRK-2-34
	-	-	
open-loop	-	-	-
	-	-	
	-	-	
	-	-	

Receiver	Frequency band	Data products	Data file type
closed-loop	X	Phase	TRK-2-34
	S	Phase	
open-loop	X	LCP voltage samples	RSR
	X	RCP voltage samples	
	S	LCP voltage samples	
	S	RCP voltage samples	

Receiver	Frequency band	Data products	Data file type
closed-loop	X	Phase	TRK-2-34
	S	Phase	
open-loop	X	LCP voltage samples	RSR
	X	RCP voltage samples	
	S	LCP voltage samples	
	S	RCP voltage samples	

7.9.4.2 Sample Rate

Table 7.9-4: Sample rate configurations for the various TVT steps

Closed-loop	1 sample / second Doppler
Open-loop	50,000 samples / second
Auxiliary data	TBD
Ground station meteo	1 sample / minute

Closed-loop	10 samples / second Doppler
Open-loop	5,000 samples / second
Auxiliary data	TBD
Ground station meteo	1 sample / minute

Closed-loop	1 sample / second Doppler 15 min ranging (simultaneous w/ Doppler)
Open-loop	-
Auxiliary data	TBD
Ground station meteo	1 sample / minute

Closed-loop	1 sample / second Doppler 15 min ranging (simultaneous w/ Doppler)
Open-loop	5,000 samples / second
Auxiliary data	TBD
Ground station meteo	1 sample / minute

7.9.4.3 Data Volume through the various TVT steps

Table 7.9-5: Default data volume 1 sec sampling closed-loop only

	Data Volume per hour
Closed-loop IFMS DSN	 1016 kByte per frequency / hour 1036 kByte per frequency / hour
Open-loop IFMS DSN	 -
Auxiliary data	TBD
Ground station meteo	Already contained in IFMS figure

Table 7.9-6: TVT data volume OL 50000 samples/second

	Data Volume per hour
Closed-loop IFMS DSN	 8,000 kByte per frequency / hour 1,036 kByte per frequency / hour
Open-loop IFMS DSN	 TBD 7,500,000 kByte / hour
Auxiliary data	TBD
Ground station meteo	Already contained in IFMS figure

Table 7.9-7: TVT data OL 5000 samples/second

	Data Volume per hour
Closed-loop IFMS DSN	 N/A N/A
Open-loop IFMS DSN	 TBD 750,000 kBytes / hour
Auxiliary data	TBD
Ground station meteo	Already contained in IFMS figure

7.9.4.4 Accuracy

Accuracy will be determined.

7.9.4.5 Availability

TBD

7.10 Grand total Data Volume

Occultations							
IFMS closed-loop	**Calculation (bytes)**	**samples per second**	**data volume one hour data recording (kBytes)**	**typical tracking pass (hours)**	**number of tracking passes**	**grand total data volume (kBytes)**	
Overhead	0.5	1	1.8	0.5	718	646.2	
Ranging	110	1	396	0.5	718	142164	
Doppler	220	1	792	0.5	718	284328	
Meteo	100	0.0167	6	0.5	718	2154	
DSN closed-loop ATDF							
Ranging Doppler	288	1	1036.8	0.5	619	320889.6	750181.8
Gravity							
IFMS closed-loop	**Calculation (bytes)**	**samples per second**	**Data volume one hour data recording (kBytes)**	**typical tracking pass (hours)**	**number of tracking passes**	**grand total data volume (kBytes)**	
Overhead	0.5	1	1.8	0.67	718	861.6	
Ranging	110	1	396	0.67	718	189552	
Doppler	220	1	792	0.67	718	379104	
Meteo	100	0.0167	6	0.67	718	2872	572389.6
Solar corona							
IFMS closed-loop	**Calculation (bytes)**	**samples per second**	**data volume one hour data recording (kBytes)**	**Typical tracking pass (hours)**	**number of tracking passes**	**grand total data volume (kBytes)**	
Overhead	0.5	1	1.8	6.5	129	1509.3	
Ranging	110	1	396	6.5	129	332046	
Doppler	220	1	792	6.5	129	664092	
Meteo	100	0.0167	6	6.5	129	5031	
DSN closed-loop ATDF							
Ranging Doppler	288	1	1036.8	6.5	129	869356.8	1872035.1
Phobos							
IFMS closed-loop	**Calculation (bytes)**	**samples per second**	**data volume one hour data recording (kBytes)**	**typical tracking pass (hours)**	**number of tracking passes**	**grand total data volume (kBytes)**	
Overhead	0.5	1	1.8	6.5	129	1509.3	
Ranging	110	1	396	6.5	129	332046	

Doppler	220	1	792	6.5	129	664092	
Meteo	100	0.0167	6	6.5	129	5031	
DSN closed-loop ATDF							
Ranging Doppler	288	1	1036.8	6.5	129	869356.8	1872035.1

Occultations							
IFMS open-loop	**Calculation (Mbytes)**	**samples per minute**	**data volume one hour data recording (MBytes)**	**typical tracking pass (hours)**	**number of tracking passes**	**grand total data volume (kBytes)**	
Overhead			0			0	
Ranging			0			0	
Doppler			0			0	
Meteo			0			0	
DSN open-loop RSR							
Ranging Doppler	0.5	1	30	0.5	619	9285	9285
Bistatic radar							
IFMS open-loop	**Calculation (Mbytes)**	**samples per minute**	**data volume one hour data recording (MBytes)**	**typical tracking pass (hours)**	**number of tracking passes**	**grand total data volume (kBytes)**	
Overhead			0			0	
Ranging			0			0	
Doppler			0			0	
Meteo			0			0	
DSN open-loop RSR							
Ranging Doppler	12.5	1	750	2	20	30000	30000
Solar Corona							
IFMS open-loop	**Calculation (Mbytes)**	**samples per minute**	**data volume one hour data recording (MBytes)**	**typical tracking pass (hours)**	**number of tracking passes**	**grand total data volume (kBytes)**	
Overhead			0			0	
Ranging			0			0	
Doppler			0			0	
Meteo			0			0	
DSN open-loop RSR							
Ranging Doppler	0.5	1	30	6.5	129	25155	25155
Phobos							
IFMS open-loop	**Calculation (Mbytes)**	**samples per minute**	**data volume one hour data recording (MBytes)**	**typical tracking pass (hours)**	**number of tracking passes**	**grand total data volume (kBytes)**	
Overhead			0			0	

Ranging			0			0	
Doppler			0			0	
Meteo			0			0	
DSN open-loop RSR							
Ranging Doppler	0.5	1	30	6.5	129	25155	25155

8

page left free

9 Sequence of Events

Sequence-of-events tables are included in the following for the operations procedures:

1. Timeline (summary)
2. Tracking Verification TVT
   TVT-ONES
   TVT-TWOS
   TVT-ONED
   TVT-TWOD
3. Occultations OCC
   OCC-DFLT
   OCC-NNOI
4. Gravity GRA
5. Bistatic Radar BRP
6. Solar Corona SCP

9.1 Operation Timeline

Cf. following pages

10 References

Asmar, S.W., and R.G. Herrera, Radio Science Handbook, JPL D-7938 Volume 4, Jet Propulsion Laboratory, Pasadena, CA, 1995.

Asmar, S.W., R.G. Herrera, and T. Priest, Radio Science Handbook, JPL D-7938 Volume 6, Jet Propulsion Laboratory, Pasadena, CA, 1995.

Asmar, S.W., and N.A. Renzetti, The Deep Space Network as an Instrument for Radio Science Research , Jet Propulsion Laboratory Publication 80-93, Rev. 1, 15 April 1993.

Bird M.K., Volland H., Pätzold M., Edenhofer P., Asmar S.W. and Brenkle J.P., The Coronal Electron Density Distribution Determined from Dual-frequency Ranging Measurements during the 1991 Solar Conjunction of the Ulysses Spacecraft, *Astrophys. J.* 426 , 373-381, 1994.

Bird, M. K., M. Allison, S. W. Asmar, D. H. Atkinson, P. Edenhofer, M. Heyl, L. Iess, D. Plettemeier, G. L. Tyler, and R. Wohlmuth, "The Huygens Doppler Wind Experiment," Special Publications Series, European Space Agency, September 13, 1995.

DSN 810-5: Deep Space Network / *Flight Project Interface Design Book* , Document 810-5, Jet Propulsion Laboratory, Pasadena, CA.

Edgett, K. S, Butler, Bryan J.; Zimbelman, J. R.; Hamilton, V. E. (1997): Geologic context of the Mars radar 'Stealth' region in southwestern Tharsis. Journal of Geophysical Research, E, Vol. 102(9), pp. 21,545-21,567.

Elliot, J. L. and P. D. Nicholson (1984). The Rings of Uranus. *Planetary Rings*. R. Greenberg and A. Brahic ed. Tucson, University of Arizona. 25-72.

Elliot, J. L., E. W. Dunham, A. S. Bosh, S. M. Slivan, L. A. Young, L. H. Wasserman and R. L. Millis (1989). “Pluto's Atmosphere.” Icarus 77(1): 148-170.

Eshleman, V. R. (1973). “The Radio Occultation Method for the Study of Planetary Atmospheres.” Planetary and Space Science 21: 1521- 1531.

Eshleman, V. R. and G. L. Tyler (1975). “Radio Occultation: Problems and Potential Solutions.” Stanford Electronics Laboratories, Stanford University. Rpt. no. 3241-3. September.

Eshleman, V. R., D. P. Hinson, G. F. Lindal and G. L. Tyler (1987). “Past and Future of Radio Occultation Studies of Planetary Atmospheres.” Advances in Space Research 7(12): 29-32.

Eshleman, V. R., G. L. Tyler, J. D. Anderson, G. Fjeldbo, G. S. Levy, G. E. Wood and T. A. Croft (1977). “Radio Science Investigations with Voyager.” Space Science Reviews 21(2): 207-232.

Fjeldbo, G. and V. R. Eshleman (1971). “The Neutral Atmosphere of Venus as Studied with the Mariner V Radio Occultation Experiment.” Astronomical Journal 76(2): 123-140.

Gurrola, E. M. (1995) Interpretation of Radar Data from the Icy Galilean Satellites and Triton, Ph.D. Dissertation, Stanford University.

Hinson, D. P., R. A. Simpson, J.D. Twicken, G. L. Tyler and F. M. Flasar. (1999) “Initial Results from Radio Occultation Measurements with Mars Global Surveyor,” JOURNAL OF GEOPHYSICAL RESEARCH (Planets), vol. 104, no E11, pp. 26,997–27,012, November 25.

Howard, H. T., G. L. Tyler, P. B. Esposito, J. D. Anderson, R. D. Reasenberg, I. I. Shapiro, G. Fjeldbo, A. J. Kliore, G. S. Levy, D. I. Brunn, R. Dickinson, R. E. Edelson, W. L. Martin, R. B. Postal, B. Seidel, T. T. Sesplaukis, D. L. Shirley, C. T. Stelzried, D. N. Sweetnam, G. E. Wood and A. I. Zygielbaum. (1974) "Mercury: Results on Mass, Radius, Ionosphere and Atmosphere Obtained from the Mariner 10 Dual frequency Radio Signals," SCIENCE, vol. 185, no. 4146, pp. 179-183, July.

Howard, H. T., V. R. Eshleman, D. P. Hinson, A. J. Kliore, G. F. Lindal, R. Woo, M. K. Bird, H. Volland, P. Edenhofer, M. Pätzold and H. Porsche. (1992). "Galileo Radio Science Investigations." Space Science Reviews 60: 565-590.

Hunten, D. M. and J. Veverka (1976). Stellar and Spacecraft Occultations by Jupiter: A Critical Review of Derived Temperature Profiles. *Jupiter*. T. Gehrels ed. Tucson, University of Arizona. 238-246.

JPLD-14027, Mars Global Surveyor Project, Telecommunications System Operations Reference Handbook, Version 2.1 (MGS 542-257), JPL Document D-14027, Jet Propulsion Laboratory,Pasadena, CA, 1996.

Konopliv and Snogren (1995)

Kliore, A. K., D. L. Cain, G. S. Levy, V. R. Eshleman, G. Fjeldbo and F. D. Drake (1965). "Occultation Experiment: Results of the First Direct Measurement of Mars' Atmosphere and Ionosphere." Science 149: 1243-1248.

Kursinski, E. R., G. A. Hajj, W. I. Bertiger, S. S. Leroy, T. K. Meehan, L. J. Romans, J. T. Schofield, D. J. McCleese, W. G. Melbourne, C. L. Thornton, T. P.Yunck, J. R. Eyre, R. N. Nagatani, (1996) "Initial results of radio occultation observations of Earth's atmosphere using the Global Positioning System," Science, vol.271, no.5252, p. 1107-10.

Lipa, B. J. and G. L. Tyler (1979). "Statistical and Computational Uncertainties in Atmospheric Profiles from Radio Occultations: Mariner 10 at Venus." Icarus 39(2): 192-208.

Muhleman, D.O.; Butler, B.J.; Grossman, A.W.; Slade, M.A. (1991). "Radar images of Mars" SCIENCE, vol.253, no.5027, p. 1508-13.

Nozette, S. (1996) et al.. The Clementine bistatic radar experiment, Science, 274, (5292), pp.1495-1498

Pätzold M. et al., Mars Express Orbiter Radio Science, *ESA-Special Publication, in press*, 2000b.

Pätzold M., Bird M.K., Edenhofer P., Asmar S.W., McElrath T.P. (1995): Dual-frequency radio sounding of the solar corona during the 1995 conjunction of the Ulysses spacecraft, *Geophys. Res. Lett.* 22, 3313—3316.

Pätzold M., Bird M.K., Edenhofer P., The change of Giotto's dynamical state during the P/Grigg-Skjellerup flyby caused by dust particle impacts, *Journ. Geophys. Res.* 98 , A12, 20911-20920, 1993.

Pätzold M., Bird M.K., Volland H., Edenhofer P. and Buschert H., Dynamics of the Giotto spacecraft in the inner dust coma of Comet P/Halley; Part 1: Observations, *Z. Flugwiss. Weltraumforsch* 15 , 89-96, 1991a.

Pätzold M., Bird M.K., Volland H., Edenhofer P. and Buschert H., Dynamics of the Giotto spacecraft in the inner dust coma of Comet P/Halley; Part 2: Interpretations, *Z. Flugwiss. Weltraumforsch* 15 , 159-164, 1991b.

Pätzold, M. et al., Rosetta Radio Science Investigations, *ESA-Special Publication*, *in press*, 2000a.

Pettengill , G. H., P.G. Ford and R.A. Simpson (1996). Electrical properties of the Venus surface from bistatic radar observations. Science 272(5268), 1628-1631.

Simpson, R.A. et al. (1984). Viking bistatic radar experiment; summary of results in near-equatorial regions, In: JGR. Journal of Geophysical Research. B89(12), pp.10,385-10,404

Simpson, R. A. (1993). "Spacecraft Studies of Planetary Surfaces Using Bistatic Radar." IEEE Transactions on Geoscience and Remote Sensing 31(2): 465-482.

Standish, E.M. (1993), Planet-X – No dynamic evidence in the optical observations. Astron. J. 105(5), 2000-2006.

Tyler, G. L, H.T. Howard (1973). Dual-Frequency Bistatic-Radar Investigations of the Moon Apollos 14 and 15. Journal of Geophysical Research 78(23), pp.4852-4874

Tyler, G. L. (1991) Magellan; electrical and physical properties of Venus' surface. Science 252(5003), pp.265-270

Tyler, G. L. (1987). "Radio Propagation Experiments in the Outer Solar System with Voyager." Proceedings of the IEEE 75(10): 1404-1431.

Tyler, G. L., G. Balmino, D. P. Hinson, W. L. Sjogren, D. E. Smith, R. A. Simpson, S. M. Asmar, P. Priest, and J. D. Twicken, "Radio Science Observations with Mars Global Surveyor: Orbit insertion through one year in mapping orbit," submitted to Journal of Geophysical Research (Planets), Special Issue on Mars Global Surveyor, August 3, 2000.

Tyler, G. L., et al. (1989). "Voyager Radio Science Observations of Neptune and Triton." Science 246(4936): 1466-1473.

Tyler, G. L., G. Balmino, D. P. Hinson, W. L. Sjogren, D. E. Smith, R. T. Woo, S. M. Asmar, M. J. Connally, C. L. Hamilton and R. A. Simpson (1992). "Radio Science Investigations with Mars Observer." Journal of Geophysical Research (Planets) 97(E5): 7759-7779.

Ware, R., M. Exner, D. Feng, M. Gorbunov, K. Hardy, B. Herman, Y. Kuo, T. Meehan, W. Melbourne, C. Rocken, W. Schreiner, S. Sokolovskiy, F. Solheim, X. Zou, R. Anthes, S. Businger, K. Trenberth. (1996) "GPS sounding of the atmosphere from low Earth orbit: preliminary results" BULLETIN OF THE AMERICAN METEOROLOGICAL SOCIETY, vol.77, no.1, p. 19-40 Jan. 1996.

Yeomans et al., Radio science results during the NEAR-Shoemaker spacecraft rendezvous with Eros, Science 289, 2085-2088, 2000.

Yeomans, D.K. et al., Estimating the mass of asteroid 253 Mathilde from tracking data during the NEAR flyby, Science 278, 2106-2109, 1997.

Yuen, J. H., Ed., . *Deep Space Telecommunications Systems*. New York, Plenum. 1983

Zisk, S. H. and Mouginis-Mark, P.J., Anomalous region on Mars: implications for near-surface liquid water, Nature, 288, 735-738, 1980